UNIVERSITE DE LIEGE
FACULTE DE MEDECINE VETERINAIRE
DEPARTEMENT DES SCIENCES CLINIQUES
SERVICE DE MEDECINE INTERNE DES ANIMAUX DE COMPAGNIE

Caractérisation des altérations du microbiote respiratoire et investigation des sous-populations de macrophages impliquées dans la fibrose pulmonaire idiopathique canine

Characterization of the alterations of the respiratory microbiota and investigation of lung macrophage clusters involved in canine idiopathic pulmonary fibrosis

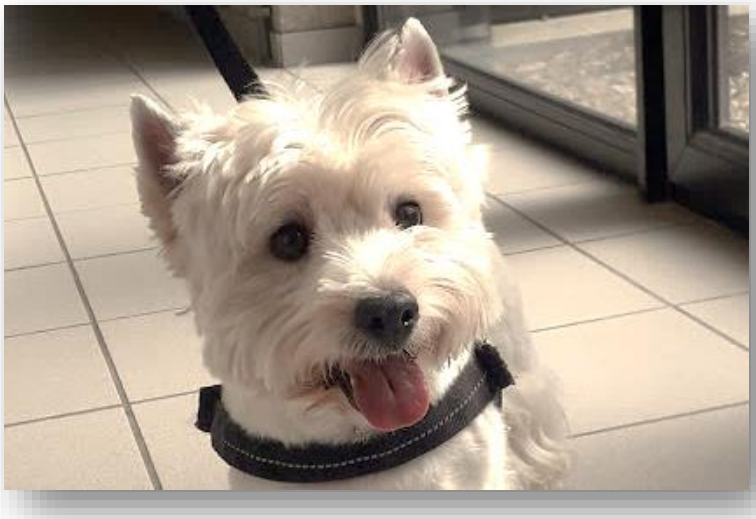

Aline FASTRES

THESE PRESENTEE EN VUE DE L'OBTENTION DU GRADE DE
Docteur en Sciences Vétérinaires

ANNEE ACADEMIQUE 2020-2021

Acknowledgements

First of all, I would like to warmly thank my promoter, Professor Cécile Clercx, for her daily support throughout this thesis, her patience, her energy and her continued motivation. Cécile, this thesis could not have been undertaken and completed without you. You offered me to start this wonderful experience and believed in my ability to carry it out. Thank you for always accepting my requests and for giving me the freedom to develop this thesis as I wanted. You have remained an attentive and always available presence during these 4 years and you have pushed me to give the best of myself and to constantly surpass myself. Your way of supervising me, always encouraging and even maternal, has made you like a second mother to me; and I'm definitely not the only one who thinks so, you have a lot of "daughters" and I'm proud to be one of them! Your passion for research, your constructive advice, all your ideas and the hours spent rereading my papers have allowed my work to evolve into what it is today. I could not have imagined having a better promotor. Just thank you!

Besides, I also would like to thank my co-promotor Pr Fabrice Bureau and all the members of my thesis committee, Pr Georges Daube and Pr Laurent Gillet for their collaboration, their help, their good ideas and the time they devoted to the evaluation and improvement of my thesis. Thank you Fabrice and Georges for opening the doors of your respective laboratories where I have always been welcomed and been able to find help.

I would like to express my gratitude to all the members of my jury, Pr Veronique Delcenserie from the faculty of Veterinary medicine of Liège, Doctor Bénédicte Machiels from the faculty of Veterinary medicine of Liège, Pr Robert P. Dickson from the University of Michigan, Pr Antoine Froidure from the Catholic University of Louvain, Dr Julien Guiot from the University hospital of Liège and Pr Mutien-Marie Garigliany from the faculty of Veterinary medicine of Liège. They kindly agreed to judge my work and provide me good suggestions to improve the manuscript. Thank you to Dr Anne-Sophie Van Laere who agreed to chair this jury.

I also would like to thank all the people who have contributed to this work, and I hope I haven’t forgotten any of them!

I would like to greatly thank all the members of the “westie team”: the cardiologists Dr Anne-Christine Merveille and Pr Kathleen McEntee who have performed all the echocardiographies for my dogs even if they were so horrible because of their ugly lungs; Dr Alexandru-Cosmin Tutunaru, my dedicated anaesthetist, for his calm and pragmatism even when the dogs were cyanotic. None of the dogs passed away during anaesthesia, it was my greatest fear! Thank you for keeping them alive and

thank you to all the anaesthetic service for their help when you were not there; Pr Géraldine Bolen, Dr Eugénie Soliveres, Dr Emilie Pierrot, Laurie Van Bossuyt and all the members of the imaging service for all their CT-scan reports and lung echographies and for their availability even during the holidays.

I would also make a special big thank to the "MIPA team": Dr Elodie Roels who helped me and showed me all the tips and tricks to begin my thesis, thank you for your support and for your always so cool comments on my papers; Dr Emilie Vangrinsven who participated with me to the recruitment of healthy dogs, who shared (not long enough) my office and was my only thesis colleague in the middle of all the clinicians at the beginning, you contributed to make me feel less alone in research; Charlotte, Elodie D., Morgane, Valérie, Nina, Lena, Aurélie, Hélène, Marine, Tom and Sébastien really thank you to make a little place for me in your special team, thank you for your kindness and all the good laughs. I would also make a big kiss to Caroline, I was so sad when you had to leave my office. Thank you for your support in difficult times!

Thank you also to the chiefs of the internal medicine service, Pr Dominique Peeters and Dr Frédéric Billen for their support and their encouragements. Dominique thank you to give me the opportunity to continue my thesis and to discover the assistant position, I really appreciated pass on my knowledge to students, thanks for believing in me! Thank you again to all the members of the small animal clinic of the faculty of Veterinary medicine of Liège and to all the students who supported me and my westies during these 4 years.

I wanted to thank all the team from the department of Food Science for their welcome and in particular Simone, Hiba, Sophie, Elisa and of course Bernard Taminiau. Bernard, you taught me to be autonomous for microbiota analysis and to deal with such enormous amounts of data. Thank you for your help in statistic and in results interpretation and for all the time you spent to pass on some of your knowledge to me. I really enjoyed all your messages when you were not at work.

I would like to express my immense gratitude to the team of the GIGA centre and more specifically to Laurence Fievez and Dimitri Pirottin for their welcome. They helped me to navigate into the meander of the fundamental science. They were always available to help me to reach our objectives with motivation, calm, kindness and stubbornness against not working experiment. Thank you for sharing your knowledge and your time. You have greatly contributed to the advancement of my research. Thank you also to Dr Thomas Marichal and Dr Christophe Desmet for their availability, their advice and their help in the performance of this work.

Of course, I would like to thank Joëlle Piret, Kim Phan Hu, Belinda Albert, Eugenia Di Biagio, Sylvain Romijn, François Delvaux and Michael Sarlet for their technical assistance. All this

work could not have been done without you! Thank you Joëlle for your availability, your patience foolproof, your good mood and your precision, I really enjoyed working with you even if most of the times it was difficult to find the good protocol! I was really lucky to work with you.

Thank you to Pr Frédéric Farnir and Evelyne Moyse for their invaluable help in statistics.

Thanks to Pr Nadine Antoine who welcomed me in her lab and helped me to find solutions to my problems in immunohistochemistry and thank you to all the team of the histopathology department for their welcome.

A special thanks to all the owners of westies who trusted me to take care of their dogs and special loves to Nahya, Jock, Dana, Blue Belle Girl, Nikki, Spiky, Noisette, Djinn, Athena, Cepia, Loona, Grany, Harry, Epsy, Elios, Kyra, Cookie, Barry, James, Lula, Logan, Fizz, Gipsy, Biscotte, Looky, Shiva, Chanel, Suus and Beau that I followed during these 4 years.

Finally, I would like to express my love to my parents and my family for always being present for me and for encouraging me. Thank you also for supporting me when I was stressed, I know how I can be horrible in such periods! Thank you, mom and dad, for always supporting me in my choices and allowing me to continue on my way. I wouldn’t be here without you and the work here presented could not have been accomplished. Mother, don’t let your key fall again; I know you are proud of me!

Abbreviations

5-HT	Serotonin
6MWD	6-minute walked distance
6MWT	6-minute walking test
AC	Amoxicillin/clavulanic acid
AE	Acute exacerbation
ALP	Alkaline phosphatase
ARDS	Acute respiratory distress syndrome
AM	Alveolar macrophage
AMOVA	Analysis of molecular variance
ATP11A	ATPase phospholipid transporting 11A
Avg_logFC	Average log2 fold change
BAL	Bronchoalveolar lavage
BALF	Bronchoalveolar lavage fluid
Br	Brachycephalic dogs
CAP	Community-acquired pneumonia
CB	Chronic bronchitis
CCL2	C-C motif chemokine ligand 2
CCL3	C-C motif chemokine ligand 3
CCL4	C-C motif chemokine ligand 4
CCL5	C-C motif chemokine ligand 5
CCL18	C-C motif chemokine ligand 18
CCR2	C-C motif chemokine receptor type 2
cDNA	Complementary desoxyribonucleic acid
CF	Cystic fibrosis
CIPF	Canine idiopathic pulmonary fibrosis
CIRD-C	Canine infectious respiratory disease complex
CLD	Connective lung disease
COPD	Chronic obstructive pulmonary disease
CRP	C reactive protein
Ct	Cycle threshold
CXCL8	C-X-C motif chemokine ligand 8

D0	Before antimicrobial drug administration
D10	10 days after discontinuation of antimicrobial drug administration
D16	16 days after discontinuation of antimicrobial drug administration
DC	Dendritic cell
DCC	Differential cell count
DEG	Differentially expressed gene
DNA	Deoxyribonucleic acid
EBP	Eosinophilic bronchopneumopathy
ECM	Extracellular matrix
ELISA	Enzyme-linked immunoassay
EMT	Epithelial-mesenchymal transition
ET1	Endothelin-1
ExpB	Experimental beagles
FGF	Fibroblast growth factor
FN1	Fibronectin 1
GEMs	Gel beads in emulsion
GER	Gastroesophageal reflux
GGO	Ground glass opacity
GO	Gene ontology
GSEA	Gene set enrichment analysis
HOMOVA	Homogeneity of the molecular variance
HP	Chronic hypersensitivity pneumonitis
HRCT	High-resolution computed tomography
IGF1	Insulin growth factor 1
ILD	Interstitial lung disease
IL1	Interleukin 1
IL1RN	Interleukin 1 receptor antagonist
IL6	Interleukin 6
IM	Interstitial macrophage
INF-α	Interferon alpha
IPF	Idiopathic pulmonary fibrosis
ITGB6	Integrin αvβ6

ITGB8	Integrin αvβ8
KL-6	Krebs Von den Lungen-6
LDA	Linear discriminant analysis
LM	Lung microbiota
LTBP	Latent TGF-β binding protein
Ma/Mo	Macrophages/monocytes
MMP	Matrix metalloproteinase
NMDS	Non-metric multidimensional scaling
NSIP	Non-specific interstitial pneumonia
OTU	Operational taxonomic unit
PaO_2	Partial pressure of oxygen in arterial blood
PCII	Type II pneumocyte
PCA	Principal component analysis
PCR	Polymerase chain reaction
PCS	Procedural control specimen
PDGF	Platelet derived growth factor
PERMANOVA	Permutational multivariate analysis of variance
PH	Arterial pulmonary hypertension
PIIINP	Procollagen type III amino terminal propeptide
P-Smad2	Phosphorylated signalling protein Smad2
QOL	Quality of life
qPCR	Quantitative polymerase chain reaction
qRT-PCR	Quantitative reverse transcriptase PCR
RNA	Ribonucleic acid
RT	Reverse transcription
S	Shepherd dogs
ScRNA-seq	Single-cell mRNA sequencing
SFTPC	Surfactant protein C
SPP1	Osteopontin
T	Terrier dogs
TBRI	TGF-β receptor I
TBRII	TGF-β receptor II

TCC	Total cell count
TGF-β1	Transforming growth factor beta 1
THBS1	Thrombospondin-1
TIMP1	Metallopeptidase inhibitor 1
TNF-α	Tumour necrosis factor alpha
t-SNE	t-distributed stochastic neighbour embedding
UIP	Usual interstitial pneumonia
UMI	Unique molecular identifier
VEGF	Vascular endothelial growth factor
WHWT	West Highland white terrier

Table of contents

Résumé - Abstract

Résumé

La fibrose pulmonaire idiopathique canine (CIPF) est une pathologie qui atteint essentiellement les chiens âgés de la race du West Highland white terrier (WHWT). Il s'agit d'une maladie chronique caractérisée par un dépôt de collagène dans l'interstitium pulmonaire entrainant une insuffisance respiratoire progressive. A ce jour, l'étiologie de cette pathologie reste inconnue, le diagnostic est difficile, la pathophysiologie peu investiguée et le pronostic sombre. Les seuls traitements possibles actuellement sont symptômatiques et visent à améliorer la qualité de vie des chiens. La CIPF est régulièrement assimilée à la fibrose pulmonaire idiopathique (IPF) qui touche l'homme, bien que les deux pathologies ne soient pas strictement identiques.

Ce travail a donc été entrepris dans le but d'améliorer les connaissances pathophysiologiques sur la CIPF et plus précisément celles relatives au microbiote pulmonaire (LM) et aux clusters de macrophages pulmonaires du liquide de lavage bronchoalvéolaire (BALF). En effet, les macrophages sont les principaux médiateurs des réactions immunitaires innées dirigées contre les bactéries dans le poumon. Ils sont capables de se polariser et de moduler leur caractéristiques phénotypiques (inflammatoires ou pro-fibrosantes) en fonction des modifications de leur environnement et notamment du LM. Récemment, des études sur l'IPF ont montré que le LM et son impact sur le système immunitaire et notamment les macrophages pourraient avoir un lien avec le développement, le maintien et l'exacerbation de la maladie donnant lieu à de nouvelles perspectives thérapeutiques.

Dans un premier temps, nous avons décrit le LM chez les chiens sains et les principaux facteurs susceptibles de l'influencer. Une première étude a eu pour objectif de déterminer l'effet à court et moyen terme d'une antibiothérapie systémique sur le LM de beagles expérimentaux. En effet, les WHWTs atteints de CIPF présentés en consultation sont régulièrement traités à l'aide d'agents antimicrobiens. Nous avons établi que le LM avant antibiothérapie est relativement stable entre les individus et composé en majorité de 4 phyla, les Protéobactéries, les Firmicutes, les Bactéroïdetes et les Actinobactéries. L'administration orale d'amoxicilline-acide clavulanique pendant 10 jours modifie la diversité globale et la composition du LM, lesquelles reviennent à un état proche de l'état initial 16 jours après l'arrêt du traitement. L'effet de l'environnement et de la race sur le LM a ensuite été investigué en comparant des groupes de chiens adultes de races différentes (terriers-WHWTs-beagles-brachycéphaliques-bergers) évoluant dans des environnements différents (domestique-expérimental). Il a été montré que le LM varie de façon significative en fonction de l'environnement et que la race joue également un rôle dans la variation du LM bien que plus anecdotique. L'âge ne semble pas avoir d'impact sur le LM chez les chiens adultes. Un LM commun à tous les chiens sains dans chaque étude sur le LM a pu être identifié. Il contient au moins les genres *Cutibacterium*, *Streptococcus*, *Acinetobacter* et *Pseudomonas*. Dans une maladie pulmonaire aiguë, la bordetellose, nous avons pu montrer que les résultats obtenus par séquençage de l'ADN 16S (technique utilisée pour étudier le microbiote) sont corrélés aux résultats d'amplification en chaîne par polymérase et de

culture (techniques classiques d'identification des infections bactériennes dans le poumon). Le séquençage de l'ADN 16S est donc une technique fiable pour identifier les bactéries, surtout rares et difficilement cultivables, impliquées dans les maladies pulmonaires infectieuses canines. Une dysbiose a également été mise en évidence chez ces chiens caractérisée par une domination d'une ou deux bactéries, une diminution de la richesse et de la diversité et une augmentation de la charge bactérienne. Finalement, nous avons pu montrer qu'entre les WHWTs atteints de CIPF et les WHWTs sains, le LM est assez similaire avec une augmentation de 6 genres par rapport aux chiens sains d'autres races (*Brochothrix*, *Curvibacter*, *Pseudarcicella*, un genre de la famille des Flavobacteriaceae, *Rhodoluna* et *Limnohabitans*). *Brochothrix*, *Pseudarcicella*, *Curvibacter* et un genre de la famille des Flavobacteriaceae sont également, bien que non significativement, plus abondants chez les WHWTs malades par rapport aux sains. Nous en avons donc déduit que chez le WHWT, la présence d'un LM particulier semble davantage liée à la race qu'à la maladie et pourrait être un facteur intervenant dans la prédisposition du WHWT à la CIPF.

Le séquençage des acides ribonucléiques messagers par cellule (scRNA-seq), une technique de séquençage à haut débit et non biaisée permettant l'analyse transcriptomique de cellules individuellement, a ensuite été validée dans le BALF de chiens sains. Quatorze clusters conservés entre les chiens ont pu être mis en évidence correspondant à 8 populations cellulaires : macrophages, lymphocytes, neutrophiles, cellules dendritiques, lymphocytes B, mastocytes, cellules épithéliales et cellules en division. Le scRNA-seq a alors été utilisé pour identifier des clusters de macrophages chez des WHWTs atteints de CIPF en comparaison de WHWTs sains. Les mêmes grandes populations cellulaires que dans l'étude précédente ont été identifiées. Les cellules identifiées comme étant des macrophages ont ensuite été sous-catégorisées en cinq clusters. Parmi ceux-ci, deux clusters, l'un identifiés comme des monocytes et l'autre comme des macrophages dérivés de monocytes, sont enrichis en gènes pro-fibrosants par rapport aux autres. Les gènes pro-fibrosants surexprimés dans ces 2 clusters incluent *CCL2, SPP1, FN1, CCL3, TIMP1, IL1RN, CXCL8* et *CCL4*, et *SFTPC*, *CCL5*, *FN1, CXCL8, ATP11A* et *SPP1,* respectivement. L'expression différentielle des gènes dans les monocytes entre les WHWTs malades et sains n'est pas différente, mais ce cluster contient significativement plus de cellules chez les WHWTs malades. Les macrophages dérivés de monocytes sont quant à eux enrichis en gènes pro-fibrosants chez les WHWTs malades par rapport aux sains mais aussi en gènes associés à l'angiogenèse et à la transition épithélio-mésenchymateuse, phénomènes intervenant dans la pathophysiologie de la fibrose. La présence de ces clusters de macrophages pro-fibrosants contribue probablement au développement et au maintien de la CIPF chez le WHWT.

Ce travail a donc permis de décrire le LM canin et ses modifications chez les WHWTs atteints de CIPF par rapport à d'autres conditions saines et pathologiques. L'utilisation du scRNA-seq dans le BALF, après validation, a permis d'identifier des clusters de macrophages pro-fibrosants chez les WHWTs atteints de CIPF. Les gènes pro-fibrosants identifiés pourraient servir dans le futur comme biomarqueur ou cible thérapeutique, ce qui offre de belles perspectives de recherche sur la CIPF.

Summary

Canine idiopathic pulmonary fibrosis (CIPF) mainly affects middle-aged to old dogs from the West Highland white terrier (WHWT) breed. CIPF is a chronic disease characterized by collagen deposition in the pulmonary interstitium inducing progressive airway failure. Despite numerous investigations, the aetiology of the disease remains unknown, the diagnosis difficult, the pathophysiology misunderstood and the prognosis poor. Currently, there is no curative therapeutic option for that condition and only symptomatic treatments can be used to maintain a quality of life as good as possible for the dogs. CIPF is frequently equated with human idiopathic pulmonary fibrosis (IPF), although the diseases are not strictly identical.

This project was therefore conducted in order to increase pathophysiological knowledges on CIPF and more precisely the ones related to the lung microbiota (LM) and bronchoalveolar lavage fluid (BALF) macrophage clusters. Indeed, macrophages are critical mediators of innate immune responses against bacteria in the lung. They are able to polarize and modulate their phenotypes (inflammatory or pro-fibrotic) to adjust to the microbial environmental conditions. Moreover, recently, studies about IPF have shown that the LM and its impact on the immune system, especially lung macrophages, could have a link with the development, the maintain and the exacerbation of the disease, providing perspectives for designing novel therapeutic strategies.

Before assessing the LM in CIPF, we described the LM in healthy dogs and determined the principal factors potentially able to alter it in healthy conditions, including antimicrobial treatment, age, breed and living conditions. As WHWTs affected with CIPF are frequently referred under antimicrobial drug, we first investigated the short and long-time impact of such treatment on the LM in healthy experimental beagles. We showed that before drug administration, the LM is quite similar among dogs with the predominance of 4 phyla: Proteobacteria, Firmicutes, Bacteroidetes and Actinobacteria. A 10-days oral amoxicillin-clavulanic acid administration induces alteration of the global diversity and the composition of the LM. However, changes nearly disappear 16 days after discontinuation of the drug. The impact of the living conditions and the breed on the LM have then been assessed by comparing different dogs' breeds (terriers, WHWTs, beagles, brachycephalic dogs and shepherds) living in different conditions (domestic or experimental). We showed that LM is significantly different depending of the living condition of dogs, while breed has a milder impact. In adult dogs, age doesn't seem to have an impact on the LM. A core microbiota has been proposed by regrouping data of all published studies related to the LM in healthy dogs and is composed by at least *Cutibacterium*, *Streptococcus*, *Acinetobacter* and *Pseudomonas* genera. In acute respiratory diseases and particularly in dogs affected with *Bordetella bronchiseptica*, we showed that 16S rDNA sequencing (the technique used to assess LM) results correlate with results of classical techniques used to assess bacterial infection in the lung (*i.e.* polymerase chain reaction and culture). This suggests that the 16S rDNA sequencing is reliable for identifying bacteria involved in canine lung infectious

diseases, mainly when rare or slow growing bacteria are concerned. A dysbiosis of the LM is also described in the dogs affected with bordetellosis characterized by a domination of one or two bacteria, a reduction of the diversity and the richness, and a higher bacterial load compared with healthy aged-matched dogs. Lastly, we showed that the LM between healthy WHWTs and WHWTs affected with CIPF is quite similar. *Brochothrix*, *Curvibacter*, *Pseudarcicella*, a genus belonging to Flavobacteriaceae family, *Rhodoluna* and *Limnohabitans* genera are increased in WHWTs either healthy or diseased compared with healthy dogs from other breeds. *Brochothrix, Pseudarcicella, Curvibacter* and a genus belonging to Flavobacteriaceae family are also more abundant in CIPF than in healthy WHWTs, however, not significantly. We therefore conclude that the presence of a specific LM in WHWTs compared to other breeds may be suspected to be one of the factors that can predispose that breed to CIPF.

In the second part of the thesis, the use of the single-cell mRNA sequencing technique (scRNA-seq) was first validated in the BALF from healthy dogs. ScRNA-seq is an unbiased and high throughput tool that enables the transcriptomic identification of thousands of single cells at a time and that has never been used in dogs before. By using this technique, we found 14 conserved clusters in the BALF of healthy dogs corresponding to 8 different cell populations: macrophages, lymphocytes, neutrophils, dendritic cells, B cells, mast cells, epithelial cells and cells in division. The scRNA-seq was then used to identify macrophages clusters in WHWTs affected with CIPF compared with healthy WHWTs. In all WHWTs, the same cell populations as described in the previous study were identified. Five clusters of macrophages were found. Among them, two were enriched in pulmonary fibrosis processes compared with other clusters, a cluster of monocytes and a cluster of monocytes-derived macrophages. Pro-fibrotic genes overexpressed in monocytes and monocytes-derived macrophages included *CCL2*, *SPP1*, *FN1*, *CCL3*, *TIMP1*, *IL1RN*, *CXCL8* and *CCL4*, and *SFTPC*, *CCL5*, *FN1*, *CXCL8*, *ATP11A* and *SPP1*, respectively. The differential gene expression in monocytes was not different between CIPF and healthy WHWTs. However, significantly more cells from this cluster were identified in CIPF dogs. Monocytes-derived macrophages were enriched in pulmonary fibrosis but also in angiogenesis and epithelial-mesenchymal transition processes in CIPF compared with healthy WHWTs. Four pro-fibrotic genes were overexpressed in CIPF compared with healthy WHWTs in that cluster including *FN1*, *SPP1*, *CXCL8* and *PLAU*. The presence of those pro-fibrotic macrophage clusters in diseased WHWTs probably participates to the onset and/or the perpetuation of CIPF.

In conclusion, this project allowed to better describe the LM in healthy dogs and its modifications in WHWTs affected with CIPF in comparison with other lung pathological conditions. The use of the scRNA-seq in dogs' BALF, after validation revealed the presence of pro-fibrotic macrophage clusters in CIPF compared with healthy WHWTs. Overexpressed pro-fibrotic genes identified in CIPF WHWTs might be used as biomarkers or be targeted for therapeutic treatment, which offers good perspectives for future research about CIPF.

General preamble

The present work will focus on a lung disease affecting middle-aged to old dogs from the West Highland white terrier (WHWT) breed called the canine idiopathic pulmonary fibrosis (CIPF). CIPF is considered as an interstitial lung disease (ILD). The ILD term was introduced in 1994 to design a heterogenous collection of diseases affecting the lung parenchyma and characterized by an initial alveolar inflammation extending to the interstitium and leading to diffuse fibrosis (MeSH PubMed). In pulmonary fibrosis cases, the lungs are progressively infiltrated with fibroblasts and collagen which results in an impairment of gas exchanges and a progressive respiratory failure (Mesh PubMed).

Since 2011, the CIPF disease has been the subject of different studies including studies conducted by our team with the contribution of our Finnish veterinary partners from the University of Helsinki. Those works aimed at improving knowledges on CIPF in terms of clinical characterization, diagnosis and prognosis, but also of pathophysiology and identification of future possible therapeutic approaches, with the expectation that findings will be translatable to the human idiopathic pulmonary fibrosis (IPF), a comparable disease in man. However, at the present time, several aspects of CIPF remain to be explored.

In the introduction, we will review what is currently known about CIPF in the WHWT breed in comparison with human findings on IPF, and what is still to be explored. In addition, in line with the objectives of the present work, part of the introduction will focus on the lung microbiota (LM), that will be studied in CIPF and another part on the single-cell mRNA sequencing (scRNA-seq) technique, a recent tool that is used in our work as well.

Introduction

1. Canine idiopathic pulmonary fibrosis

1.1. Generalities

CIPF was properly described for the first time in 1999 by Corcoran and colleagues in a cohort of 29 WHWTs (Corcoran *et al.*, 1999). Initially, the disease was characterized by a diffuse interstitial pattern on radiographs, and an increase of respiratory sounds with the presence of inspiratory crackles on lung auscultation (Corcoran *et al.*, 1999). The term CIPF was first employed in 2005 by Johnson and colleagues due to similarity between the canine disease and the IPF disease described in human medicine. Indeed, the two pathologies correspond to specific form of chronic, progressive, fibrosing ILDs of unknown cause, occurring primarily in older patients or dogs and limited to the lungs. They are characterized by an accumulation of collagen in the interstitium leading to progressive dyspnoea, impaired gas exchange and death (ATS and ERS, 2000; Raghu *et al.*, 2011; Raghu *et al.*, 2018; Clercx, Fastrès and Roels, 2018; Lynch *et al.*, 2018; Laurila and Rajamäki, 2020). CIPF has also been called chronic pulmonary disease (Corcoran *et al.*, 1999; Schober and Baade, 2006), chronic idiopathic pulmonary fibrosis (Lobetti, Milner and Lane, 2001; Webb and Armstrong, 2002), idiopathic pulmonary fibrosis (Norris, Griffey and Walsh, 2002; Reinero, 2019a) and interstitial lung disease (Norris, Naydan and Wilson, 2005; Reinero and Cohn, 2007).

In 2019, a large review classified ILDs in dogs and cats (Figure 1) in order to help in understanding more about aetiology, clinical features, pathogenesis and response to treatment (Reinero, 2019a; Reinero, 2019b). As in human, the term ILDs in dogs groups large and heterogenous non-infectious, non-neoplastic disorders characterized by various types of inflammation and fibrosis (Reinero, 2019a; Reinero, 2019b; Wakwaya and Brown, 2019; Farris, 2020). Among ILDs, CIPF is considered as a familial fibrotic ILD and is the best-described ILDs affecting dogs, probably because of its potential utility as spontaneous model for IPF in human (Reinero, 2019a; Reinero, 2019b). Indeed, the potential role of WHWTs as model for IPF has been considered as striking similarities in clinical presentations were observed between the two species (Williams and Roman, 2016; Tashiro *et al.*, 2017; Barnes *et al.*, 2019). With the improvement of CIPF characterization, differences between IPF and CIPF have been highlighted in thoracic imaging and histopathological findings indicating that the diseases are not identical (Syrjä *et al.*, 2013; Clercx, Fastrès and Roels, 2018; Laurila and Rajamäki, 2020). Nevertheless, the spontaneity of the disease development in the dog as well as its submission to similar environmental living conditions as men support their superiority as model compared to those induced, in particular for testing mechanisms of action and effectiveness of novel therapies (Clercx, Fastrès and Roels, 2018; Barnes *et al.*, 2019).

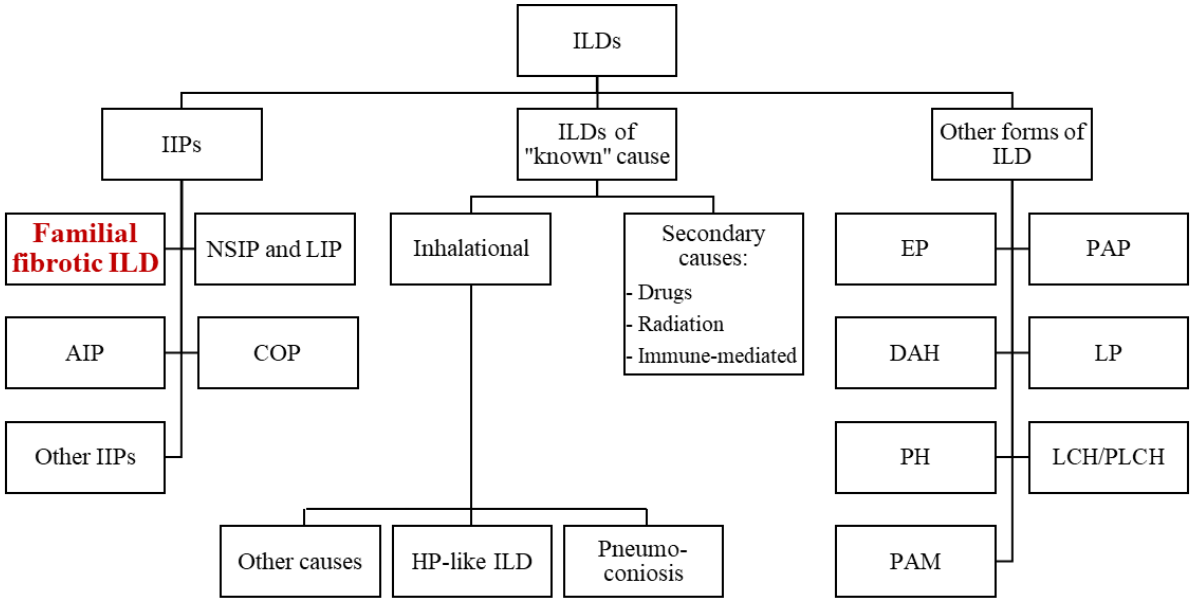

Figure 1. *Classification of canine and feline interstitial lung diseases (ILDs). Canine idiopathic pulmonary fibrosis belongs to familial fibrotic ILDs. IIPs, idiopathic interstitial pneumonias; NSIP, non-specific interstitial pneumonia; LIP, lymphocytic interstitial pneumonitis; AIP, acute interstitial pneumonia; COP, cryptogenic organizing pneumonia; HP-like ILD, hypersensitivity-like interstitial lung disease; EP, eosinophilic pneumonia; PAP, pulmonary alveolar proteinosis; DAH, diffuse alveolar haemorrhage; LP, lipid/lipoid pneumonia; PH, pulmonary hyalinosis; LCH/PLCH, Langerhans' cell histiocytosis/pulmonary Langerhans' cell histiocytosis; PAM, pulmonary alveolar microlithiasis. Figure adapted from Reinero et al., 2019.*

1.2. Epidemiology and clinical presentation

Currently, the prevalence and the incidence of CIPF are unknown. The difficulty to diagnose the disease, the presence of misdiagnosis and the lack of knowledges about WHWTs population contribute to the absence of epidemiologic data about the disease (Clercx, Fastrès and Roels, 2018; Laurila and Rajamäki, 2020).

Age of the dogs at presentation ranges from 5 to 16 years (Heikkilä *et al.*, 2011; Syrjä *et al.*, 2013; Roels *et al.*, 2017a; Thierry *et al.*, 2017; Holopainen *et al.*, 2019; Roels *et al.*, 2019), although rare younger CIPF cases have also been reported (Johnson *et al.*, 2005; Schober and Baade, 2006). No sex predisposition is reported (Clercx, Fastrès and Roels, 2018; Laurila and Rajamäki, 2020). The disease develops slowly allowing adaptation to progressive respiratory impairment. Indeed, early stage of the disease are frequently confounded by the owners with normal ageing process and dogs are usually bright and alert at their presentation except for more severe cases (Corcoran *et al.*, 1999;

Heikkila-Laurila and Rajamaki, 2014). The duration of clinical signs prior diagnosis varies between around 1 month and 4 years with great individual variation. As in human IPF, common clinical signs reported include either exercise intolerance or chronic cough or both. Other classical clinical signs include restrictive dyspnoea, tachypnoea, cyanosis, syncope, gagging and panting (Heikkila-Laurila and Rajamaki, 2014; Roel *et al.*, 2017; Thierry *et al.*, 2017; Holopainen *et al.*, 2019; Kishaba, 2019b; Roels *et al.*, 2019).

At clinical examination, presence of bilateral, inspiratory crackles is a characteristic finding on lung auscultation, which is also typically reported in IPF (Clercx, Fastrès and Roels, 2018; Raghu *et al.*, 2018; Sgalla *et al.*, 2018; Hochhegger *et al.*, 2019; Laurila and Rajamäki, 2020). Moreover, in some dogs, crackles can even be heard without stethoscope when the dog is breathing with an open mouth (Clercx, Fastrès and Roels, 2018; Laurila and Rajamäki, 2020). Other common clinical examination findings include positive laryngo-tracheal reflex, tachypnoea and dyspnoea. In severely affected dogs, cyanosis, respiratory distress, and an abdominal breathing pattern are commonly present (Corcoran *et al.*, 1999; Heikkila-Laurila and Rajamaki, 2014). Some dogs develop complications secondary to CIPF such as secondary respiratory tract infection or arterial pulmonary hypertension (PH). In this case, a low-grade, right-sided, and systolic murmur can be heard because of tricuspid reflux due to PH (Heikkila-Laurila and Rajamaki, 2014). The presence of PH is also documented in IPF patients and is associated with a decrease in survival, an increase risk of death and a reduce quality of life (QOL) (Raghu *et al.*, 2015a; Torrisi *et al.*, 2018; Alfaro and Cordeiro, 2020).

1.3. Aetiology and risk factors

The aetiology of CIPF is still unknown. As the disease principally occurs in WHWTs, a genetic predisposition is strongly suspected (Heikkila-Laurila and Rajamaki, 2014). Indeed, a genetic relationship with another dog affected with CIPF was associated with an increased risk to develop CIPF (Roels *et al.*, 2018). However, not all old WHWTs are affected with CIPF, which suggests the involvement of other factors in the disease development (Clercx, Fastrès and Roels, 2018; Laurila and Rajamäki, 2020). Anecdotal pulmonary fibrosis cases have also been described in other terrier breeds, such as the American Staffordshire terrier, the Bull terrier, the Cairn terrier and the Scottish terrier (Corcoran *et al.*, 1999; Lobetti, Milner and Lane, 2001; Norris, Griffey and Walsh, 2002; Johnson *et al.*, 2005; Krafft *et al.*, 2013). However, it is unknown if the disease in those breeds is exactly the same as in the WHWT breed. In human, several genetic mutations have been clearly associated with an increased risk to develop IPF and include essentially mutations in the mucin 5B gene, surfactant protein genes and telomerase genes (Wakwaya and Brown, 2019). Despite investigations, none of these mutations have consistently been associated with CIPF in WHWTs (Clercx, Fastrès and Roels, 2018; Laurila and Rajamäki, 2020). Recently, a genome-wide association study identified genetic variants associated with CIPF in the WHWT breed, located in a region encompassing the cleavage and

polyadenylation specific factor 7 (*CPFS7*) and the succinate dehydrogenase complex assembly factor 2 (*SDHAF2*) genes (Piras *et al.*, 2020). These two overlapping genes include 15 and 8 informative single nucleotide polymorphisms, respectively. However, in this study, the disease was self-reported by the owners which raises questions about CIPF diagnosis as no clinical confirmation of CIPF, knowledge of whether they had progressive lung fibrosis and information about lifespan were known by the authors (Piras *et al.*, 2020). Further studies are required to validate those results. Another genome-wide association analysis was also recently performed in WHWTs affected with atopic dermatitis, a heritable disease condition affecting between 6.5 and 52% of WHWTs (O' Neill *et al.*, 2019; Favrot *et al.*, 2020; Rostaher *et al.*, 2020). A missense variant in the gene coding for the coagulation factor II thrombin receptor (*F2R*) that segregated between healthy and diseased WHWTs was identified (Agler *et al.*, 2019). The activation of this receptor has been shown to play a role especially in wound healing, inflammation and fibrosis and may be at the origin to the increased local chemokine C-C motif ligand 2 (CCL2) release and epithelial-mesenchymal transition (EMT) process occurring in CIPF (Mercer and Chambers, 2013; Wygrecka *et al.*, 2013; Ungefroren *et al.*, 2018). However, to our knowledge, there is no study assessing the link between atopic dermatitis and CIPF and between the activation of this receptor and CIPF in the WHWT breed.

Several environmental factors have also been associated with CIPF such as living in an old house, absence of a ventilation system and frequent grooming in dedicated facilities (Roels *et al.*, 2018).

Certain infectious causes described in lung fibrotic diseases in other species have also been investigated in CIPF-affected WHWTs. In men, horses, and rodents, an association between pulmonary fibrotic pathologies and gamma herpesvirus infection has been identified (Williams, 2014). However, gamma herpesviruses infection in CIPF WHWTs is unlikely as lung and blood polymerase chain reaction (PCR) failed to identify viral desoxyribonucleic acid (DNA) in diseased dogs (Roels *et al.*, 2016). A recent study also screened for fungal DNA in the lungs of CIPF and healthy WHWTs, using a pan-fungal PCR test targeting the internal transcribed spacer region conserved in the fungal reign (Roels *et al.*, 2017b). In the same study, serum samples were also tested for precipitins from common environmental fungi using electrosyneresis. Results suggest that fungal infection is not associated with CIPF while a lung sensitization to fungal allergens might be involved in the pathogenesis of the disease as an increased prevalence of environmental fungal exposure in CIPF dogs was found compared with controls (Roels *et al.*, 2017b). Infection by bacteria has been associated with an increased risk of IPF development in human (Molyneaux and Maher, 2013; Williams, 2014; Fastrès *et al.*, 2017a; Olson *et al.*, 2018; Sgalla *et al.*, 2018). Indeed, it is suspected that the presence of certain bacteria by causing epithelial alveolar injury on their own or through inflammatory and pro-fibrotic cascades activation could be associated with disease development and may also drive disease

progression or acute exacerbation (AE) (Molyneaux and Maher, 2013; Fastrès *et al.*, 2017a; Olson *et al.*, 2018; Sgalla *et al.*, 2018). Recently, the development of modern microbiological techniques has allowed the study of the LM as developed below. The exact role of the LM as risk factor or in the pathophysiology of IPF remains unclear. However, its involvement in the disease is supported by the findings that immunosuppressive therapies are associated with an increased risk of death and hospitalization and antibiotics administration decreases mortality rate, increases QOL and reduces respiratory infections (Fastrès *et al.*, 2017a). The role of lung bacteria as a risk factor or in the development and progression of CIPF in WHWTs has not yet been assessed and represents a promising field of investigation.

Microaspirations secondary to gastroesophageal reflux (GER) are also suggested to be associated with CIPF and could be one of the factors which could predispose WHWTs to the disease. Indeed, increased total bile acid bronchoalveolar lavage fluid (BALF) concentrations were found in CIPF and healthy WHWTs compared to healthy dogs of other breeds (Määttä *et al.*, 2018). In human, GER and secondary microaspirations have been reported in 0 to 94% of IPF patients (Raghu *et al.*, 2015a). Microaspirations are suspected to induce repetitive alveolar damages in susceptible patients at the origin of an aberrant wound healing leading to lung fibrosis (Torrisi *et al.*, 2018; Bédard Méthot, Leblanc and Lacasse, 2019; Alfaro and Cordeiro, 2020). However, they can also appear secondary to the reduce lung compliance induced by IPF leading to an increase thoracic pressure and to further GER (Alfaro and Cordeiro, 2020).

1.4. Pathogenesis

As in human IPF, CIPF pathophysiology remains elusive and a lot of mechanisms are still to be discovered with the willing to identify new therapeutic targets.

In IPF, it is now widely assumed that repetitive alveolar epithelial injuries in susceptible people (aged people with specific genetic susceptibility and environmental exposures) act as the first driver of an abnormal wound healing process leading ultimately to the development and the sustainment of lung fibrosis (Figure 2) (Richeldi, Collard and Jones, 2017; Sgalla *et al.*, 2018; Selman and Pardo, 2020). The presence of fibroblastic foci typically located next to hyperplastic or apoptotic alveolar epithelial cells supports that hypothesis (Richeldi, Collard and Jones, 2017). Secondary to epithelial damages, lung epithelial cells develop aberrant regenerative behaviour and produce and release high amount of inflammatory and fibrogenic cytokines and growth factors such as TNF-α (tumour necrosis factor alpha), transforming growth factor-β1 (TGF-β1), platelet derived growth factor (PDGF), fibroblast growth factor (FGF), vascular endothelial growth factor (VEGF) and CCL2. Those molecules create and maintain an environment supportive of exaggerated fibroblasts migration, proliferation and differentiation into myofibroblasts which contribute to excessive extracellular matrix

(ECM) and collagen deposition and destroy normal lung architecture in particular via the formation of fibroblastic foci (O'Dwyer, Ashley and Moore, 2016; Richeldi, Collard and Jones, 2017; Sgalla *et al.*, 2018; Glass *et al.*, 2020; Selman and Pardo, 2020). Epithelial damages also activate the coagulation cascade which reduces the degradation of ECM, also resulting in a profibrotic effect, and inducing differentiation of fibroblasts into myofibroblasts (Sgalla *et al.*, 2018). Finally, the inflammation may also play an important role in IPF. Inflammatory cells produce cytokines that can stimulate an inflammatory response, but also induce alveolar damages and participate to the transition to a reparative environment (Sgalla *et al.*, 2018).

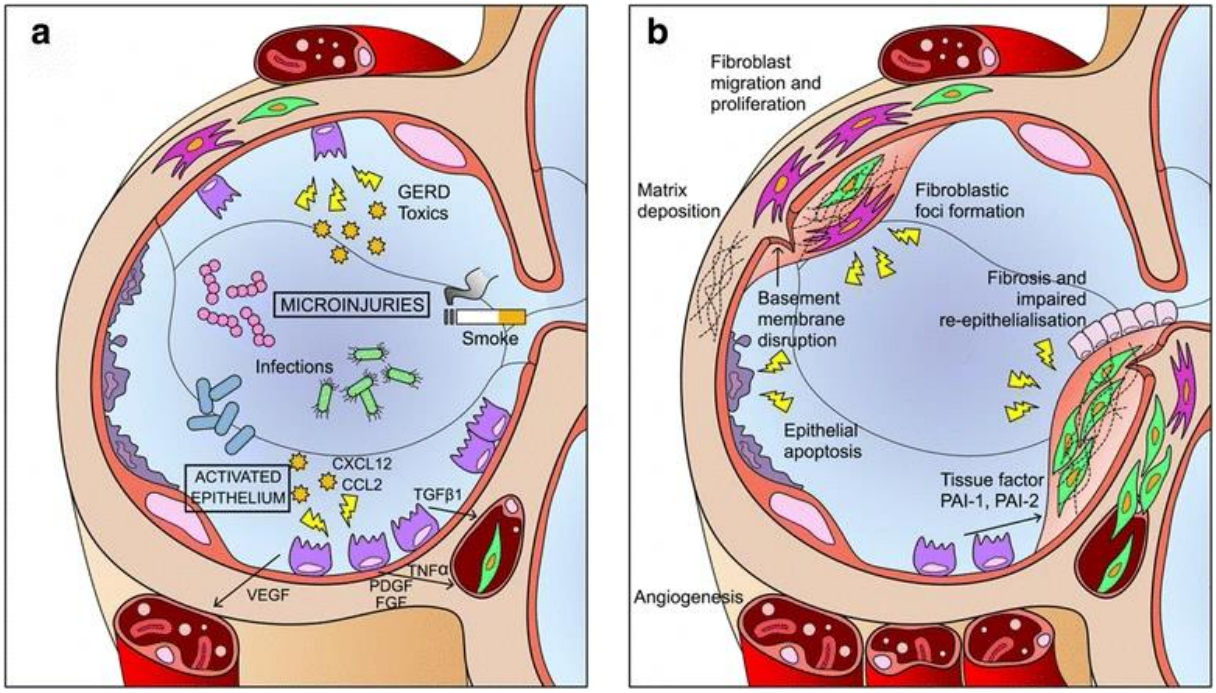

Figure 2. *Schematic view of IPF pathogenesis. Repeated injuries over time lead to maladaptive repair process, characterized by type 2 pneumocytes apoptosis, proliferation and epithelium-mesenchymal cross-talk* ***(a)*** *and following fibroblasts, myofibroblasts proliferation and accumulation of extracellular matrix* ***(b)****.CCL2, chemokine C-C motif ligand 2; CXCL12, C-X-C motif chemokine ligand 12; FGF, fibroblast growth factor; PAI-1, plasminogen activator inhibitor 1; PAI-2, plasminogen activator inhibitor 2; PDGF, platelet-derived growth factor; TGF-β1, Transforming growth factor-β1; TNF-α, tumour necrosis factor-alpha; VEGF, vascular endothelial growth factor (Sgalla et al., 2018).*

Among all pro-fibrotic molecules involved in IPF, it is now well recognized that TGF-β1 is a key-molecule conducting to the disease (Chanda *et al.*, 2019). Its main roles in IPF development include the promotion of epithelial cell apoptosis, migration and EMT, the production of other growth factors and profibrotic and proangiogenic mediators, the recruitment of fibrocytes and the activation, proliferation and differentiation of fibroblasts into myofibroblasts (Grimminger, Günther and Vancheri, 2015; Sgalla *et al.*, 2018). The role of TGF-β1 as a key mediator of fibrosis has also been

investigated in CIPF in two studies (Krafft *et al.*, 2014; Lilja-Maula *et al.*, 2014). The alteration of TGF-β1 signalling pathways found in CIPF dogs are resumed in Figure 3. The first study investigated by immunohistochemistry TGF-β1 signalling activity by targeting phosphorylated signalling protein Smad2 (P-Smad2), and regulation by targeting ECM regulatory proteins including latent TGF-β1 binding proteins (LTBPs) and fibrillin-2 (Lilja-Maula *et al.*, 2014). An increased P-Smad2 immunoreactivity predominantly localized in the altered alveolar epithelium was found in WHWTs affected with CIPF compared to healthy WHWTs. LTBP1 immunoreactivity was also increased in diseased compared to healthy dogs in peribronchial, perivascular, as well as altered alveolar epithelium area. No significant difference in fibrillin-2 immunoreactivity was reported between WHWTs affected with CIPF and healthy WHWTs (Lilja-Maula *et al.*, 2014). In addition to the assessment of some TGF-β1 signalling (P-Smad2/3) and regulatory proteins (LTBP-1, -2 and -4 and Smad7), the second study also investigated in diseased compared with healthy dogs serum concentration of TGF-β1, and lung expression and localization of TGF-β1, TGF-β receptor I (TBRI), and TGF-β1 activation proteins including the integrins αvβ6 (ITGB6) and αvβ8 (ITGB8) and the thrombospondin-1 (THBS1) (Krafft *et al.*, 2014). Authors found that TGF-β1 circulated in higher concentration in predisposed breeds. TGF-β1 was not overexpressed in CIPF compared to healthy dogs, while an increased TGF-β1 protein immunoreactivity was found in CIPF lungs with intense interstitial labelling. TBRI and P-Smad2/3 immunoreactivity was more observed in CIPF dogs in alveolar epithelial cells and particularly hyperplastic type II pneumocytes (PCIIs). The expression of LTBP4 as well as ITGB8 was decreased in CIPF compared to healthy dogs, while THBS1 expression was increased. Finally, the expression of the inhibitory Smad7 protein did not differ between healthy and diseased dogs (Krafft *et al.*, 2014). All that results suggested that altered epithelial cells may have a central role in the pathophysiology of CIPF (Krafft *et al.*, 2014; Lilja-Maula *et al.*, 2014). In addition, modifications of activation, regulation and storage pathways of TGF-β1 might probably be involved in the pathophysiological mechanisms leading to CIPF (Krafft *et al.*, 2014).

The involvement of other pro-fibrotic molecules like activins A and B have also been studied in CIPF dogs (Lilja-Maula *et al.*, 2015). Activins are cytokines belonging to the TGF-β superfamily that can bind TBR and drive Smad phosphorylation cascade (Derynck and Budi, 2019). Activin B was detected in BALF of WHWT affected with CIPF by western blot analysis, especially in WHWTs with AE of the disease. The molecule was also strongly expressed in altered alveolar epithelium in the lungs of WHWTs with CIPF compared to healthy WHWTs. Those data suggest that Activin B could to play a role in fibrosis and might act as a marker of alveolar epithelial damage (Lilja-Maula *et al.*, 2015).

In human, altered haemostatic, fibrinolytic and inflammatory profiles have been associated with the exuberant wound process (Sgalla *et al.*, 2018). However, no clear evidence of an altered

systemic haemostatic, fibrinolytic or inflammatory state was found in WHWTs affected with CIPF compared with healthy dogs. Nevertheless, higher platelet counts and fibrinogen concentrations were found in WHWTs compared with other breeds which may be a predisposing factor for CIPF or simply reflects biological variation in the breed (Roels *et al.*, 2019).

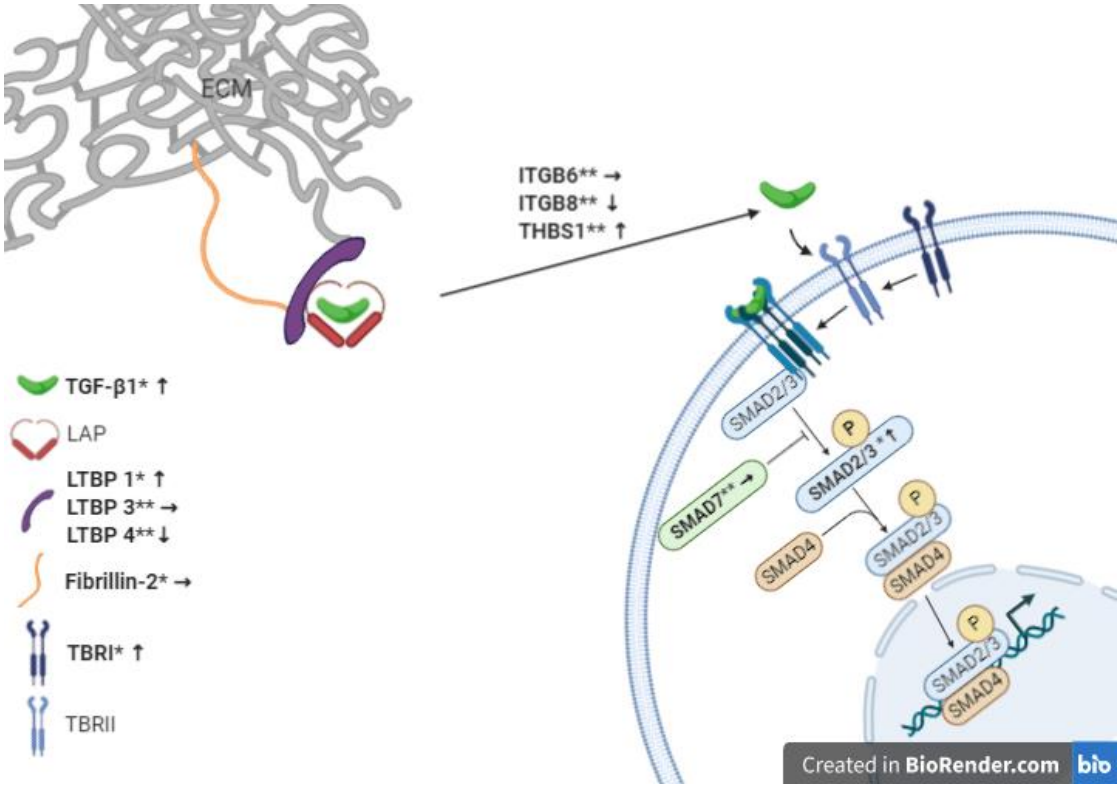

Figure 3. *Transforming growth factor-β1 (TGF-β1) pathways investigated in canine idiopathic pulmonary fibrosis (Krafft et al., 2014; L. Lilja-Maula et al., 2014). TGF-β1 is stored linked to the latency-associated peptide (LAP) as a latent form and is bound to either component of the extracellular matrix (ECM) or fibrillin-2 by latent TGF-β1 binding proteins (LTBPs). After activation of TGF-β1 notably mediated by integrins such as integrins αvβ6 (ITGB6) and αvβ8 (ITGB8) or thrombospondin-1 (THBS1), TGF-β1 binds its receptor the TGF-β receptor II (TBRII). TGF-β1 binding promotes the formation and stabilization of receptor complexes formed by two TGF-β receptors I (TBRIs) and two TBRIIs. Upon receptors activation, effectors Smads are phosphorylated and translocate into the nucleus to repress or activate the transcription of TGF-β1 dependent molecules. The phosphorylation of effector Smads is inhibited by Smad7 (Derynck and Budi, 2019). *, immunohistochemistry findings; **, quantitative reverse transcription polymerase chain reaction findings; ↑, significantly increased compared with healthy dogs; ↓, significantly decreased compared with healthy dogs; →, no significant difference compared with healthy dogs.*

Recently, lung bacterial communities and their interactions with immune cells were suspected to be involved in IPF pathogenesis. Indeed, genetic mutations in genes involved in immune response found in IPF leads to reduced bacterial clearance and altered immune response (Glass *et al.*, 2020). Presence of specific bacteria and increase bacterial burden was associated with worse IPF outcome

and disease progression, supporting the role for bacteria in IPF pathogenesis (Fastrès *et al.*, 2017a; Glass *et al.*, 2020). By themselves, bacteria can cause epithelial damages but, they can also activate immune cells which in turn can induce epithelial injuries by producing pro-inflammatory molecules. Moreover, during the course of the disease, the presence of specific bacteria can contribute to maintain alveolar inflammation and to induce AE of the disease (Fastrès *et al.*, 2017a; Molyneaux *et al.*, 2017a; Spagnolo *et al.*, 2019). Primarily or secondary to the alteration of the LM, an accumulation of active pro-fibrotic macrophages was confirmed in the lungs of IPF patients (O'Dwyer, Ashley and Moore, 2016; Heukels *et al.*, 2019). Products secreted by those macrophages notably include TGF-β, FGF, PDGF, insulin-like growth factor 1 (IGF1) and VEGF (Desai *et al.*, 2018; Heukels *et al.*, 2019). CCL18 (C-C motif chemokine ligand 18) most probably also produced by those pro-fibrotic macrophages and increased in BALF of IPF patients activates fibroblasts producing collagen and recruits T-cells that in turn can stimulate macrophages in a positive feed-back loop to produce CCL18 (Heukels *et al.*, 2019). Pro-inflammatory macrophages producing cytokines such as TNFα, IL-1 (interleukin 1), and IL-6 (interleukin 6) have also been described in IPF, and are suspected to cause alveolar epithelium injury and to maintain tissue inflammation (Heukels *et al.*, 2019). Monocytes attracted in the lung via the CCR2-CCL2 axis also play a role in IPF by producing pro-inflammatory cytokines, including IFN-α (interferon alpha), CCL3 (C-C motif chemokine ligand 3) and CCL4 (C-C motif chemokine ligand 4), which promote myofibroblasts differentiation. In the lung, monocytes progressively differentiate into macrophages or fibrocytes able to promote fibrosis (O'Dwyer, Ashley and Moore, 2016; Heukels *et al.*, 2019). Such changes in lung microbial communities and macrophages polarization have not yet been investigated in WHWTs affected with CIPF.

1.5. Diagnostic work up

The diagnosis of CIPF is based on clinical findings, diagnostic imaging, and the exclusion of other cardiac and respiratory diseases able to mimic clinical signs of CIPF (Clercx, Fastrès and Roels, 2018; Laurila and Rajamäki, 2020). A strong suspicion of CIPF can be achieved after a complete work-up including history assessment, clinical examination, complete blood work, 6-minute walking test (6MWT), echocardiography, thoracic imaging, bronchoscopy and BALF analysis, although a definite diagnosis can only be obtained by histopathological examination (Clercx, Fastrès and Roels, 2018; Laurila and Rajamäki, 2020).

In IPF, clinical practice guidelines to diagnose the disease has been published in order to guide clinicians and consist in (1) the exclusion of other known causes of ILD and either (2) the presence of usual interstitial pneumonia (UIP) pattern on thoracic high resolution computed tomography (HRCT) or (3) the specific combination of thoracic HRCT and histopathology patterns in patients with lung biopsies (Raghu *et al.*, 2011; Raghu *et al.*, 2018). However, the diagnostic of IPF as in CIPF remains quite challenging. The specific clinical challenges are to differentiate IPF from connective lung

diseases (CLDs) which develop secondary to immune disorders, chronic hypersensitivity pneumonitis (HP) and familial pulmonary fibrosis (Lynch *et al.*, 2018).

1.5.1. 6-minute walking test

The 6MWT consists in the assessment of the distance covered by the dog over 6 minutes of time (Clercx, Fastrès and Roels, 2018; Laurila and Rajamäki, 2020). It is a well-tolerated and non-invasive technique used for evaluation of exercise intolerance. The 6MWT is, with the arterial blood gas assessment, one of the 2 cardiopulmonary function tests performed in WHWTs affected with CIPF (Clercx, Fastrès and Roels, 2018; Laurila and Rajamäki, 2020). Indeed, the 6-minute walked distance (6MWD) was shown to be moderately correlated (Kendall′s tau-b = 0.69) with the arterial partial pressure in oxygen (PaO_2), although being only statistically significant at 10% (Lilja-Maula *et al.*, 2014). In numerous studies, the test was performed and a significantly reduced distance was reported in WHWTs affected with CIPF compared with healthy WHWTs (Clercx, Fastrès and Roels, 2018; Laurila and Rajamäki, 2020). Moreover, repetitive assessment of the 6MWD can be used to monitor changes in exercise intolerance in WHWTs with CIPF and, therefore, the progression of the disease (Lilja-Maula *et al.*, 2014).

As in dogs, an oxygen desaturation during 6MWT and a reduction in exercise performance is classically observed in IPF patients (Hochhegger *et al.*, 2019; Kishaba, 2019b). Moreover, the 6MWT alone or in combination with other parameters can be used in human IPF to predict the severity and the prognosis of the disease (Hochhegger *et al.*, 2019; Kishaba, 2019b; Somogyi *et al.*, 2019).

1.5.2. Arterial blood gas analysis

Arterial blood gas analysis is another classical cardiopulmonary function test used in CIPF WHWTs (Clercx, Fastrès and Roels, 2018; Laurila and Rajamäki, 2020). It is considered as the gold standard test for evaluating oxygenation and ventilation (Balakrishnan and Tong, 2020). In CIPF and IPF, it provides information about disease severity and disease progression in case of repeated measures (Lilja-Maula *et al.*, 2014; Hochhegger *et al.*, 2019; Kishaba, 2019b; Somogyi *et al.*, 2019). Moderate (80-60 mmHg) to severe (< 60mmHg) hypoxemia and increased alveolar-arterial oxygen gradient have been reported in more than 90% of the dogs suffering from CIPF (Clercx, Fastrès and Roels, 2018; Laurila and Rajamäki, 2020). Hypoxemia in CIPF probably does not only result from alveolo-capillary diffusion impairment due to thickened alveolo-capillary membrane. Indeed, in human IPF, the main reason for hypoxemia was ventilation–perfusion mismatch (Plantier *et al.*, 2018). Change in arterial partial pressure of carbon dioxide is not reported in CIPF cases (Heikkilä *et al.*, 2011; Roels *et al.*, 2017a; Holopainen *et al.*, 2019).

1.5.3. Blood work

Haematology and biochemistry analyses are unremarkable in WHWTs affected with CIPF and are commonly performed only to exclude other diseases (Clercx, Fastrès and Roels, 2018; Laurila and Rajamäki, 2020). As in human IPF, polycythaemia is not associated with the disease in dogs (Crystal *et al.*, 1976; Laurila and Rajamäki, 2020). Only serum concentration of alkaline phosphatase (ALP) and platelet count are frequently higher than reference ranges which seems to be breed-related as those values did not differ between healthy and diseased WHWTs (Heikkila-Laurila and Rajamaki, 2014; Roels *et al.*, 2015a; Thierry *et al.*, 2017; Roels *et al.*, 2019). The increased ALP activity in WHWTs could possibly be attributed to benign subclinical hyperadrenocorticism as suspected in Scottish terriers (Zimmerman *et al.*, 2010).

In IPF, serological testing for C-reactive protein, erythrocyte sedimentation rate, rheumatoid factor, anti-cyclic citrullinated peptide, myositis panel, and anti-nuclear antibody can be helpful to differentiate IPF from CLD, although slightly positive results for rheumatoid factor, anti-nuclear antibody and cyclic citrullinated peptide have been demonstrated in 29% of IPF patients without clinical significance (Hochhegger *et al.*, 2019; Wakwaya and Brown, 2019). There is no evidence for or against the dosage of serum precipitins for the screening of HP (Wakwaya and Brown, 2019). Finally, the screening for other forms of ILDs using diagnostic blood biomarkers is not recommended (Raghu *et al.*, 2018; Wakwaya and Brown, 2019).

1.5.4. Bronchoscopy and bronchoalveolar lavage fluid analysis

Bronchoscopic results described in WHWTs affected with CIPF are non specific. Because bronchoscopy requires general anaesthesia, which could be tricky in some severe cases, the performance of the test should be discussed in term of benefits versus risks. Bronchoscopy should be performed, especially when there is discrepancy between clinical data and thoracic HRCT findings or suspicion of infection or other disease process (Clercx, Fastrès and Roels, 2018; Laurila and Rajamäki, 2020).

Findings reported in diseased dogs include tracheal collapse, bronchial mucosal irregularity, mild to moderate amount of bronchial mucus, dynamic airway collapse, bronchiectasis and bronchomalacia. Bronchial mucosal irregularity and tracheal collapse are also described in healthy WHWTs and could be aged-related changes (Heikkila-Laurila and Rajamaki, 2014).

Analyses of BALF commonly indicate an increase of the total cell count (TCC) related to an increased in macrophages, neutrophils and mast cells. BALF bacterial culture is rarely positive (Heikkila-Laurila and Rajamaki, 2014).

In IPF, BALF analysis can be used to exclude alternative diagnoses (Raghu *et al.*, 2018; Wakwaya and Brown, 2019). However, giving the wide range of cell proportions and the low number of studies and patients included in the studies comparing BALF analyses in patient with IPF and other fibrosing ILDs, the usefulness of BALF to discriminate ILDs is unclear. In addition, the BALF procedure remains invasive for the patient, has some risk of complications and needs to be carefully considered in term of benefits (Raghu *et al.*, 2018).

1.5.5. Diagnostic imaging

1.5.5.1. Echocardiography

Echocardiography is essential to exclude primarily cardiac disease which can mimic clinical signs of CIPF, but also to look after secondary PH which can affect up to 60% of CIPF WHWTs at diagnosis (Clercx, Fastrès and Roels, 2018; Laurila and Rajamäki, 2020; Roels *et al.*, 2021). The prevalence of PH in IPF patients is also high ranging from 31 to 46% and increases with the disease severity (Raghu *et al.*, 2015a; Torrisi *et al.*, 2018; Somogyi *et al.*, 2019; Alfaro and Cordeiro, 2020). In IPF, PH is associated with a decrease in survival, an increase risk of death and a reduce QOL (Raghu *et al.*, 2015a; Torrisi *et al.*, 2018). In CIPF, although the presence of moderate to severe PH at diagnosis doesn't seem to be associated with a shorter survival, detecting PH is important for making therapeutic decisions as treatment can improve clinical signs and QOL of the dogs (Clercx, Fastrès and Roels, 2018; Johnson and Stern, 2020; Laurila and Rajamäki, 2020; Roels *et al.*, 2021).

At echocardiography, PH is classically assessed in dogs by measuring the peak velocity of the tricuspid regurgitation jet. Other echocardiographic measures can aid for PH assessment including assessment of the size of the right ventricle and the right atrium, the systolic flattening of the interventricular septum, the pulmonary artery diameter to aortic diameter ratio, the pulmonary artery flow profile, the caudal vena cava size, the acceleration time to ejection time ratio of the pulmonary artery flow, the right pulmonary artery distensibility index and the right pulmonary vein to pulmonary artery ratio (Schober and Baade, 2006; Visser *et al.*, 2016; Reinero *et al.*, 2020; Roels *et al.*, 2021).

1.5.5.2. Thoracic radiography

As in IPF, thoracic radiography is neither specific nor sensitive for CIPF diagnosis (Heikkila-Laurila and Rajamaki, 2014; Wallis and Spinks, 2015). It is more useful to exclude other pulmonary diseases such as neoplasia for example (Heikkila-Laurila and Rajamaki, 2014). Moreover, thoracic radiography findings cannot be used to assess disease progression in CIPF dogs (Laurila and Rajamäki, 2020).

The most common radiographic finding identified in WHWTs affected with CIPF is a moderate to severe generalized bronchointerstitial pattern which can also be identified in control dogs, although in less severe proportion (Johnson *et al.*, 2005; Corcoran *et al.*, 2011; Heikkilä *et al.*, 2011; Heikkila-Laurila and Rajamaki, 2014; Thierry *et al.*, 2017). Right-side cardiomegaly and pulmonary arterial enlargement can also be visualized in WHWTs affected with CIPF, in case of secondary PH (Johnson *et al.*, 2005; Heikkila-Laurila and Rajamaki, 2014). Bronchial pattern and patchy alveolar opacities with indistinct margins are also reported in addition to interstitial infiltrates (Johnson *et al.*, 2005; Heikkila-Laurila and Rajamaki, 2014). Representative examples of radiographic changes in CIPF dogs are shown in Figure 4.

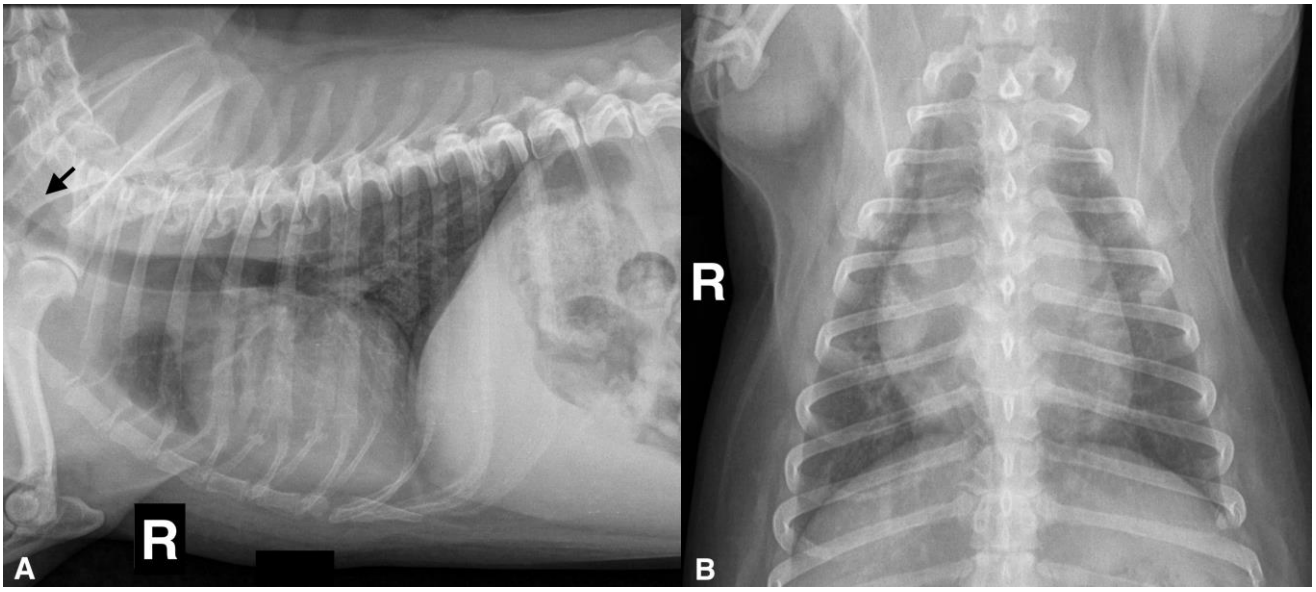

Figure 4. *Representative thoracic radiographies obtained from a 13-year-old West Highland white terrier affected by canine idiopathic pulmonary fibrosis.* ***(A)*** *right lateral view and* ***(B)*** *ventro-dorsal view. A diffuse, severe unstructured interstitial pattern, a moderate bronchial to peribronchial pattern and a small thoracic volume are observed on both views which are consistent with pulmonary fibrosis considering the breed of the patient. The right heart and the liver are enlarged. A large soft-tissue band (black arrow) is superimposed to the dorsal aspect of the cervical trachea and is compatible with tracheal flaccidity.*

1.5.5.3. <u>Thoracic high resolution computed tomography</u>

Thoracic HRCT is considered as essential for the diagnosis of IPF in men and CIPF in dogs, as it allows the investigation of the lung in a better spatial resolution than radiography (Heikkilä *et al.*, 2011; Heikkila-Laurila and Rajamaki, 2014; Lynch *et al.*, 2018). Moreover, in CIPF, a positive and a negative correlation between the severity of pulmonary HRCT findings and either clinical signs or survival time after diagnosis are reported, respectively. Those findings support the benefit of thoracic

HRCT to provide information about the characterization and the prognosis of the disease (Thierry *et al.*, 2017; Holopainen *et al.*, 2019).

In CIPF dogs, thoracic HRCT findings have been described in several studies (Johnson *et al.*, 2005; Corcoran *et al.*, 2011; Heikkilä *et al.*, 2011; Roels *et al.*, 2017a; Thierry *et al.*, 2017; Holopainen *et al.*, 2019). Moderate to severe ground glass opacity pattern (GGO) defined as hazy increased attenuation with preservation of the bronchial and vascular margins are recorded in all WHWTs affected with CIPF (Johnson *et al.*, 2005; Corcoran *et al.*, 2011; Heikkilä *et al.*, 2011; Roels *et al.*, 2017a; Thierry *et al.*, 2017; Holopainen *et al.*, 2019). The GGO pattern is found in all stages of the disease (mild, moderate and severe) but became more diffuse as the clinical stage of the disease worsened (Johnson *et al.*, 2005; Heikkilä *et al.*, 2011; Thierry *et al.*, 2017). Parenchymal bands and patchwork of regions of differing attenuation called mosaic attenuation pattern (Corcoran *et al.*, 2011; Heikkilä *et al.*, 2011; Thierry *et al.*, 2017; Holopainen *et al.*, 2019), subpleural lines (Corcoran *et al.*, 2011; Heikkilä *et al.*, 2011; Holopainen *et al.*, 2019), subpleural and peribronchovascular interstitial thickening (Corcoran *et al.*, 2011; Heikkilä *et al.*, 2011), consolidations (Heikkilä *et al.*, 2011; Holopainen *et al.*, 2019) and nodules (Roels *et al.*, 2017a; Thierry *et al.*, 2017) are also described and associated with moderate and severe stages of the disease (Johnson *et al.*, 2005; Thierry *et al.*, 2017). Finally, traction bronchiectasis defined as irregular bronchial dilatation with abnormal surrounding parenchyma (Corcoran *et al.*, 2011; Heikkilä *et al.*, 2011; Thierry *et al.*, 2017; Holopainen *et al.*, 2019) and honeycombing (subpleural cystic airspaces) (Corcoran *et al.*, 2011; Heikkilä *et al.*, 2011; Thierry *et al.*, 2017) are only seen in severe cases and are associated with severe stages of the disease (Johnson *et al.*, 2005; Thierry *et al.*, 2017).

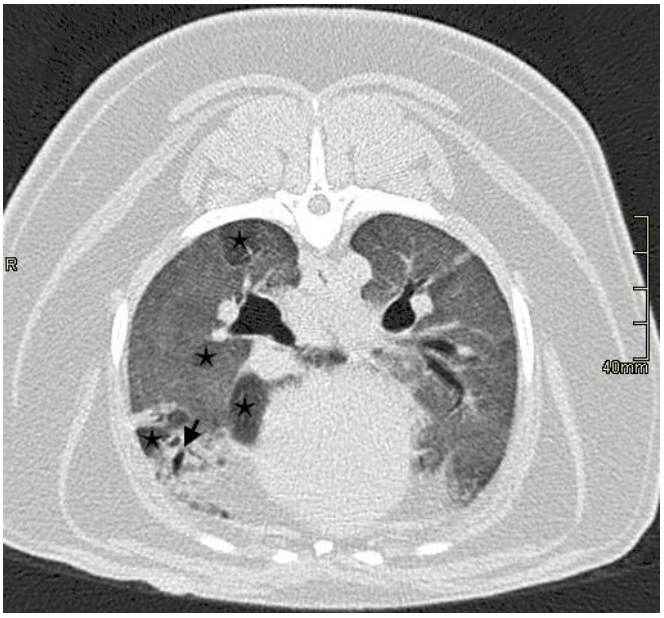

Figure 5. *Representative transverse image of thoracic high resolution computed tomography (HRCT) in a lung window in inspiratory phase, obtained from a 7-year-old West Highland white terrier affected by canine idiopathic pulmonary fibrosis. A diffuse ground glass opacity is observed. Multiple well-defined hypo-attenuating areas (black stars) compared to the surrounding parenchyma are present, mostly in the right lung which defines a mosaic attenuation pattern. Traction bronchiectasis is visible in the ventral aspect of the right caudal lung lobe (black arrow). The surrounding parenchyma is consolidated.*

In human, different patterns have been described with the aim to help to better diagnose the disease with the UIP pattern considered as the hallmark imaging pattern of IPF (Raghu et al., 2018). UIP pattern is characterized by honeycombing with or without traction bronchiectasis and traction bronchiolectasis (Raghu et al., 2018). The presence of a GGO pattern is uncommon in the UIP pattern and is usually accompanied by a superimposed reticular pattern (Raghu et al., 2018). The classical localization of the UIP pattern in IPF is subpleural with basal predominance (Raghu et al., 2018). While the honeycombing and the traction bronchiectasis found in CIPF dogs are in favour of an UIP pattern, the extensive GGO pattern is more suggestive of another ILDs (Lynch *et al.*, 2018; Raghu *et al.*, 2018). However, even in men, the diagnosis of IPF should not be excluded if the thoracic HRCT finding is not in favour of an UIP pattern (Lynch *et al.*, 2018; Raghu *et al.*, 2018).

The only problem regarding the use of classical thoracic HRCT in CIPF WHWTs is that it requires general anaesthesia, which might not be possible in severely affected dogs as an increased aesthetic risk is present especially in WHWTs with substantial hypoxemia (Heikkila-Laurila and Rajamaki, 2014). Alternatives to thoracic HRCT on dogs under general anaesthesia have been assessed in two recent studies in which thoracic HRCT has been performed on awaken dogs with or without sedation (Roels *et al.*, 2017a; Holopainen *et al.*, 2019). However, some lesions such as the GGO pattern can vary in terms of extent and severity in such conditions which could modify the identification and grading of CIPF (Roels *et al.*, 2017a). Moreover, inability to obtain images during specific respiration phases may cause secondary artefactual changes such as consolidation during expiration and motion artifacts which could also potentially impact the assessment of the parenchymal lesions (Holopainen *et al.*, 2019). These differences should be taken into consideration when general anaesthesia is contraindicated (Roels *et al.*, 2017a; Holopainen *et al.*, 2019).

1.5.6. Histopathological features

Histopathological examination of lung tissue is generally performed after the animal's death due to the invasiveness of the procedure. Therefore, the diagnosis is often confirmed at necropsy (Clercx, Fastrès and Roels, 2018). In human, the performance of lung biopsies should be considered when HRCT finding is not definitive for UIP pattern or when the clinical features suggest an alternative diagnosis than IPF (Raghu *et al.*, 2018; Hochhegger *et al.*, 2019).

Lesions reported in WHWTs shares features of the 2 most common ILDs in human, UIP pattern, classically found in IPF, and nonspecific interstitial pneumonia (NSIP) pattern (Table 1) (Syrjä *et al.*, 2013).

Table 1. *Comparison between the main histological criteria required for the diagnoses UIP or NSIP pattern in human and the findings in CIPF in WHWTs.*

Criteria	UIP	CIPF in WHWT	NSIP (fibrosing)
Pattern	Patchy, subpleural or paraseptal	Diffuse with subpleural/peribronchiolar accentuation	Relatively diffuse
Interstitial fibrosis	Marked, distorting, replacing alveolar tissue	Mild to marked, not obliterating alveolar architecture	Variable degree
Honeycombing	Yes	Yes	Not characteristic
Fibroblastic foci	Yes	No	Absent or inconspicuous
Interstitial inflammation	Minimal, mild	Mild to moderate	Mild to moderate
SM hyperplasia	Yes	Yes	Not characteristic
PCII	Hyperplasia	Hyperplasia, atypia	Hyperplasia in areas of inflammation
Bronchiolar epithelium	Bronchial metaplasia of alveolar epithelium	Bronchial metaplasia of alveolar epithelium	Not recorded

UIP, usual interstitial pneumonia; NSIP, non-usual interstitial pneumonia; CIPF, canine idiopathic pulmonary fibrosis; WHWT, West Highland white terrier; SM, smooth muscle; PCII, type II pneumocyte. Table extracted from Syrjä et al., 2013.

The lung of CIPF-affected dogs is characterized by a mild to moderate, diffuse, mature fibrosis of the interstitium which resembles to NSIP pattern in human (Figure 6). In addition, multifocal areas of more severe and cellular fibrosis are found in most dogs which is more characteristic of human UIP pattern (Figure 6) (Syrjä *et al.*, 2013). In those areas of immature fibrosis, honeycombing, profound alveolar epithelial changes (*i.e.*, PCIIs hyperplasia, multinucleated PCIIs), diffuse presence of myofibroblasts in alveolar interstitium, bronchial metaplasia of alveolar epithelium (*i.e.*, epithelial pseudostratification and squamous metaplasia), and alveolar luminal changes (*i.e.*, distortion of alveolar architecture, acute alveolar damage with hyaline membrane formation and emphysematous changes) can also be present (Syrjä *et al.*, 2013; Heikkila-Laurila and Rajamaki, 2014). In dogs, fibroblastic foci, found specifically in the UIP pattern, are not described (Syrjä *et al.*, 2013). As in human IPF, in most CIPF cases, there is no evidence of inflammatory change in either the parenchyma or the airways (Heikkilä *et al.*, 2011).

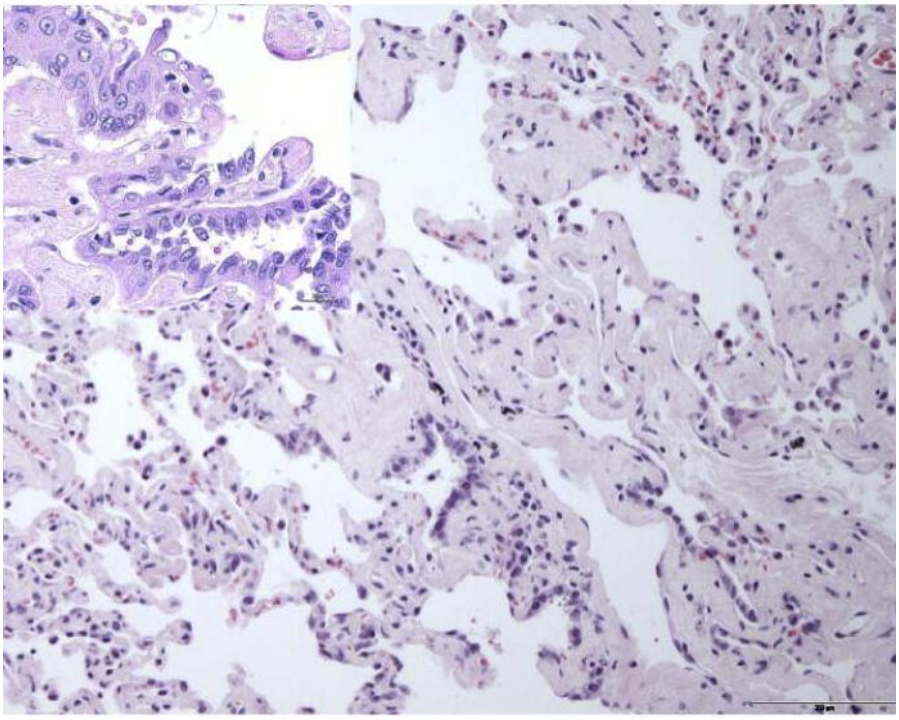

Figure 6. *Example of histopathological features found in West Highland white terrier affected with canine idiopathic pulmonary fibrosis. Transition from mild diffuse fibrosis on the left, to a focus of accentuated disease, with severe interstitial fibrosis on the right. Haematoxylin and eosin. Bar, 200 μm. Inset: Type 2 pneumocytes hyperplasia and squamous metaplasia of the alveolar epithelium. Figure extracted from Syrjä et al., 2013.*

1.5.7. Biomarkers

Several studies have been conducted to find biomarkers. Specifically, those studies aimed to identify biomarkers able to differentiate CIPF from healthy conditions and from other chronic lower respiratory diseases (*i.e.*, diagnostic biomarkers) and to predict disease severity and outcome (*i.e.*, prognostic biomarkers). Two different methods were used to search for biomarkers in CIPF including screening techniques (*i.e.* pulmonary gene expression by microarray analysis (Krafft *et al.*, 2013) and analysis of the BALF proteome (Lilja-Maula *et al.*, 2013)) and targeting techniques (*i.e.* BALF and serum identification of known pro-fibrotic molecules).

Similar research on biomarkers has been performed in human IPF to predict mortality and disease evolution with the objective to improve patient counselling, and treatment related decisions including reference for lung transplantation evaluation (Wakwaya and Brown, 2019). However, despite investigations, reliable and routinely available predictive and therapeutic biomarkers are still missing and the search must be continued (Somogyi *et al.*, 2019).

1.5.7.1. C-C motif chemokine ligand 2

CCL2 also named monocyte chemoattractant protein 1 is mainly expressed in epithelial cells and macrophages of lung tissue in patients with ILDs (Xue *et al.*, 2019). In IPF mouse model and in IPF, CCL2, acting preferentially through its receptor the C-C motif chemokine receptor type 2 (CCR2), has been shown to contribute to fibrosis through a wide variety of mechanisms involving inflammation, angiogenesis and myofibroblasts accumulation (Moore *et al.*, 2005; Raghu *et al.*, 2015b; Osafo-Addo and Herzog, 2017).

In CIPF, an increased expression of *CCL2* gene, confirmed by quantitative reverse transcriptase PCR (qRT-PCR), was shown in lung samples from WHWTs affected with CIPF compared with control dogs of various breeds (Krafft et al., 2013). Serum and BALF CCL2 concentrations measured by enzyme-linked immunoassay (ELISA) tests were elevated in dogs affected with CIPF, compared with healthy controls of the same breed suggesting that CCL2 could be useful as diagnostic biomarker (Krafft *et al.*, 2013; Roels *et al.*, 2015b). In addition, high serum CCL2 concentrations at the time of diagnosis were shown to be negatively associated with survival time (Roels *et al.*, 2015a; Roels *et al.*, 2015b). Finally, serum CCL2 concentrations were also higher in WHWTs compared with healthy dogs from other breeds which might be related to the breed predisposition of the WHWT for CIPF (Roels *et al.*, 2015a).

1.5.7.2. C-X-C motif chemokine ligand 8

The C-X-C motif chemokine ligand 8 (CXCL8) is a neutrophils chemo-attractant cytokine secreted by a wide range of cell types including blood monocytes, alveolar macrophages (AMs), fibroblasts, endothelial cells, and epithelial cells. In addition to serve as a chemoattractant molecule, CXCL8 promotes cellular proliferation, motility and invasion, as well as EMT and angiogenesis (Ha, Debnath and Neamati, 2017). Serum CXCL8 levels have been associated with disease progression and survival in IPF patients (Guiot *et al.*, 2017).

Serum and BALF CXCL8 concentrations were measured in WHWTs either healthy or affected with CIPF and in healthy dogs from other breeds by ELISA. BALF CXCL8 concentrations were higher in WHWTs affected with CIPF compared with healthy WHWTs. However, no difference was identified in serum concentrations between healthy and diseased WHWTs (Roels *et al.*, 2015b). In healthy dogs, serum CXCL8 concentrations were higher in WHWTs compared with other breeds which could be due to the predisposition of the WHWT breed to develop the disease (Roels *et al.*, 2015a).

1.5.7.3. Endothelin-1

The endothelin-1 (ET1), a vasoactive peptide, is suggested to be an important contributor in the pathobiology of fibrosing disorders (Swigris and Brown, 2010). In the lung, ET-1 is secreted by fibroblasts, endothelial cells, AMs, epithelial cells and polymorphonuclear leukocytes and is known to promote fibroblasts activation, proliferation, as well as differentiation into myofibroblasts (Swigris and Brown, 2010). In IPF, an increase in lung tissue and BALF ET-1 levels has been reported. In addition, studies on IPF mouse models showed that the use of ET-1 receptor antagonist could limit bleomycin-induced fibrosis (Swigris and Brown, 2010).

Serum and BALF ET-1 concentrations were assessed by ELISA in dogs either suffering from CIPF, chronic bronchitis (CB), and eosinophilic bronchopneumopathy (EBP), or healthy of either the beagle or the WHWT breed. Higher serum ET-1 concentrations were found in CIPF WHWTs compared with all the other groups. A cut-off serum concentration value of 1.8 pg/mL has been determined for the detection of CIPF with a sensitivity of 100% and a specificity of 81.2%. BALF ET-1 concentrations were under the detection threshold of the ELISA in healthy WHWTs and in dogs with CB, while they were above in all CIPF WHWTs (Krafft *et al.*, 2011).

1.5.7.4. Procollagen type III amino terminal propeptide

Procollagen type III amino terminal propeptide (PIIINP) is used as a marker of connective tissue metabolism. The propeptide release depends on the amount of collagen produced (Low *et al.*, 1992). In IPF, PIIINP level, analysed in order to be able to stage the disease and monitor the course of the patients, was elevated in both serum and BALF and correlated with disease activity and progression (Low *et al.*, 1992).

In CIPF, PIIINP concentrations were analysed in serum and BALF of dogs either affected with CIPF, CB, EBP or healthy, by radioimmunoassay. Serum PIIINP concentrations did not differed between the different groups, whereas BALF PIIINP levels were significantly increased in CIPF and EBP dogs compared with CB and healthy dogs (Heikkilä *et al*., 2013). The higher PIIINP level found in EBP was already reported and is probably due to secondary fibrosis development (Clercx and Peeters, 2007).

1.5.7.5. Transforming growth factor beta

The potential interest of serum TGF-ß1 concentration as biomarker of CIPF has been investigated in WHWTs affected with CIPF, healthy WHWTs and healthy dogs from other breeds. An increase in serum TGF-ß1 concentration was detected both in diseased and healthy WHWTs

suggesting that TGF-ß1 could be one of the factors predisposing WHWTs to CIPF (Krafft *et al.*, 2014).

1.5.7.6. Activins

As already said, activin B was detected in the BALF of WHWTs affected with CIPF mostly if they had concurrent AE or diffuse alveolar damage, while the molecule was not detected in healthy WHWTs. It indicates that activin B could be used as marker of alveolar damage. However, further studies are required to confirm those data as they are based on a relative low number of dogs (Lilja-Maula *et al.*, 2015).

1.5.7.7. Matrix metalloproteinases

Matrix metalloproteinases (MMPs) are essential for ECM degradation, wound healing and angiogenesis but also for immune response regulation. They have pro and anti-fibrotic capacities. In IPF, an imbalance between the pro and anti-fibrotic mediators is reported, driven fibrosis development by inducing the activation of latent TGF-β1, EMT, fibrocytes migration, macrophages polarization and myofibroblasts differentiation (Mahalanobish *et al.*, 2020). MMP-7 is overexpressed in plasma of IPF patients compared with healthy patients and patients with other ILDs (Guiot *et al.*, 2017). In addition, MMP-7 is significantly increased in epithelial cells both at the gene and protein levels and also significantly correlated with disease severity (Guiot *et al.*, 2017; Todd *et al.*, 2020). Increased circulating MMP-2 and -9 have been detected in IPF patients compared to healthy controls (Todd *et al.*, 2020). Moreover, increased total MMP-9 concentrations have been observed in BALF of IPF patients compared with healthy and high BALF total MMP-9 concentrations were found in IPF patients with rapid disease progression (Mckeown *et al.*, 2009).

Serum and BALF activities of both pro-MMP-2, -7 and -9 and active MMP-2, -7 and -9 were assessed by zymography in CIPF WHWTs, healthy WHWTs, healthy dogs from other breeds and dogs with CB and EBP (Määttä *et al.*, 2020). Higher serum pro-MMP-7 activities were found in CIPF WHWTs compared with healthy dogs from other breeds, dogs with CB or dogs with EBP. In CIPF WHWTs with severe hypoxemia ($PaO_2 \leq 60$ mmHg), serum pro-MMP-7 activity was significantly associated with increased risk of death. In BALF, pro-MMP-2 and pro-MMP-9 activities were significantly increased in CIPF WHWTs compared with healthy WHWTs and dogs with CB. Pro-MMP-2 activity was also significantly higher in CIPF WHWTs compared with EBP dogs. Finally, active MMP-9 was only detected in BALF of CIPF and EBP dogs (Määttä *et al.*, 2020).

1.5.7.8. Krebs Von den Lungen-6

The glycoprotein Krebs Von den Lungen-6 (KL-6) is classified as a human transmembrane mucin and is expressed by the PCIIs and the bronchiolar epithelial cells (Hamai *et al.*, 2016; Guiot *et al.*, 2017; Sokai *et al.*, 2017; Wakamatsu *et al.*, 2017). KL-6 is considered as the best and the more reliable serum diagnostic and outcomes predicting biomarker for human ILDs (Ishikawa *et al.*, 2012; Bonella *et al.*, 2019). The increased level of KL-6 in ILDs has been associated with the repairing of PCIIs and the increasing of intracellular permeability. KL-6 promotes the proliferation and the migration of pulmonary fibroblasts which act during the fibrosis process (Hu *et al.*, 2017; Sokai *et al.*, 2017).

Serum KL-6 concentrations were not different between CIPF and healthy WHWTs but higher concentrations were observed in terrier breeds. Whether this may reflect a predisposing factor for CIPF development merits further investigations (Fastrès *et al.*, 2018).

1.5.7.9. Serotonin

The serotonin (5-hydroxytryptamine, 5-HT) is a multifunctional signalling molecule expressed in the lung by platelet-derived 5-HT as well as endothelial cells, mast cells and pulmonary neuroendocrine cells (Löfdahl *et al.*, 2021). In human IPF, an enhanced activation of serotonergic signalling has been reported. Several studies indicated that 5-HT induces TGF-β1. In addition, in *in vivo* IPF models and *in vitro* human cells experiments, 5-HT receptor antagonist treatment was shown to produce significant anti-fibrotic effects (Löfdahl *et al.*, 2021).

5-HT serum concentration was not assessed in CIPF dogs. In healthy WHWTs compared with healthy dogs from other breeds, 5-HT serum and BALF concentrations do not indicate relevant interbreed differences and are not in favour of any influence of basal 5-HT concentrations on CIPF development in WHWT (Roels *et al.*, 2015a).

1.5.7.10. Vascular endothelial growth factor

VEGF is an angiogenic molecule considered as an essential regulator of fibroblasts proliferation, migration and transformation. It also partially acts by increasing expression of MMPs largely involved in IPF pathogenesis as discussed above (Grimminger, Günther and Vancheri, 2015). In IPF, there are several evidences that BALF and serum VEGF levels can predict disease progression and severity (Grimminger, Günther and Vancheri, 2015). In addition, nintedanib, one of the approved treatments for IPF, competitively binds VEGF receptor (Wind *et al.*, 2019).

Despite such interest in IPF studies, VEGF BALF and serum concentrations have been assessed by ELISA in only one study in healthy dogs from different breeds including WHWTs (Roels et al., 2015a). Unfortunately, values obtained were under the detection limit of the kit which prevented the authors to give any conclusive results (Roels et al., 2015a).

1.5.7.11. Serum C-reactive protein

The C-reactive protein (CRP) is a major acute phase protein in human and dogs and is used as biomarkers of inflammation, infection and trauma (Eckersall and Bell, 2010). CRP can be used in IPF to discriminate between healthy and diseased patients and to predict disease progression and mortality (Somogyi *et al.*, 2019).

Serum CRP concentrations were not increased in dogs affected with CIPF and were not significantly different between WHWTs affected with CIPF and control dogs (Viitanen *et al.*, 2014; Roels *et al*., 2019).

1.5.7.12. Others

In their microarray analysis, Krafft and colleagues (2013) also found up-regulation of numerous other genes with a confirmed overexpression by qRT-PCR including C-C motif chemokine ligand 7, C-X-C motif chemokine ligand 14 and fibroblast activation protein α (Krafft *et al.*, 2013). However, the potential interest of those molecules as biomarker was not further investigated.

1.6. Treatment

To date, there is no effective treatments for CIPF (Clercx, Fastrès and Roels, 2018; Laurila and Rajamäki, 2020). In human IPF, two anti-fibrotic drugs, nintedanib and pirfenidone, have been approved for the management of the disease (Sgalla *et al.*, 2018; Maher and Strek, 2019). Both drugs were shown to slow disease progression and impact survival of IPF patients (Glassberg, 2019). In addition, there is growing evidence that the use of either pirfenidone or nintedanib decreases the risk of acute degradations of lung function and improves life expectancy (Maher and Strek, 2019). However, the drugs were not documented in CIPF dogs (Clercx, Fastrès and Roels, 2018). Therefore, management of CIPF dogs is primarily symptomatic and includes cough suppression, cardiac support in case of PH and, when present, control of secondary infection and inflammation with the aim to reduce the severity of clinical signs and secondary complications and improve the perceived QOL (Clercx, Fastrès and Roels, 2018; Laurila and Rajamäki, 2020).

Oral or inhaled corticosteroids appear to relieve cough in most dogs, especially when concurrent bronchial changes are reported (Corcoran *et al.*, 1999; Heikkilä *et al.*, 2013). Antitussive

drugs may also be considered against cough (Clercx, Fastrès and Roels, 2018; Laurila and Rajamäki, 2020). As in human IPF, the use of sildenafil, a phosphodiesterase-5 inhibitor, in case of concomitant PH was shown to improve clinical signs and QOL (Clercx, Fastrès and Roels, 2018; Sgalla *et al.*, 2018; Johnson and Stern, 2020; Laurila and Rajamäki, 2020). In IPF, proton pump inhibitors or histamine H_2 receptor blockers to treat microaspirations remains recommended because of the low cost and risk of adverse effect of such therapy even if no proof of action on survival is documented (Raghu *et al.*, 2018; Sgalla *et al.*, 2018; Wakwaya and Brown, 2019). Their use in CIPF dogs might also be benefit as supported by the increase of microaspirations rate in WHWTs (Määttä *et al.*, 2018; Laurila and Rajamäki, 2020). Finally, again as in human IPF, causes of acute worsening of respiratory function, such as bacterial pneumonia for example, should be investigated and treated appropriately (Sgalla *et al.*, 2018; Somogyi *et al.*, 2019; Laurila and Rajamäki, 2020).

Other general recommendations include weight loss in obese patients in order to increased thoracic wall compliance and decreased extrathoracic and intra-abdominal adipose tissue. Environmental modifications such as the improvement of air quality, and the reduction of recognized triggers of clinical signs such as frequent grooming for example can also be recommended (Roels *et al.*, 2018; Reinero *et al.*, 2020). Keeping routine daily walks is encouraged unless the dog shows signs of exhaustion (Laurila and Rajamäki, 2020). Indeed, lower routine physical activity in IPF patients is associated with worse survival rates and pulmonary rehabilitation can be helpful to decrease dyspnoea and breathlessness and seems at least during the first 6 months of implementation to improve QOL, 6MWD and reduce anxiety and depression (Sgalla *et al.*, 2018; Somogyi *et al.*, 2019).

1.7. Prognosis

The prognosis of the disease is poor. Lilja-Maula and colleagues (2014) reported a median survival time of 32 months (range: 2–51 months) from onset of clinical signs, and 11 months (0–40 months) from diagnosis in 7 WHWTs with CIPF-related death. In another study about 16 CIPF WHWTs, median survival time after diagnosis was 255 days (1–1375 days) (Thierry *et al.*, 2017). Finally, in an online questionnaire–based survey filled in by 458 WHWT owners, the overall survival time after CIPF diagnosis was 1.4 years (0–8.5 years) and the cause of the death was CIPF-related in 76.7% of cases (Roels *et al.*, 2018). The lack of prognostic biomarker as well as the variability in individual disease progression contribute to the difficulty to predict disease progression in WHWTs affected with CIPF (Clercx, Fastrès and Roels, 2018).

The median survival time of IPF patient is of 3-5 years. However, as in CIPF, IPF outcome is difficult to predict as the clinical course of the disease is highly heterogenous among patients with patients who remains relatively stable with episodes of acute deterioration, patients who have a slow but progressive clinical course, and patients who have an evolution rapidly leading to death from

respiratory failure (Richeldi, Collard and Jones, 2017; Kishaba, 2019a; Somogyi *et al.*, 2019; Wakwaya and Brown, 2019).

1.8. Unexplored fields

Despite consequent research on CIPF, there is still many unexplored fields (Clercx, Fastrès and Roels, 2018; Laurila and Rajamäki, 2020). The prevalence and the incidence of the disease remain unknown and difficult to establish (Clercx, Fastrès and Roels, 2018; Laurila and Rajamäki, 2020). Early identification of affected dogs is challenging for the owners because of clinical signs that may mimic ageing. Moreover, disease is easily confounded by veterinarians with other illnesses sharing similar presentation and clinical signs, such as congestive left heart failure, chronic bronchopneumonia with bronchomalacia, lung neoplasia and angyostrongylosis for example (Corcoran *et al.*, 1999; Heikkila-Laurila and Rajamaki, 2014; Clercx, Fastrès and Roels, 2018; Laurila and Rajamäki, 2020). The diagnosis requires at least the performance of thoracic HRCT which is not available in all veterinary structures. Besides, only histopathological examination, which may be sometimes unconclusive, can confirm CIPF (Heikkilä *et al.*, 2011; Syrjä *et al.*, 2013; Roels *et al.*, 2017a; Holopainen *et al.*, 2019). Disease progression is highly variable between dogs and difficult to predict. Despite numerous investigations to identify biomarkers for disease diagnostic and prognostic assessment, reliable and routinely available biomarkers are still missing (Fastrès *et al.*, 2018; Krafft *et al.*, 2011; Krafft *et al.*, 2013; Krafft *et al.*, 2014; Heikkilä *et al.*, 2013; Lilja-Maula *et al.*, 2013; Lilja-Maula *et al.*, 2015; Viitanen *et al.*, 2014; Roels *et al.*, 2015a; Roels *et al.*, 2015b; Määttä *et al.*, 2020). CIPF causes have not yet been identified and are probably multiple. While viral and fungal infection doesn't seem to be associated with CIPF (Roels *et al.*, 2016), genetic predisposition, presence of increase rate of GER and specific environmental exposures are suspected to play a role in disease development and pathogenesis (Maatta *et al.*, 2017; Clercx, Fastrès and Roels, 2018; Roels *et al.*, 2018; Piras *et al.*, 2020). However, further studies are needed to clearly establish it. The exact pathophysiology leading to the development and the progression of lung fibrosis is not yet completely understood. Better understanding of pathways leading to CIPF would allow to identify therapeutic targets with the aim to prevent, slow or even cure the disease. Indeed, currently, therapeutic options are only symptomatic and there are still no specific ongoing therapeutic trials in CIPF (Clercx, Fastrès and Roels, 2018; Laurila and Rajamäki, 2020).

2. The lung microbiota

The LM corresponds to the collection of bacteria that colonize the lung. Table 2 collects most of the terms commonly employed to describe the microbiota and that will be used in the present work.

Table 2. *Microbiota definitions.*

Microbiota	All the bacteria found in a region or habitat
Microbiome	The totality of the microbes (bacteria, fungi and viruses) with their genes and the environment in which they interact
16S ribosomal DNA	A specific DNA gene that is unique to bacteria and that comports variable and common regions between each bacterium
Taxonomy	The science that identifies and classifies the species. Bacteria are classified in taxonomic groups corresponding to phylum, class, order, family, genus and species in descending order
OTU	Specific sequences based on sequence similarity (typically threshold is 97%) to reference genes. This is taken as a proxy measure for species-level divergence
Taxon	A group of phylogenetically related microbes that belong to the same taxonomic group
Amplicon	An amplified fragment of DNA from a region of a marker gene (such as 16S rDNA) that is generated by PCR
Richness	Number of different taxa within a sample
Evenness	Equality of the relative abundances among different taxa. The evenness varies from 0 to 1 and the more the relative abundances of taxa differ the lower the evenness is
α-diversity	Amount of variation in sequences composition among a sample
β-diversity	Amount of variation in sequences composition among sampling units
Ecological parameters	Refers to the richness, the evenness and the diversity
Resilience	The capacity of the microbiome to absorb disturbance and reorganize itself while undergoing change, so as to retain essentially the same function, structure, and identity
Dysbiosis	A condition in which the normal structure of the microbiome is disturbed, often through external pressures

DNA, deoxyribonucleic acid; OTU, Operational taxonomic unit; PCR, polymerase chain reaction.

Table adapted from (Segal et al., 2014; Rogers et al., 2015; Ricotta, 2017; Costa et al., 2018).

2.1. History

Historically, conventional culture-based techniques that imply to isolate *ex vivo* and culture bacteria were used to study bacterial communities based on morphological and biochemical characteristics (Dickson *et al.*, 2016). However, the vast majority of the bacteria were not detected by culture. Indeed, some are unculturable, most require specific growth conditions (culture media, incubation conditions, *etc.*) that have not or cannot be reproduced experimentally and some are rare, slow growing and may be missed (Streit and Schmitz, 2004; Woo *et al.*, 2008).

Secondary to the development of culture-independent techniques, a large project named the Human Microbiome Project has been launched in 2007 by the National Institutes of Health to study the microbiota in 18 parts of the human body. It provided significant insights into the function and diversity of the human microbiota (The Human Microbiome Project Consortium, 2012). However, the lung was not targeted by this project as it was considered as sterile. The sterility of the lung was

supported by three concepts: (1) the absence of growth in lung specimens using classic culture-based protocols designed to detect respiratory pathogens, (2) the thought that the bacteria identified in the lungs only reflect contamination from upper airways and (3) the thougth that there is no resident flora that can reproduce into the lung environment (Dickson *et al.*, 2016).

The first study about the LM using culture-independent technique was published in 2010 by Hilty and colleagues. It provided two major results further validated by other papers including the description of the LM in healthy patients and the description of LM alteration in asthmatic patients (Hilty *et al.*, 2010). Numerous studies were then published about the LM, in various lung diseases, contributing to improvement of the knowledge in this field.

In healthy dogs, the first report about the presence of a LM was published in 2016 by Ericsson *et al.* They described the LM in a cohort of healthy experimental beagle dogs (Ericsson *et al.*, 2016). A pilot study and a poster communication were also produced by our team at the same period of time assessing the LM in healthy dogs from different breeds and in dogs affected with CIPF and comparing the LM between healthy WHWTs living either in Finland or in Belgium, respectively (Fastrès *et al.*, 2017b; Roels *et al.*, 2017c).

2.2. Techniques used to describe the lung microbiota

2.2.1. The 16s rDNA amplicon sequencing

The study of lung microbial communities was made possible thank to the development of culture-independent methods. The use of those methods becomes attractive secondary to the reduction of the cost linked to such studies and the development of sequencing technologies and bioinformatics analytic tools facilitating results analysis (Dickson *et al.*, 2016). Culture-independent methods are based on the direct analysis of bacterial DNA or ribonucleic acid (RNA), without any cultural step. Different culture-independent methods are available to study the microbiota, however, in this research, only the partial 16S rDNA amplicon sequencing method was used. In this section, a brief description of this technique is presented. Several reviews are available describing all the different culture-independent methods that can be used to analyse the microbiota (Fraher *et al.*, 2012; Doggett *et al.*, 2016; Boers *et al.*, 2017; Slatko *et al.*, 2018; Vargas-Albores *et al.*, 2019)

The 16S rDNA amplicon sequencing technique is the most commonly used method to study bacterial communities (Moffatt and Cookson, 2017; Slatko *et al.*, 2018). The advantages of the 16S rDNA amplicon sequencing technique include the low cost of the technique, the high sensitivity allowing bacterial identification at species level in 62 to 92% of cases, the rapidity, and the possibility to classify the bacteria into classes similar to the phylogenetic classification (Woo *et al.*, 2008). Indeed, the 16S rRNA gene is an non-coding gene, ubiquitous among bacterial communities that has

kept a constant structure and function over time (Woese, 1987; Fraher *et al.*, 2012; Vargas-Albores *et al.*, 2019). It is composed by nine highly conserved regions across taxa, that enables the design of PCR primers, and nine hypervariable regions (V1-V9) used to distinguish between taxa and that yield a phylogenetic signal useful for bacterial identification (Clarridge, 2004; Fraher *et al.*, 2012; Moffatt and Cookson, 2017; Vargas-Albores *et al.*, 2019). Thanks to these characteristics, the 16S rRNA gene is considered as the universal target for bacterial identification using sequencing. The bacterial classification based on the 16S rRNA gene was developed in the 1970s (Woese and Fox, 1977). The large used of the 16S rRNA gene to study and classify bacteria in the following years leads to the availability of large reference databases increasing the bacterial identification rate (Woo *et al.*, 2008; Dickson *et al.*, 2016). First studies typically sequenced the entire 16S rRNA gene which is about 1,550 base pairs long (Boers, Jansen and Hays, 2019). However, sequencing of long fragment reduced the sequencing depth, limiting the diversity. Therefore, massively parallel sequencing technologies progressively focused on the sequencing of shorter fragments at greater depth (Boers, Jansen and Hays, 2019).

The 16S rDNA amplicon sequencing technique includes several steps. Firstly, after the collection of the sample of interest, DNA present in the sample is extracted, purified and quantified. Secondly, a fragment of the 16S rDNA is amplified by PCR using primers targeting constant regions of the gene. Amplicons obtained are then purified and prepared to form libraries. The libraries are sequenced. Finally, sequences are cleaned and assessed for quality before being clustered in operational taxonomic units (OTUs) and aligned to bacterial genome database for identification (Boers *et al.*, 2019). The taxonomic level of identification will depend on the percentage of homology between sequences. By convention, clustered sequences in OTUs with 97% of homology allows identification until genus- or species-level phylogeny (Větrovský and Baldrian, 2013).

2.2.2. Challenges associated with the study of the lung microbiota

Numerous parameters (*e.g.*, sampling procedure, contaminations, sequencing strategy, 16S rDNA region sequenced, taxonomic classifier, *etc*.) are able to influence results of lung bacterial community studies. The absence of standardization of these parameters makes it difficult to compare studies of the LM. Principal challenges associated with the study of the LM using the 16S rDNA amplicon sequencing technique are reported in this section.

First, the LM can be studied from different types of samples including BALF, sputum, protected brush and lung tissue. Depending on the sample type, variations in contamination, sampling volume, lung area investigated, *etc.* can provide different results. For example, increased diversity and different β-diversity have been reported in sputum compared with BALF and brush samples (Hogan *et al.*, 2016). The bacterial load is also higher in sputa compared with BALF specimens (Marsh *et al.*,

2018). In human, several studies indicated that using BALF to study LM was not confounded by oral microbiota contamination and was considered as an acceptable technique to investigate the LM (Morris *et al.*, 2013; Segal *et al.*, 2013; Bassis *et al.*, 2015). Even if oral contaminations are more likely in sputum, it doesn't seem to alter the meaningful microbial signal (Dickson *et al.*, 2016).

Variability of LM results associated with the used of the 16S rDNA amplicon sequencing includes notably the choice of the fragment amplified which is variable between studies. In all cases, sequencing of only a part of the 16S rRNA gene decreases the diversity compared with the sequencing of the full-length gene at similar sequencing depth. To study the LM, it has been showed that more accurate estimation of the bacterial richness could be reached by amplifying either V1–V3 or V1–V4 regions of the gene (Kim, Morrison and Yu, 2010). By sequencing partial sequences of the 16S rRNA gene and depending on the sequences selected, different degrees of segregation can be achieved between bacteria (Mizrahi-Man *et al.*, 2013; Boers *et al*., 2019). For some bacteria, the discriminatory power is generally restricted to the genus level. This could contribute to reduce the diversity by preventing identification of bacteria with close genetic background. However, it could also artificially increase the diversity when same bacteria are identified as 2 different entities because of mutations inducing more that 3% of variability. Indeed, sequences are grouped together when they shared 97% of homogeneity and separated when they differed from more than 3%. In the same idee, depending on the fragment amplified, different results can be obtained at least at the species level (Boers *et al.*, 2019). A number ranging from 1 to 15 of copies of the 16S rDNA can be identified depending on the bacteria (Klappenbach *et al.*, 2001). Moreover, the number of copies can even vary in bacteria from the same species (Stoddard *et al.*, 2015) which complicates the analysis, could artificially increase the relative abundance of certain bacteria and may result in a false community structure (Větrovský and Baldrian, 2013; Stoddard *et al.*, 2015; Vargas-Albores *et al.*, 2019).

Another important challenge is to deal with the fact that the 16S rDNA amplicon sequencing technique is based on PCR that suffers from numerous biases such as amplification biases for example. As a consequence, avoiding contaminations with the use of this method is crucial especially in lung samples, in which the bacterial load is low (Salter *et al.*, 2014; Marsh *et al.*, 2018). Indeed, amplification of contaminant bacterial DNAs can lead to completely aberrant results. In LM studies, contaminations can occur at different steps including sampling and laboratory analyses and can come from different sources such as the upper respiratory airways and laboratory reagents for example (Salter *et al.*, 2014; Dickson *et al.*, 2017a; Marsh *et al.*, 2018). To control and detect contaminations, it is important to process negative controls alongside clinical specimens through all analytic steps from the sampling to the sequencing. Controls of any equipment or media used during the analyses are also relevant such as bronchoscope wash for example. In addition to negative control samples, strict laboratory controls of all reagents and machines are required. To avoid variations in background

contamination, batched analyses are also recommended (Salter *et al.*, 2014; Marsh *et al.*, 2018). Contaminations from upper airways cannot be prevented totally, however, they seem to minimally alter the LM in BALF specimens obtained through bronchoscopy (Charlson *et al.*, 2011; Bassis *et al.*, 2015; Dickson *et al.*, 2015; Dickson *et al.*, 2017a). The contamination from upper airways and saliva in sputum specimens remains unknown (Moffatt and Cookson, 2017). Other PCR biases could also come from inaccurate amplification, such as preferential annealing or chimeric PCR products and undetection of some genes due to low bacterial abundance in samples (Kanagawa, 2003; Jany and Barbier, 2008).

The impact of the sequencing strategy (*i.e.*, read length, single or paired end) on LM results was not clearly investigated in the literature (Mizrahi-Man *et al.*, 2013). Numerous reference databases can be used to generate identification of bacteria based on the 16S rDNA amplicon sequencing including SILVA (Pruesse *et al.*, 2007), RDP (Cole *et al.*, 2003), GreenGenes (DeSantis *et al.*, 2006), or NCBI database (Federhen, 2012). The accuracy of the identification obtained using these databases will depend on their quality and their completeness knowing that all reference databases contain poorly annotated or unidentified sequences (Boers *et al.*, 2019).

Finally, the 16S rDNA amplicon sequencing method is frequently criticized because of its inability to distinguish dead from alive bacteria (Doggett *et al.*, 2016). Recent developments exist to bypass this problem by degrading free DNA and DNA in permeable and thus dead bacteria before PCR amplification (Codony, Dinh-Thanh and Agustí, 2020). However, these techniques also suffered from biases as they can damage living bacteria and generate wrong conclusions (Codony *et al*., 2020). The presence of different effective mechanisms of clearance in lungs such as AMs (Joshi *et al.*, 2018) and the speed of about 10 mm/min of the mucociliary escalator (Whaley, Wolff and Muggenburg, 1987), might prevent the amplification of free DNA coming from dead bacteria. Moreover, the detection of dead bacteria could be clinically relevant as they are able to induce immune response (Beck, Young and Huffnagle, 2012; Morris *et al.*, 2013).

2.3. Role of the lung microbiota

It is now clear that the LM plays an important role in the homeostasis of the lungs by its action on the metabolism, the development of the immune system and the protection against pathogens (Lloyd and Marsland, 2017; Wang *et al*., 2017). Indeed, dysbiosis and altered LM, especially in early life, has been associated with numerous lung diseases and is able to affect risk of diseases, exacerbations, response to drugs and clinical outcomes (Wang *et al.*, 2016; Man *et al.*, 2017; Shukla *et al.*, 2017; Wang *et al.*, 2017). However, it remains unknown whether the LM alterations are a cause or a consequence of lung diseases (Fastrès *et al.*, 2017a; Huang *et al.*, 2017).

The principal function of the lungs is the exchange between oxygen and carbon. The perpetual entry of air and foreign substances represents a constant stimulation of the local immune system which have to remain tolerant and not react except above a certain threshold (Wang *et al.*, 2017). The LM is suspected to contribute to the establishment of this threshold (Man *et al*., 2017). Indeed, in germ-free mice the absence of lung bacteria induces higher susceptibility to pulmonary pathogens, house dust and asthma by increasing the Th2 immune response, notably (Brown *et al*., 2017; Man *et al.*, 2017). Several data also suggest that the presence of specific bacteria at certain periods of the life is crucial for shaping the adaptative immune response and developing correct immune tolerance (Man *et al.*, 2017; Pattaroni *et al.*, 2018). Moreover, in human the development of the LM is associated with a decrease in lung inflammation, recruitment of inflammatory cells and production of pro-inflammatory cytokines (Man *et al.*, 2017; Wang *et al.*, 2017). Investigating how the LM may regulate innate immunity has recently gained interest (O'Dwyer, Dickson and Moore, 2016; Zhang *et al.*, 2020), and a role for constitutive sensing of microbes and their metabolites has been proposed (Zhang *et al.*, 2020). The gut microbiota seems to affect pulmonary immunity and a link between the gut microbiota and the lungs, named the gut–lung axis, has been described (O'Dwyer, Dickson and Moore, 2016; Zhang *et al.*, 2020). Indeed, dysbiosis of the gut microbiota in early age is associated with chronic lung diseases development such as asthma and increases the susceptibility to pulmonary infectious diseases (O'Dwyer, Dickson and Moore, 2016). This interaction between the gut and the lung is bidirectional and changes in LM also affect the gut microbial communities (Dumas *et al.*, 2018; Zhang *et al.*, 2020). Endotoxins, microbial metabolites, cytokines, and hormones as well as regulatory T cells acting via the bloodstream connection have been proposed as mediators of modulation of immune responses and inflammation between the gut and the lungs (O'Dwyer, Dickson and Moore, 2016; Zhang *et al.*, 2020).

The microbiota has also an action on the protection of the lungs by promoting the innate response against pathogens and their clearance from the airways (Brown *et al.*, 2017; Man *et al.*, 2017). Finally, the LM is also showed to increase resistance to lung infection (Brown *et al.*, 2017).

2.4. Lung microbiota in healthy condition

2.4.1. Development and composition in human

The presence of a LM has been reported in human early in gestation (Al Alam *et al.*, 2020). Temporal changes in the LM were identified during the foetal development although the causes and the factors influencing this maturation are unknown (Al Alam *et al.*, 2020). Some overlaps between the placental and the foetal LM has been shown (Piersigilli *et al.*, 2020). After birth, the microbiota is relatively homogenous across organs and resembles that of the mother (Dominguez-Bello *et al.*, 2010). The resilience of the LM to environmental pressure, such as the delivery mode, is increased in term infant compared with preterm infant (Pattaroni *et al.*, 2018). After birth, the microbiota in all organs

rapidly differentiates before stabilizing (Dickson *et al.*, 2016). Indeed, the gut microbiota is largely variable in young children until the age of 3 years old, when it resembles that of the adults (Yatsunenko *et al.*, 2012). Same pattern of variation is described in the upper airways microbiota (Biesbroek *et al.*, 2014). In human, the maturation of the LM is rapid, occurring in the 2 first months of age (Pattaroni *et al.*, 2018). Different factors throughout life can play a role in the development of the LM including host genetics, environmental parameters such as antibiotic administration, diet composition, living conditions (air pollution, cigarette smoke), contact with pathogens, and host immunity (O'Dwyer, Dickson and Moore, 2016; Shukla *et al.*, 2017; Wang *et al.*, 2017; Yang *et al.*, 2020).

In adults, the LM has a low bacterial load which can vary depending on the sample type, the sample volume and clinical parameters (*e.g.*, age, lung disease, *etc.*). In general, bacterial load is between $10^{4.5}$ and $10^{8.5}$ 16S copies/mL in BALF and up to 10^{8} 16S copies/mL in sputum which is approximatively 2 to 4 times lower than in the oral microbiota (Charlson *et al.*, 2011; Dickson *et al.*, 2016; Shukla *et al.*, 2017; Marsh *et al.*, 2018). In healthy adult patients, the LM is composed by a majority of facultative anaerobic bacteria with a large predominance of Bacteroidetes and Firmicutes phyla. Other major phyla include Proteobacteria, Fusobacteria and Actinobacteria (Hilty *et al.*, 2010; Erb-Downward *et al.*, 2011; Morris *et al.*, 2013; Dickson *et al.*, 2016; O'Dwyer, Dickson and Moore, 2016). A core microbiota was defined at the genus level, and includes *Prevotella*, *Veillonella*, *Streptococcus*, *Pseudomonas*, *Fusobacterium*, *Haemophilus* and *Porphyromonas* (Hilty *et al.*, 2010; Charlson *et al.*, 2011; Erb-Downward *et al.*, 2011; Beck *et al.*, 2012; Morris *et al.*, 2013; Dickson *et al.*, 2016). The LM is close to that of the mouth. Indeed, the oral cavity is considered as the principal source of the bacteria composing the LM of healthy patients, although the similarity between the mouth and the LM vary among people (Hilty *et al.*, 2010; Erb-Downward *et al.*, 2011; Morris *et al.*, 2013; Dickson *et al.*, 2016). Little variations of the LM between pulmonary lobes are reported. However the LM is considered as quite homogeneous in human (Dickson *et al.*, 2015)

2.4.2. Composition in dogs

In healthy dogs the LM as in human is also closer to the oral microbiota than to the nasal or the faecal microbiota and has a weak bacterial biomass (Ericsson *et al.*, 2016). Four major phyla are described including Proteobacteria, Firmicutes, Actinobacteria and Bacteroidetes (Figure 7) (Ericsson *et al.*, 2016; Roels *et al.*, 2017c). Dominant genera identified in the canine LM include *Pseudomonas*, *Acinetobacter*, *Cutibacterium*, *Streptococcus* and Pasteurellaceae genus (Ericsson *et al.*, 2016; Roels *et al.*, 2017c).

Compared with human, a large predominance of Proteobacteria is found in the canine LM. In their study, Ericsson and colleagues (2016) also described a more uniform community structure

between dogs than what was reported in human which could be related to the greater homogeneity of their samples (experimental beagle dogs co-housed in a stable environment and fed with the same food).

Roels and colleagues (2017) identified differences between healthy experimental beagles and healthy client-owned WHWTs raising the hypothesis that specific modifications of the LM in dogs could be related to the breed and/or the living conditions. An impact of the environment on LM in dogs was also documented by the identification of differences in the LM of healthy WHWTs living either in Finland or in Belgium (Fastrès *et al.*, 2017b).

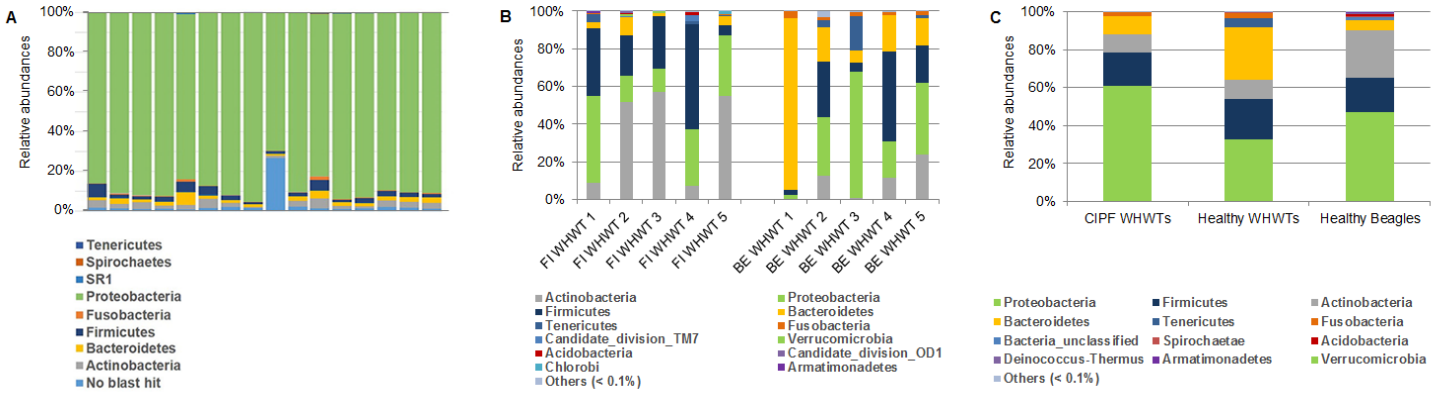

Figure 7. *Phylum-level composition of airway microbiota in healthy dogs.* ***(A)*** *Bar charts showing relative abundance of all taxa detected in bronchoalveolar lavage fluid (BALF) collected from 16 intact adult female dogs, analysed using amplification of the V4 region of the 16S rDNA and annotated to the taxonomic level of phylum using the Greengenes database (Ericsson et al., 2016).* ***(B)*** *Bar charts showing relative abundance of all taxa detected in BALF collected from 10 healthy West Highland white terriers (WHWTs) coming from either Finland (FI) (n = 5) or Belgium (BE) (n = 5), analysed using amplification of the V1-V3 region of the 16S rDNA and annotated to the taxonomic level of phylum using the SILVA database (Fastrès et al., 2017b).* ***(C)*** *Bar charts showing relative abundance of all taxa detected in BALF collected from 10 adult beagle dogs, 5 healthy WHWTs and 7 WHWTs affected with canine idiopathic pulmonary fibrosis (CIPF), analysed using amplification of the V1-V3 region of the 16S rDNA and annotated to the taxonomic level of phylum using the SILVA database (Roels et al., 2017c).*

2.4.3. Composition in other species

In horses, only one study has been published about the LM (Fillion-Bertrand *et al.*, 2018). Results of the study showed that BALF samples have also a low bacterial load compared with nasal and oral specimens and a lower richness and diversity. Predominating phyla in horses include Proteobacteria, Acidobacteria and Firmicutes. No dominant OTU characteristic of the LM has been

identified. Finally, modifications in environmental living conditions (*i.e.*, food and housing) as well as diseased status are found to modify the LM.

The LM in pigs and sheep has been studied as a model for human but also because bacterial respiratory diseases, especially infectious pneumonia, represent an important economic loss in the swine industry (Glendinning *et al.*, 2016; Huang *et al.*, 2019). In swine, commonly identified phyla include Proteobacteria, Firmicutes, Tenericutes and Bacteroidetes (Siqueira *et al.*, 2017; Huang *et al.*, 2019; Li *et al.*, 2021). The dominant genus reported in pigs is *Mycoplasma*. Other major genera reported include *Escherichia-Shigella*, *Lactotococcus*, *Macrococcus*, *Methylotenera*, *Ureaplasma* and *Phyllobacterium* (Huang *et al.*, 2019; Li *et al.*, 2021). As in other species, changes in LM have been associated with diseased conditions (Siqueira *et al.*, 2017; Huang *et al.*, 2019; Li *et al.*, 2021). In sheep, the LM is dominated by *Corynebacterium*, *Bacillus*, *Enterococcus*, *Klebsiella*, *Mannheimia*, *Micrococcus*, *Moraxella*, *Pasteurella*, *Pseudomonas*, *Staphylococcus* and *Streptococcus* (Glendinning *et al.*, 2016). As in human, different degrees of spatial variability are identified between different lung segments in sheep (Dickson *et al.*, 2015; Glendinning *et al.*, 2016).

Finally, the LM of rodents as a model for human has also extensively been studied in healthy and diseased conditions. Studies in healthy mice have confirmed that the LM is different of that from other body sites, such as the oral cavity or the gut (Barfod *et al.*, 2015; Dickson *et al.*, 2018; Kostric *et al.*, 2018). The mice LM communities are composed mainly at the phylum level by Firmicutes, Proteobacteria and Actinobacteria, while being composed mainly at the genus level by *Delftia*, *Lactobacillus*, *Propionibacterium*, *Rhodococcus*, and *Streptococcus* (Kostric *et al.*, 2018). In rat lungs, a large predominance of Proteobacteria followed by lower percentage of Firmicutes, Bacteroidetes, and Actinobacteria phyla is reported. Prominent genera include *Serratia*, and in smaller proportions *Ralstonia* and *Brucella* (Li *et al.*, 2017a; Finn *et al.*, 2018). The diversity (Kostric *et al.*, 2018) and the richness (Singh *et al.*, 2017; Kostric *et al.*, 2018) of the mice LM have been shown to increase with the age, while, in adults, the LM seems to be quite similar among individuals (Barfod *et al.*, 2015; Kostric *et al.*, 2018). As in mice, the LM of adult rats is consistent between individuals (Finn *et al.*, 2018). The sex also seems to have an impact on the LM in mice (Barfod *et al.*, 2015). The LM in early-life mice has been showed to cluster by environment and to change rapidly according to environmental alterations, while a higher resilience towards environmental variations is found in adults (Dickson *et al.*, 2018; Kostric *et al.*, 2018). Environmental changes by exposition of rats to particle matter also result in an altered microbial composition with an increase in bacterial diversity and in abundance of potentially pathogenic bacteria (Li *et al.*, 2017a). Finally, studies performed in healthy mice and rats have shown that antimicrobial drug administration can alter the LM compared to non treated animals (Barfod *et al.*, 2015; Dickson *et al.*, 2018; Finn *et al.*, 2019).

2.5. Variation of the lung microbiota in healthy and diseased states

The LM is considered as a dynamic ecosystem which results from the balance between three phenomena: bacterial immigration, elimination and local growth (Charlson *et al.*, 2011; Bassis *et al.*, 2015; Dickson *et al.*, 2016). In healthy conditions, immigration and elimination predominate while local growths are more predominant in diseased conditions (Figure 8) (Dickson *et al.*, 2015).

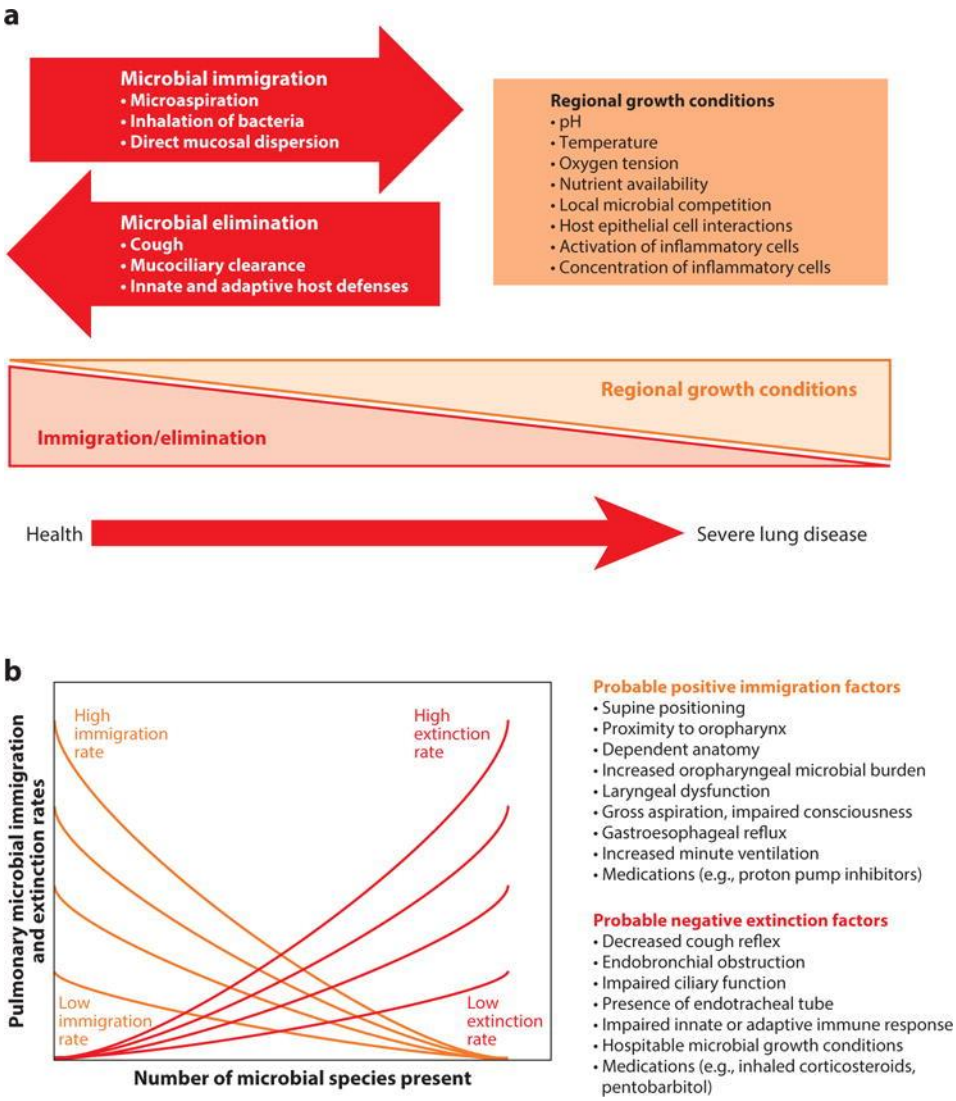

Figure 8. *Ecological modelling of the respiratory microbiome (Dickson et al., 2016).* ***(a)*** *The constitution of the respiratory microbiome is determined by three factors: microbial immigration, microbial elimination, and the relative reproduction rates of its members. In health, community membership is determined primarily by immigration and elimination; in advanced lung disease, membership is determined primarily by regional growth conditions.* ***(b)*** *The adapted island model of lung biogeography. Community richness in health for a given site in the respiratory tract is a function of immigration and elimination factors.*

Bacterial immigration includes 3 phenomena: microaspirations, inhalation and dispersion along mucosae and is considered as the primary source of bacteria in the lungs (Dickson *et al.*, 2016). This hypothesis is supported in human and dogs by the presence of overlaps between the oral and the LM (Bassis *et al.*, 2015; Ericsson *et al.*, 2016; Dickson *et al.*, 2017a). Microaspirations are common and ubiquitous in healthy individuals and are considered as the principal mode of microbial immigration (Gleeson, Eggli and Maxwell, 1997; Dickson *et al.*, 2017a). Microaspirations also occur in dogs, although it is less studied and seems to be related to the facial conformation (Määttä *et al.*, 2018). Approximatively 10^4-10^6 bacteria per mm^3 are contained in the inhaled air and could contribute to the LM (Dickson, Erb-Downward and Huffnagle, 2014). The dispersion of the bacteria directly along mucosa has not yet been clearly proved and remains theoretical (Dickson *et al.*, 2016; Dickson *et al.*, 2017a).

The elimination of microbial communities is driven by mechanical, immunological and bacterial mechanisms in the lungs (Dickson *et al.*, 2016; O'Dwyer, Dickson and Moore, 2016). Mechanical elimination is driven by the muco-ciliary escalator that constantly carries bacteria along the mucus layer to the upper airways where they are swallowed or expectorated. The cough also contributes to the mechanical elimination of the bacteria. Finally, the lungs possess a large arsenal of innate and adaptative immune defences able to recognize, kill and clear the airways. The bacteria themselves play also a role in the elimination of their members (Dickson *et al.*, 2016; O'Dwyer, Dickson and Moore, 2016).

Changes in local growth conditions also impact microbial communities. In healthy conditions, small variations of the LM have been identified between different pulmonary segments (Charlson *et al.*, 2011; Segal *et al.*, 2013; Dickson *et al.*, 2015). However, intra-individual variations were not identified in all subjects and were less important than inter-individual ones (Dickson *et al.*, 2015). Local variations of the LM are suspected to be related to local changes in the lung microenvironment such as the temperature, the oxygen tension, the pH, *etc.* (O'Dwyer, Dickson and Moore, 2016). Such changes in the lung environment are particularly important in diseased lungs and are suspected to induce pressure across bacteria, favouriting the growth of more adapted ones (Dickson, Erb-Downward and Huffnagle, 2014; Dickson *et al.*, 2016; O'Dwyer, Dickson and Moore, 2016). Changes in the LM, also named dysbiosis (Table 2) then occur. Dysbiosis of the LM has been associated with various chronic and acute respiratory diseases. However, it is still challenging to identify the mechanisms beyond the generation and the alteration of the LM and to determine its contribution to lung diseases development (Dickson *et al.*, 2016; O'Dwyer, Dickson and Moore, 2016). As alterations of the microbiota could act in the pathogenesis of numerous diseases, microbiota manipulations therefore potentially represent a potential therapeutic target.

2.5.1. Acute diseases

The LM has been studied in acute pulmonary diseases such as pneumonia, trauma and acute respiratory distress syndrome (ARDS) (Dickson *et al.*, 2014; Dickson *et al.*, 2016; Dickson *et al.*, 2020; Dickson *et al.*, 2017b). These pathologies are characterized by an abrupt increase in bacterial load and decrease in bacterial richness and diversity (Dickson *et al.*, 2014). Predominance of one or two taxonomic groups is also reported (Dickson et al., 2014; Dickson *et al.* 2016; Dickson, Erb-Downward and Huffnagle, 2014). The dysbiosis has been associated with an increase in inflammatory markers (Dickson *et al.*, 2017b). Alterations of the LM can predict outcomes and the response to treatment in critically ill patients. Indeed, the enrichment of the LM with bacteria mainly found in the gut microbiota such as species from the Lachnospiraceae and Enterobacteriaceae families (*Escherichia coli*, *Enterobacter spp.*, and *Klebsiella pneumoniae*) is frequent in patients with worse outcomes (Dickson *et al.*, 2017b; Dickson *et al.*, 2020). The detection of gut-associated bacteria is also associated with the presence of ARDS (Dickson *et al.*, 2020).

In dogs, a dysbiosis of the LM has also been associated with pneumonia. The LM composition, mostly in communities acquired pneumonia (CAP), is shaped towards a domination of specific taxa and a loss of the bacterial communities found in healthy conditions (Vientós-plotts *et al.*, 2019). Moreover, the LM alterations identified by 16S rDNA amplicon sequencing are in the majority of the cases in good agreement with culture results (Vientós-plotts *et al.*, 2019).

Studies in acute pulmonary diseases helped to better understand the microbial field and suggest that the LM assessment could help to guide the selection of antimicrobial drugs especially when culture results are negative (Woo *et al.*, 2008; Johansson *et al.*, 2019; Vientós-plotts *et al.*, 2019).

2.5.2. Chronic diseases

The LM has been extensively described in chronic lung diseases including asthma, chronic obstructive pulmonary disease (COPD), cystic fibrosis (CF), bronchiectasis and IPF. In the majority of chronic lung diseases, a shift in the microbiota composition from Bacteroidetes phylum towards Proteobacteria phylum has been described together with a decrease in diversity and an increase in richness and bacterial burden (Dickson and Huffnagle, 2015). Baseline differences in microbial population abundance and in microbial diversity have been associated with exacerbation in IPF (Molyneaux *et al.*, 2017a) and in COPD (Jubinville *et al.*, 2018), higher mortality and poorer outcomes (Molyneaux *et al.*, 2014; Takahashi *et al.*, 2018). However, whether the LM alteration represents a cause or a consequence of the disease is still not clear (Fastrès *et al.*, 2017a; Huang *et al.*, 2017), despite the increasing number of studies investigating microbiota modifications.

More precisely, in asthma and allergy, clear evidence has shown that greater environmental bacterial exposure and increased bacterial diversity at an early age has a protective role on disease susceptibility (Dickson *et al.*, 2016; Wang, Li and Tian, 2017; Mathieu *et al.*, 2018; Heul, Planer and Kau, 2019). The presence of a specific microbiota enriched in Proteobacteria is found in asthmatic compared to healthy patients (Hilty *et al.*, 2010). Moreover, the presence of specific bacteria, especially *Streptococcus*, *Haemophilus*, and *Moraxella* spp. is suggested to alter local immune responses and increase disease severity and inflammation (Teo *et al.*, 2015; Heul, Planer and Kau, 2019). However, in asthmatic patients, the exact impact of dysbiosis on disease development and progression remains unclear (Mathieu *et al.*, 2018). In COPD, an increased proportion of Proteobacteria and Actinobacteria is found compared with healthy patients (Hilty *et al.*, 2010; Sze *et al.*, 2012). Certain bacteria are also associated with the disease such as *Pseudomonas aeruginosa* and *Haemophilus* spp. (Hilty *et al.*, 2010; Stefano *et al.*, 2017). The dysbiosis, and particularly the presence of those bacteria and the decrease of the bacterial diversity, is associated with disease severity, poor prognosis and increased inflammatory markers (Erb-Downward *et al.*, 2011; Langille *et al.*, 2013; Wang *et al.*, 2016; Stefano *et al.*, 2017; Mayhew *et al.*, 2018; Filho *et al.*, 2019). Moreover, dysbiosis can predict exacerbations, and lung remodelling such as bronchiectasis and emphysema (Erb-Downward *et al.*, 2011; Langille *et al.*, 2013; Wang *et al.*, 2016; Stefano *et al.*, 2017; Mayhew *et al.*, 2018; Filho *et al.*, 2019). In patients with CF, bacterial infections have a great impact on morbidity and mortality (Moffatt and Cookson, 2017). Alterations of bacterial communities have been showed both during stable and exacerbation of CF. However, the changes seem to be patient-specific (Dickson *et al.*, 2016; Huang and LiPuma, 2017; Moffatt and Cookson, 2017). Despite this heterogeneity, a core microbiota has been proposed in CF and includes *Streptococcus*, *Prevotella*, *Rothia*, *Veillonella*, and *Actinomyces* (Coburn *et al.*, 2015; Blanchard and Waters, 2019). When classic CF pathogens such as *Pseudomonas*, *Burkholderia*, *Stenotrophomonas*, or *Achromobacter* are found in the LM of CF patients, they tend to predominate (Coburn *et al.*, 2015; Moffatt and Cookson, 2017; Blanchard and Waters, 2019). A decrease in bacterial diversity is also reported in CF patients but is more likely due to cumulative antibiotic exposure rather than an increase in disease severity (Dickson *et al.*, 2016). In bronchiectasis, the LM is also highly heterogeneous between patients, although Proteobacteria enrichment and predominance of *Pseudomonas*, *Haemophilus* and *Streptococcus* are frequently reported (Dickson *et al.*, 2016; Moffatt and Cookson, 2017; Richardson *et al.*, 2019). The predominance of *Pseudomonas* and *Haemophilus* in the LM is associated with disease progression and an increase in exacerbation frequency (Dickson *et al.*, 2016; Richardson *et al.*, 2019).

In IPF, the LM is suspected to induce alveolar epithelial lesions and apoptosis by itself and/or by activation of immune cells producing pro-inflammatory molecules and to modulate the host response. In addition, it is suspected to play a role as a cofactor of fibrosis initiation in genetically predisposed individuals (O'Dwyer *et al.*, 2019; Spagnolo *et al.*, 2019). Bacteria can trigger disease

progression as infections carry a high morbi-mortality, whereas immunosuppressive treatment increases the risk of death and hospitalizations (Fastrès *et al.*, 2017a; Spagnolo *et al.*, 2019). *Haemophilus influenzae*, *Haemophilus parainfluenzae*, *Streptococcus pneumoniae*, *Moraxella catarrhalis*, *Pseudomonas aeruginosa* and *Proteus mirabilis* have been identified by culture-dependent technique in 36% of IPF patients (n = 22), suggesting that occult bacterial infections may contribute to the development of IPF (Harrison, 2009). In their study on 55 IPF patients, Han and colleagues (2014) showed that *Prevotella*, *Veillonella* and *Escherichia* spp. are the most common species identified in IPF patients, although their presence is also reported in healthy LM (Han *et al.*, 2014). The presence of either a specific strain of *Streptococcus* spp. or *Staphylococcus* spp., which has been reported in less than half of the patients, is strongly associated with disease progression (Han *et al.*, 2014). Molyneaux and colleagues (2014) assessed the LM in BALF of 65 IPF patients and 44 controls and showed that the bacterial load was higher in IPF patients. Moreover, they showed that the baseline bacterial burden can predict disease progression and survival, findings which have been later confirmed (Molyneaux *et al.*, 2014; O'Dwyer *et al.*, 2019). Potentially pathogenic bacteria including *Haemophilus*, *Streptococcus*, *Neisseria* and *Veillonella* spp. have also been identified in higher abundance in IPF compared to healthy patients (Molyneaux *et al.*, 2014). Host-microbiome interactions have also been studied and a correlation has been found between the immune response, the abundance of specific bacteria and the survival (Huang *et al.*, 2017). Genetic mutations in genes involved in immune response are found in IPF that also lead to reduce bacterial clearance and altered immune response (Glass *et al.*, 2020). Finally, O'Dwyer and colleagues (2019) shown that dysbiosis precedes the peak of inflammation and the development of fibrosis in the lungs of bleomycin mouse model (O'Dwyer *et al.*, 2019). Moreover, germ-free mice are protected against mortality following bleomycin exposition even if they develop similar severity of fibrosis compared to conventional mice (O'Dwyer *et al.*, 2019).

The role of bacterial infections as a trigger of AE in IPF have also recently been investigated. Bacterial load is increased in AE (n = 20) compared with stable (n = 15) disease and a shift in bacterial communities is reported towards an increase in *Campylobacter* and *Stenotrophomonas* spp. and a decrease in *Veillonella* spp. (Molyneaux *et al.*, 2017a). However, in 170 IPF patients (48 with AE and 122 with a stable disease) in which 38 different bacterial strains including a majority of Gram-negative bacteria (89.5%) were detected, no differences in detection rate between stable and AE IPF patients was reported. *Klebsiella pneumonia*, *Mycobacterium tuberculosis* and *Acinetobacter baumannii* were the most abundant bacteria identified in both stable and AE IPF patients (Weng *et al.*, 2019). Those results suggest that dysbiosis can play a role in at least some cases of AE, although it remains unclear whether LM alteration is a cause or a consequence of AE (Molyneaux *et al.*, 2017a). Finally, the higher abundance of *Campylobacter* spp., a digestive bacteria, detected in AE supports the hypothesis of a role of GER in exacerbations development (Invernizzi and Molyneaux, 2019).

3. Single-cell mRNA sequencing

The first use of the scRNA-seq performed on a next-generation sequencing platform was reported in 2009 (Hedlund and Deng, 2018; Hwang, Lee and Bang, 2018; See *et al.*, 2018). The method allows the comprehensive quantification of gene-expression heterogeneity at the single-cell level (Hedlund and Deng, 2018; Hwang, Lee and Bang, 2018; Chen, Ning and Shi, 2019). Before the development of single-cell transcriptomic analysis strategies, bulk RNA-sequencing technologies have been widely used to study averaged gene expression across cell populations limiting the assessment of cellular heterogeneity. Indeed, the transcriptome can differ between cells even in similar cell types and this variability can be masked in bulk analysis (Hwang, Lee and Bang, 2018). It is important to be able to characterize cells as they are considered as the fundamental, structural and functional units of an organism (Mesh PubMed). They are working in concert to respond to stimuli in order to maintain health. Unfortunately, cell characterization using conventional flow cytometry techniques was also limited to a certain number of markers and required prior knowledges to identify cells (Salomon *et al.*, 2019). In the past several years, the scRNA-seq was used to overcome these limitations and study the biology at a microscopic resolution in an unbiased way (Hedlund and Deng, 2018).

As a consequence, the scRNA-seq reshaped our ability to identify novel cell types and states as well as to understand molecular processes of tissues in health and disease (Salomon *et al.*, 2019). It also provided insights into tissue cellular composition (Hedlund and Deng, 2018; Salomon *et al.*, 2019). Indeed, it has been widely used to dissect cellular heterogeneity in various tissue at different times and in different conditions for investigating developmental processes, cell responses to different stimuli/diseases/treatments, regulatory mechanisms, *etc.* (Haque *et al.*, 2017; Stubbington *et al.*, 2017; Hedlund and Deng, 2018; Papalexi and Satija, 2018; Salomon *et al.*, 2019). The technique has been used in humans (Muraro *et al.*, 2016; Mould *et al.*, 2019; Suryawanshi *et al.*, 2019), mice (He *et al.*, 2018) and other species (Davie *et al.*, 2018; Farnsworth *et al.*, 2020) but to our knowledge, not yet in dogs.

3.1. Method

Different methods of scRNA-seq have been developed (Hedlund and Deng, 2018; See *et al.*, 2018; Chen, Ning and Shi, 2019). However, we will focus on the droplet-based technique which was used in this work to assess in an unbiased way the heterogeneity of BALF cells and especially macrophages in dogs. This method has the advantage to be the most cost effective and time saving while at the same time increasing cellular throughput (Macosko *et al.*, 2015; Zheng *et al.*, 2017; Chen, Ning and Shi, 2019; Salomon *et al.*, 2019). Indeed, it works with small volume reaction chambers which results in decreasing reagents cost and increasing sensitivity (Macosko *et al.*, 2015; Salomon *et al.*, 2019).

The droplet-based scRNA-seq method relies on the rapid encapsulation of individual cells with barcoded beads in suspension into a water-in-oil droplet (Macosko *et al.*, 2015; Zheng *et al.*, 2017). The different steps of the process are resumed in Figure 9. Droplets are formed into a microfluidic system where water and oil are brought together at the junction between channels (Macosko *et al.*, 2015; Zheng *et al.*, 2017). New microfluidic platforms, such as the 10X Genomics Chromium system used in this work, are now capable of generating an emulsion of thousands of droplets in a few minutes (Zheng *et al.*, 2017; Salomon *et al.*, 2019). The emulsion results in the formation of gel beads in emulsion (GEMs) containing a single cell, a barcoded bead and different reagents. The barcoded beads are recovered by multiple oligonucleotides composed by: (1) sequencing adapters/primers for molecular amplification and sequencing of the transcripts; (2) cell barcode, an unique sequence of nucleotides identical to each oligonucleotide on the bead which allows the identification for each amplified transcript of the cell origin; (3) unique molecular identifier (UMI), an unique sequence of nucleotides that individually tag each polyadenylated RNA captured and allows the identification of PCR duplicates; and (4) poly-d(T) region to prime polyadenylated RNA transcripts (Macosko *et al.*, 2015; Zheng *et al.*, 2017; Salomon *et al.*, 2019). After encapsulation, cells are lyzed into the GEMs, polyadenylated RNA are linked by the poly-d(T) sequences on the bead and the reverse transcription (RT) occurs. During this first-strand synthesis, the cell barcode and the UMI are incorporated into the complementary DNA (cDNA) molecules (Zheng *et al.*, 2017). The emulsion is then broken and all the next steps are conducted onto the mix of all cDNAs obtained. Following the emulsion breakage, cDNAs are amplified via PCR. Libraries are prepared by incorporation of compatible adapters for sequencing and sequencing is then performed. After the sequencing, data generated must be processed into a matrix displaying for each cell the number of transcripts (UMIs) of each gene detected (Zheng *et al.*, 2017; Salomon *et al.*, 2019). Based on the matrix cells sharing similar transcriptomic information can be clustered. Using the differentially expressed genes (DEGs) between the clusters, each of them can be characterized. The identification of DEGs is also crucial for interpreting the biological differences between compared clusters and conditions. Enrichment in specific functions or phenomena can also be calculated by comparing DEGs with known gene lists (Macosko *et al.*, 2015; Zheng *et al.*, 2017; Stuart and Satija, 2019).

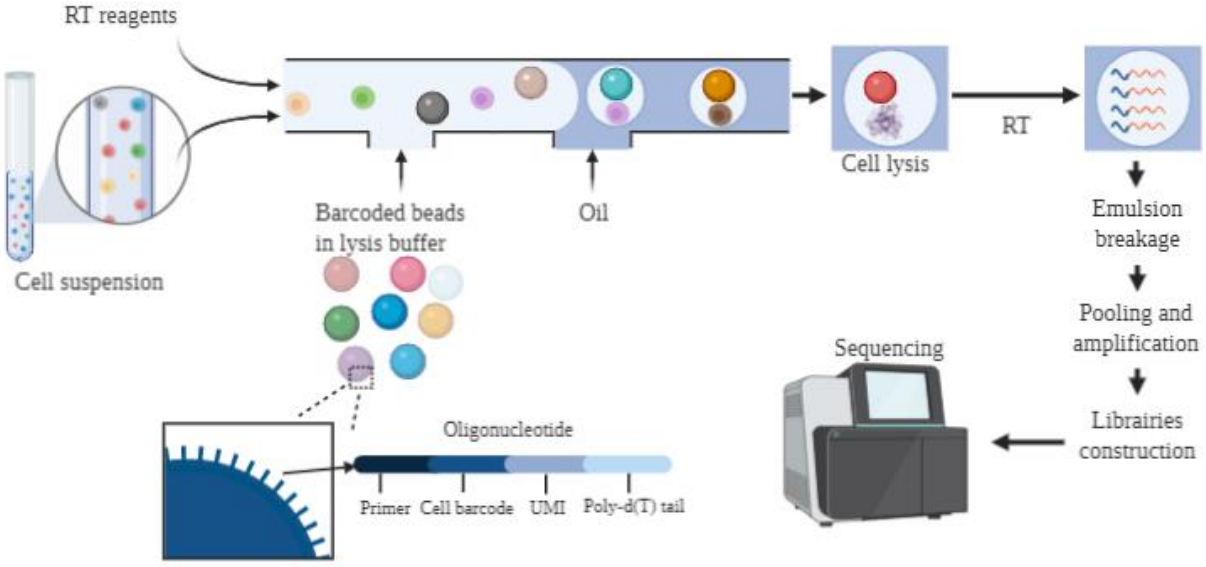

Figure 9. *Illustration of the single-cell mRNA sequencing process from the samples obtention to the sequencing. RT, reverse transcription; UMI, unique molecular identifier. Created in BioRender.com.*

3.2. Limitations

The droplet-based scRNA-seq technique has several limitations which have to be taken into account. First, the technique requires fresh samples that have to be rapidly processed to minimize the perturbation of the cell transcriptome after samples collection and to produce high quality transcriptomic data (Zheng *et al.*, 2017). Broken or dead cells can generate low-quality data and may lead to misinterpretation by releasing their RNA content into the suspension. The released material can be encapsulated within droplets and processed with a cell thereby changing its expression profile (Salomon *et al.*, 2019). The speed, reproducibility and high cell capture rate of droplet-based scRNA-seq methods allow to reduce this contamination (Zheng *et al.*, 2017; Chen, Ning and Shi, 2019). In addition, during encapsulation, a certain percentage of doublets (coencapsulation of 2 cells in the same droplet) can be achieved also conducting to misinterpretation of scRNA-seq data. Doublets can be prevented by reducing the concentration of both cells and beads which increases both waste and cost by reducing the droplet occupancy (Chen, Ning and Shi, 2019; Salomon *et al.*, 2019). Detection and removal of broken cells, dead cells and doublets can also be performed by controlling the scRNA-seq data quality which is crucial in such analysis. Accordingly, cells with few or extremely high number of reads corresponding respectively to broken/dead cells and doublets must be excluded. Detection of a higher rate of reads mapping to mitochondrial genome is also informative for identifying low-quality cells (Chen, Ning and Shi, 2019).

Secondly, with the Chromium 10X system, used in this work, the rate of coencapsulation of a cell and a bead into a droplet corresponds to ~50% of input cells (Zheng *et al.*, 2017). In addition, it has been established that only 10-20% of cell transcripts are captured and reverse transcribed (Hwang,

Lee and Bang, 2018). This low efficiency results in the misdetection of rare cell populations if insufficient cell numbers are analysed and in the inability to detect poorly expressed messenger RNAs (See *et al.*, 2018; Chen, Ning and Shi, 2019).

Finally, especially in dogs, the lack of annotation of the genome, as well as the lack of knowledge on cell identity markers are great challenges to overcome to provide sufficient information from samples using this method. Indeed, the mapping ratio of reads is an important indicator of the overall quality of scRNA-seq data (Chen, Ning and Shi, 2019). Incomplete genome database may prevent the identification of transcripts and the interpretation of the data.

Objectives

Objectives

In this work, we specifically decided to improve knowledge on CIPF pathogenesis by exploring LM dysbiosis and macrophage clusters alterations in the disease. Indeed, the importance of lung bacterial communities and their interaction with immune cells have gained interest in IPF pathogenesis but also in other lung diseases. A role for bacteria in the development and progression of lung diseases is strongly suspected. In the lung, bacterial communities are directly in contact with immune cells, especially macrophages which play an important role in tissue homeostasis. Macrophages represent almost 70% of all immune cells in the lung tissue and this percentage reaches more than 80% in BALF (O'Dwyer, Ashley and Moore, 2016; Yu *et al.*, 2016; Lee *et al.*, 2018; Zhang *et al.*, 2018; Nelson and Couto, 2020). The role of macrophages in lung diseases has also recently gained interest with the development of new technologies such as the scRNA-seq able to identify extremely heterogeneous cell populations upon different conditions (Desai *et al.*, 2018; Zhang *et al.*, 2018). In IPF, pro-fibrotic and pro-inflammatory macrophage clusters have been described promoting lung fibrosis and inflammation (O'Dwyer, Ashley and Moore, 2016; Heukels *et al.*, 2019). All these recent discoveries are in favour of an impact of the LM and the innate immunity in lung diseases and specifically in IPF which represent a promising field of investigation at the origin of the performance of this work.

1. Assessment of the lung microbiota in dogs

The role of microorganisms such as viruses and fungi has been investigated in CIPF WHWTs (Roels *et al.*, 2016; Roels *et al.*, 2017b). However, the potential role of bacteria in CIPF development and progression has not yet assessed. In IPF patients, bacterial infections have been associated with higher probability to develop IPF. Moreover, bacteria, directly or indirectly through immune response activation, are suspected to play a role in IPF onset, as well as in IPF progression and AE triggering (Molyneaux and Maher, 2013; Fastrès *et al.*, 2017a; Olson *et al.*, 2018; Sgalla *et al.*, 2018). The development of culture-independent techniques, at the origin of the performance of studies on bacterial populations, allowed a better understanding of the LM and its impact on lung diseases (Dickson *et al.*, 2016). Therefore, exploring lung bacterial communities and their alterations in WHWTs affected with CIPF was the first objective of this work.

At the time of the beginning of this thesis, only few studies on the LM were performed in dogs (Ericsson *et al.*, 2016; Roels *et al.*, 2017c; Fastrès *et al.*, 2017b), and factors able to change the canine LM were unknown. Accordingly, we first described the LM in healthy dogs, investigated factors known to alter it in other species and/or that could have an impact on our results on CIPF WHWTs. We also assessed the reliability of the 16S rDNA sequencing to study canine LM. Specifically, we aimed (1) to assess the short- and medium-term effect of a widely used oral antimicrobial drug on the

LM, as WHWTs and dogs with chronic respiratory diseases often have been treated or are being treated with antimicrobial drug at the time of their presentation; (2) to assess the LM in healthy dogs and study the impact of the breed and the living conditions on it in these dogs; and (3) to analyse the LM in dogs with an acute respiratory disease, the bordetellosis, and correlate results of the 16S rDNA amplicon sequencing with quantitative PCR (qPCR) and culture results, conventional techniques used to identify bacterial infection in dogs.

We then aimed to investigate the LM in WHWTs affected with CIPF compared with healthy age-matched WHWTs and healthy dogs from other breeds in order to describe variations of the LM associated with the disease and potential variations of the LM associated with the WHWT breed which could potentially predispose to the disease.

2. Assessment of macrophage clusters in canine bronchoalveolar lavage fluid

In the second part of this work, we wished to study macrophage populations in CIPF dogs via an unbiased approach, the scRNA-seq. As said in the introduction, the technique is recent and allows high-throughput and high-resolution transcriptomic analysis of thousands of cells at the same time without prior cell markers knowledge (See *et al.*, 2018; Poczobutt and Eickelberg, 2019; Stuart and Satija, 2019). The objective was to identify possible specific pro-fibrotic macrophage clusters, but also DEGs in diseased compared with healthy condition. We were interested in macrophages as they represent a large part of lung immune cells and they are the first cell in contact with lung bacterial communities. Moreover, in IPF studies, they are recognized to increase in number and to secrete high amount of pro-fibrotic molecules (O'Dwyer, Ashley and Moore, 2016; Desai *et al.*, 2018; Zhang *et al.*, 2018). With the use of scRNA-seq, pro-fibrotic roles for macrophages were also described in IPF patients and IPF mouse models suggesting that targeting either specific macrophage and monocyte clusters, or macrophages products could be useful for IPF prevention and treatment (Heukels *et al.*, 2019).

Therefore, our first aim was to validate the use of the scRNA-seq technique in BALF from healthy dogs. Indeed, the technique was quite recent and its use in dogs was not yet reported. Moreover, BALF cell populations were only phenotypically described by cytological examination and further BALF cell clusters were only investigated for lymphocytes by flow cytometry (Dirscherl *et al.*, 1995; Vail, Mahler and Soergel, 1995; Clercx *et al.*, 2002; Out *et al.*, 2002; Spużak *et al.*, 2008; Finke, 2013; Nelson and Couto, 2014). Accordingly, we also wished to provide an atlas of the canine BALF cells in healthy dogs which could be used after as a base resource for further investigations of the BALF cell subpopulations in disease conditions. Secondly, after validation of the scRNA-seq technique in canine BALF, we aimed to characterize using this tool disease-related heterogeneity within macrophage clusters in BALF from CIPF compared with healthy WHWTs.

Experimental section

Experimental section

Part 1 :

Assessment of the lung microbiota in dogs

Preamble

The first part of the experimental section groups three studies related to the LM in dogs. Figure 10 represents a summary of principal results obtained in these studies. In all those studies, the same technique was used to obtain LM data (Figure 10).

We first described the LM in healthy experimental and client-owned dogs and focused on factors able to affect the LM in healthy dogs (Figure 10) (Study 1 and study 2). We showed that oral antimicrobial drug administration changed the LM in a microbiologically predictable manner (Study 1). The LM seemed to return at its initial stage 2 weeks after the last administration of the drug (Study 1). In dogs, the living conditions, especially experimental compared with client-owned living conditions, had an impact on the LM and induced changes in bacterial richness and communities (Study 2). Discriminant taxa were identified in each canine breed, indicating also an impact of the breed on the LM (Study 2). However, no change in bacterial communities and ecological data were reported between breeds except in the WHWT breed (Study 2). Finally, we showed that in adult dogs, the age had no impact on the LM (Study 2).

In diseased conditions, the LM was first studied in dogs affected with *Bordetella bronchiseptica*, a bacterial agent of the canine infectious respiratory disease complex (CIRD-C) and results were compared with conventional culture-based and qPCR ones. Good agreement was found between the 16S rDNA amplicon sequencing and the culture and the PCR results (Study 3). A dysbiosis was highlighted in CIRD-C compared with healthy dogs (Figure 10) (Study 3). Finally, LM was investigated in WHWTs affected with CIPF compared to healthy WHWTs and healthy dogs from other breeds. In WHWTs either healthy or affected with CIPF, the LM was quite similar. *Brochothrix*, *Pseudarcicella*, *Curvibacter* and a genus belonging to Flavobacteriaceae family were more abundant in WHWTs compared with healthy dogs from other breeds and more abundant in CIPF WHWTs compared with healthy WHWTs, although not significantly (Figure 10). Results were in favour of the hypothesis that the LM alterations in CIPF WHWTs are most likely related to the breed and might accordingly be among the factors able to predispose to CIPF (Study 2).

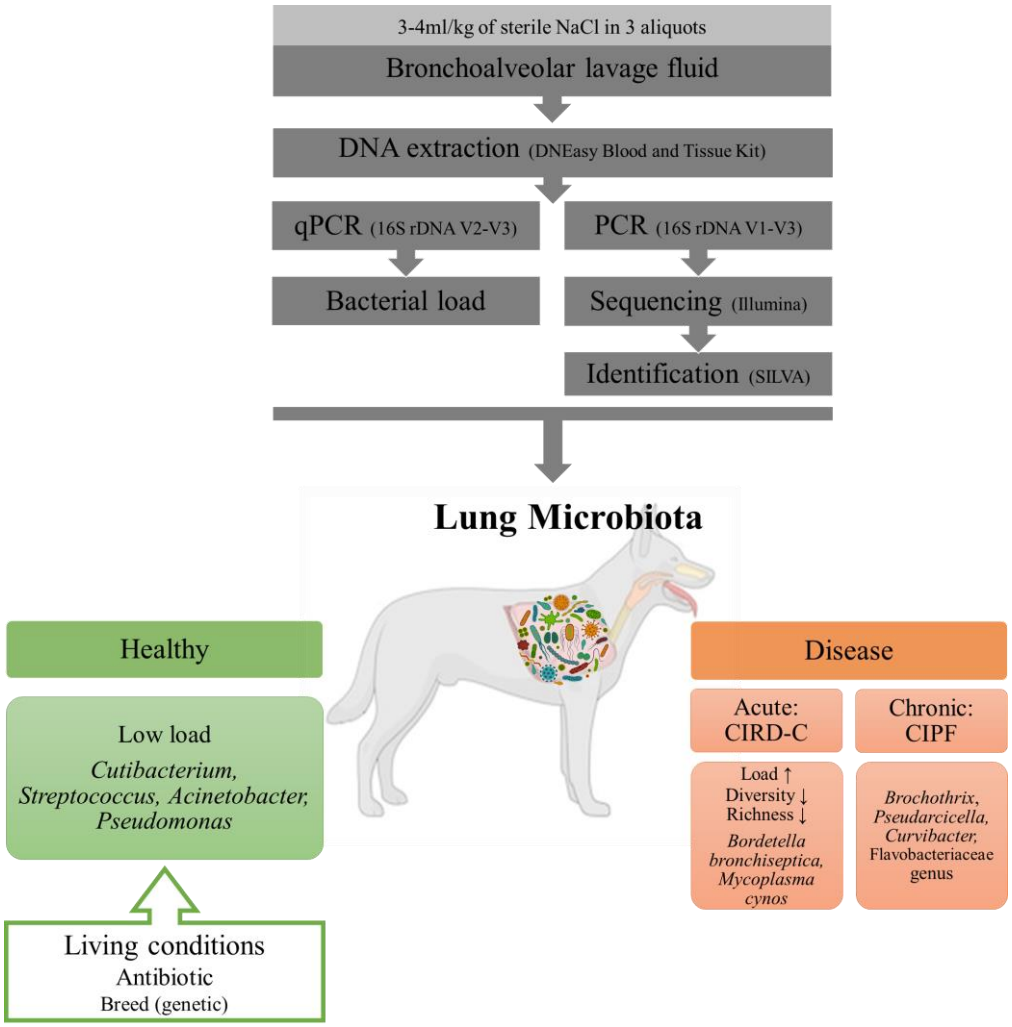

Figure 10. *Obtention, composition and factors affecting the lung microbiota (LM) (Study 1-3). LM data were obtained from bronchoalveolar lavage fluid and assessed using the 16S rDNA amplicon sequencing technique targeting the V1-V3 region of the gene. After sequencing, bacterial communities were identified with an operational taxonomic unit clustering distance of 97% of homogeneity based on the SILVA v1.32 database. Bacterial load was obtained by quantitative polymerase chain reaction (qPCR) targeting the V2-V3 region of the 16S rDNA. Four major genera colonize the airways of the healthy lung: Cutibacterium, Streptococcus, Acinetobacter and Pseudomonas. In healthy condition, the microbial density in the lung is low. Factors such as living conditions, antimicrobials drug administration and breed can influence the microbiota composition. In dogs affected with canine infectious respiratory disease complex (CIRD-C), a dysbiosis characterized by an increase in bacterial load, a decrease in richness and diversity and the domination of B. bronchiseptica and/or M. cynos was highlighted compared with healthy dogs. In West Highland white terriers (WHWTs) affected with canine idiopathic pulmonary fibrosis (CIPF), the LM was enriched with Brochothrix, Pseudarcicella, Curvibacter and a genus belonging to Flavobacteriaceae family, similarly compared with healthy WHWTs, although in higher proportion.*

Experimental section

Part 1

Study 1 :

Effect of an antimicrobial drug on lung microbiota in healthy dogs

Heliyon 5:e02802

Aline Fastrès, Bernard Taminiau, Emilie Vangrinsven, Alexandru-Cosmin Tutunaru, Evelyne Moyse, Frederic Farnir, Georges Daube, Cécile Clercx

Abstract

Alterations of the lung microbiota (LM) are associated with clinical features in chronic lung diseases (CLDs) with growing evidence that an altered LM contributes to the pathogenesis of such disorders. The common use of antimicrobial drugs in the management of CLDs likely represents a confounding factor in the study of the LM. The aim of the present study was to assess the effect of oral administration of amoxicillin/clavulanic acid (AC) on the LM in healthy dogs ($n = 6$) at short (immediately after stopping AC [D10]) and medium-term (16 days after stopping AC [D26]).

Metagenetic analyses were performed on the V1–V3 hypervariable region of 16S rDNA after extraction of total bacterial DNA from samples of bronchoalveolar lavage fluid (BALF).

AC did not induce significant changes in BALF cellular counts or in the bacterial load or microbial richness, evenness and α-diversity, while the β-diversity was clearly modified at D10 compared with D0 (before AC administration) and D26 ($P < 0.01$). The relative abundance of Bacteroidetes and Proteobacteria increased at D10 ($P < 0.01$) in comparison with D0 and D26 ($P < 0.01$). The relative abundance of Firmicutes decreased from D0 to D10 ($P < 0.01$) and increased from D10 to D26 ($P < 0.01$), but was still lower than at D0 ($P < 0.01$). The proportion of Actinobacteria increased at D26 compared with D0 and D10 ($P < 0.01$).

Significant differences between timepoints at the level of family, genus or species were not found. In conclusion, in healthy dogs, oral administration of AC induces significant changes in LM at the phyla level and in the β-diversity. Most changes normalize within 2 weeks after discontinuation of AC.

Introduction

The lung microbiota (LM) represents the collection of microbes from the lung (Segal *et al.*, 2014). In healthy people, the lung microbiota closely resembles that of the oral cavity, although the bacterial biomass is lower (Dickson *et al.*, 2016). In order to study the LM, at least in healthy individuals, bronchoalveolar lavage (BAL) is considered to be an acceptable sampling method (Dickson *et al.*, 2015). In the majority of human chronic lung diseases (CLDs), LM alterations have been associated with the disease (Costa *et al.*, 2018). However, whether the LM alterations represent a cause or a consequence of the disease is still not clear (Fastrès *et al.*, 2017a; Huang *et al.*, 2017). In dogs, the LM has been studied much more recently than in man and the literature is sparse (Ericsson *et al.*, 2016; Roels *et al.*, 2017c). Ericsson et al. (2016) assessed the LM from samples of bronchoalveolar lavage fluid (BALF) in healthy adult experimental beagle dogs (Ericsson *et al.*, 2016). They found that the LM was dominated by the phylum Proteobacteria with a relative abundance of >80%. In parallel, the LM from BALF obtained in healthy adult experimental beagle dogs and client-owned dogs from another breed was studied (Roels *et al.*, 2017c); results suggest a possible effect on the LM of breed and/or living conditions (Ericsson *et al.*, 2016; Roels *et al.*, 2017c).

In man, the effect of antimicrobial drugs on the gut microbiota has been investigated and a decrease in richness, diversity and modification in up to 30% of the relative abundance of the taxa was shown (Zaura *et al.*, 2015; Thiemann *et al.*, 2016). Recently, the LM has been shown to be altered by antimicrobial treatment in mice (Dickson *et al.*, 2018). To our knowledge, the effect of antimicrobial drugs on the LM in healthy individuals has not yet been investigated neither in man nor in dogs.

In the context of the study of the LM alterations in CLD, and since canine patients with CLD often have been treated or are being treated with antimicrobial treatment at the time of referral, there is a need to know how antimicrobial drugs interfere with the LM. Moreover, the time delay needed after cessation of treatment, in order to avoid any interaction of the drug with the LM, has not yet been studied. Therefore, the aim of the present study was to assess the short- and medium-term effect of a widely used oral antimicrobial drug on the LM in healthy adult dogs. The results of the study should provide key information for further investigations of the role of the LM in canine CLDs.

Materials and methods

1. Dog population

Six healthy experimental beagle dogs (four females and two males) aged between 1 and 11 years (mean 4.4 years), with a mean ± standard deviation body weight of 13.6 ± 1.3 kg, were included in the experimental study approved by the Ethical Committee of the University of Liège (protocol #1910). The dogs were housed on woodchip litter with outdoor access for 3–6 h each day. They had access to clean drinking water ad libitum and were fed with premium commercial dry food. There was no modification in the diet or the living conditions during the study period. The dogs did not receive any antimicrobial drug for at least 1 year prior to the study. At inclusion, the dogs were confirmed to be healthy, based on absence of clinical signs, normal physical examination, normal haematology and serum biochemistry analysis, normal gross appearance during bronchoscopy, and absence of abnormalities in the BALF analysis.

2. Protocol

For each dog, 20 mg/kg of amoxicillin/clavulanic acid (AC) (Amoxiclav-VMD, VMD, Arendonk, Belgium) was administered orally twice daily for 10 days. BALF sampling was repeated on each dog at three different timepoints: before AC administration (D0) and immediately (D10) as well as 16 days (D26) after discontinuation of AC.

3. Samples collection and processing

Dogs were anaesthetized without intubation. The bronchoscope was cleaned and disinfected before each use. A procedural control specimen (PCS) was obtained prior to each BAL procedure by injection of 10 mL of sterile saline solution through the bronchoscope channel followed by aspiration through the same channel into a sterile container using a low-power suction pump. The bronchoscope was then inserted through the oral cavity of the dog. The BAL was performed by injecting 3–4 mL/kg of sterile saline solution divided into three aliquots, including two aliquots with the endoscope inserted into the right diaphragmatic lobe, followed by a third aliquot placed into the left diaphragmatic lobe. Each aliquot was directly aspirated by gentle suction and the fluids recovered from the three aliquots were pooled. After sampling, both PCS and BALF were transferred into cryotubes and stored at -80C until analysis. A small amount of BALF was used for calculation of the total cell count (TCC) as well as for cytospin preparation (centrifugation at 221 g, for 4 min at 20C, Thermo Shandon Cytospin©4). Cytospin preparations were stained by Diff Quick and were used for differential cell count (DCC) determination by counting a minimum of 100 cells.

4. 16S rDNA extraction and high throughput sequencing

The analysis of the LM for all dogs and for all 3 timepoints was performed on a single occasion for each step of the LM analysis which included DNA extraction, polymerase chain reactions (PCRs), sequencing and post-sequencing analysis. As required, strict laboratory controls were done to avoid contamination from the PCR reagents and laboratory materials.

Total DNA was extracted from BALFs and PCSs using the DNEasy Blood and Tissue kit (QIAGEN Benelux BV, Antwerp, Belgium) according to the manufacturer's instructions. DNA was eluted into DNase/RNase free water for a total volume of 30µL and the concentration and purity were evaluated using an ND-1000 spectrophotometer (NanoDrop ND1000, Isogen, De Meern, The Netherlands).

The bacterial load was assessed by quantitative PCRs (qPCRs) targeting the V2–V3 region of the 16S rDNA. Duplicate qPCRs were conducted in a final volume of 20 µL containing 2.5 µL of template DNA, 0.5 µL of forward primer (5'-ACTCCTACGGGAGGCAGCAG-3'; 0.5 µM), 0.5 µL of reverse primer (5'-ATTACCGCGGCTGCTGG-3'; 0.5 µM) [12], 10 µL of No Rox SYBR 2x MasterMix (Eurogentec, Seraing, Belgium), and 6.5 µL of water. The run also contained non-template controls and a 10-fold dilution series of a V2–V3 purified (Wizard®SV Gel and PCR Clean-Up System, Promega, Leiden, The Netherlands) PCR product quantified by PicoGreen targeting double-stranded DNA (Promega, Leiden, The Netherlands) and used to build the standard curve. Data acquisition was obtained using an ABI 7300 real-time PCR system, with the following cycling sequence: 1 cycle of 50°C for 2 min; 1 cycle of 95°C for 10 min; 40 cycles of 94C for 15 s; and 1 cycle of 60°C for 1 min. After the PCR, a melting curve was constructed in the range of 64–99°C. Results were expressed in logarithm base 10 copy numbers per millilitre.

For bacterial identification, PCR targeting the V1–V3 region of the 16S rDNA was performed with the following primers: forward (5'-GAGAGTTTGATYMTGGCTCAG-3') and reverse (5'-ACCGCGGCTGCTGGCAC-3') and Illumina overhand adapters (Ngo *et al.*, 2018). Amplicons were purified with the Agencourt AMPure XP beads kit (Beckman Coulter, Villepinte, France) and submitted to a second PCR for indexing using the Nextera XT index primers 1 and 2. After purification, amplicons were quantified by PicoGreen (ThermoFisher Scientific, Waltham, MA, USA) before normalization and pooling. PCSs and the negative control from the extraction and the PCR steps were not sequenced as their PCR products after amplification were <1 ng/µL. Bacterial 16S rDNA amplicon libraries were then sequenced on a MiSeq Illumina sequencer using V3 reagents. A positive control using 20 defined bacterial species DNA was included in the run. Sequence read processing including a first cleaning step for length and sequence quality and a screening for chimera with UCHIME algorithm was made using, respectively, MOTHUR v1.39 and Vsearch (Edgar *et al.*,

2011; Rognes *et al.*, 2016). 16S rDNA reference alignment and taxonomical assignation with an operational taxonomic unit (OTU) clustering distance of 0.03 were based on the SILVA database v1.32 using the cluster.split command in MOTHUR v1.39 (Kozich *et al.*, 2013). A final subsampling was performed to have an identical mean of reads per samples at 5,400 reads.

5. Data analysis

Comparisons between events for TCC, DCC and the bacterial load were made using Friedman tests in XLStat (Addinsoft, Paris, France).

Good's coverage index and ecological indicators, including the bacterial richness (Chao1 index), evenness (Simpson index-based measure) and α-diversity (inverse Simpson's index) were calculated with MOTHUR v1.39 and compared between timepoints using Friedman tests in XLStat.

Non-metric multidimensional scaling (NMDS) graph was performed based on a Bray-Curtis dissimilarity matrix at the species level to assess the global bacterial composition (β-diversity) between timepoints (R vegan package). Significant differences between timepoints were calculated with MOTHUR v1.39 using AMOVA and HOMOVA tests. The AMOVA test is a non-parametric analysis for testing the hypothesis that genetic diversity within each timepoint is not significantly different from the genetic diversity in all timepoints together (Schloss, 2013). The HOMOVA test is a nonparametric analysis used to test the hypothesis that the genetic diversity within the different timepoints is homogeneous (Schloss, 2018).

Differences in bacterial relative abundances between timepoints were assessed in R using a mixed linear model with Benjamini Hotchberg FDR correction for multiple comparisons.

Results were expressed as median and interquartile range.

All sample raw reads were deposited at the National Centre for Biotechnology Information (NCBI) and are available under Bioproject ID PRJNA507075.

Results

1. BALF cell analysis

There were no significant differences between timepoints for TCC and DCC (Table 1).

Table 1. *Median and interquartile range of the total and differential bronchoalveolar lavage fluid cell count between timepoints.*

Timepoints	Total cell count cells/µL	Macrophages %	Neutrophils %	Lymphocytes %	Eosinophils %
D0	800.0 (702.5-890.0)	82.5 (80.0-86.5)	5.5 (4.2-7.5)	6.0 (0.2-17.0)	2.0 (1.2-2.8)
D10	470.0 (275.0-635.0)	92.0 (90.2-98.2)	3.0 (0-6.0)	0.5 (0-2.5)	1.5 (0.2-2.0)
D26	220.0 (125.0-330.0)	78.0 (74.8-81.2)	5.0 (4.2-9.5)	9.0 (7.0-11.8)	0.5 (0-4.0)
P-value between the 3 timepoints	0.07	0.07	0.31	0.40	0.25

D0, before antimicrobial drug administration; D10, just after antimicrobial drug discontinuation; D26, 16 days after antimicrobial drug discontinuation.

2. BALF microbiota analysis

Good's coverage index was >95.91% in all samples (98.74% (97.22–99.04)) and was not different between timepoints (P = 0.31) indicating the same sampling effort per timepoint. A total of 2,236,209 reads were recovered with a median length of 498 nucleotides. After the first cleaning step, 1,691,396 reads were kept and screened for chimera. 1,607,398 reads per samples were retained and used for OTU clustering before the final subsampling.

The differences in the bacterial load between timepoints were not significant (P = 0.51) (Figure 1). In PCSs, the bacterial load was 2.46 (2.41–2.65) copies per millilitre; about 100 times lower than in the BALF samples.

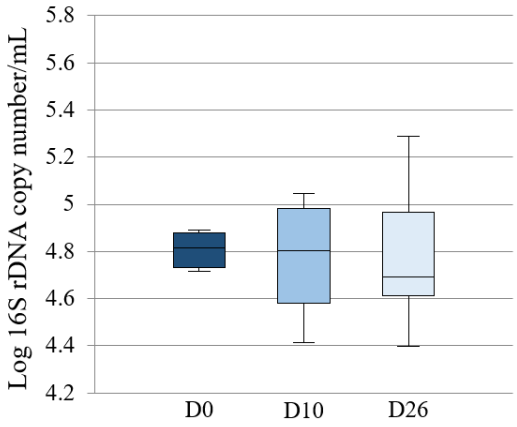

Figure 1. *Box plot representing the logarithm of the number of 16S rDNA copies per microliter (bacterial load) between timepoints. The medians are represented by the central horizontal bars. The lower and upper limits of the box are the first and third quartiles, respectively. There were no significant differences between timepoints.*

Phyla, families, genera and species making up the dog's LM, before AC administration, with a relative abundance of >1.00%, are presented in Table 2.

Table 2. *The top 25 most abundant taxa present in the lung microbiota at the level of phyla, families, genera and species in healthy dogs before administration of the antimicrobial drug.*

Phylum	Family	Genus	Species	Median relative abundance, %
Firmicutes	Streptococcaceae	*Streptococcus*	*Streptococcus mitis*	3.5 (2.1-4.1)
			Streptococcus cristatus	0.5 (0.2-0.8)
			Streptococcus salivarius	0.4 (0-1.0)
	Staphylococcaceae	*Staphylococcus*	*Staphylococcus epidermidis*	1.8 (1.7-2.7)
			Staphylococcus warneri	0.8 (0.4-2.2)
			Staphylococcus xylosus	0.5 (0.1-0.7)
	Erysipelotrichaceae	*Allobaculum*	*Allobaculum* HM124340	1.3 (0.1-3.5)
			Allobaculum DQ113686	0.5 (0.2-1.3)
			Allobaculum 16S_OTU48	0.3 (0-1.3)
		Turicibacter	*Turicibacter* FJ880353	0.3 (0.1-0.6)
	Veillonellaceae	*Veillonella*	*Veillonella* JQ449520	1.1 (0.8-1.4)
	Bacillales Family XI	*Gemella*	*Gemella haemolysans*	0.9 (0.4-1.0)
Actinobacteria	Propionibacteriaceae	*Propionibacterium*	*Propionibacterium acnes*	7.0 (5.2-17.0)
	Corynebacteriaceae	*Corynebacterium_1*	*Corynebacterium_1 tuberculostearicum*	1.1 (0.4-1.5)
	Micrococcaceae	*Micrococcus*	*Micrococcus luteus*	0.6 (0.4-0.8)
		Rothia	*Rothia mucilaginosa*	0.6 (0.1-1.0)
			Rothia dentocariosa	0.4 (0-0.9)
Proteobacteria	Moraxellaceae	*Acinetobacter*	*Acinetobacter_johnsonii*	0.4 (0.1-2.5)
		Enhydrabacter	*Enhydrobacter_osloensis*	0.4 (0.1-1.0)
Bacteroidetes	Flavobacteriaceae	*Flavobacterium*	*Flavobacterium* EU802240	0.7 (0.1-1.1)
		Elizabethkingia	*Elizabethkingia miricola*	0.6 (0.1-1.0)
		Chryseobacterium	*Chryseobacterium haifense*	0.4 (0-1.0)
Fusobacteria	Fusobacteriaceae	*Fusobacterium*	*Fusobacterium* AJ867041	0.6 (0-1.6)
			Fusobacterium nucleatum	0.4 (0.1-0.9)
Verrucomicrobia	Verrucomicrobiaceae	*Verrucomicrobiaceae_ge*	*Verrucomicrobiaceae_ge* 16S_OTU17	0.8 (0.4-2.2)

The relative abundances are presented in median and interquartile range.

The bacterial richness, evenness and α-diversity were not significantly modified between timepoints (P = 0.31, 0.61 and 0.85 respectively) (Figure 2).

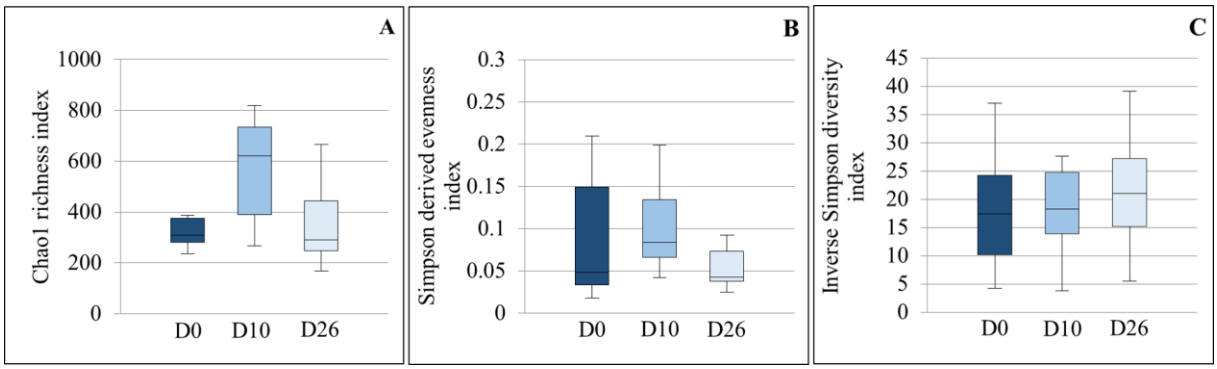

Figure 2. *Box plot graphs representing the bacterial richness (A), evenness (B) and alpha diversity (C) at the 3 timepoints. The medians are represented by the central horizontal bars. The lower and upper limits of the box are the first and third quartiles, respectively.*

The NMDS graph of the β-diversity showed clear differences between D10 and the other timepoints (Figure 3). Significant differences were found between timepoints with the AMOVA test ($P < 0.001$) with significant differences in the post-hoc tests between D0 and D10 ($P = 0.002$) and D10 and D26 ($P < 0.001$), but not between D0 and D26. The HOMOVA test showed significant differences between timepoints ($P = 0.009$) with significant difference in the post-hoc tests only between D10 and D26 ($P = 0.004$).

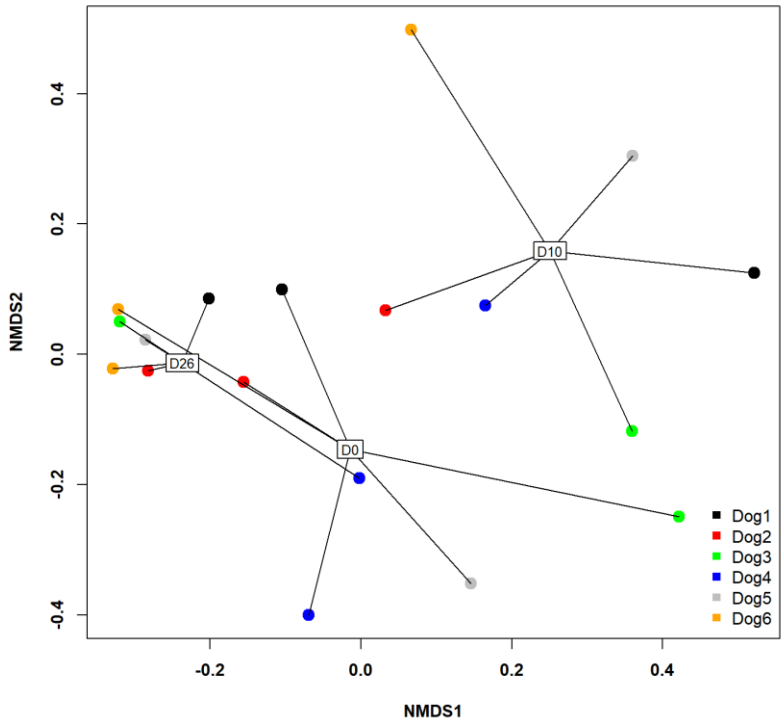

Figure 3. *Two-dimensional non-parametric representation of the global bacterial composition at the species level between timepoints for each dog based on a Bray-Curtis matrix of dissimilarity. Lung communities are clustered by timepoints. D0: before antimicrobial administration; D10: just after antimicrobial discontinuation; D26: 16 days after antimicrobial discontinuation; NMDS: non-metric multidimensional scaling.*

Figure 4 illustrates the distribution of bacterial relative abundance at the phyla level in all dogs at the different timepoints. The Bacteroidetes (Figure 5A), the Proteobacteria (Figure 5B), the Firmicutes (Figure 5C) and the Actinobacteria (Figure 5D) were significantly different between timepoints. No significant differences were shown between timepoints at the level of families, genera and species. However, as shown in Figure 6, at D10, some genera decreased, such as *Streptococcus spp.* (Firmicutes), *Staphylococcus spp.* (Firmicutes) and *Lactobacillus spp.* (Firmicutes), others increased, such as *Pseudomonas spp.* (Proteobacteria), *Flavobacterium spp.* (Bacteroidetes) and *Chryseobacterium spp.* (Bacteroidetes), while some remained stable, such as *Propionibacterium spp.*

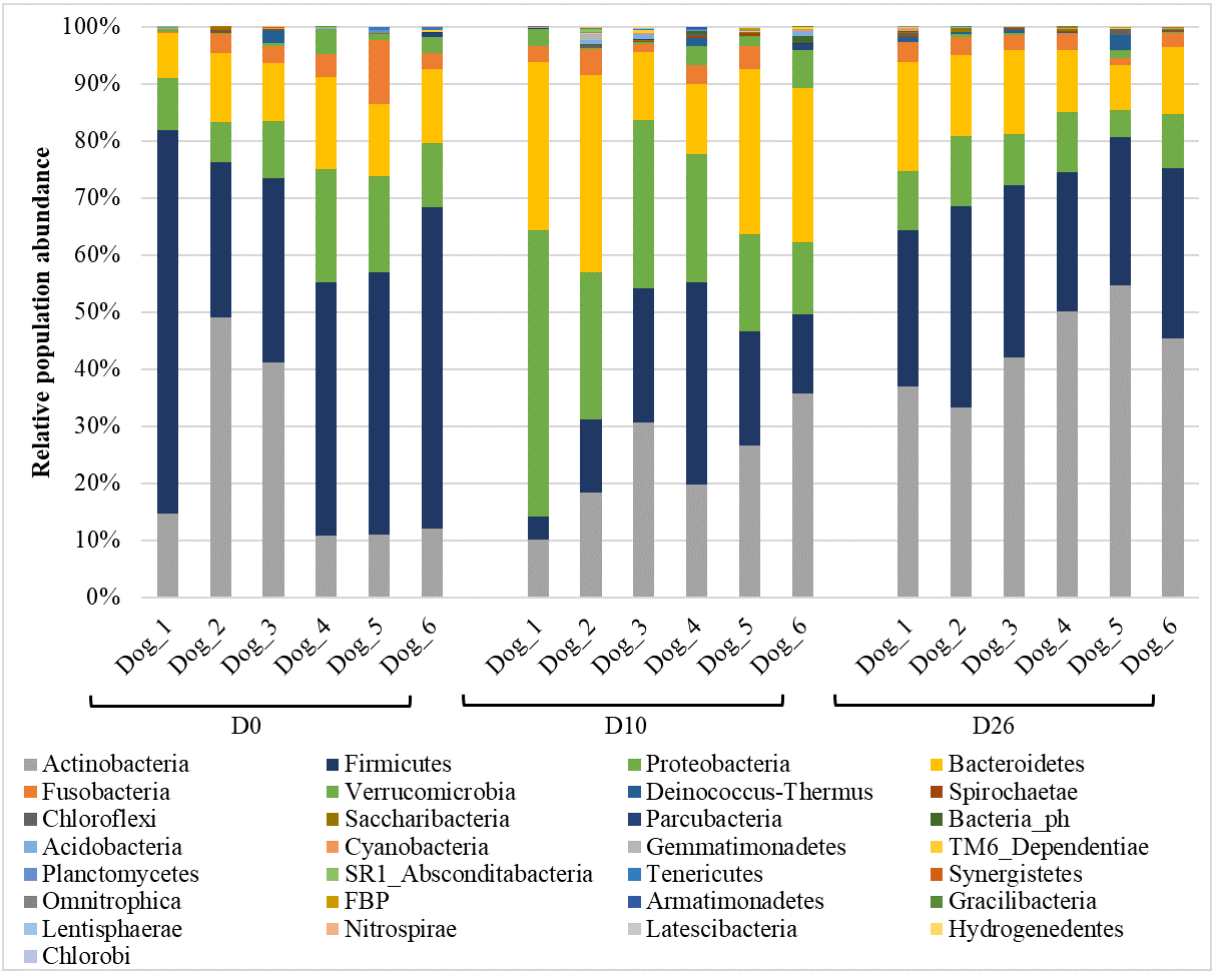

(Actinobacteria).

Figure 4. *Phyla-level composition of bronchoalveolar lavage fluid (BALF) microbiota at the 3 timepoints. Bar charts showing relative abundance annotated to the taxonomic level of phylum of all taxa detected in BALF collected from 6 healthy adult beagle dogs, before (D0) and 10 days (D10) as well as 16 days after the discontinuation of the drug.*

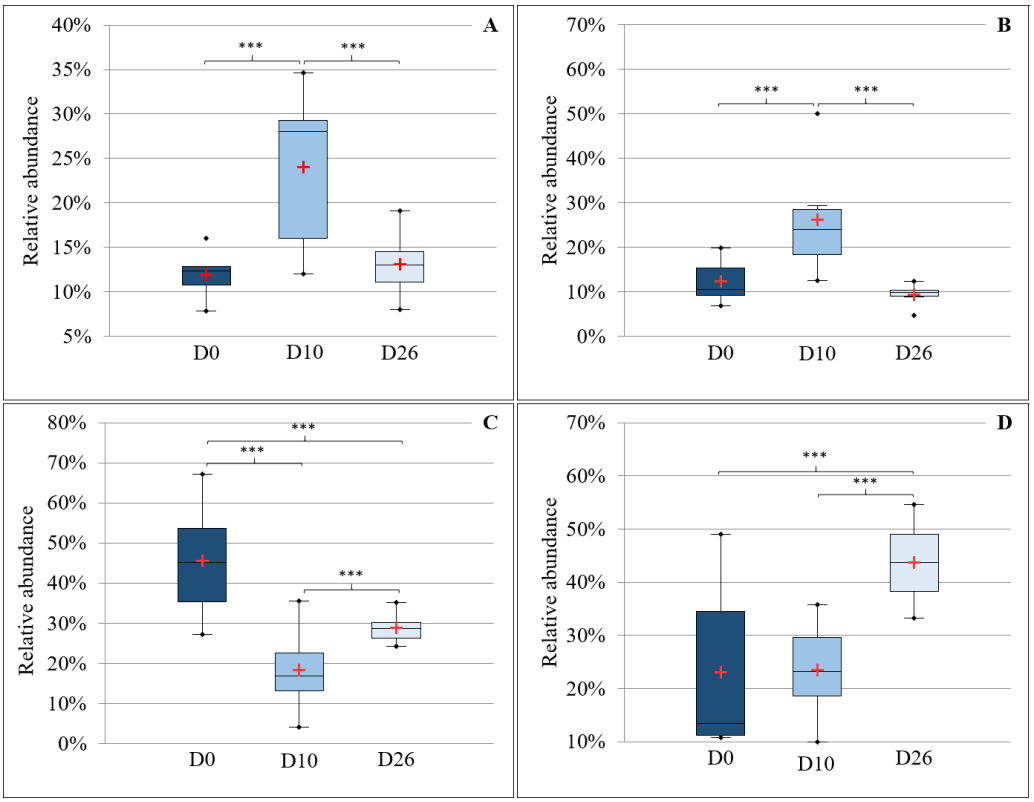

Figure 5. *Box plot graphs representing Bacteroidetes (A), Proteobacteria (B), Firmicutes (C) and Actinobacteria (D) relative abundances between timepoints. The means and the medians are represented by the cross and the central horizontal bars respectively. The lower and upper limits of the box are the first and third quartiles, respectively. Points are considered as outliers. ***Statistically different (P<0.001).*

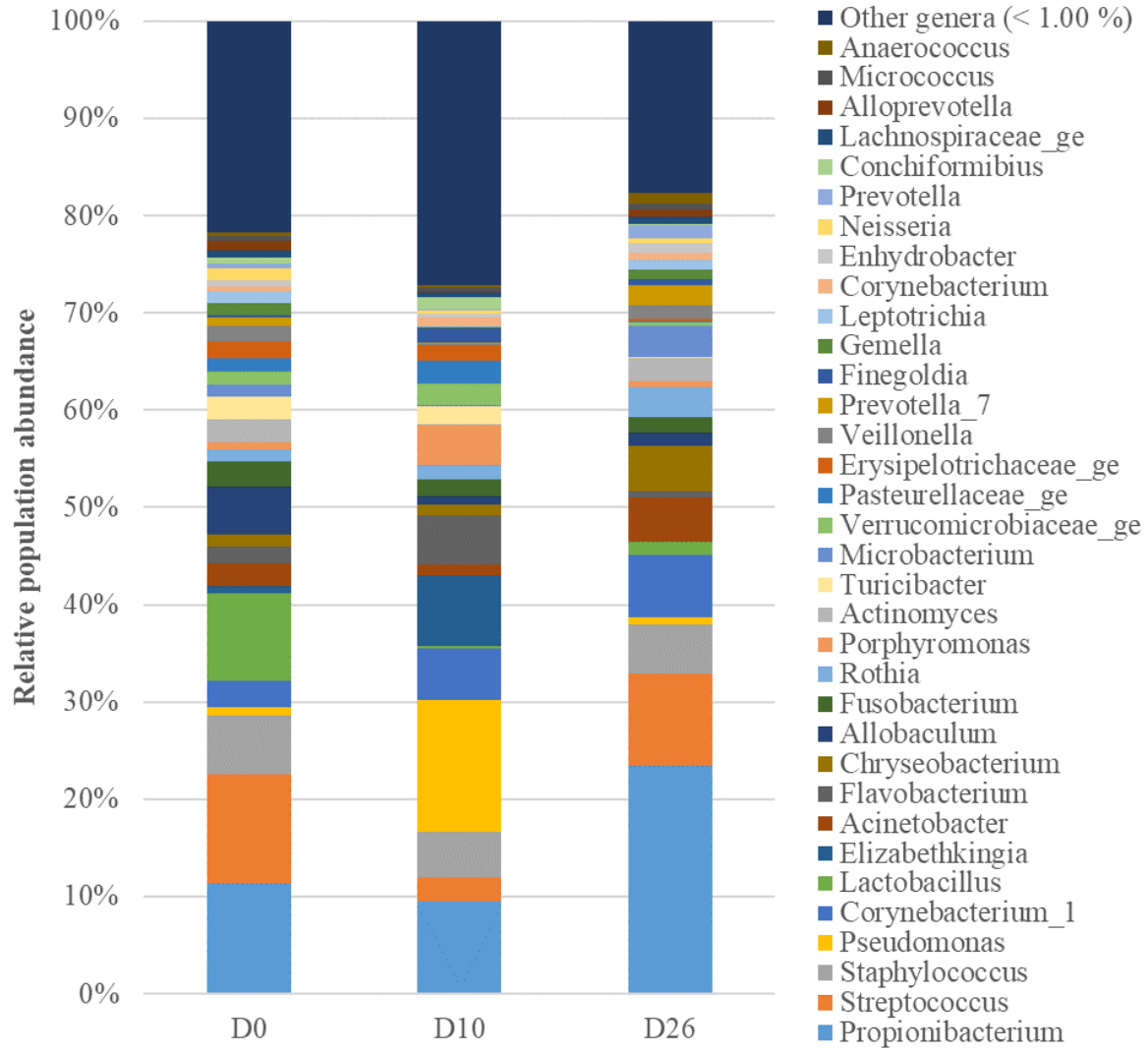

Figure 6. *Genus-level composition of bronchoalveolar lavage fluid (BALF) microbiota at the 3 timepoints. Bar charts showing relative abundance annotated to the taxonomic level of genus of all taxa detected in BALF collected from 6 healthy adult beagle dogs, before (D0) and 10 days (D10) as well as 16 days after the discontinuation of the antimicrobial drug.*

Discussion

To the best of our knowledge, this is the first study in dogs investigating how an antimicrobial drug interferes with the LM. Since the use of antimicrobial drugs such as oral treatment with AC is common in the management of canine CLDs, this study is a prerequisite before assessing the role of alterations of the LM in the pathogenesis of canine CLDs. In the present study, oral administration of AC to healthy beagles induced an obvious shift in the β-diversity of the LM as well as significant changes in the proportion of the major phyla, and the majority of these changes were no longer present at 2 weeks after drug discontinuation. Furthermore, the bacterial load and the ecological indices of richness, evenness and α-diversity were not significantly modified.

In the study of the LM, avoiding bacterial contamination is crucial, because of the low bacterial biomass of the respiratory tract (Dickson *et al.*, 2016; Marsh *et al.*, 2018). Amplification of contaminants could modify the data obtained and provide aberrant results (Salter *et al.*, 2014). Origins of contamination can be numerous and may occur at different steps involving the laboratory analyses, the materials, mainly the bronchoscope, and the sampling procedure (Salter *et al.*, 2014; Dickson *et al.*, 2017a). In order to minimize contamination from extraction and sequencing reagents, strict laboratory controls of all reagents and machines were performed. PCSs were collected before each sampling in order to detect contamination via the bronchoscope itself, the sterile saline solution and the device used for the lavage. In the present study, analysis of PCSs indicated that this source of contamination could only minimally alter our results (Bassis *et al.*, 2015). Finally, during the procedure, care was taken to avoid contact with the oropharyngeal, laryngeal and tracheal mucosae during insertion of the bronchoscope. In spite of these handling precautions, some contamination during passage of the bronchoscope through the upper airway cannot be excluded. However, it has been shown that such contamination only minimally alters the LM in bronchoscopically-acquired specimens (Bassis *et al.*, 2015; Dickson *et al.*, 2015; Dickson *et al.*, 2017a).

In the present study, the four major phyla (Firmicutes, Actinobacteria, Proteobacteria and Bacteroidetes) found in the lung of healthy beagles were the same as described in previous studies in beagles, although the abundance order differed (Ericsson *et al.*, 2016; Roels *et al.*, 2017c). The observed differences in relative abundance of major phyla can be attributed to several factors. Firstly, the LM largely depends on the environmental conditions (Dickson *et al.*, 2016; Lloyd and Marsland, 2017) and differences in housing, type of food, geographical area and dog behaviour may have had an impact on the LM (Dickson and Huffnagle, 2015; Dickson *et al.*, 2016). Secondly, the technique used to sample and analyse BALF in the present study differs from that used by Ericsson et al. (2016), in which a catheter was passed through a sterile endotracheal tube to collect the BALF. In the present study the use of a bronchoscope was chosen, according to a technique that has been approved for investigation of the LM in man (Bassis *et al.*, 2015). Finally, the relative abundance of Firmicutes in

this study compared with others performed on beagles was higher. This elevated percentage of Firmicutes might have been slightly overestimated because bacteria composing the Firmicutes phylum appear to have more 16S rDNA copies in their genome than bacteria in other phyla (Větrovský and Baldrian, 2013).

In order to limit the variations between samples related to contamination or factors influencing the LM as mentioned above, the dogs in the present study were from the same breed, co-housed in a stable environment and fed with the same standardized diet. The sampling procedure was highly standardized and repeated identically at the three timepoints. Moreover, each step of the LM analysis (DNA extraction, PCRs, sequencing and post sequencing analysis) was performed at a single occasion for all samples together (from all dogs and from all 3 timepoints).

The stability of the LM over time is an important source of experimental and clinical variability and might have interfered with our results. Indeed, it has been shown in mice, that the LM is dynamic and rapidly converges in cohoused mice placed in shared cages (Dickson *et al.*, 2018). Dogs of our study were housed in the same conditions before and during the study period. As a consequence, it is reasonable to expect that such a stable environment helped to reduce time-induced variations.

AC, a beta-lactam antimicrobial drug, is a broad-spectrum antimicrobial drug acting against Gram-positive and to a lesser extent Gram-negative bacteria (Kaur *et al.*, 2011). AC was chosen as an antimicrobial agent since it is largely used by veterinarians in dogs with lower airway disease. Moreover, AC is a drug recommended in both human and veterinary medicine for the treatment of acute pneumonia, including acute aspiration pneumonia (File, 2007; Lappin *et al.*, 2017). The dosage currently used in canine practice and recommended for pulmonary infections was used (Plumb, 2015).

Significant modifications were found at the phyla level after AC administration. As expected, the Firmicutes phylum mainly represented by bacteria that are sensitive to AC decreased. The increased relative abundance in the phylum Proteobacteria appeared to be related to an increase in the genus Pseudomonas spp., which is known to be resistant to AC (Plumb, 2015). Finally, the main genera composing the phylum Bacteroidetes increased at D10 were Gram-negative bacteria which are less sensitive to AC (Kaur *et al.*, 2011). According to these results and to the significant modification in the β-diversity shown just after discontinuation of the drug, AC appears to have an effect on the LM in healthy dogs, even if differences were not significant under the phyla level.

Absence of significant differences in the relative abundances under the phyla level and in bacterial load, richness, evenness and α-diversity might be attributed to a possible high resilience of the LM to disturbances, compared with microbiota from other sites of the body. Such a hypothesis is

supported by the fact that differences in resilience of microbiota have been shown, according to their niche. For example, the salivary microbiota was shown to be more resilient to disturbance after antimicrobial drug administration compared to that of the gut (Zaura *et al.*, 2015). Another explanation would be that in healthy individuals, such as the dogs in this study, the permeability of the alveolar-capillary wall is lower than in diseased lungs (Brusse-Keizer *et al.*, 2015), leading to a limited penetration of AC into the parenchyma and airways and therefore a limited effect on the LM. Indeed, it has been shown that amoxicillin concentration in the sputum in man may differ according to different host- and drug-related factors, such as alveolar-capillary permeability (Pennington, 1981; Honeybourne, 1994). As alveolar-capillary permeability increases in the case of inflammation, the concentration of AC, which passively diffuses in the alveolar space (Honeybourne, 1994), is probably decreased in healthy airways. It should be remembered that the use of another antimicrobial drug with improved airways penetration could have induced different LM modifications.

The inability to highlight significant differences under the phyla level might also be due to the number of data, including about 5,400 sequences per sample, as well as to the limited number of dogs included in the study. This contributed to a lack of power of the statistical tests mainly associated with the corrections for multiple tests more significant with a large dataset (Desquilbet, 2015).

Conclusion

In summary, in healthy dogs, oral administration of a commonly used broad-spectrum antimicrobial drug induced significant changes in the pulmonary microbial population and the majority of these changes were no longer present at 2 weeks after the discontinuation of the drug. As a consequence, for investigation of associations between the LM and CLDs in dogs, discontinuance of any antimicrobial medication at a minimum of 2 weeks before sampling is advised. However, further studies are warranted to investigate the effect of other antimicrobial drugs and to identify the optimal delay between antimicrobial drug discontinuation and sampling, in order to avoid any interference with the LM analysis.

Acknowledgments

We thank Sylvain Romijn and Belinda Albert for their help in the sample collection and processing. We thank Dr. Dickson R.P. and his laboratory team, especially Mr. Brown C. for their help in statistical analyses and in the presentation of data. Finally, we would like to thank Pr. Day M.J. for proofreading the English text.

References

Bassis C.M., Erb-Downward J.R., Dickson R.P., Freeman C.M., Schmidt T.M., Young V.B., et al. (2015). Analysis of the upper respiratory tract microbiotas as the source of the lung and gastric microbiotas in healthy individuals. mBio, 6(2), e00037-15. doi: 10.1128/mBio.00037-15.

Bindels L.B., Neyrinck A.M., Salazar N., Taminiau B., Druart C., Muccioli G.G., et al. (2015). Non digestible oligosaccharides modulate the gut microbiota to control the development of leukaemia and associated cachexia in mice. PLoS One., 10 (6), e0131009. doi: 10.1371/journal.pone.0131009.

Brusse-Keizer M., Vander Valk P., van der Zanden R.W., Nijdam L., van der Palen J., Hendrix R., et al. (2015). Amoxicillin concentrations in relation to beta-lactamase activity in sputum during exacerbations of chronic obstructive pulmonary disease. International Journal of COPD, 10, pp. 455–461. doi: 10.2147/COPD.S70355.

Costa A.N., da Costa F.M., Campos S.V., Salles R.K., Athanazio R.A., Costa A.N., et al. (2018) The pulmonary microbiome: challenges of a new paradigm. Jornal Brasileiro de Pneumologia, 44(5), pp. 424–432. doi: 10.1590/s1806-37562017000000209.

Desquilbet L. (2015). Puissance statistique d'une étude version 3. Available at: https://eve.vet-alfort.fr/course/view.php?id=353 (Accessed: 3 May 2018).

Dickson R. P., Erb-Downward J.R., Freeman C.M., McCloskey L., Beck J.M., Huffnagle G.B., et al. (2015). Spatial variation in the healthy human lung microbiome and the adapted island model of lung biogeography. Annals of the American Thoracic Society, 12(6), pp. 821–830. doi: 10.1513/AnnalsATS.201501-029OC.

Dickson R. P., Erb-Downward J.R., Martinez F.J., Huffnagle G.B. (2016). The Microbiome and the Respiratory Tract. Annual Review of Physiology, 78(1), pp. 481–504. doi: 10.1146/annurev-physiol-021115-105238.

Dickson R.P., Erb-Downward J.R., Freeman C.M., McCloskey L., Falkowski N.R., Huffnagle G.B., et al. (2017). Bacterial topography of the healthy human lower respiratory tract. mBio, 8(1), e02287-16. doi: 10.1128/mBio.02287-16.

Dickson R.P., Erb-Downward J.R., Falkowski N.R., Hunter E.M., Ashley S.L., Huffnagleet G.B. (2018) The lung microbiota of healthy mice is highly variable, cluster by environment, and

reflect variation in baseline lung innate immunity. American Journal of Respiratory and Critical Care Medicine, 198(4), pp. 497–508. doi: 10.1164/rccm.201711-2180OC.

Dickson R.P. and Huffnagle G.B. (2015). The lung microbiome: new principles for respiratory bacteriology in health and disease. PLoS Pathogens, 11(7), e1004923. doi: 10.1371/journal.ppat.1004923.

Edgar R.C., Haas B.J., Clemente J.C., Quince C., Knight R. (2011). UCHIME improves sensitivity and speed of chimera detection. Bioinformatics, 27(16), pp. 2194–2200. doi: 10.1093/bioinformatics/btr381.

Ericsson A.C., Personett A.R., Grobman M.E., Rindt H., Reinero C.R. (2016). Composition and predicted metabolic capacity of upper and lower airway microbiota of healthy dogs in relation to the faecal microbiota. PLoS One, 11(5), e0154646. doi: 10.1371/journal.pone.0154646.

Fastrès A., Felice F., Roels E., Moermans C., Corhay J.-L., Bureau F., et al. (2017). The lung microbiome in idiopathic pulmonary fibrosis: a promising approach for targeted therapies. International Journal of Molecular Sciences, 18(12), 2735. doi: 10.3390/ijms18122735.

File T.M. (2007). The development of pharmacokinetically enhanced amoxicillin/clavulanate for the management of respiratory tract infections in adults. International Journal of Antimicrobial Agents, 30, pp. 131–134. doi: 10.1016/j.ijantimicag.2007.07.038.

Honeybourne D. (1994). Antibiotic penetration into lung tissues. Thorax, 49(2), pp. 104–106. doi: 10.1136/thx.49.2.104.

Huang Y., Ma S.-F., Espindola M.S., Vij R., Oldham J.M., Huffnagle G.B., et al. (2017). Microbes are associated with host innate immune response in idiopathic pulmonary fibrosis. American Journal of Respiratory and Critical Care Medicine, 196(2), pp. 208–219. doi: 10.1164/rccm.201607-1525OC.

Kaur S.P., Rao R. and Nanda S. (2011). Amoxicillin: A broad spectrum antibiotic. International Journal of Pharmacy and Pharmaceutical Sciences, 3(3), pp. 30–37.

Kozich J. J., Westcott S.L., Baxter N.T., Highlander S.K., Schloss P.D. (2013). Development of a dual-index sequencing strategy and curation pipeline for analyzing amplicon sequence data on the MiSeq. Applied and Environmental Microbiology, 79(17), pp. 5112–5120. doi: 10.1128/AEM.01043-13.

Lappin M.R., Blondeau J., Boothe D., Breitschwerdt E.B., Guardabassi L., Lloyd D.H., et al. (2017). Antimicrobial use guidelines for treatment of respiratory tract disease in dogs and cats: antimicrobial guidelines working group of the international society for companion animal infectious diseases. Journal of Veterinary Internal Medicine, 31, pp. 279–294. doi: 10.1111/jvim.14627.

Lloyd C.M. and Marsland B.J. (2017). Lung homeostasis: influence of age, microbes, and the immune system. Immunity, 46(4), pp. 549–561. doi : 10.1016/j.immuni.2017.04.005.

Marsh R.L., Nelson M.T., Pope C.E., Leach A.J., Hoffman L.R., Chang A.B., et al. (2018). How low can we go? The implications of low bacterial load in respiratory microbiota studies. Pneumonia, 10(1), 7. doi: 10.1186/s41479-018-0051-8.

Ngo J., Taminiau B., Fall P.A., Daube G., Fontaine J. (2018). Ear canal microbiota – a comparison between healthy dogs and atopic dogs without clinical signs of otitis externa. Veterinary Dermatology, 29(5), 425-e140. doi: 10.1111/vde.12674.

Pennington, J. (1981). Penetration of antibiotics into respiratory secretions. Reviews of Infectious Disease, 3(1), pp. 67–73. doi: 10.1093/clinids/3.1.67.

Plumb D.C. (2015) Plumb's veterinary drug handbook, eighth edition. Wiley-Blackwell. Ames, Iowa, pp.80-84.

Roels E., Taminiau B., Darnis E., Neveu F., Daube G., Clercx C. (2017). Comparative analysis of the respiratory microbiota of healthy dogs and dogs with canine idiopathic pulmonary fibrosis. Journal of Veterinary Internal Medicine, 31(1), pp. 230–231. doi: 10.1111/jvim.14600.

Rognes T., Flouri T., Nichols B., Quince C., Mahé F. (2016). VSEARCH: a versatile open source tool for metagenomics. PeerJ, 4, e2584. doi: 10.7717/peerj.2584.

Salter S.J., Cox M.J., Turek E.M., Calus S.T., Cookson W.O., Moffatt M.F., et al. (2014). Reagent and laboratory contamination can critically impact sequence-based microbiome analyses. BMC Biology, 12, 87. doi: 10.1186/s12915-014-0087-z.

Schloss P. (2013). Amova. Available at: https://www.mothur.org/wiki/Amova (Accessed: 21 October 2019).

Schloss P. (2018). Homova. Available at: https://www.mothur.org/wiki/Homova (Accessed: 21 October 2019).

Segal L.N., Rom W.N. and Weiden M.D. (2014). Lung microbiome for clinicians: New discoveries about bugs in healthy and diseased lungs. Annals of the American Thoracic Society, 11(1), pp. 108–116. doi: 10.1513/AnnalsATS.201310-339FR.

Thiemann S., Smit N. and Strowig T. (2016). Antibiotics and the intestinal microbiome: individual responses, resilience of the ecosystem, and the susceptibility to infections. Current Topics in Microbiology and Immunology, 398, pp. 123–146. doi: 10.1007/82_2016_504.

Větrovský T. and Baldrian P. (2013). The variability of the 16S rRNA gene in bacterial genomes and its consequences for bacterial community analyses. PLoS One, 8(2), e57923. doi: 10.1371/journal.pone.0057923.

Zaura E., Brandt B., Teixeira de Mattos M.J., Buijs M., Caspers M., Rashid M., et al. (2015) Same exposure but two radically different responses to antibiotics: resilience of the salivary microbiome versus long-term microbial shifts in feces. mBio, 6(6), e01693-15. doi: 10.1128/mBio.01693-15.

Supplemental material

Data associated with this study has been deposited at the National Centre for Biotechnology Information (NCBI) under the accession number PRJNA507075.

Experimental section

Part 1

Study 2 :

Assessment of the lung microbiota in dogs: influence of the type of breed, living conditions and canine idiopathic pulmonary fibrosis

BMC Microbiology 20 :84

Aline Fastrès, Elodie Roels, Emilie Vangrinsven, Bernard Taminiau, Hiba Jabri, Géraldine Bolen, Anne-Christine Merveille, Alexandru-Cosmin Tutunaru, Evelyne Moyse, Georges Daube, Cécile Clercx

Abstract

Literature about the lung microbiota (LM) in dogs is sparse. Influence of breed and living conditions on the LM in healthy dogs is currently unknown, as well as the influence of chronic respiratory diseases such as canine idiopathic pulmonary fibrosis (CIPF) in West highland white terriers (WHWTs). Aims of this study were (1) to assess the characteristics of the healthy LM according to breed and living conditions, and (2) to study LM changes associated with CIPF in WHWTs. Forty-five healthy dogs divided into 5 groups: domestic terriers ($n = 10$), domestic shepherds ($n = 11$), domestic brachycephalic dogs ($n = 9$), domestic WHWTs ($n = 6$) (H-WHWTs) and experimental beagles ($n = 9$) and 11 diseased WHWTs affected with CIPF (D-WHWTs) were included in the study to achieve those objectives.

In healthy domestic dogs, except in H-WHWTs, the presence of few discriminant genera in each type of breed was the only LM modification. LM of experimental dogs displayed a change in b-diversity and an increased richness compared with domestic dogs. Moreover, *Prevotella_7* and *Dubosiella* genera were more abundant and 19 genera were discriminant in experimental dogs. LM of both H-WHWTs and D-WHWTs revealed increased abundance of 6 genera (*Brochothrix*, *Curvibacter*, *Pseudarcicella*, a genus belonging to Flavobacteriaceae family, *Rhodoluna* and *Limnohabitans*) compared with other healthy domestic dogs. *Brochothrix* and *Pseudarcicella* were also discriminant in D-WHWTs compared with H-WHWTs and other healthy domestic dogs.

In domestic conditions, except for H-WHWT, the breed appears to have minor influence on the LM. LM modifications were found in experimental compared with domestic living conditions. LM modifications in H-WHWTs and D-WHWTs compared with other healthy domestic dogs were similar and seemed to be linked to the breed. Whether this breed difference might be related with the high susceptibility of WHWTs for CIPF requires further studies.

Introduction

The term "microbiota" refers to all the bacteria that are found in a particular region or habitat (Segal *et al.*, 2014). While the lung has been for long considered sterile, it is now well recognized that it hosts a diverse, low biomass bacterial population (Dickson *et al.*, 2016). The lung microbiota (LM) in healthy experimental dogs is composed of a microbial population similar to the one in heathy humans, with major phyla including Firmicutes, Actinobacteria, Proteobacteria and Bacteroidetes (Ericsson *et al.*, 2016; Roels *et al.*, 2017c; Fastrès *et al.*, 2019). In a pilot study from Roels et al. (2017), based on a limited number of dogs, LM differences were found between healthy experimental beagles ($n = 6$) and healthy client-owned West Highland white terriers (WHWTs) ($n = 5$) suggesting a possible association with the breed and/or the living conditions. In the same study, differences in the LM were also highlighted between healthy client-owned WHWTs and WHWTs affected with canine idiopathic pulmonary fibrosis (CIPF) ($n = 7$) suggesting an influence of the disease on the LM.

Whether the LM varies according to the type of breed in dogs is unknown. We hypothesize that inter-breed differences in genetic, morphological or physiological characteristics, or in breathing pattern could alter the LM which might be among the factors that favour lower airway diseases with breed predisposition.

The living conditions are suspected to play a role in the LM, although it has not yet been investigated in dogs. Indeed, the respiratory tract is in constant contact with the external environment which is known to be one of the factors that impacts the LM (Dickson *et al.*, 2016). The influence of the living conditions on the LM has been specifically studied in horses and mice (Dickson *et al.*, 2018; Fillion-Bertrand *et al.*, 2018). In horses, it has been shown that lung communities are more similar between horses living in the same environment than living in different areas (Fillion-Bertrand *et al.*, 2018). In mice, the LM clusters highly by cage, shipment and vendor suggesting a clear impact of the living conditions (Dickson *et al.*, 2018). The living conditions could then represent an important source of variations of the LM and might also be among the factors able to predispose to lung diseases in dogs as it has been shown for asthma in human medicine for example (Chung, 2017; Karvone *et al.*, 2019; Ver Heul *et al.*, 2019).

CIPF is a poorly understood parenchymal lung disease mimicking notably idiopathic pulmonary fibrosis (IPF) in man. CIPF affects old dogs of the WHWTs breed, suggesting a breed predisposition for the disease (Heikkila-Laurila and Rajamaki, 2014; Clercx *et al.*, 2018). In man, numerous studies have been published supporting the hypothesis that the LM could be a trigger or a perpetuation factor in IPF (Dickson and Huffnagle, 2015; O'Dwyer *et al.*, 2016; Hewitt and Molyneaux, 2017; Molyneaux *et al.*, 2017b). In dogs, the alteration of the LM in CIPF dogs has not yet been investigated in a large number of animals.

The aims of this study were to assess [1] differences in the LM associated with the breed and the living conditions in healthy dogs; and [2] the LM alterations associated with CIPF in the WHWT breed. Therefore, the LM of healthy dogs from different breeds and living conditions was compared. Additionally, the LM of WHWTs affected with CIPF was compared with the LM of healthy WHWTs and of domestic dogs from other breeds.

Results

1. Influence of the breed on the LM

A total of 45 healthy adult dogs were included in the study and categorized into 5 groups according to the type of breed: terriers (T), shepherds (S), brachycephalic dogs (Br), WHWTs (H-WHWTs) and beagles (ExpB). Groups' characteristics are reported in the Table 1. No age differences were found between groups ($P = 0.052$).

***Table 1**. Characteristics of the groups according to the type of breed.*

	T	**S**	**Br**	**H-WHWT**	**ExpB**
N	10	11	9	6	9
Sex (M/F)	6/4	3/8	5/4	4/2	4/5
Age, yr	7.01 (6.05-8.57)	6.96 (4.34-7.33)	3.61 (1.43-4.49)	8.68 (7.65-10.11)	4.82 (2.95-10.85)
Weight, kg	6.80 (5.55-9.18) [a,b]	27.90 (23.35-31.15) [a,c,d]	11.90 (9.50-13.30) [c]	9.40 (8.65-9.70) [d]	13.80 (12.70-16.20) [b]
Breeds	7 Jack Russel terriers, 3 Yorkshire terriers	5 Belgian Malinois, 3 Australian shepherds and 1 white Swiss shepherd, 2 border collies	6 French and 1 English bulldogs, 1 pug, 1 Cavalier King Charles spaniel	WHWTs	Beagles

Data are expressed as median and interquartile range. Superscript letters reflect paired statistical difference ($P < 0.002$) according to Kruskal-Wallis and Dunn post-hoc tests. M, male; F, female; T, terriers group; S, shepherds group; Br, brachycephalic dogs group; H-WHWT: healthy West Highland white terriers group; ExpB, experimental beagles group.

The bacterial load in bronchoalveolar lavage fluids (BALFs) was not significantly different between the types of breeds ($P = 0.22$) (Figure 1A).

Bacterial richness (Figure 1C) was significantly higher in ExpB than in T and S groups, but there were no differences for the α-diversity and the evenness between groups (Figures 1B and D; $P = 0.87$ and 0.14 respectively). The β-diversity (Figure 1E) was different between the groups ($P = 0.002$) with differences between ExpB and T, S and Br ($P = 0.04$, 0.01 and 0.05 respectively).

Four major phyla were shared between the groups, including in descending order, Proteobacteria, Actinobacteria, Firmicutes and Bacteroidetes. At the genus level, inter-individual variability was observed between the dogs (Figure 1G)) and a lot of genera were present in very small proportions (*i.e.*, $< 0.05\%$). The 10 most abundant genera in median across groups were *Cutibacterium*, *Staphylococcus*, *Streptococcus*, *Pseudomonas*, *Corynebacterium_1*, Pasteurellaceae genus, *Acinetobacter*, *Conchiformibius*, *Flavobacterium* and *Porphyromonas*. Taken

together, all these genera represented 22.96% (9.59–56.64) of the global relative abundance across the groups. The linear discriminant analysis (LDA), used to determine the genera most likely to explain the differences between the groups (Segata *et al.*, 2011), revealed a total of 29 genera, 1 in T, 2 in S, 1 in Br, 9 in H-WHWT and 16 in ExpB, which were discriminant between the groups (Figure 1F). Significant differences in the relative abundance of the taxa at the genus level were only found between H-WHWTs and the other groups and are reported in the Table 2.

Table 2. *Relative abundance of taxa at the genus level significantly different between the type of breed.*

Genus	T	S	Br	H-WHWT	ExpB	P-value
Brochothrix	0% [a]	0% [b]	0% [c]	0.28% (0.05-0.45) [a,b,c]	0% (0-0.04)	[a,c] $P < 0.05$ [b] $P < 0.01$
Limnohabitans	0% [a]	0% [b]	0% [c]	0.24% (0.06-0.39) [a,b,c,d]	0% [d]	[a,b,c] $P < 0.01$ [d] $P < 0.05$
Rhodoluna	0% [a]	0% [b]	0% [c]	0.45% (0.09-0.95) [a,b,c,d]	0% [d]	[a] $P < 0.001$ [b,c] $P < 0.01$ [d] $P < 0.05$
Curvibacter	0% [a]	0% [b]	0% [c]	0.06% (0.01-0.10) [a,b,c,d]	0% [d]	[a,b,c] $P < 0.001$ [d] $P < 0.01$
Pseudarcicella	0% [a]	0% [b]	0% [c]	0.20% (0.05-0.23) [a,b,c,d]	0% [d]	[a,b,c] $P < 0.01$ [d] $P < 0.05$
Sporichthyaceae genus	0% [a]	0% [b]	0% [c]	0.11% (0.01-0.18) [a,b,c,d]	0% [d]	[a,b,c] $P < 0.001$ [d] $P < 0.05$

Results were expressed as median percentage of the relative abundance and interquartile range. Superscript letters reflect paired statistical difference by raw according to Kruskal-Wallis and Tukey post hoc tests. T group: terrier dogs; S group: shepherd dogs; Br group: brachycephalic dogs; H-WHWT: healthy West Highland white terrier dogs; ExpB group: experimental beagle dogs.

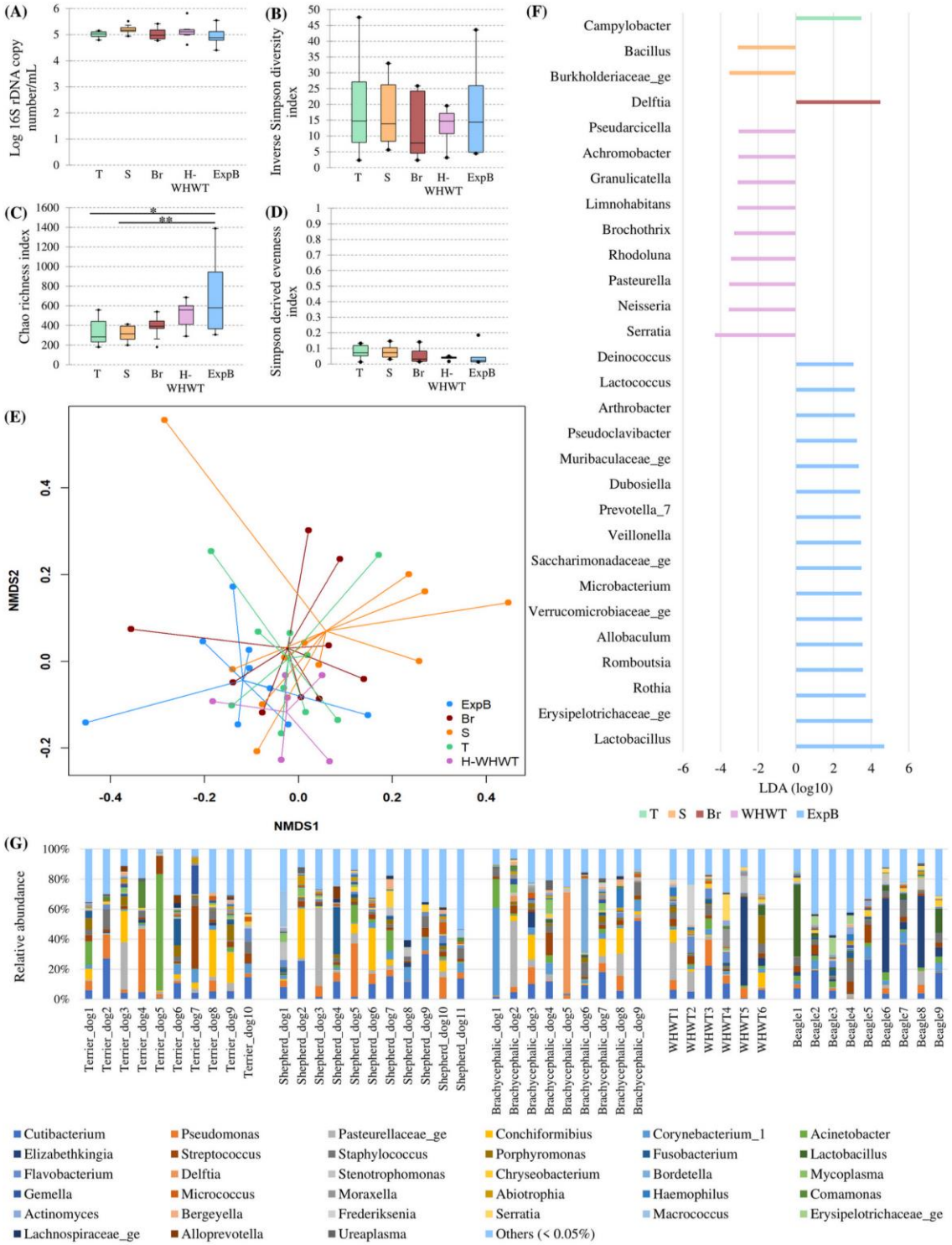

Figure 1. *Influence of the type of breed on the lung microbiota.* *The influence of the type of breed on the lung microbiota was evaluated by comparison between 5 groups including domestic terrier dogs (T), domestic shepherd dogs (S), domestic brachycephalic dogs (Br), healthy domestic West Highland white terriers (H-WHWTs) and experimental beagles (ExpB). The parameters studied to assess the lung microbiota included; the bacterial load (**A**), the α-diversity (**B**), the richness (**C**), the evenness (**D**), the β-diversity (**E**) represented by a non-metric multidimensional scaling (NMDS) graph based on a Bray-Curtis matrix and the linear discriminant analysis (LDA) where only significant genera were represented (**F**). The distribution of the relative abundance of taxa at the genus level for each dog in each type of breed concerned only genera of more than 0.05% (**G**). *P = 0.002, **P = 0.001.*

2. Influence of the living conditions on the LM

The LM has been then compared between dogs living in experimental versus domestic conditions. Domestic conditions were further divided into rural and urban conditions based on owner's information. The same 45 dogs included in the first part of this study were used and re-categorized into the three living conditions (Table 3). No age difference was reported between groups.

Table 3. *Characteristics of the groups according to the living condition.*

	Rural	**Urban**	**ExpB**
N	20	16	9
Sex (M/F)	8/12	8/8	4/5
Age, yr	7.01 (3.70-7.79)	6.58 (3.36-7.93)	4.82 (2.95-10.85)
Weight, kg	9.65 (7.10-13.45)	16.50 (9.70-29.08)	13.80 (12.70-16.20)
Breeds repartition	T: 9/10, S: 5/11, Br: 4/9, H-WHWT: 2/6	T: 1/10, S: 4/11, Br: 5/9, H-WHWT: 4/6	ExpB: 9/9

Data are expressed as median and interquartile range. M, male; F, female; T, terriers group; S, shepherds group; Br, brachycephalic dogs group; H-WHWT: healthy West Highland white terriers group; ExpB, experimental beagles group.

The bacterial load (Figure 2A) was not significantly different between the living conditions ($P = 0.24$).

There were no differences between living conditions for the α-diversity and the evenness (Figures 2B and D; $P = 0.93$ and 0.24 respectively). The richness was higher in experimental compared with rural and urban conditions (Figure 2C). The β-diversity (Figure 2E) was different between the groups ($P = 0.001$) with significant differences between experimental and rural and between experimental and urban conditions ($P = 0.003$ and 0.039 respectively). No significant difference in the β-diversity was present between rural and urban conditions ($P = 0.92$). The LDA revealed a total of 22 genera, 1 in rural, 2 in urban and 19 in experimental conditions, which were discriminant between living conditions (Figure 2F). Significant differences found between living conditions in the relative abundance of the taxa at the genus level are reported in the Table 4.

Table 4. *Relative abundance of taxa significantly different between the living conditions.*

Genera	**Rural**	**Urban**	**ExpB**
Prevotella_7	0% (0-0.002) [a]	0% [b]	0.23% (0.18-0.33) [a,b]
Dubosiella	0% [a]	0% [b]	0.04% (0-0.53) [a,b]

Results were expressed as median percentage of the relative abundance and interquartile range. Superscript letters reflect paired statistical difference by raw ($P < 0.05$) according to Kruskal-Wallis and Tukey post hoc tests. ExpB, experimental beagle dogs.

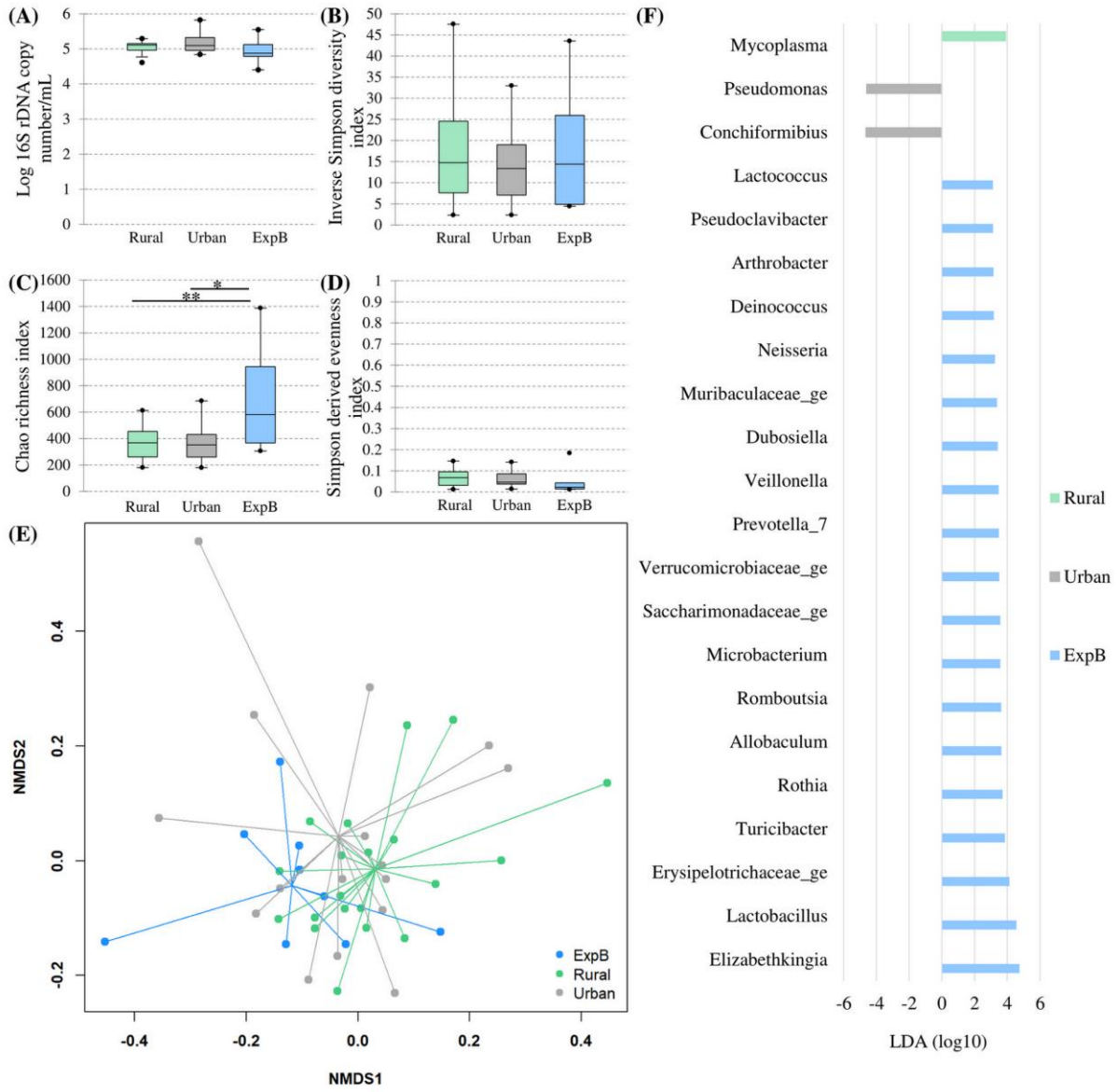

Figure 2. *Influence of the living conditions on the lung microbiota. The influence of the living conditions on the lung microbiota was evaluated by comparison between domestic dogs living either in rural or urban condition and experimental beagle dogs (ExpB). The parameters studied to assess the lung microbiota included; the bacterial load (**A**), the α-diversity (**B**), the richness (**C**), the evenness (**D**), the β-diversity (**E**) represented by a non-metric multidimensional scaling (NMDS) graph based on a Bray-Curtis matrix and the linear discriminant analysis (LDA) where only significant genera were represented (**F**). *P = 0.017, **P = 0.015.*

3. The LM in CIPF WHWTs

To assess the LM in dogs affected with CIPF, we compared 11 WHWTs affected with CIPF (D-WHWTs) with age-matched healthy WHWTs and with all the other healthy domestic dogs (T, S and Br). The clinical characteristics of the groups are reported in the Table 5.

Table 5. *Characteristics of the groups according to the disease status.*

	Healthy domestic dogs other than WHWTs	**H-WHWTs**	**D-WHWTs**
N	30	6	11
Sex (M/F)	14/16	4/2	4/7
Age, yr	6.25 (3.53-7.39) [a]	8.68 (7.65-10.11)	11.52 (10.51-12.33) [a]
Weight, kg	12.45 (7.68-23.68)	9.40 (8.65-9.70)	9.5 (9.25-10.45)

Data are expressed as median and interquartile range. Superscript letters reflect paired statistical difference (P < 0.0001) according to Kruskal-Wallis and Dunn post hoc tests. H-WHWTs: healthy West Highland white terriers; D-WHWTs: West Highland white terriers affected with canine idiopathic pulmonary fibrosis; M, male; F, female; BALF, bronchoalveolar lavage fluid.

The bacterial load (Figure 3A) was not different between the groups ($P = 0.88$).

There were no differences between groups for the α-diversity and the evenness (Figures 3B and D; $P = 0.86$ and 0.13 respectively). The richness was significantly higher in H-WHWTs compared with healthy domestic dogs other than WHWTs (Figure 3C). The β-diversity (Figure 3E) was significantly different between the groups ($P = 0.001$) with significant differences only between D-WHWTs and healthy domestic dogs other than WHWTs ($P = 0.003$). No difference in the β-diversity was present between D-WHWTs and H-WHWTs ($P = 0.18$) and between H-WHWTs and healthy domestic dogs other than WHWTs ($P = 0.13$).

The LDA revealed a total of 13 genera, 1 in healthy domestic dogs other than WHWTs, 7 in H-WHWT and 5 in D-WHWT, which were discriminant between groups (Figure 3F). Significant differences found between the groups in the relative abundance of the taxa at the genus level are reported in the Table 6.

Table 6. *Relative abundance of taxa significantly different between the disease status.*

Genera	**Healthy domestic dogs other than WHWTs**	**H-WHWTs**	**D-WHWTs**	**P-value**
Limnohabitans	0% [a,c]	0.24% (0.06-0.39) [a,b]	0.14% (0.06-0.34) [b,c]	[a] P < 0.001 [b] P < 0.01 [c] P < 0.05
Brochothrix	0% [a,b]	0.28% (0.05-0.45) [a]	0.5% (0.29-0.92) [b]	[a] P < 0.01 [b] P < 0.001
Curvibacter	0% [a,b]	0.06% (0.01-0.10) [a]	0.07% (0-0.12) [b]	[a] P < 0.05 [b] P < 0.001
Rhodoluna	0% [a,c]	0.45% (0.09-0.95) [a,b]	0.27% (0.06-0.70) [b,c]	[a] P < 0.001 [b,c] P < 0.05
Pseudarcicella	0% [a,b]	0.20% (0.05-0.23) [a]	0.34% (0.04-0.58) [b]	[a] P < 0.01 [b] P < 0.001
Genus belonging to Sporichthyaceae family	0% [a]	0.11% (0.01-0.18) [a]	0.10% (0-0.22)	[a] P < 0.01
Genus belonging to Candidatus Nomurabacteria phylum	0% [a]	0.16% (0.02-0.37) [a,b]	0.06% (0.02-0.09) [b]	[a,b] P < 0.001
Serratia	0% (0-0.02) [a]	0.42% (0.18-1.60) [a]	0.03% (0-0.13)	[a] P < 0.05
Genus belonging to Flavobacteriaceae family	0.01% (0-0.03) [a,b]	0.23 (0.04-0.47) [a]	0.26% (0.09-0.37) [b]	[a] P < 0.001 [b] P < 0.05

Results were expressed as median percentage of the relative abundance and interquartile range. Superscript letters reflect paired statistical difference by raw according to Kruskal-Wallis and Tukey post hoc tests. H-WHWTs, healthy West Highland white terriers; D-WHWTs, West Highland white terriers affected with canine idiopathic pulmonary fibrosis.

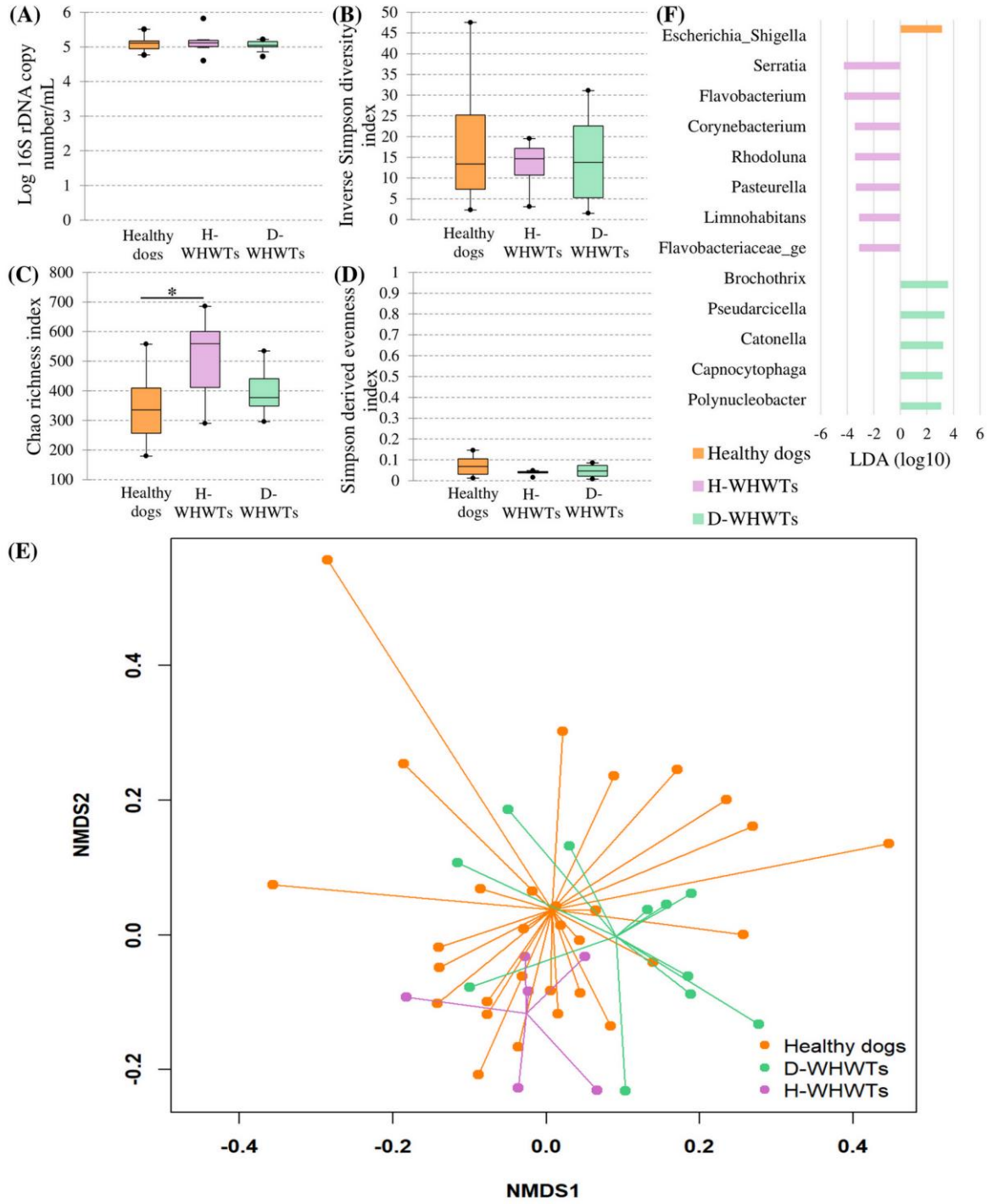

Figure 3. *The lung microbiota in West Highland white terrier affected with canine idiopathic pulmonary fibrosis (CIPF). The influence of CIPF on the lung microbiota was evaluated by comparison between healthy domestic dogs from different breeds (healthy dogs), healthy West Highland white terriers (H-WHWTs) and WHWTs affected with CIPF (D-WHWTs). The parameters studied to assess the lung microbiota included; the bacterial load (**A**), the α-diversity (**B**), the richness (**C**), the evenness (**D**), the β-diversity (**E**) represented by a non-metric multidimensional scaling (NMDS) graph based on a Bray-Curtis matrix and the linear discriminant analysis (LDA) where only significant genera were represented (**F**). *P = 0.007.*

Discussion

Results of the present study revealed that in healthy dogs, except for H-WHWTs and ExpB, the impact of the type of breed only seemed to concern the presence of few discriminant genera in each group. The LM in dogs living in experimental condition compared with the LM in dogs living in domestic condition was characterized by a change in the β-diversity with an increase of the bacterial richness. Moreover, *Prevotella_7* and *Dubosiella* genera were found in higher relative abundance and 19 genera were identified as discriminant in experimental compared with domestic living conditions. The LM in WHWTs either healthy or affected with CIPF was quite similar. In the LM of both healthy and diseased WHWTs, 6 genera were more abundant compared with the LM of healthy domestic dogs other than WHWTs and included *Brochothrix*, *Curvibacter*, *Pseudarcicella*, a genus belonging to Flavobacteriaceae family, *Rhodoluna* and *Limnohabitans.* *Brochothrix* and *Pseudarcicella* genera were also identified as discriminant genera in D-WHWTs.

In all samples from healthy dogs, four major phyla were detected, including in descending order, Proteobacteria, Actinobacteria, Firmicutes and Bacteroidetes. These four phyla are the same as those reported in previous studies in dogs (Ericsson *et al.*, 2016; Roels *et al.*, 2017c; Fastrès *et al.*, 2019) and also correspond to the major phyla found in the human LM, although not in the same order; in man Bacteroidetes and Firmicutes are the 2 most abundant (Dickson *et al.*, 2016). *Cutibacterium* (previously named *Propionibacterium*), *Staphylococcus*, *Streptococcus*, *Pseudomonas*, *Corynebacterium_1*, Pasteurellaceae genus, *Acinetobacter*, *Conchiformibius*, *Flavobacterium* and *Porphyromonas* were the most abundant genera across all healthy dogs and represented together 22.96% of the LM at the genus level. Among these genera, Pasteurellaceae genus, *Pseudomonas*, *Acinetobacter*, *Cutibacterium*, *Streptococcus* and *Porphyromonas* were also found in high relative abundance in the study from Ericsson et al. (2016). In another study, the genera *Cutibacterium*, *Streptococcus*, *Staphylococcus*, *Pseudomonas*, *Corynebacterium_1* and *Acinetobacter* were part of the 10 most abundant genera composing the LM (Fastrès *et al.*, 2019). We therefore propose that the core genera of the LM in healthy dogs include at least the genera *Cutibacterium*, *Streptococcus*, *Acinetobacter* and *Pseudomonas*. *Cutibacterium* and *Streptococcus* genera contain Gram-positive anaerobic and aero-anaerobic bacteria respectively (Abranches *et al.*, 2018; Dréno *et al.*, 2018). In the study from Ericsson et al. (2016), *Cutibacterium* genus was only found in BALF samples, not in nasal, oropharyngeal and faeces swabs. *Cutibacterium* genus is also commonly found in the healthy skin microbiota where it plays a role in skin homeostasis and in the protection against other harmful pathogen notably by pH reduction (Dréno *et al.*, 2018). *Streptococcus* was reported as one of the main genera colonizing the oral and the lung microbiota in healthy but also in diseased patients (Ericsson *et al.*, 2016; Abranches *et al.*, 2018; Wypych *et al.*, 2020). Different strains of *Streptococcus* exist specialized in carbohydrate catabolism and environment acidification. Moreover, *Streptococcus*

bacteria possess multiple high-affinity adhesins that mediate binding and biofilm formation preventing the growth of other potentially pathogen bacteria (Abranches *et al.*, 2018). Bacteria in those 2 genera could exert same functions in the lung. *Pseudomonas* and *Acinetobacter* genera contain aerobic Gram-negative bacteria belonging to the Proteobacteria phylum. *Pseudomonas* genus represents a diverse group of bacteria characterized by a high ability to grow preventing the growth of other potentially pathogen bacteria and a capacity to produce and degrade a number of compounds including toxic materials for the host (Novik *et al.*, 2015). *Acinetobacter* bacteria could play an anti-inflammatory role in the LM. Indeed, a link was found between IL10 production, an anti-inflammatory cytokine, and *Acinetobacter* in asthma and atopic dermatitis (Wypych *et al.*, 2020). However, *Streptococcus*, *Acinetobacter* and *Pseudomonas* genera are also involved in chronic infections particularly in ventilated patient and patient affected with chronic lung diseases. Knowing their capacity to form biofilms and resist to antimicrobial drugs (Antunes *et al.*, 2011; Novik *et al.*, 2015; Abranches *et al.*, 2018; Ciofu and Tolker-Nielsen, 2019; Wypych *et al.*, 2020); indeed, in dogs under antimicrobial treatment It has been shown that *Pseudomonas* relative abundance increased (Fastrès *et al.*, 2019); it is important to take into account that those bacteria might be part of the core LM in dogs.

1. Influence of the type of breed on the LM

The results of the LDA showed that few genera were identified as discriminant between groups of breeds, the number of discriminant taxa being more important in ExpB and H-WHWTs. No other modifications of the LM including in the relative abundance of the taxa, the bacterial load and the ecological parameters (diversity, richness and evenness) were identified between the groups except in ExpB and H-WHWTs. Those data indicate that in domestic healthy dogs other than WHWTs, the different types of breeds minimally alter the LM. That fact might be of interest when interpreting data about the microbiota in dogs from various breeds. The slight breed influence on the LM found in that study could be due to differences in the genetic or the morphology of the breeds as it has been shown in the gut where modification of the bacterial populations were described in relation with the dog's size (Simpson *et al.*, 2002). Since a clear link has been established between the gut microbiota and the LM (Anand and Mande, 2018), an influence, even slight, of the breed on the LM is not a surprising finding. Additional explanations for differences in LM encountered between breeds include differences in airways and lung anatomy and breathing strategy (Amis and Kurpershoek, 1986).

Of note, the fact that we included several breeds in the T, S and Br groups could have potentially masked certain breed-related differences. Moreover, it is also possible that the number of dogs included in each group was not sufficient to show more differences in the LM.

2. Influence of the living conditions on the LM

The differences found between experimental and domestic living conditions overlap the influence of both the type of breed and the living conditions, as we were unable to recruit beagle dogs living in domestic conditions. In ExpB compared with T, S and Br, the β-diversity was different, the richness was higher and 16 discriminant genera were identified. When comparing dogs based on the living conditions (experimental vs domestic either rural or urban), similar changes were found; the β-diversity was different and the richness higher in experimental compared with domestic living conditions. More discriminant genera were identified in experimental conditions, including *Prevotella_7* and *Dubosiella* also found in higher relative abundance in experimental compared with domestic living conditions. Accordingly, we believe that the modifications of the LM in ExpB are most likely due to the living conditions rather than the breed. The importance of the close living conditions on the LM has already been reported in mice, where the LM highly clusters by cage, shipment and vendor (Dickson *et al.*, 2018) and in horses where lung communities are more similar between horses in the same environment than across environments (Fillion-Bertrand *et al.*, 2018). In ExpB, the majority of the discriminant genera identified such as *Lactobacillus, Prevotella 7, Turicibacter,* Verrucomicrobiaceae genus and Erysipelotrichaceae genus, are bacteria living in the intestinal tract and found in dog's stools (Hooda *et al.*, 2012). The presence of these bacteria might be linked to the living conditions of ExpB. Indeed, ExpB are housed by group on litter, in close contact with faeces and they frequently exhibit a coprophagy behaviour. Ingestion and sniffing of faeces present in the direct environment of dogs most probably influence their LM as it results mainly from microaspiration, inhalation and direct dispersion along respiratory mucosa (Dickson *et al.*, 2016).

In domestic dogs, we did not show differences related to the fact that dogs were living mainly in either rural or urban area. However, it must be noted that this study was not designed to specifically assess the effect of such differences. Indeed, living areas in domestic dogs were arbitrary determined based on owner's information. Additionally, if the global environment (rural or urban) of the domestic dogs was different, the housing conditions were quite similar when animals were inside house. By contrast, living conditions between experimental and domestic dogs strongly differed.

3. The LM in CIPF WHWTs

Brochothrix, Curvibacter, Pseudarcicella and a genus belonging to Flavobacteriaceae family were found in higher relative abundance in healthy and diseased WHWTs compared with other healthy domestic dogs. Moreover, those genera were more abundant in D-WHWTs compared with H-WHWTs although not significantly. *Brochothrix* and *Pseudarcicella* genera were also discriminant for D-WHWTs. *Rhodoluna* and *Limnohabitans* genera were also found in higher relative abundance in WHWTs compared with domestic dogs from other breeds, but were higher in H-WHWTs than in D-

WHWTs. These bacteria preferentially contaminate food (*Brochothrix* (Stanborough *et al.*, 2017)) and water (*Curvibacter* (Ding and Yokota, 2010), *Rhodoluna* (Hahn *et al.*, 2014), *Limnohabitans* (Kasalický *et al.*, 2013), and genera belonging to Flavobacteriaceae family (McBride, 2014)), and can be ingested by dogs. Their presence in the LM of WHWTs could be associated with the higher abundance of gastroesophageal reflux reported in that breed compared with other breeds (Määttä *et al.*, 2018). The higher rate of gastroesophageal reflux in WHWTs has been hypothesized to play a role in the onset and/or in the progression of CIPF (Määttä *et al.*, 2018). In man, gastroesophageal reflux is associated with IPF although the role of these exposures in the pathogenesis of IPF is still only hypothetical (Bédard Méthot *et al.*, 2019).

A pathogenic role of *Rhodoluna*, *Limnohabitans Brochothrix*, *Curvibacter*, *Pseudarcicella* and genera belonging to Flavobacteriaceae family in the lung has only been reported for bacteria of the Flavobacteriaceae family (McBride, 2014). Indeed, some genera of the Flavobacteriaceae family, are known as opportunistic pathogen notably in human and animal such as *Elizabethkingia spp.* for example (McBride, 2014). Bacteria of the Flavobacteriaceae family present different mechanisms of pathogenicity including cellular adhesion, gliding motility, proteolytic activity and resistance to immune system and antimicrobial drug (McBride, 2014). Bacteria of the *Curvibacter* genus can expressed genes involved in carbon metabolism and fatty acid degradation, which is useful for the colonization of the mucus layer present in the lung (Pietschke *et al.*, 2017). They also had a flagellar structure able to promote their motility, their adherence and their penetration of mucosal barriers but also able to act as an activator of the immune system via Toll-like receptor signalling (Ding and Yokota, 2010; Pietschke *et al.*, 2017). Therefore, the presence in the LM of WHWTs of these 2 genera could activate the immune system, alter the airway epithelium and induce or perpetuate the airway inflammation in CIPF. Little is known about the metabolism and the potential pathogenic role of bacteria of the *Brochothrix, Pseudarcicella*, *Rhodoluna* and *Limnohabitans* genera (Kämpfer *et al.*, 2012; Kasalický *et al.*, 2013; Hahn *et al.*, 2014; Stanborough *et al.*, 2017; Lorenzo *et al.*, 2018; Cruaud *et al.*, 2020).

Data of the present study showed that both healthy and CIPF WHWTs had a distinct microbiota compared with other healthy domestic dogs. The majority of the genera found in higher relative abundance in H-WHWTs compared with other healthy domestic dogs were also found in higher relative abundance in D-WHWTs. This is in favour of the hypothesis that the LM modifications in WHWTs are most likely related to the breed. Accordingly, the LM might be among the factors able to predispose to CIPF. That hypothesis is supported by the fact that in mice with bleomycin-induced lung fibrosis, the dysbiosis precedes the peak of lung injury and persists in the fibrotic lung (O'Dwyer *et al.*, 2019).

In human medicine, the LM in IPF patients was clearly modified compared with the LM of healthy patients on the contrary of what we observed in D-WHWTs compared to H-WHWTs. In IPF, the diversity decreased and the bacterial load increased in association with the disease progression, the presence of certain genera, not found in CIPF dogs, has also been associated with IPF such as *Haemophilus*, *Streptococcus*, *Neisseria*, *Staphylococcus* and *Veillonella* (Molyneaux and Maher, 2013; Dickson *et al.*, 2016; Fastrès *et al.*, 2017a; Huang *et al.*, 2017; Salisbury *et al.*, 2017; Takahashi *et al.*, 2018; O'Dwyer *et al.*, 2019). Of course, human and dogs are 2 different animal species with their own LM specificities. Moreover, the lack of common LM disturbances between IPF and CIPF may be related to the fact that the diseases, although presenting similarities, are different as suggested by well stablished differences in thoracic high resolution computed tomography (HRCT) (Heikkila-Laurila and Rajamaki, 2014; Thierry *et al.*, 2017) and histopathological (Syrjä *et al.*, 2013) characteristics.

Conclusion

In domestic conditions, at the exception of the WHWT, differences between the types of breeds appear to have minor influence on the LM and should only minimally impact results of clinical studies comparing dogs of different types of breeds.

Differences in living conditions (experimental vs domestic dogs) were associated with modifications of the LM including a shift in the β-diversity, higher richness and identification of a large number of discriminant genera. Such differences need to be taken into account when results on the LM in experimental conditions are extrapolated to domestic dogs.

The LM found in WHWTs was distinct from the LM of other healthy domestic dogs. Therefore, LM changes in WHWTs seem to be associated with the breed. No clear modifications of the LM were found in CIPF compared with healthy WHWTs. Accordingly, the differences in the LM found in WHWTs might be related to the high susceptibility of that breed for CIPF and don't seem to be induced by the disease. Further long-term follow-up studies before and during the course of CIPF and studies assessing the role of the bacteria specifically found in D-WHWTs including *Brochothrix*, *Curvibacter*, *Pseudarcicella* and a genus belonging to Flavobacteriaceae family are needed to assess whether the LM play a role as a trigger of CIPF and as a contributor for the perpetuation of the disease.

Materials and Methods

1. Study population

The study was performed at the veterinary clinic of companion animals of the University of Liège (CVU, Liège, Belgium). Adult dogs were prospectively included and classified into different groups based on their types of breeds, living conditions and disease status. The different breeds recruited included experimental beagles (ExpB), domestic shepherds (S), domestic terriers (T), domestic brachycephalic dogs (Br) and domestic healthy WHWTs (H-WHWTs). H-WHWTs were selected in view of their high predisposition for CIPF; ExpB dogs were chosen for their experimental living conditions; T were recruited because they belong to the same kind of breed and are morphologically similar to WHWTs but are not predisposed to CIPF; S were chosen because they are larger, athletic dogs with a thin and deep thorax; Br were selected based on their facial morphology causing a partial upper airways obstruction and a different pattern of breathing (Amis and Kurpershoek, 1986; Bernaerts *et al.*, 2010; Yu *et al.*, 2017). The living conditions were classified into experimental and domestic conditions. Besides, domestic conditions were further subdivided into rural or urban. For investigation of LM alterations associated with the disease, the group including WHWTs affected with CIPF (D-WHWTs) was compared to the group of H-WHWTs, and to a group including all the other healthy domestic dogs (T, S and Br groups combined).

Samples from healthy domestic dogs and dogs affected with CIPF were collected between May 2017 and April 2019. All dogs were privately owned (*i.e.* domestic dogs) and were housed in house or apartment, with or without outdoor access, and fed with various diets. For healthy dogs, owners were asked whether they lived in urban (inside a city of more than 2000 inhabitants) or rural area (in the countryside or in villages of less than 2000 inhabitants). Samples from ExpB were collected in December 2017. The beagles were experimental dogs housed in the experimental kennel of the University of Liège, by pair on woodchip litter, with a large concrete outdoor access, along a heavily used highway road 3 to 6 h per day and fed with a standardized commercial food.

At inclusion, the status of the dogs was confirmed based on clinical signs, physical examination, haematology and plasma biochemistry (Idexx, Hoofddorp, The Nertherlands), gross appearance of the respiratory tract during bronchoscopy and analysis of the BALF. Moreover, in WHWTs, CIPF was diagnosed or excluded according to a previously described approach (Heikkila-Laurila and Rajamaki, 2014) based on history, presence or absence of marked crackles on lung auscultation, and compatible findings or absence of abnormalities on thoracic HRCT. Dogs under antimicrobial drug or corticoids were not included in the study.

2. Sample collection

BALFs were obtained in each dog under anaesthesia as previously described (Fastrès *et al.*, 2019). Briefly, dogs were anesthetized by a veterinary anaesthetist with a premedication with butorphanol 0.2 mg/kg intravenously (Butomidor® 10 mg/mL, Richter Pharma AG, Wels, Austria). Anaesthesia was then induced and maintained with intravenous propofol (Diprivan® 1%, Asen Pharma Trading Limited, Dublin, Ireland) infusion on demand; animals were not intubated except WHWT dogs which were intubated with a sterile endotracheal tube and maintained under anaesthesia with isoflurane during the HRCT before being extubated for the bronchoalveolar lavage (BAL) procedure. Before each use, the flexible paediatric endoscope (FUJINON© Paediatric Video-Bronchoscope EB-530S) used for the bronchoscopy was cleaned and disinfected. Then, 3 to 4 mL/kg of sterile saline solution were injected into the bronchoscope channel wedged in the respiratory tract of dogs and directly reabsorbed in a sterile recipient. BALFs were stored just after the collection without any processing at − 80 °C until DNA extraction. Dogs were awakened after the BAL procedure and returned to their owners for domestic dogs or brought back to the kennel for experimental dogs.

3. DNA extraction

Analysis of the LM was performed as previously described (Fastrès *et al.*, 2019). Briefly, total DNA was extracted from BALFs according to manufacturer's instructions with the DNeasy Blood and Tissue kit (QIAGEN Benelux BV, Antwerp, Belgium), using the pre-treatment for Gram-positive bacteria protocol. This protocol was preceded by a beat beating step with glass beads > 106 µM and glass beads soda-lime (Sigma-Aldrich, Overijse, Belgium, Cat. G4649 and Z265926). DNA was eluted into DNase/RNase-free water for a final volume of 30 µL and the concentration and purity were evaluated using a ND-1000 spectrophotometer (NanoDrop ND-1000, Isogen, De Meern, The Netherlands). All DNA extractions were done at the same time with the same kit and procedure.

4. 16S quantitative PCR

The bacterial load was assessed in all samples by duplicate quantitative polymerase chain reactions (qPCRs) targeting the V2-V3 region of the 16S rDNA with the following primers, forward (5′-ACTCCTACGGGAGGCAGCAG-3′) and reverse (5′-ATTACCGCGGCTGCTGG-3′) (Bindels *et al.*, 2015) as previously described (Fastrès *et al.*, 2019). Results obtained were then expressed in base 10 logarithm of the total 16S rDNA copy numbers per mL.

5. 16S rDNA library preparation, sequencing and informatics

For bacterial identification, polymerase chain reactions (PCRs) targeting the V1-V3 hypervariable regions of the 16S rDNA were performed for all samples at the same time with the

following primers: forward (5′-GAGAGTTTGATYMTGGCTCAG-3′) and reverse (5′-ACCGCGGCTGCTGGCAC-3′) and Illumina overhand adapters as already described (Ngo *et al.*, 2018; Fastrès *et al.*, 2019). Amplicons obtained were purified, quantified and submitted to a second PCR round for indexing. A final quantification of all samples was performed by qPCR before normalization and pooling of the amplicons to form libraries. Libraries obtained were then sequenced on a MiSeq Illumina sequencer (Illumina, San Diego, CA, USA) using V3 reagents. After sequencing, 8,930,807 reads with a median length of 508 nucleotides were obtained.

After a first cleaning step (length and sequences quality), 6,991,349 reads were screened for chimera using Vsearch algorithm (Rognes *et al.*, 2016). Six million six hundred ninety-nine thousand five hundred seventy-two reads were retained for alignment and clustering using MOTHUR v1.40 (Kozich *et al.*, 2013). Taxonomical assignations with an operational taxonomic unit (OTU) clustering distance of 0.03 were based on the SILVA database v1.32. A final subsampling was performed with a median reads per sample of 10,000.

All sample raw reads associated with this study have been deposited at the National Centre for Biotechnology Information (NCBI) under the accession number PRJNA594816.

6. Identification of procedural contaminants and validation of the sequencing

Procedural control specimens (PCSs) were obtained in order to evaluate the general contamination during sampling just before each BAL by injection and direct reabsorption into the bronchoscope channel of 10 mL of sterile saline solution (NaCl 0.9%). PCSs were then stored at − 80 °C until further analysis. PCS were then treated exactly the same way as the BALF samples. Briefly, DNA was extracted with the same technique, same extraction kit and at the same time as samples. Bacterial load in PCSs was obtained by duplicate qPCRs performed in the same run as samples, by the same technique. The bacterial load was about 100 times lower in the PCS than in the corresponding BALF samples ($P < 0.0001$). PCR targeting the V1-V3 region of the 16S rDNA were performed as for the samples. The PCS amplification products were < 1 ng/μL and were then not sequenced.

A positive control using 20 defined bacterial species DNA and a negative control from the PCR step were included into the run to validate the sequencing.

7. Statistical analysis

The influence of the type of breed was assessed by comparing the 5 groups of healthy dogs. The influence of the living conditions was evaluated by comparing experimental, rural and urban

conditions. Finally, the influence of CIPF on the LM was evaluated by comparing all healthy domestic dogs other than WHWTs, H-WHWTs and D-WHWTs.

Normality was first checked using the Shapiro-Wilk test for each analysis. Characteristics of the groups were compared using Kruskal-Wallis test and post-hoc Dunn tests with Bonferroni correction using XLStat (Addinsoft, Paris, France).

Statistical differences in the relative abundance of taxa were assessed with Kruskal-Wallis test using Benjamini Hotchberg procedure and a false discovery rate of 10% for multiple comparisons, followed by Tukey-Kramer post hoc tests, using STAMP software (Parks and Beiko, 2010). The LDA was performed to detect discriminant bacteria between groups at the genus level with MOTHUR v1.40. For the LDA interpretation, differences were considered as significant for a $P < 0.05$ and a LDA score > 3.0 (Segata *et al.*, 2011).

Metrics of richness (Chao1 index), evenness (Simpson index-based measure) and α-diversity (inverse Simpson's index) were assessed with MOTHUR v1.40 at the OTUs level and compared between groups using Kruskal-Wallis test and Dunn post-hoc tests with Bonferroni correction using XLStat. The same test was used to compare the bacterial load between groups. Non-metric multidimensional scaling (NMDS) figures were performed based on a Bray-Curtis dissimilarity matrix at the OTUs level to represent the global bacterial composition (β-diversity) between groups (R vegan package). The β-diversity between types of breeds, living conditions and disease status was calculated using R (vegan package) by a permutational multivariate analysis of variance (PERMANOVA) followed by pairwise tests with Bonferroni correction.

Results are expressed in median and interquartile range. A P-value < 0.05 was considered as statistically significant.

Acknowledgments

The authors would like to thank Albert Belinda, Phan Kim-Thu and Romijn Sylvain for their help in samples collection and storage.

References

Abranches J., Zeng L., Kajfasz J.K., Palmer S., Chakraborty B., Wen Z., et al. (2018). Biology of Oral *Streptococci*. Microbiology Spectrum, 6(5), pp. 426–434. doi: 10.1128/9781683670131.ch26.

Amis T.C. and Kurpershoek C. (1986). Pattern of breathing in brachycephalic dogs. American Journal of Veterinary Research, 47(10), pp. 2200–2204.

Anand S. and Mande S.S. (2018). Diet, microbiota and gut-lung connection. Frontiers in Microbiology, 9, p. 2147. doi: 10.3389/fmicb.2018.02147.

Antunes L.C.S., Imperi F., Carattoli A., Visca P. (2011). Deciphering the multifactorial nature of acinetobacter baumannii pathogenicity. PLoS One, 6(8), e22674. doi: 10.1371/journal.pone.0022674.

Bédard Méthot D., Leblanc É. and Lacasse Y. (2019). Meta-analysis of gastroesophageal Reflux disease and idiopathic pulmonary fibrosis. Chest, 155(1), pp. 33–43. doi: 10.1016/J.CHEST.2018.07.038.

Bernaerts F., Talavera J., Leemans J., Hamaide A., Claeys S., Kirschvink N., et al. (2010). Description of original endoscopic findings and respiratory functional assessment using barometric whole-body plethysmography in dogs suffering from brachycephalic airway obstruction syndrome. The Veterinary Journal, 183(1), pp. 95–102. doi: 10.1016/j.tvjl.2008.09.009.

Bindels L.B., Neyrinck A.M., Salazar N., Taminiau B., Druart C., Muccioli G.G., et al. (2015). Non digestible oligosaccharides modulate the gut microbiota to control the development of leukemia and associated cachexia in mice. PLoS One, 10(6), e0131009. doi: 10.1371/journal.pone.0131009.

Chung K.F. (2017). Clinical reviews in allergy and immunology airway microbial dysbiosis in asthmatic patients = A target for prevention and treatment? Journal of Allergy and Clinical Immunology, 139(4), pp. 1071–1081. doi: 10.1016/j.jaci.2017.02.004.

Ciofu O. and Tolker-Nielsen T. (2019). Tolerance and resistance of *Pseudomonas aeruginosa* biofilms to antimicrobial agents-How *P. aeruginosa* can escape antibiotics. Frontiers in Microbiology, 10,913. doi: 10.3389/fmicb.2019.00913.

Clercx C., Fastrès A. and Roels E. (2018). Idiopathic pulmonary fibrosis in the West Highland white terrier: an update. The Veterinary Journal, 242, pp. 53–58.

Cruaud P., Vigneron A., Fradette M.S., Dorea C.C., Culley A.I., Rodriguez M.J., et al. (2020). Annual bacterial community cycle in a seasonally ice-covered river reflects environmental and climatic conditions. Limnology and Oceanography, 65, pp. S21–S37. doi: 10.1002/lno.11130.

Dickson R.P., Erb-Downward J.R., Martinez F.J., Huffnagle G.B. (2016). The Microbiome and the Respiratory Tract. Annual Review of Physiology, 78(1), pp. 481–504. doi: 10.1146/annurev-physiol-021115-105238.

Dickson R.P., Erb-Downward J.R., Falkowski N.R., Hunter E.M., Ashley S.L., Huffnagle G.B. (2018). The lung microbiota of healthy mice are highly variable, cluster by environment, and reflect variation in baseline lung innate immunity. American Journal of Respiratory and Critical Care Medicine, 198(4), pp. 497–508. doi: 10.1164/rccm.201711-2180OC.

Dickson R.P. and Huffnagle G.B. (2015). The lung microbiome: new principles for respiratory bacteriology in health and disease. PLoS Pathogens, 11(7), e1004923. doi: 10.1371/journal.ppat.1004923.

Ding L. and Yokota A. (2010). *Curvibacter fontana* sp. nov., a microaerobic bacteria isolated from well water. The Journal of General and Applied Microbiology, 56(3), pp. 267–271. doi: 10.2323/jgam.56.267.

Dréno B., Pécastaings S., Corvec S., Veraldi S., Khammari A., Roques C. (2018). *Cutibacterium acnes* (*Propionibacterium acnes*) and *acne vulgaris*: a brief look at the latest updates. Journal of European Academy of Dermatology and Venereology, 32(2), pp. 5–14. doi: 10.1111/jdv.15043.

Ericsson A.C., Personett A.R., Grobman M.E., Rindt H., Reinero C.R. (2016). Composition and predicted metabolic capacity of upper and lower airway microbiota of healthy dogs in relation to the faecal microbiota. PLoS One, 11(5), e0154646. doi: 10.1371/journal.pone.0154646.

Fastrès A., Felice F., Roels E., Moermans C., Corhay J.L., Bureau F., et al. (2017). The lung microbiome in idiopathic pulmonary fibrosis: a promising approach for targeted therapies. International Journal of Molecular Sciences, 18(12), 2735. doi: 10.3390/ijms18122735.

Fastrès A., Taminiau B., Vangrinsven E., Tutunaru A.C., Moyse E., Farnir F, et al. (2019). Effect of an antimicrobial drug on lung microbiota in healthy dogs. Heliyon. Elsevier, 5(11), e02802. doi: 10.1016/J.HELIYON.2019.E02802.

Fillion-Bertrand G., Dickson R.P., Boivin R., Lavoie J.P., Huffnagle G.B., Leclere M. (2018). Lung microbiome is influenced by the environment and asthmatic status in an equine model of asthma. American Journal of Respiratory Cell and Molecular Biology, 60(2), pp. 189–197. doi: 10.1165/rcmb.2017-0228OC.

Hahn M.W., Schmidt J., Taipale S.J., Doolittle W.F., Koll U. (2014). *Rhodoluna lacicola* gen. nov., sp. nov., a planktonic freshwater bacterium with stream-lined genome. International Journal Of Systematic and Evolutionary Microbiology, 64, pp. 3254–3263. doi: 10.1099/ijs.0.065292-0.

Heikkila-Laurila H.P. and Rajamaki M.M. (2014). Idiopathic pulmonary fibrosis in West Highland white terriers. Veterinary Clinics of North America: Small Animal Practice, 44, pp. 129–142. doi: 10.1016/j.cvsm.2013.08.003.

Heul V.A., Planer J. and Kau A.L. (2019). The human microbiota and asthma. Clinical Reviews in Allergy and Immunology, 57(3), pp. 350–363.

Hewitt R.J. and Molyneaux P.L. (2017). The respiratory microbiome in idiopathic pulmonary fibrosis. Annals of Translational Medicine, 5(12), 250. doi: 10.21037/atm.2017.01.56.

Hooda S., Minamoto Y., Suchodolski J.S., Swanson K.S. (2012). Current state of knowledge: the canine gastrointestinal microbiome. Animal health research reviews, 13(1), pp. 78–88. doi: 10.1017/S1466252312000059.

Huang Y., Ma S.F., Espindola M.S., Vij R., Oldham J.M., Huffnagle G.B., et al. (2017). Microbes are associated with host innate immune response in idiopathic pulmonary fibrosis', American Journal of Respiratory and Critical Care Medicine, 196(2), pp. 208–219. doi: 10.1164/rccm.201607-1525OC.

Kämpfer P., Busse H.J., Longaric I., Rosselló-Móra R., Galatis H., Lodders N. (2012). *Pseudarcicella hirudinis* gen. nov., sp. nov., isolated from the skin of the medical leech hirudo medicinalis. International Journal of Systematic and Evolutionary Microbiology, 62(9), pp. 2247–2251. doi: 10.1099/ijs.0.037390-0.

Karvone A.M., Kirjavainen P.V., Taubel M., Jayaprakash B., Adams R.I., Sordillo J.E., et al. (2019). Indoor bacterial microbiota and development of asthma by 10.5 years of age. Journal of Allergy and Clinical Immunology, 144(5), pp. 1402–1410. doi: 10.1016/j.jaci.2019.07.035.

Kasalický V., Jezbera J., Hahn M.W., Šimek K. (2013). The diversity of the *Limnohabitans* genus, an important group of freshwater bacterioplankton, by characterization of 35 isolated strains. PLoS One, 8(3), e58209. doi: 10.1371/journal.pone.0058209.

Kozich J.J., Westcott S.L., Baxter N.T., Highlander S.K., Schloss P.D. (2013). Development of a dual-index sequencing strategy and curation pipeline for analyzing amplicon sequence data on the MiSeq. Applied and Environmental Microbiology, 79(17), pp. 5112–5120. doi: 10.1128/AEM.01043-13.

Lorenzo J.M., Munekata P.E., Dominguez R., Pateiro M., Saraiva J.A., Franco D. (2018). Main groups of microorganisms of relevance for food safety and stability: General aspects and overall description. In Innovative technologies for food preservation: Inactivation of spoilage and pathogenic microorganisms. Elsevier. St Louis, Missouri: Elsevier Inc., pp. 53–107. doi: 10.1016/B978-0-12-811031-7.00003-0.

Määttä O.L.M., Laurila H.P., Holopainen S., Lilja-Maula L., Melamies M., Viitanen S.J., et al. (2018). Reflux aspiration in lungs of dogs with respiratory disease and in healthy West Highland white terriers. Journal of Veterinary Internal Medicine, 32(6), pp. 2074–2081. doi: 10.1111/jvim.15321.

McBride M.J. (2014). The family Flavobacteriaceae. In: Rosenberg E., DeLong E.F., Lory S., Stackebrandt E., Thompson F. (eds). The prokaryotes. Springer-Verlag. Berlin, Germany, pp. 643–676.

Molyneaux P.L., Willis-Owen S.A.G., Cox M.J., James P., Cowman S., Loebinger M., et al. (2017). Host-microbial interactions in idiopathic pulmonary fibrosis. American Journal of Respiratory and Critical Care Medicine, 195(12), pp. 1640–1650. doi: 10.1164/rccm.201607-1408OC.

Molyneaux P.L. and Maher T.M. (2013). The role of infection in the pathogenesis of idiopathic pulmonary fibrosis. European Respiratory Review, 22, pp. 376–381. doi: 10.1183/09059180.00000713.

Ngo J., Taminiau B., Fall P.A., Daube G., Fontaine J. (2018). Ear canal microbiota – a comparison between healthy dogs and atopic dogs without clinical signs of otitis externa. Veterinary Dermatology, 29(5), pp. 425-e140. doi: 10.1111/vde.12674.

Novik G., Savich V. and Kiseleva E. (2015). Microbiology in agriculture and human health. In Mohammad Manjur Shah (ed) Microbiology in Agriculture and Human Health. IntechOpen. London, United Kingdom, pp. 73–105. doi: 10.5772/60502.

O'Dwyer D.N., Shanna A.L., Gurczynski S.J., Meng X., Wilke C., Falkowski N.R., et al. (2019). Lung microbiota contribute to pulmonary inflammation and disease progression in pulmonary fibrosis. American Journal of Respiratory and Critical Care Medicine, 199, pp. 1127–1138. doi: 10.1164/rccm.201809-1650OC.

O'Dwyer D.N., Dickson R.P. and Moore B.B. (2016). The lung microbiome, immunity, and the pathogenesis of chronic lung disease. The Journal of Immunology, 196(12), pp. 4839–4847. doi: 10.4049/jimmunol.1600279.

Parks D.H. and Beiko R.G. (2010). Identifying biologically relevant differences between metagenomic communities. Bioinformatics, 26(6), pp. 715–721. doi: 10.1093/bioinformatics/btq041.

Pietschke C., Treitz C., Forêt S., Schultze A., Künzel S., Tholey A., et al. (2017). Host modification of a bacterial quorum-sensing signal induces a phenotypic switch in bacterial symbionts. Proceedings of the National Academy of Sciences of the United States of America, 114(40), E8488–E8497. doi: 10.1073/pnas.1706879114.

Roels E., Taminiau B., Darnis E., Neveu F., Daube G., Clercx C. (2017). Comparative analysis of the respiratory microbiota of healthy dogs and dogs with canine idiopathic pulmonary fibrosis. Journal of Veterinary Internal Medicine, 31(1), pp. 230–231. doi: 10.1111/jvim.14600.

Rognes T., Flouri T., Nichols B., Quince C., Mahé F. (2016). VSEARCH: a versatile open source tool for metagenomics. PeerJ, 4, e2584. doi: 10.7717/peerj.2584.

Salisbury M.L., Han M.K., Dickson R.P., Molyneaux P.L. (2017). Microbiome in interstitial lung disease: from pathogenesis to treatment target. Current Opinion in Pulmonary Medicine, 23(5), pp. 404–410. doi: 10.1097/MCP.0000000000000399.

Segal L.N., Rom W.N. and Weiden, M.D. (2014). Lung microbiome for clinicians: New discoveries about bugs in healthy and diseased lungs. Annals of the American Thoracic Society, 11(1), pp. 108–116. doi: 10.1513/AnnalsATS.201310-339FR.

Segata N., Izard J, Waldron L., Gevers D., Miropolsky L., Garrett W.S., et al. (2011). Metagenomic biomarker discovery and explanation. Genome Biology, 12(6). doi: 10.1186/gb-2011-12-6-r60.

Simpson J.M., Martineau B., Jones W.E., Ballam J.M., Mackie R.I. (2002). Characterization of faecal bacterial populations in canines: Effects of age, breed and dietary fiber. Microbial Ecology, 44(2), pp. 186–197. doi: 10.1007/s00248-002-0001-z.

Stanborough T., Fegan N., Powell S.M., Tamplin M., Chandry P.S. (2017). Insight into the genome of *Brochothrix thermosphacta*, a problematic meat spoilage bacterium. Applied and Environmental Microbiology, 83(5), e02786-16. doi: 10.1128/AEM.02786-16.

Syrjä P., Heikkilä H.P., Lilja-Maula L., Krafft E., Clercx C., Day M.J., et al. (2013). The histopathology of idiopathic pulmonary fibrosis in West Highland white terriers shares features of both non-specific interstitial pneumonia and usual interstitial pneumonia in man. Journal of Comparative Pathology, 149(2–3), pp. 303–313. doi: 10.1016/j.jcpa.2013.03.006.

Takahashi Y., Saito A., Chiba H., Kuronuma K., Ikeda K., Kobayashi T., et al. (2018). Impaired diversity of the lung microbiome predicts progression of idiopathic pulmonary fibrosis. Respiratory Research. Respiratory Research, 19, 34. doi: 10.1186/s12931-018-0736-9.

Thierry F., Handel I., Hammond G., King L.G., Corcoran B.M., Schwarz T. (2017). Further characterization of computed tomographic and clinical features for staging and prognosis of idiopathic pulmonary fibrosis in West Highland white terriers. Veterinary Radiology and Ultrasound, 58(4), pp. 381–388. doi: 10.1111/vru.12491.

Wypych L.C., Wickramasinghe T.P. and Marsland B.J. (2020). The influence of the microbiome on respiratory health. Nature immunology, 20, pp. 1279–1290.

Yu C., Liu Y., Sun L., Wang D., Wang Y., Zhao S. (2017). Chronic obstructive sleep apnea promotes aortic remodelling in canines through miR-145/Smad3 signalling pathway. Oncotarget, 8(23), pp. 37705–37716. doi: 10.18632/oncotarget.17144.

Supplemental material

All sample raw reads associated with this study have been deposited at the National Centre for Biotechnology Information (NCBI) under the accession number PRJNA594816.

Experimental section

Part 1

Study 3 :

Analysis of the lung microbiota in dogs with *Bordetella bronchiseptica* infection and correlation with culture and quantitative polymerase chain reaction

BMC Veterinary Research 51:46

Aline Fastrès, Morgane A. Canonne, Bernard Taminiau, Frédéric Billen, Mutien-Marie Garigliany, Georges Daube, Cécile Clercx

Abstract

Infection with *Bordetella bronchiseptica* (*Bb*), a pathogen involved in canine infectious respiratory disease complex, can be confirmed using culture or qPCR. Studies about the canine lung microbiota (LM) are recent, sparse, and only one paper has been published in canine lung infection. In this study, we aimed to compare the LM between *Bb* infected and healthy dogs, and to correlate sequencing with culture and qPCR results. Twenty *Bb* infected dogs diagnosed either by qPCR and/or culture and 4 healthy dogs were included. qPCR for *Mycoplasma cynos* (*Mc*) were also available in 18 diseased and all healthy dogs. Sequencing results, obtained from bronchoalveolar lavage fluid after DNA extraction, PCR targeting the V1–V3 region of the 16S rDNA and sequencing, showed the presence of *Bb* in all diseased dogs, about half being co-infected with *Mc*. In diseased compared with healthy dogs, the β-diversity changed ($P = 0.0024$); bacterial richness and α-diversity were lower ($P = 0.012$ and 0.0061), and bacterial load higher ($P = 0.004$). *Bb* qPCR classes and culture results correlated with the abundance of *Bb* ($r = 0.71$, $P < 0.001$ and $r = 0.70$, $P = 0.0022$). *Mc* qPCR classes also correlated with the abundance of *Mc* ($r = 0.73$, $P < 0.001$). *Bb* infection induced lung dysbiosis, characterized by high bacterial load, low richness and diversity and increased abundance of *Bb*, compared with healthy dogs. Sequencing results highly correlate with qPCR and culture results showing that sequencing can be reliable to identify microorganisms involved in lung infectious diseases.

Introduction

Bordetella bronchiseptica, a Gram-negative, aerobic, coccobacillus, is regarded as one of the principal pathogens involved in canine infectious respiratory disease complex (CIRD-C)(Schulz *et al.*, 2014; Viitanen *et al.*, 2015; Canonne *et al.*, 2016; Maboni *et al.*, 2019). Its prevalence in dogs with infectious respiratory diseases ranges from 5.2 to 78.7% (Schulz *et al.*, 2014; Rheinwald *et al.*, 2015; Decaro *et al.*, 2016; Maboni *et al.*, 2019). According to the taxonomical classification, the bacterium *B. bronchiseptica* belongs to the Proteobacteria phylum, the Alcaligenaceae family and the *Bordetella* genus (NCBI, 2019a). CIRD-C or formerly "kennel cough" is considered as one of the most common infectious diseases in dogs worldwide despite vaccination, and affects mostly young and kennel dogs (Ford, 2012). Viruses such as canine adenovirus, canine distemper virus, canine parainfluenza virus, canine respiratory coronavirus, pneumovirus and influenza A virus and bacteria other than *B. bronchiseptica* such as *Mycoplasma cynos* and *Streptococcus equi* subsp. *zooepidermicus* are primary infectious agents involved in the complex (Ford, 2012; Maboni *et al.*, 2019). Because of the numerous infectious aetiologies as well as possible co-infections, clinical signs of CIRD-C are highly variable and difficult to predict ranging from mild illness to severe pneumonia or death (Ford, 2012). Among the bacteria, *Mycoplasma cynos*, a Gram-negative organism is considered as an emerging bacterium in CIRD-C (Priestnall *et al.*, 2014; Maboni *et al.*, 2019). This bacterium belongs to the Tenericutes phylum, the Mycoplasmataceae family and the *Mycoplasma* genus (NCBI, 2019b). The diagnosis of *B. bronchiseptica* infection can be confirmed either by culture or by specific quantitative polymerase chain reaction (qPCR) on various samples including bronchoalveolar lavage fluid (BALF). The bacteria can also be observed on cytological preparations, adhering to the top of the cilia of respiratory epithelial cells (Canonne *et al.*, 2016). The treatment against *B. bronchiseptica* can be challenging as the bacterium is localized at the top of the cilia, can adopt a biofilm lifestyle and may drive an immunosuppressive response (Anderton *et al.*, 2004; Skinner *et al.*, 2005; Pilione and Harvill, 2006; Buboltz *et al.*, 2009; Cattelan *et al.*, 2016). In such cases, classical oral or parenteral antimicrobial drug may not be sufficient even if in vitro susceptibility is shown (Steinfeld *et al.*, 2012). Recently, it has been shown that gentamycin nebulization was helpful to achieve therapeutic concentration on the apical surface of bronchial epithelium, mostly when classical antimicrobial drugs failed to be curative (Bemis and Appel, 1977; Vieson *et al.*, 2012; Canonne *et al.*, 2018).

The 16S rDNA amplicon sequencing is a technique less sensitive than a qPCR but which allows rapid and accurate identification of all the bacteria composing the microbiota, which refers to the global microbial population of an area, including rare, unknown, slow-growing and unculturable bacteria (Woo *et al.*, 2008; Segal *et al.*, 2014; Scher *et al.*, 2016; Patelet *al.*, 2017). Moreover, this technique allows highlighting the complexity of the microbial populations and their alterations in

disease processes (Woo *et al.*, 2008; Patel *et al.*, 2017). In man, the 16S rDNA amplicon sequencing is increasingly being used in clinical contexts such as in acute pneumonia. Acute pneumonia is considered as an abrupt, emergent phenomenon with the predominance of specific taxonomic groups, low microbial diversity and high bacterial load (Dickson *et al.*, 2014, 2016; Dickson, Erb-Downward and Huffnagle, 2014). Studies in acute pneumonia indicate that the 16S rDNA sequencing improves the microbiological yield and could help to guide antimicrobial therapy (Woo *et al.*, 2008; Johansson *et al.*, 2019). In dogs, the lung microbiota (LM) has only been studied in bacterial secondary or community-acquired pneumonia (CAP) and only few data are available in experimental healthy beagles (Ericsson *et al.*, 2016; Fastrès *et al.*, 2019; Vientós-plotts *et al.*, 2019) and healthy dogs from other breeds (Fastrès *et al.*, 2020a). In dogs with pneumonia, a dysbiosis of the LM was observed with the loss of bacteria found in health and the domination, mostly in CAP, of one or two bacteria (Vientós-plotts *et al.*, 2019). Moreover a good agreement was found between the results of 16S rDNA amplicon sequencing and culture, although some discrepancies concerning the number of unique taxa identified and presence or absence of predominating taxa were noticed (Vientós-plotts *et al.*, 2019). Results suggest that the 16S rDNA amplicon sequencing could be useful for causal bacteria detection in parallel with culture, mostly if culture is negative (Vientós-plotts *et al.*, 2019).

The aims of this study were to analyse the LM in a series of cases with *B. bronchiseptica* infection in comparison with healthy dogs and to correlate results of the 16S rDNA amplicon sequencing with qPCR and culture results.

Materials and methods

1. Case selection criteria

Client-owned dogs referred to the veterinary hospital of the University of Liège, between January 2014 and December 2018, with a diagnosis of *B. bronchiseptica* infection, were recruited. Infection with *B. bronchiseptica* was confirmed by either positive culture ($> 10^4$ colony forming unit/mL), or positive qPCR, or both, on BALF samples and by the resolution of the clinical signs after adapted antimicrobial drug administration. Another inclusion criterion concerned the availability of BALF banked at −80 °C, for LM analysis. Data were collected from the medical records and included signalment, history, clinical signs, thoracic radiography, bronchoscopy findings and BALF analysis results, as well as culture and qPCR results.

BALF samples from healthy dogs involved in an independent study analysing the effect of the type of breed on the LM composition were also used. Those samples were obtained according to a protocol approved by the Ethical Committee of the University of Liège (protocol #1435) and after the owner consent. Healthy status was confirmed based on a complete history without abnormalities, normal physical examination, blood work (haematology and biochemistry), bronchoscopy and BALF analysis (gross appearance and cell counts). Healthy dogs did not receive any kind of antimicrobial drugs or probiotics for the year preceding the study.

2. BALF collection and processing

Bronchoscopy, bronchoalveolar lavage (BAL) procedure, and BALF processing and analysis were performed as already described (Canonne *et al.*, 2016; Fastrès *et al.*, 2019). Briefly, dogs were anesthetized using various protocols at the discretion of a board-certified anaesthesiologist. A flexible paediatric endoscope (FUJINON© Paediatric Video-Bronchoscope EB-530S) cleaned and disinfected before each use was inserted into the trachea until the extremity was wedged into the bronchi. Three to four mL/kg of sterile saline solution (NaCl 0.9%) divided into three aliquots were instilled into at least two different lung lobes, followed by aspiration by gentle suction. The recovered BALF was pooled. Before each BAL in dogs, a procedural control specimen (PCS) was obtained by injection and aspiration of 10 mL of sterile saline solution (NaCl 0.9%) through the bronchoscope.

Just after BALF collection, total (TCC) and differential cells counts (DCC) were determined using respectively a hemacytometer and a cytospin preparation (centrifugation at 221 *g*, for 4 min at 20 °C, Thermo Shandon Cytospin©4), by counting a total of 200 cells at high power field. Part of the crude BALF was promptly stored in cryotubes at −80 °C for the microbiota analysis and the remaining

BALF was centrifuged at 3500 × *g* 15 min at 4 °C and divided into pellets and supernatant also stored separately at −80 °C. The PCSs were stored in cryotubes at −80 °C without processing.

3. Culture

Cultures from crude fresh BALF samples were performed for aerobic bacteria detection. Cultures were conducted at 35 °C on several agar plates (Chapman's, Mac Conkey's, CAN and TSS agar). Standard biochemical methods were used to identify the bacteria (Synlab Laboratories, Liège, Belgium). Due to challenging growth requirements and as it is not classically performed in clinic, *Mycoplasma* sp. was not cultured. BALF samples from healthy dogs were not submitted to conventional bacterial culture.

4. *B. bronchiseptica* and *M. cynos* qPCR

In diseased dogs, qPCR targeting *B. bronchiseptica* and *M. cynos* were performed either on crude fresh BALF when performed immediately after the BAL procedure or on pellet and crude frozen BALF when performed later. In healthy dogs, qPCRs were performed on frozen pellet BALF (Department of Veterinary Pathology, Liège, Belgium).

DNA was extracted from samples using the NucleoMag Vet kit (Macherey-Nägel GmbH & Co. KG, Düren, Germany) according to the protocol provided by the manufacturer. Total DNA quantity and purity were measured after extraction using the ND-1000 spectrophotometer (NanoDrop ND-1000, Isogen, De Meern, The Netherlands).

For *B. bronchiseptica* and *M. cynos* detection, duplicate qPCR reactions (20 µL) included 2 µL of DNA template, 10 µL Luna Universal Probe qPCR Master Mix (Bioké, The Netherlands), 6 µL of water and 2 µL of the primers mix. For *B. bronchiseptica*, the primers mix contained 20 µL of the forward primer (5′-ACTATACGTCGGGAAATCTGTTTG -3′) and the reverse primer (5′-CGTTGTCGGCTTTCGTCTG -3′) at 10 µM and 10 µL of the probe (5′-FAM-CGGGCCGATAGTCAGGGCGTAG-BHQ1-3′) at 10 µM (Helps *et al.*, 2005). The cycling conditions started with an initial denaturation step at 95 °C for 10 min, followed by 45 cycles of denaturation at 95 °C for 30 s, primer annealing at 55 °C for 20 s and elongation at 72 °C for 1 min. For *M. cynos*, the primers mix contained 20 µL of the forward primer (5′-GTGGGGATGGATTACCTCCT-3′) and the reverse primer (5′-GATACATAAACACAACATTATAATATTG-3′) at 10 µM and 10 µL of the probe (5′-TCTACGGAGTACAAGTTACAATTCATTTTAGT-3′) at 10 µM (Sakmanoglu *et al.*, 2017). The cycling conditions were as follows: an initial denaturation step at 95 °C for 10 min, followed by 45 cycles of denaturation at 95 °C for 30 s, primer annealing at 50 °C for 20 s and elongation at 72 °C for 1 min.

Results obtained were further categorized into 6 classes for the correlation with the LM calculation according to a previously published study (Canonne *et al.*, 2016). Briefly, classes were defined based on the cycle threshold (Ct) values: very high load (Ct < 20), high load (20.1–24), moderate load (24.1–28), low load (28.1–32), very low load (> 32.1), and negative results.

5. 16S rDNA amplicon sequencing

Analysis of the LM in all samples was performed for each step (DNA extraction, polymerase chain reactions (PCRs), sequencing and post sequencing analysis) on a single occasion for all samples. As required, strict laboratory controls were done to avoid contaminations from PCR reagents and laboratory materials.

DNA was extracted from crude BALFs and PCSs previously banked at −80 °C, following the protocol provided with the DNeasy Blood and Tissue kit (QIAGEN Benelux BV; Antwerp, Belgium) as already described (Ngo *et al.*, 2018; Fastrès *et al.*, 2019). Total DNA quantity and purity were measured after extraction using the ND-1000 spectrophotometer (NanoDrop ND-1000, Isogen, De Meern, The Netherlands).

Duplicate qPCRs targeting the V2-V3 region of the 16S rDNA were performed to evaluate the bacterial load in the lung as already described (Bindels *et al.*, 2015; Fastrès *et al.*, 2019). qPCRs were conducted in a final volume of 20 µL containing 2.5 µL of template DNA, 0.5 µL of forward primer (5′-ACTCCTACGGGAGGCAGCAG-3′; 0.5 µM), 0.5 µL of reverse primer (5′-ATTACCGCGGCTGCTGG-3′; 0.5 µM), 10 µL of No Rox SYBR 2 × MasterMix (Eurogentec, Seraing, Belgium), and 6.5 µL of water. Data were recorded using an ABI 7300 real-time PCR system, with the following cycling sequence: 1 cycle of 50 °C for 2 min; 1 cycle of 95 °C for 10 min; 40 cycles of 94 °C for 15 s; and 1 cycle of 60 °C for 1 min. A melting curve was constructed in the range of 64–99 °C and the end of the cycle. The run contained also non-template controls and a tenfold dilution series of a V2–V3 PCR product purified (Wizard® SV Gel and PCR Clean-Up System, Promega, Leiden, The Netherlands), quantified by PicoGreen targeting double-stranded DNA (Promega) and used to build the standard curved. The results reflecting the bacterial load were expressed in logarithm with base 10 of the copy number per millilitre.

To characterize the bacterial populations in samples, the V1–V3 region of the bacterial 16S rDNA gene was amplified using the forward primer (5′-GAGAGTTTGATYMTGGCTCAG-3′) and the reverse primer (5′-ACCGCGGCTGCTGGCAC-3′) with Illumina overhand adapters as previously described (Ngo *et al.*, 2018; Fastrès *et al.*, 2019). PCRs were conducted and amplicons obtained purified with the Agencourt AMPure XP beads kit (Beckman Coulter, Villepinte, France), indexed using the Nextera XT index primers 1 and 2 and quantified by PicoGreen (ThermoFisher Scientific,

Waltham, MA, USA) before normalization and pooling to form libraries. The amplification products < 1 ng/µL were not sequenced.

Sequencing was performed on a Miseq Illumina sequencer using V3 reagents with positive controls and negative controls from the PCR step.

A total of 3 254 346 reads were obtained after sequencing with a median length of 510 nucleotides. After a first cleaning step, 3 116 730 reads were screened for chimera using Vsearch (Rognes *et al.*, 2016). 3 040 049 reads were retained for alignment and clustering using MOTHUR v1.40 (Kozich *et al.*, 2013). The taxonomical assignations with an operational taxonomic unit (OTU) clustering distance of 0.03 were based on the SILVA database v1.32. A final subsampling was performed with a median reads per samples of 10 000 reads.

All sample raw reads were deposited at the National Centre for Biotechnology Information and are available under Bioproject ID PRJNA575149.

6. Statistical analyses

To compare diseased and healthy dogs, a subpopulation of dogs with *B. bronchiseptica* infection was selected to be age-matched with the population of healthy dogs (Mann–Whitney tests using XLStat software).

Normality was checked with Shapiro–Wilk tests before each comparison between healthy and diseased dogs. Mann–Whitney tests were used to compared TCC and DCC between diseased and healthy dogs using XLStat software. Differences in relative abundances between groups at all the taxonomic levels were assessed by Welch's t-tests and Benjamini–Hochberg–false discovery rate of 10% correction (O'Dwyer *et al.*, 2019), with STAMP software. The β-diversity was evaluated by a permutational analysis of the variance (PERMANOVA) and visualized with a principal component analysis (PCA) using R (R vegan package). Other ecological parameters of the LM were calculated using MOTHUR v1.40 and compared between healthy and diseased dogs with Mann–Whitney tests using XLStat software. The α-diversity was based on the inverse Simpson index, the richness on the chao index and the evenness was derived from the Simpson index. The bacterial load was compared between groups with Mann–Whitney tests using XLStat software. The bacterial loads in PCSs were compared with the corresponding bacterial load in BALF samples with a Wilcoxon signed-rank test using XLStat software.

Correlations between the lung bacterial communities at each taxonomic level and the Ct classes for either *B. bronchiseptica* or *M. cynos*, and the culture results, were measured with Spearman tests using XLStat software.

Data were expressed as median and interquartile range. A P value < 0.05 was considered as statistically significant.

Results

1. Animals

Twenty dogs with a diagnosis of *B. bronchiseptica* infection and 4 healthy dogs were included in the study (Table 1). In all dogs, median age was 9 months (range 3-18) and medium weight was 11.5 kg (1.3–41.0). From the 20 diseased dogs, seven (dogs no. 3, 9, 14, 15, 18, 19 and 20) were selected and compared with the 4 healthy dogs. No significant difference in the age was found between the subpopulation of diseased dogs and the healthy dogs ($P = 0.073$). For the TCC, DCC and all LM parameters (including relative abundances at all taxonomic levels, the bacterial load and the ecological parameters including the β and α-diversity, the richness and the evenness), differences between the subpopulations of diseased dogs selected or not for the comparison with healthy dogs were not significant indicating that the subsampling is representative of all the diseased group (see Additional file 1).

Table 1: *Characteristics of the dogs included in the study.*

Dogs	Status	Age at sampling (years)	Sex	Breed	Antibiotic treatment at sampling	Ct *B. bronchiseptica*	Ct *M. cynos*	Culture
1	Diseased	0.60	M	French bulldog	-	28.4	22.9	/
2	Diseased	0.40	M	Malamute	+ (amoxicillin/clavulanic acid 12.5 mg/kg BID and enrofloxacin 5 mg/kg SID, PO, for 1 day)	22.3	18.5	-
3	Diseased	1.05	F	French bulldog	-	25.3	-	+ (*B. bronchiseptica*)
4	Diseased	0.43	F	Boxer	-	21.9	-	+ (*B. bronchiseptica*)
5	Diseased	0.65	F	French bulldog	+ (doxycycline 5 mg/kg BID, PO, for 10 days)	24.2	LOD	+ (*B. bronchiseptica*)
6	Diseased	0.32	F	English bulldog	+ (marbofloxacin 3 mg/kg SID, PO, for 7 days)	?	?	-
7	Diseased	0.35	F	Jack Russel terrier	-	/	/	+ (*B. bronchiseptica*)
8	Diseased	0.54	M	Boxer	+ (amoxicillin/clavulanic acid 12.5 mg/kg BID, PO for 1 day)	26.5	24.0	-
9	Diseased	0.99	F	Munster lander	-	23.6	-	+ (*B. bronchiseptica*)
10	Diseased	0.38	F	French bulldog	-	?	/	/
11	Diseased	0.56	F	Chihuahua	-	24.0	?	-
12	Diseased	0.51	F	Cavalier king Charles spaniel	-	24.0	-	+ (*B. bronchiseptica*)

Dogs	Status	Age at sampling (years)	Sex	Breed	Antibiotic treatment at sampling	Ct *B. bronchiseptica*	Ct *M. cynos*	Culture
13	Diseased	0.57	F	German shepherd	-	21.5	LOD	+ (*B. bronchiseptica*)
14	Diseased	0.68	F	Cavalier king Charles spaniel	-	25.6	23.7	+ (*B. bronchiseptica*, *Acinetobacter baumanii*)
15	Diseased	0.99	M	Spitz	-	17.6	-	+ (*B. bronchiseptica*)
16	Diseased	0.53	M	Boxer	-	25.3	32.8	/
17	Diseased	0.27	M	Yorkshire terrier	-	21.8	-	+ (*B. bronchiseptica*)
18	Diseased	0.90	F	Spitz	-	23.5	-	+ (*Pantoea agglomerans*, *Serratia marcescens*)
19	Diseased	1.51	M	Chinese crested	+ (doxycycline, one injection, dose unknown)	32.0	-	-
20	Diseased	0.72	M	Cavalier king Charles spaniel	-	21.5	-	+ (*B. bronchiseptica*)
21	Healthy	1.26	M	Beauceron	-	-	-	/
22	Healthy	1.19	M	French bulldog	-	-	-	/
23	Healthy	1.40	M	French bulldog	-	38.0	-	/
24	Healthy	1.43	M	Pug	-	-	-	/

qPCR, quantitative polymerase chain reaction; Ct, cycle threshold value; +, positive result; -, negative result; ?, positive qPCR result but Ct value not known; /, test not performed; LOD, only one replicate was above the detection's limit; SID, once a day; BID, twice a day; PO, oral administration.

French bulldogs, boxers and Cavalier King Charles spaniels were among the most represented breeds and counted for 50% of the recruited dogs affected with *B. bronchiseptica*. Chronic productive daily cough of at least 1 week to 4 month's duration (median of 1 month) was reported in all diseased cases. At presentation, 5 dogs were receiving oral antimicrobial agents (Table 1) without improvement including amoxicillin/clavulanic acid ($n = 1$), amoxicillin/clavulanic acid with enrofloxacin ($n = 1$), doxycycline ($n = 2$) and marbofloxacin ($n = 1$). Vaccinal status was recorded for 15 dogs, 6 dogs were not vaccinated against *B. bronchiseptica* and 9 received only one subcutaneous vaccinal injection (Pneumodog©, Merial, Lyon, France) between one and 12 months (median 2 months) before the development of symptoms. Physical examination was normal in 5 dogs, positive laryngo-tracheal reflex was noted in 10 dogs, 5 dogs had bilateral nasal discharge, 2 had dyspnoea and 1 had mild hyperthermia (39.1 °C). Thoracic radiography revealed the presence of a ventral alveolar pattern in 9 dogs, a broncho-interstitial pattern in 8 dogs and no abnormalities in 3 dogs. The diagnosis of *B. bronchiseptica* infection was confirmed by a positive qPCR ($n = 9$), a positive culture ($n = 1$) or both ($n = 10$).

2. Bronchoscopy and BALF analysis

During the bronchoscopy procedure, in diseased dogs, mucopurulent material was seen in the trachea and bronchi in 14 dogs, oedema and/or erythema and/or thickening of the bronchial wall was noted in 10 dogs, bronchomalacia was reported in 4 dogs. TCC and DCC were available in the BALF of 18 and 17 diseased dogs, respectively. In all the diseased dogs, median TTC was 1740 cells/µL (1080–3515) and the median differential cell count included 39% (12–63) of macrophages, 41% (24–77) of neutrophils, 7% (4–12) of lymphocytes and 1% (0–5) of eosinophils.

Compared with healthy dogs, the TTC in the subpopulation of dogs affected with *B. bronchiseptica* was significantly higher with more neutrophils and less macrophages (Table 2).

***Table 2**: Total and differential cell counts between the subpopulation of diseased dogs and healthy dogs.*

	Total cell count (cells/µL)	Macrophages (%)	Neutrophils (%)	Lymphocytes (%)	Eosinophils (%)
Subpopulation of diseased dogs (n = 7)	1300 (1040 - 3622)	33 (15.8 – 47.2)	48 (35.8 – 68.5)	9.5 (6.2 – 15.8)	2 (1 – 6.8)
Healthy dogs (n = 4)	270 (243.8 - 380)	91.5 (85.5 – 96.2)	2.5 (2 – 3.2)	6 (0.8 – 11.2)	0.5 (0 – 1.5)
P-value	0.0061	< 0.001	0.014	0.29	0.32

Results are expressed as median (range). Significant P-values are in bold. The subpopulation of diseased dogs corresponds to the dogs n°3, 9, 14, 15, 18, 19 and 20 in the Table 1.

3. Culture results

In the diseased dogs, the result of the culture was positive for *B. bronchiseptica* in 6/11 dogs (54.5%) and negative in 5 dogs from which 4 were under antimicrobial treatment.

4. *B. bronchiseptica* and *M. cynos* quantitative PCR

All qPCR results were positive for *B. bronchiseptica* in the diseased dogs (19/19) and included 1 very high load result, 9 high load results, 5 moderate load results and 2 low load results, one of them corresponding to a dog receiving doxycycline. Two qPCRs were positive without information available on the Ct level. qPCR results for *M. cynos* were positive in 7/18 (38.9%) and included 1 very high load result, 3 high load results and 1 very low load result. Two qPCR results were positive but Ct values were unknown.

In the healthy group, one dog had a positive qPCR result for *B. bronchiseptica* at a very low load, while the results were negative in the 3 other dogs. qPCRs for *M. cynos* were all negative in the healthy group.

5. Microbiota analysis

The PCSs were not sequenced as their amplification products after purification were < 1 ng/µL. An internal study performed in our laboratory (Taminiau B and Daube G, unpublished observations) showed that under this value, the sequencing is not reliable. Moreover, the bacterial load was about 100 times lower in the PCSs compared with the samples ($P = 0.016$).

B. bronchiseptica was found in each of the 20 diseased dogs with a relative abundance of more than 50% in 13 of them. Only 2 dogs (dogs n°1 and 11) had a relative abundance of *B. bronchiseptica* of less than 5% (Figure 1). Among the diseased dogs, 40% (8/20) were co-infected with *M. cynos* and/or *Pseudomonas* sp. and other strain of *Mycoplasma* than *M. cynos*. Other bacteria were also found in high relative abundance (> 5%) including, *Elizabethkingia meningoseptica*, *Stenotrophomonas* sp., *Ureaplasma* sp., Alcaligenaceae_genus sp., *Elizabethkingia meningoseptica*, *Fusobacterium* sp., *Methylotenera* sp. and *Escherichia-Shigella* sp. (Figure 1).

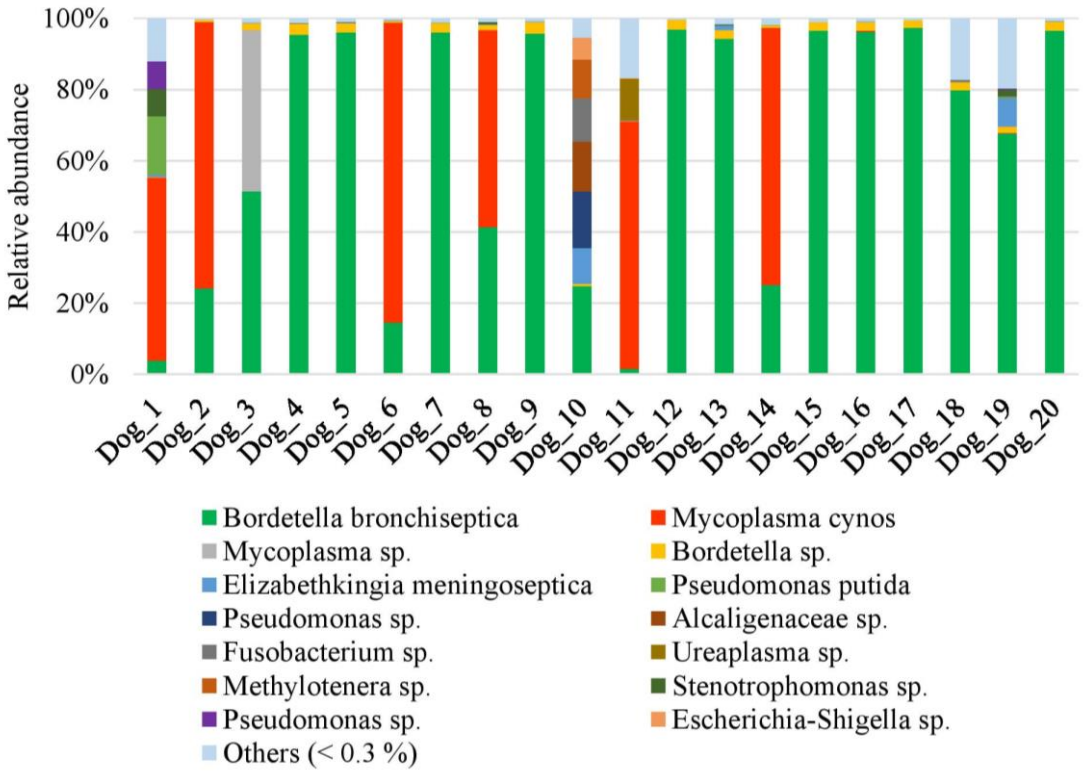

Figure 1. *Species-level composition of the lung microbiota in dogs affected with B. bronchiseptica. Bar charts showing relative abundance annotated to the taxonomic level of species of all taxa detected in the bronchoalveolar lavage fluid of 20 dogs affected with B. bronchiseptica.*

In healthy dogs, *B. bronchiseptica* was found by amplicon sequencing in one dog and *M. cynos* in 3 dogs in a very low relative abundance (0.43 and 0.55, 0.52 and 0.61% respectively).

In diseased compared with healthy dogs, a shift was observed in the bacterial populations with more Alcaligenaceae in diseased compared with healthy dogs (82.3% (62.6-99.4) versus 2.2% (1.3–3.8); *P*-value corrected = 0.058) at the family level (Figure 2B). At the genus level (Figure 2C), there were more *Bordetella* in diseased compared with healthy dogs (82.3% (61.7-99.4) versus 0% (0–0.1); *P*-value corrected = 0.11). There was no significant difference at the phylum (Figure 2A) and at the species levels (Figure 2D), although a marked increase in Proteobacteria (94.3% (67.6-99.6) versus 38.9% (30.4–49.0); *P*-value corrected = 0.30) phylum reflecting the increase in *B. bronchiseptica* (79.8% (59.5–96.2) versus 0% (0–0.1); *P*-value corrected = 0.40) species was noted in diseased compared with healthy dogs. The β-diversity (Figure 3) assessed by the PERMANOVA was significantly different between healthy and diseased dogs ($P = 0.0024$). The α-diversity (Figure 4A) as well as the richness (Figure 4B) were significantly lower in diseased compared with healthy dogs. There was no difference between healthy and diseased dogs for the evenness ($P = 0.10$) ((Figure 4C). Finally, the bacterial load was significantly higher in dogs with *B. bronchiseptica* infection compared with healthy dogs (Figure 5).

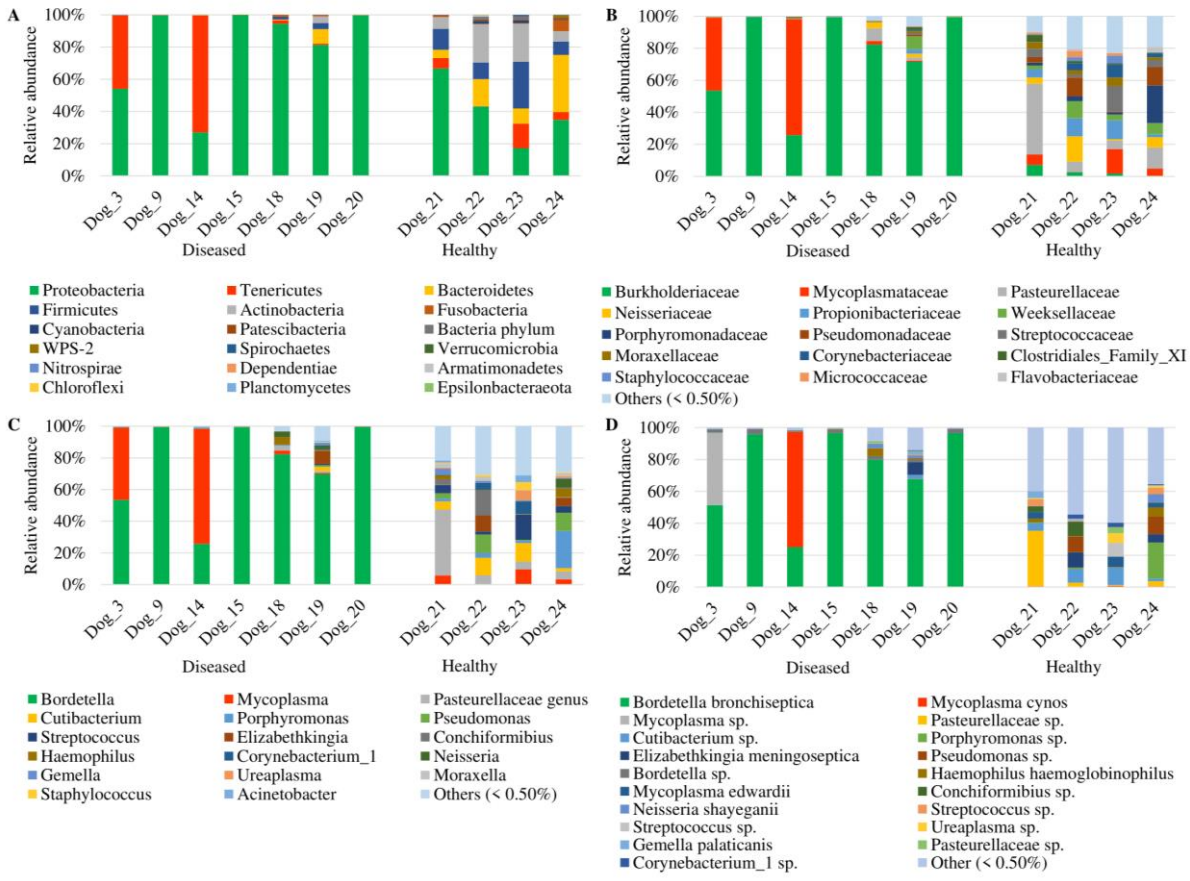

Figure 2. *Taxa detected in healthy dogs and dogs affected with B. bronchiseptica. Bar charts showing the relative abundance of all taxa detected in the bronchoalveolar lavage fluid of 4 healthy dogs and 7 dogs affected with B. bronchiseptica, annotated to the taxonomic level of phylum (A), family (B), genus (C) and species (D).*

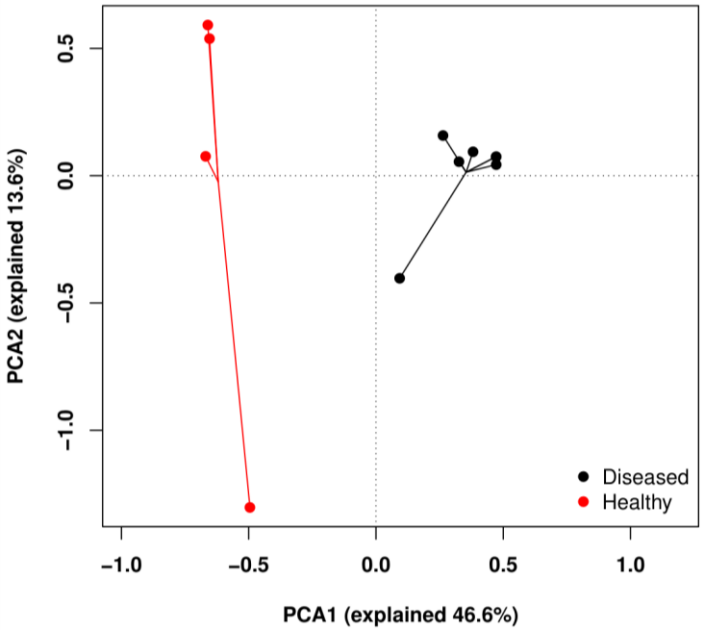

Figure 3. *Principal component analysis representing the β-diversity between healthy dogs and dogs affected with B. bronchiseptica. Lung communities are clustered by groups (diseased (n = 7) and healthy (n = 4) dogs).*

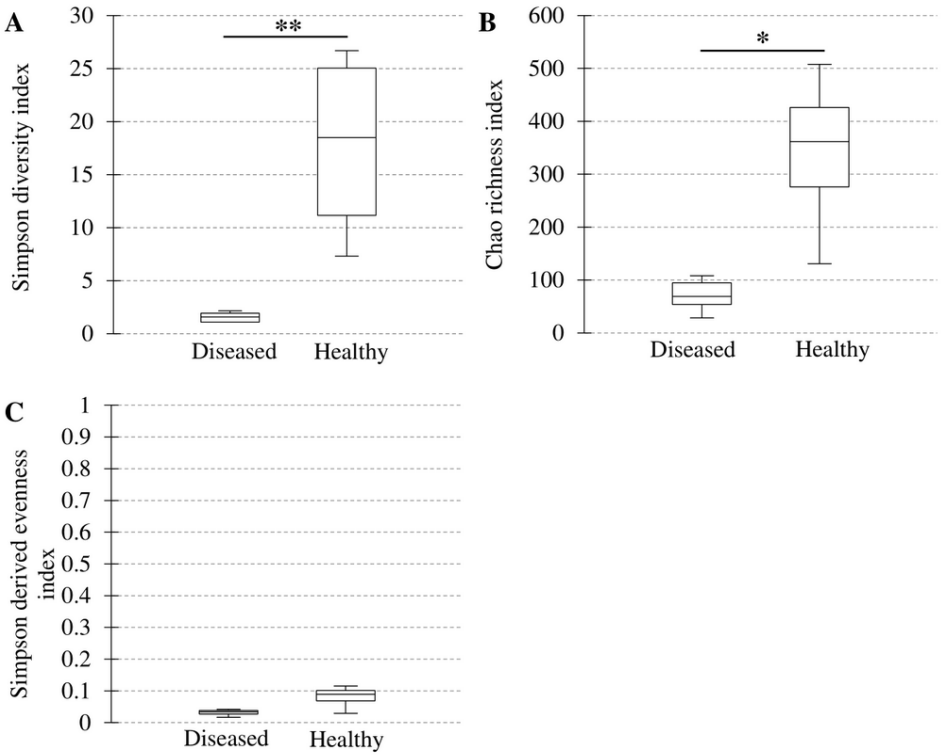

Figure 4. *Ecological parameters comparison between healthy dogs and dogs affected with B. bronchiseptica. Box plot graphs representing the bacterial alpha diversity (A), richness (B) and evenness (C) in healthy (n = 4) compared with diseased dogs (n = 7). The medians are represented by the central horizontal bars. The lower and upper limits of the box are the first and third quartiles, respectively. *P = 0.012; **P = 0.006.*

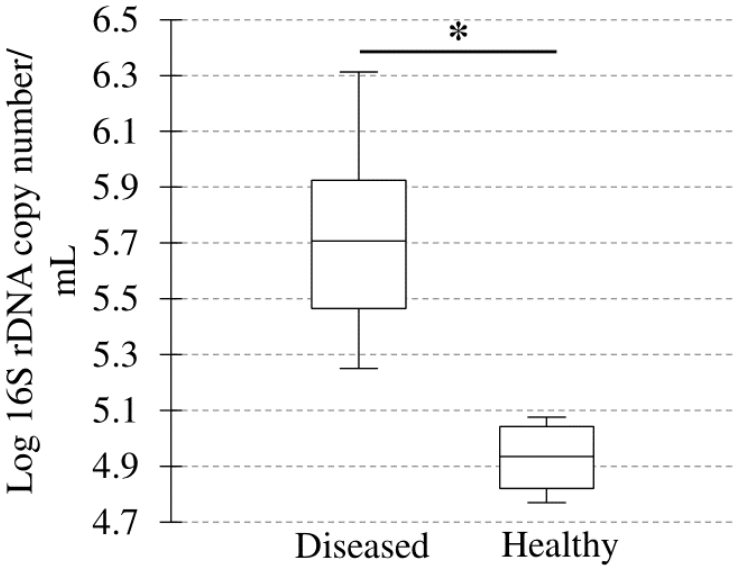

Figure 5. *Bacterial load in healthy dogs and dogs affected with B. bronchiseptica. Box plot representing the logarithm of the number of 16S rDNA copies per microliter (bacterial load) between healthy (n = 4) and diseased dogs (n = 7). The medians are represented by the central horizontal bars. The lower and upper limits of the box are the first and third quartiles, respectively. *P = 0.004.*

A significant positive correlation was found between the bacterial composition in *B. bronchiseptica* and *M. cynos* at each taxonomic level obtained by the 16S rDNA amplicon sequencing and the Ct classes for *B. bronchiseptica* and *M. cynos*, and the culture results as shown in Table 3. In all cases where a positive culture was found for *B. bronchiseptica*, the relative abundance for *B. bronchiseptica* was highly elevated (96.01% (94.87–96.56)). In 2 dogs, other bacteria were identified by culture including *Acinetobacter baumanii*, *Pantoea agglomerans* and *Serratia marcescens* (Table 1) but were not identified by sequencing.

Table 3: *Correlation between the 16S rDNA amplicon sequencing and either Ct classes or culture.*

			B. bronchiseptica				*M. cynos*	
			qPCR results		Culture results		qPCR results	
			r	P-value	r	P-value	r	P-value
16S rDNA amplicon sequencing results	Phyla	Proteobacteria	0.54	0.012	0.70	0.0022		
		Tenericutes					0.66	0.0018
	Families	Alcaligenaceae	0.66	0.0015	0.70	0.0021		
		Mycoplasmataceae					0.66	0.0018
	Genera	*Bordetella*	0.73	< 0.001	0.70	0.0022		
		Mycoplasma					0.66	0.0018
	Species	*Bordetella_bronchiseptica*	0.71	< 0.001	0.70	0.0022		
		Mycoplasma_cynos					0.73	< 0.001
		Bordetella_Otu00473	0.70	< 0.001	0.68	0.0017		

Significant positive correlation results between the bacterial composition of the LM in all dogs (n = 24) for B. bronchiseptica and M. cynos at each taxonomic level and either B. bronchiseptica and M. cynos Ct classes or the culture. qPCR, quantitative polymerase chain reaction; r, Spearman correlation coefficient.

Discussion

In the present study, we described the LM in dogs with CIRD-C and *B. bronchiseptica* infection. We showed a clear dysbiosis of the LM with a significant decrease in α-diversity and richness, as well as an increased bacterial load, in dogs affected with *B. bronchiseptica* compared with healthy dogs. The Alcaligenaceae family and the *Bordetella* genus were overrepresented in diseased dogs. In the sequencing profile, about half of the diseased dogs were co-infected, the majority with *M. cynos*. Finally, a positive correlation was found between the bacterial composition of the LM for *B. bronchiseptica* and *M. cynos* at each taxonomic level and the corresponding qPCR or culture result.

In this study, the major phyla found in healthy dogs were the Proteobacteria, the Bacteroidetes, the Actinobacteria and the Firmicutes. The same major phyla have already been reported in the LM of healthy dogs (Ericsson *et al.*, 2016; Fastrès *et al.*, 2019; Fastrès *et al.*, 2020a). Despite their implication in CIRD-C, *B. bronchiseptica* and *M. cynos* are commensal bacteria found in the respiratory tract of healthy dogs (Ford, 2012; Canonne *et al.*, 2016; Maboni *et al.*, 2019). In the present study, the amplicon sequencing technique detected *B. bronchiseptica* at very low level in 1 healthy dog, in which qPCR revealed a very low load. The absence of dysbiosis associated with the presence of *B. bronchiseptica* at a very low level in that dog, corroborates the fact that this bacterium is a commensal bacterium which is not always associated with lung disease (Ford, 2012; Canonne *et al.*, 2016; Maboni *et al.*, 2019). The amplicon sequencing technique also detected *M. cynos* in low relative abundance in 3 of the healthy dogs, while qPCR results were negative. Since different aliquots from a same initial sample of BALF were used for qPCR and amplicon sequencing technique, a lack of homogeneity between the aliquots could explain this slight discrepancy.

Compared with healthy dogs, a dysbiosis was observed in the diseased dogs, with a shift in microbial populations as shown by a clear difference in the β-diversity. The Proteobacteria and the Tenericutes phylum were more abundant in the diseased dogs, logically reflecting an increased prevalence of *Bordetella* and *Mycoplasma*. The incapacity to show significant differences between healthy and diseased dogs at the species level was probably due to a lack of power in the statistical tests related to the low number of control dogs included in the study as well as to the high number of data (10 000 sequences per sample). Indeed, large dataset requires more severe corrections for multiple tests (Desquilbet, 2015). In dogs affected with *B. bronchiseptica* infection, in comparison with heathy dogs, the LM was composed in majority by only one or two bacteria, a finding that has also been reported in dogs with CAP (Vientós-plotts *et al.*, 2019). In pneumonia in man, the dominant pathogenic strain also usually represents the majority of the detected sequences (74% or more) (Dickson *et al.*, 2016); a low alpha-diversity and low richness reflecting the high predominance of one or two bacteria are also described together with an increased bacterial load (Dickson, Erb-Downward

and Huffnagle, 2014). In the present study, we observed identical modifications since the α-diversity and the richness were drastically lower and the bacterial load higher in diseased compared with healthy dogs. These modifications are supported by the ecological modelling of the LM proposed by Dickson et al. (2014). In healthy individuals, the bacterial communities found in the LM are mainly determined by the balance between immigration and elimination while in injured respiratory tract, the local growth conditions are altered creating a pressure across bacterial members and improving the reproduction rate of adapted bacteria which results in an increase in the bacterial load and a decrease in the richness and the diversity, together with the emergence of dominating bacteria (Dickson, Erb-Downward and Huffnagle, 2014).

The prevalence of bacterial co-infections in dogs affected with *B. bronchiseptica* found in this study by sequencing is quite elevated (40%) in comparison with data from the literature, where bacterial co-infections are reported in 7.69% to 53% of cases (Viitanen, Lappalainen and Rajamäki, 2015; Canonne *et al.*, 2016; Decaro *et al.*, 2016). Reported co-infecting bacteria in CIRD-C also found in that study by sequencing included *M. cynos* (Canonne *et al.*, 2016), other *Mycoplasma* species (Viitanen, Lappalainen and Rajamäki, 2015; Decaro *et al.*, 2016) and *Pseudomonas* sp. (Ford, 2012). Other bacteria with a relative abundance > 5% that have been associated with pneumonia such as *Stenotrophomonas* sp., *Ureaplasma* sp., *Escherichia-Shigella* sp. in dogs (Chalker, 2005; Rheinwald *et al.*, 2015; Johnson *et al.*, 2016; Lappin *et al.*, 2017; Vientós-plotts *et al.*, 2019), or *Elizabethkingia meningoseptica* in men (Jean *et al.*, 2014) were found in that study. Although it is unclear if they are just colonizing or co-infecting bacteria, and if they could potentially play a role in CIRD-C. The high rate of co-infections in this study could be associated with the selection of the diseased dogs. Indeed, in CIRD-C, the disease is often self-limiting and resolves spontaneously within 2 weeks without complications (Ford, 2012) while co-infections are usually associated with more severe and chronic clinical signs (Maboni *et al.*, 2019). The diseased dogs were referral cases with clinical signs for a median duration of 1 month. Higher bacterial co-infection rate could also be related to underlying viral infection (Ford, 2012; Maboni *et al.*, 2019), which was not assessed in this study.

As previously reported and confirmed in this study, the qPCR is a very sensitive technique to diagnose *B. bronchiseptica* infection (Canonne *et al.*, 2016). All infected dogs tested in this study had a positive qPCR result for *B. bronchiseptica* generally at moderate to very high load. The result of the culture was negative in 5/11 dogs which could partially be related to the fact that four of those dogs had recently been treated with antimicrobial drugs which may impair culture growth. Negative culture results have also already been described in dogs with *B. bronchiseptica* infection and could be associated with the sensitivity of the technique (Canonne *et al.*, 2016). In man, it has been shown that the culture sensitivity in *Bordetella sp.* infections was lower than the PCR sensitivity (Reizenstein *et al.*, 1993). In the present study, *B. bronchiseptica* was found by 16S rDNA amplicon sequencing in

high amount in all the diseased dogs. The results of the amplicon sequencing at each taxonomic level were correlated with the Ct classes and the culture results. Such good agreement between positive culture results and 16S rDNA sequencing results has already been reported (Vientós-plotts *et al.*, 2019), with a high relative abundance of the taxa found by culture. Also, as already reported, some ubiquitous bacteria identified by culture were not found with the 16S rDNA amplicon sequencing which could be due to a mis annotation of the SILVA database or to a contamination of the culture which could lead to errors in culture-based antimicrobial drug selection (Vientós-plotts *et al.*, 2019). Other co-infecting and/or colonizing bacteria were detected by the sequencing, showing that the 16S rDNA amplicon sequencing can be an interested technique to identified new potential pathogens. Moreover, the sequencing depicts the global bacterial population on the contrary of the qPCR and culture. Indeed, the qPCR is specific of the targeted sequence and is not useful to detect new bacteria (Maddocks and Jenkins, 2017). Culture is quite challenging; some bacteria like *Mycoplasma* sp. requires specific culture conditions, some bacteria are unculturable and other bacteria are rare and slow growing and therefore may be missed (Woo *et al.*, 2008). The present study has some limitations. Firstly, qPCR Ct and culture results were not available in all dogs. Moreover, the qPCRs were performed on different type of materials (frozen or fresh, pellet or crude BALF). Some dogs were treated with antimicrobial drugs at the time of sampling which could have an impact on culture, qPCR and sequencing results. Culture results of BALF samples from healthy dogs were not available. We consider that such results are not essential since our study focuses on the evaluation of the 16S rDNA amplicon sequencing technique in diseased dogs, in a clinical context. Besides, we have a quite limited number of control dogs and in order to compare age-matched groups, we have selected a subpopulation of our diseased dogs for the comparison. Indeed, although in dogs the effect of aging has not been studied, in man, the LM has been reported to be different in young children of less than 3 years compared with adults (Dickson *et al.*, 2016). Healthy dogs were not breed-matched with the diseased dogs. However, the breed impact on the LM seemed to be subtle (Fastrès *et al.*, 2020a). No differences between the selection of diseased dogs and the rest of the diseased group were shown suggesting that the selection is representative of the diseased group.

Conclusion

In dogs with CIRD-C and *B. bronchiseptica* infection, there is a major dysbiosis of the LM, characterized by high bacterial load, low richness and diversity and increased abundance of *B. bronchiseptica*, in comparison with healthy dogs.

Co-infections, mostly with *M. cynos*, are frequent in CIRD-C dogs with *B. bronchiseptica* infection and could have an impact on the duration of the disease and the response to treatment.

The sequencing results highly correlated with results obtained by specific qPCR of *B. bronchiseptica* and *M. cynos* and culture of *B. bronchiseptica.* Therefore, 16S rDNA amplicon sequencing is reliable to identify potential causal bacterial microorganism involved in lung infectious diseases, to understand the global interaction between bacteria in the lung and could be useful to identify new species potentially involved in respiratory diseases in dogs.

In the future, with the development of 16S technologies, it could be interesting to include those analyses in the diagnostic work-up, mostly in dogs with a suspicion of lower airway infection, especially when the classical culture is negative or when there is no or only poor response to classical treatment. However, in such case, additional culture will still be needed to detect bacterial resistance to antimicrobial drugs.

Acknowledgments

The authors thank Sylvain Romijn and Belinda Albert for their technical assistance. Authors also thank Eveline Moyse for her contribution to statistical analysis.

References

Anderton, T.L., Maskell, D.J. and Preston A. (2004). Ciliostasis is a key early event during colonization of canine tracheal tissue by *Bordetella bronchiseptica*. Microbiology, 150, pp. 2843–2855. doi: 10.1099/mic.0.27283-0.

Bemis D. and Appel M. (1977). Aerosol Nolvasan treatment of *Bordetella bronchiseptica* in dogs. Veterinary Clinic of North America: Small Animal Practice, 72(1), pp. 53–55.

Bindels L.B., Neyrinck A.M., Salazar N., Taminiau B., Druart C., Muccioli G.G., et al. (2015). Non digestible oligosaccharides modulate the gut microbiota to control the development of leukemia and associated cachexia in mice. PLoS One, 10(6), e0131009. doi: 10.1371/journal.pone.0131009.

Buboltz A.M., Nicholson T.L., Weyrich L.S., Harvill E.T. (2009). Role of the Type III Secretion System in a hypervirulent lineage of *Bordetella bronchiseptica*. Infection and Immunity, 77(9), pp. 3969–3977. doi: 10.1128/IAI.01362-08.

Canonne A.M., Billen F., Tual C., Ramery E., Roels E., Perters I., Clercx C. (2016). Quantitative PCR and cytology of bronchoalveolar lavage fluid in dogs with *Bordetella bronchiseptica* infection. Journal of veterinary internal medicine, 30(4), pp. 1204–1209. doi: 10.1111/jvim.14366.

Canonne M., Roels E., Billen F., Benchekroun G., Clercx C. (2018). Comparison of two aerosolized gentamicin protocols for *Bordetella bronchiseptica* lower airway infection in dogs. Journal of Veterinary Internal Medicine, 32, pp. 2306–2307. doi: 10.1111/jvim.15092.

Cattelan N., Dubey P., Arnal L., Yantorno O.M., Deora R. (2016). *Bordetella* biofilms : a lifestyle leading to persistent infections. Pathogens and Disease, 74, ftv108. doi: 10.1093/femspd/ftv108.

Chalker V. (2005). Canine mycoplasmas. Research in Veterinary Science, 79(1), pp. 1–8. doi: 10.1016/j.rvsc.2004.10.002.

Decaro N., Mari V, Larocca V., Losurdo M., Lanave G., Stella M., et al. (2016). Molecular surveillance of traditional and emerging pathogens associated with canine infectious respiratory disease. Veterinary Microbiology, 192, pp. 21–25. doi: 10.1016/j.vetmic.2016.06.009.

Desquilbet L. (2015) Puissance statistique d'une étude version 3. Available at: https://eve.vet-alfort.fr/course/view.php?id=353 (Accessed: 3 May 2018).

Dickson R.P., Erb-Downward J.R., Prescott H.C., Martinez F.J., Curtis J.L., Lama V.N., et al. (2014). Analysis of culture-dependent versus culture-independent techniques for identification of bacteria in clinically obtained bronchoalveolar lavage fluid. Journal of Clinical Microbiology, 52(10), pp. 3605–3613. doi: 10.1128/JCM.01028-14.

Dickson R.P. Erb-Downward J.R., Martinez F.J., Huffnagle G.B. (2016). The microbiome and the respiratory tract. Annual Review of Physiology, 78(1), pp. 481–504. doi: 10.1146/annurev-physiol-021115-105238.

Dickson R.P., Erb-Downward J.R. and Huffnagle G. B. (2014). Towards an ecology of the lung: New conceptual models of pulmonary microbiology and pneumonia pathogenesis. The Lancet Respiratory Medicine, 2(3), pp. 238–246. doi: 10.1016/S2213-2600(14)70028-1.

Ericsson A.C. Personett A.R., Grobman M.E., Rindt H., Reinero C.R. (2016). Composition and predicted metabolic capacity of upper and lower airway microbiota of healthy dogs in relation to the faecal microbiota. PLOS One, 11(5), p. e0154646. doi: 10.1371/journal.pone.0154646.

Fastrès A., Taminiau B., Vangrinsven E., Tutunaru A.C., Moyse E., Farnir F., et al. (2019). Effect of an antimicrobial drug on lung microbiota in healthy dogs. Heliyon, 5(11), e02802. doi: 10.1016/J.HELIYON.2019.E02802.

Fastrès A., Vangrinsven E., Taminiau B., Tutunaru A.C., Jabri H., Daube G., et al. (2020). Assessment of lung microbiota in healthy dogs: impact of breed and living conditions. Proceedings of the 29th ECVIM-CA Congress, Milano, Italia. Journal of Veterinary Internal Medicine, 34, p. 361. doi: 10.1111/jvim.15658.

Ford, R. (2012). Canine infectious tracheobronchitis. In Greene CE. Infectuous diseases of the dog and cat. 4th ed. Elsevier. Saint Louis, Missouri, pp. 55–65.

Helps C.R., Lait P., Damhuis A., Björnehammar U., Bolta D., Brovida C., et al. (2005). Factors associated with upper respiratory tract disease caused by feline herpesvirus, feline calicivirus, *Chlamydophila felis* and *Bordetella bronchiseptica* in cats: Exerience from 218 European catteries. Veterinary Record, 156(21), pp. 669–673. doi: 10.1136/vr.156.21.669.

Jean S.S., Lee W.S., Chen F.L., Ou T.Y., Hsueh P.R. (2014). *Elizabethkingia meningoseptica* : an important emerging pathogen causing healthcare-associated infections. Journal of Hospital Infection, 86, pp. 244–249. doi: 10.1016/j.jhin.2014.01.009.

Johansson N., Vondracek M., Backman-Johansson C., Sköld M.C., Andersson-Ydsten K., Hedlund J. (2019). The bacteriology in adult patients with pneumonia and parapneumonic effusions : increased yield with DNA sequencing method. European Journal of Clinical Microbiology & Infectious Diseases, 38, pp. 297–304. doi: 10.1007/s10096-018-3426-0.

Johnson L. R., Johnson E.G., Vernau W., Kass P.H., Byrne B.A. (2016). Bronchoscopy, imaging, and concurrent diseases in dogs with bronchiectasis: (2003 – 2014). Journal of Veterinary Internal Medecine, 30, pp. 247–254. doi: 10.1111/jvim.13809.

Kozich J.J., Westcott S.L., Baxter N.T., Highlander S.K., Schloss P.D. (2013). Development of a dual-index sequencing strategy and curation pipeline for analysing amplicon sequence data on the MiSeq. Applied and Environmental Microbiology, 79(17), pp. 5112–5120. doi: 10.1128/AEM.01043-13.

Lappin M.R., Blondeau J., Boothe D., Breitschwerdt E.B., Guardabassi L., Lloyd D.H., et al. (2017). Antimicrobial use guidelines for treatment of respiratory tract disease in dogs and cats: antimicrobial guidelines working group of the international society for companion animal infectious diseases. Journal of Veterinary Internal Medicine, 31, pp. 279–294. doi: 10.1111/jvim.14627.

Maboni G., Seguel M., Lorton A., Berghaus R., Sanchez S. (2019). Canine infectious respiratory disease: New insights into the aetiology and epidemiology of associated pathogens. PLoS One, 14(4), e0215817. doi: 10.1371/journal.pone.0215817.

Maddocks S. and Jenkins R. (2017). Chapter 4 - Quantitative PCR: things to consider. In Understanding PCR. Academic Press, Cambridge, United Kingdom, pp. 45–52. doi: 10.1016/B978-0-12-802683-0.00004-6.

NCBI (2019a). Taxonomy browser. *B. bronchiseptica*. Available at: https://www.ncbi.nlm.nih.gov/Taxonomy/Browser/wwwtax.cgi?id=518. (Accessed : 06 September 2019).

NCBI (2019b). Taxonomy browser. *M. cynos*. Available at: https://www.ncbi.nlm.nih.gov/Taxonomy/Browser/wwwtax.cgi. (Accessed 06 September 2019).

Ngo J., Taminiau B., Fall P.A., Daube G., Fontaine J. (2018). Ear canal microbiota – a comparison between healthy dogs and atopic dogs without clinical signs of otitis externa. Veterinary Dermatology, 29(5), 425-e140. doi: 10.1111/vde.12674.

O'Dwyer D.N., Shanna A.L., Gurczynski S.J., Meng X., Wilke C., Falkowski N.R., et al. (2019). Lung microbiota contribute to pulmonary inflammation and disease progression in pulmonary fibrosis. American Journal of Respiratory and Critical Care Medicine, 199, pp.1127-1138. doi: 10.1164/rccm.201809-1650OC.

Patel A., Harris K.A. and Fitzgerald F. (2017). What is broad-range 16S rDNA PCR? Archives of Disease in Childhood: Education and Practice Edition, 102(5), pp. 261–264. doi: 10.1136/archdischild-2016-312049.

Pilione M.R. and Harvill E.T. (2006). The *Bordetella bronchiseptica* type III secretion system inhibits gamma interferon production that is required for efficient antibody-mediated bacterial clearance. Infection and Immunity, 74(2), pp. 1043–1049. doi: 10.1128/IAI.74.2.1043.

Priestnall S.L., Mitchell J.A., Walker C.A., Erles K. (2014). New and emerging pathogens in canine infectious respiratory disease. Veterinary Pathology, 51(2), pp. 492–504. doi: 10.1177/0300985813511130.

Reizenstein E., Johansson B., Mardin L., Abens J., Möllby R., Hallander H.O. (1993). Diagnostic evaluation of polymerase chain reaction discriminative for *Bordetella pertussis*, *B. parapertussis*, and *B. bronchiseptica.* Diagnostic Microbiology and Infectious Disease, 17(3), pp. 185–191. doi: 10.1016/0732-8893(93)90094-N.

Rheinwald M., Hartmann K., Hähner M., Wolf G., Straubinger R.K., Schulz B. (2015). Antibiotic susceptibility of bacterial isolates from 502 dogs with respiratory signs. Veterinary record, 176(15), 383. doi: 10.1136/vr.102694.

Rognes T., Flouri T., Nichols B., Quince C., Mahé F. (2016). VSEARCH: a versatile open source tool for metagenomics. PeerJ, 4, e2584. doi: 10.7717/peerj.2584.

Sakmanoglu A., Sayin Z., Ucan U.S., Pinarkara Y., Uslu A., Erganis O. (2017). Comparison of five methods for isolation of DNA from *Mycoplasma cynos.* Journal of Microbiological Methods, 140, pp. 70–73. doi: 10.1016/J.MIMET.2017.07.003.

Scher J.U., Joshua V., Artacho A., Abdollahi-Roodsaz S., Öckinger J., Kullberg S. et al. (2016). The lung microbiota in early rheumatoid arthritis and autoimmunity. Microbiome, 4, 60. doi: 10.1186/s40168-016-0206-x.

Schulz B.S., Kurz S., Weber K., Balzer H.J., Hartmaan K. (2014). Detection of respiratory viruses and *Bordetella bronchiseptica* in dogs with acute respiratory tract infections. The Veterinary Journal, 201(3), pp. 365–369. doi: 10.1016/J.TVJL.2014.04.019.

Segal L.N., Rom W.N. and Weiden M.D. (2014). Lung microbiome for clinicians: New discoveries about bugs in healthy and diseased lungs. Annals of the American Thoracic Society, 11(1), pp. 108–116. doi: 10.1513/AnnalsATS.201310-339FR.

Skinner J.A., Pilione M.R., Shen H., Harvill E.T., Yuk M.H. (2005). Bordetella type III secretion modulates dendritic cell migration resulting in immunosuppression and bacterial persistence. The Journal of Immunology, 175, pp. 4647–4652. doi: 10.4049/jimmunol.175.7.4647.

Steinfeld A., Prenger-Berninghoff E., Bauer N., Weiß R., Moritz A. (2012). Bacterial susceptibility testings of the lower airways of diseased dogs. Tierarztl Prax Ausg K Kleintiere Heimtiere, 40(5), pp. 309–317. doi: 10.1055/s-0038-1623659.

Vientós-plotts A.I., Ericsson A.C., Rindt H., Reinero C.R. (2019). Respiratory dysbiosis in canine bacterial pneumonia : standard culture vs. microbiome sequencing. Frontiers in Veterinary Science, 6, 354. doi: 10.3389/fvets.2019.00354.

Vieson M.D., Piñeyro P. and LeRoith T. (2012). A review of the pathology and treatment of canine respiratory infections. Veterinary Medicine: Research and Reports, 3, pp. 25–39. doi: 10.2147/VMRR.S25021.

Viitanen S. J., Lappalainen A. and Rajamäki M.M. (2015). Co-infections with respiratory viruses in dogs with bacterial pneumonia. Journal of Veterinary Internal Medicine, 29(2), pp. 544–551. doi: 10.1111/jvim.12553.

Woo P.C.Y., Lau S.K.P., Teng J.L.L., Tse H., Yuen K.Y. (2008). Then and now : use of 16S rDNA gene sequencing for bacterial identification and discovery of novel bacteria in clinical microbiology laboratories. Clinical Microbiology and Infection, 14(10), pp. 908–934. doi: 10.1111/j.1469-0691.2008.02070.x.

Supplemental material

All sample raw reads were deposited at the National Centre for Biotechnology Information and are available under Bioproject ID PRJNA575149.

Additional file 1. *Comparison between the subpopulations of diseased dogs selected or not for the comparison with healthy dogs.*

Variable		Subpopulation of diseased dogs selected to be compared with healthy dogs (n = 7)	Subpopulation of diseased dogs not selected to be compared with healthy dogs (n = 13)	P-value
Clinical findings	Age (y)	0.99 (0.81-1.02)	0.51 (0.38-0.56)	<0.001†
	Gender (F/M)	4/3	8/5	
BALF analysis	TCC (cell/µL)	1300 (1040-3622)	1780 (1391-3510)	0.71†
	Macrophages (%)	33 (15.8-47.2)	49 (13-66)	0.42†
	Neutrophils (%)	48 (35.8-68.5)	34 (21.5-77)	0.85†
	Lymphocytes (%)	9.5 (6.2-15.8)	7 (3-10)	0.20†
	Eosinophils (%)	2 (1-6.8)	1 (0-4.5)	0.42†
Lung microbiota parameters	β-diversity	/	/	0.30††
	α-diversity (Inverse Simpson index	1.56 (1.08-1.92)	1.12 (1.08-1.98)	0.88†
	Richness (chao index)	69.1 (54-94.8)	61.3 (37-98)	0.64†
	Evenness (Simpson derived index)	0.034 (0.027-0.038)	0.045 (0.028-0.072)	0.28†
	Bacterial load (log 16S rDNA copy numbers/mL)	5.71 (5.47-5.92)	5.79 (5.66-6.04)	0.64†

BALF, bronchoalveolar lavage fluid; †, Mann-Whitney tests; ††, permutational analysis of variance. The subpopulation of diseased dogs selected to be compared with healthy dogs corresponds to the dogs n°3, 9, 14, 15, 18, 19 and 20 in the Table 1.

Experimental section

Part 2:

Assessment of macrophage subpopulations in canine bronchoalveolar lavage fluids

Preamble

The second part of the experimental section was dedicated to the analysis of the cell clusters in the BALF from healthy dogs and to the alteration in macrophage clusters in CIPF compared with healthy WHWTs (Study 4 and study 5).

The scRNA-seq, a technique which has never been used in dogs before, was employed to identify cell clusters of the canine BALF (Study 4). Four healthy dogs from different breeds and ages were included. The study aimed to assess the feasibility of the technique in dogs as well to provide a base resource regarding cell populations and clusters of the canine BALF. A total of 5710 cells were analysed corresponding to 14,994 genes detected. Cells were clustered into 14 distinct clusters sharing similar transcriptomic profile and common at all the four dogs except for one cluster of minor cell number. The clusters were characterized as providing from eight different cells types including macrophages/monocytes (Ma/Mo) (50.4%), T lymphocytes (27.1%), neutrophils (4.1%), dendritic cells (DCs) (3.9%), B cells (1.2%), epithelial cells (9.5%), mast cells (1%) and cells in division (2.2%). Specific overexpressed markers were found in each of these cell types including *MARCO*, *MSR1*, *HLA-DRB1*, *CD163*, *CD86*, *MRC1*, *CD68* and *CD63* for Ma/Mo, *CD3E* and *CD3D* for T cells, *SELL* and *ITGAM* for neutrophils, *CD1E*, *CD83* and *CCR7* for DCs, *BCR*, *FCRLA* and *CD19* for B cells, *TFF3*, *TFF1* and *KRT19* for epithelial cells, *KIT*, *FCER1G* and *MS4A2* for mast cells and finally, *PCALF*, *TOP2A* and *Ki67* for cells in division. Four distinct Ma/Mo clusters were found, 3 were identified as AMs based on *MARCO* expression and were enriched in functions involved respectively in immune response and cell activation, regulation of the immune response, and cell homeostasis. The last cluster of macrophages was considered as either monocytes or monocyte-derived macrophages. T cells included $CD8^+$ and $CD8^-CD4^-$ clusters. Ciliated and non-ciliated epithelial cells as well as mature and immature DCs were also recorded. All these findings represent a highly useful dataset for the identification and subsequent interpretation of cell populations and molecular signatures alterations in future studies on canine lung diseases.

We then analysed the cell clusters of the BALF from 5 WHWTs affected with CIPF compared to 3 healthy WHWTs which corresponded to 19,255 cells (6,703 from healthy and 12,552 from diseased dogs) coding for 11,722 genes (Study 5). Again, 14 cell clusters divided into the 8 cell types found in our first study were found and included 5 Ma/Mo clusters, $CD8^+$ and $CD8^-CD4^-$ T cells, neutrophils, mature and immature DCs, B cells, epithelial cells, mast cells and cells in division. Among Ma/Mo, 2 clusters were identified as AMs, one as monocytes, one as monocyte-derived macrophages and the last one was not further identified. Significantly more monocytes were found in CIPF compared with healthy dogs. Monocytes and monocyte-derived macrophages were also enriched compared with the other Ma/Mo clusters in genes involved in profibrotic process including *CCL2*, *SPP1*, *FN1*, *CCL3*, *TIMP1*, *IL1RN*, *CXCL8* and *CCL4*, and *SFTPC*, *CCL5*, *FN1*, *CXCL8*, *ATP11A* and

SPP1, respectively. DEGs between CIPF and healthy WHWTs were only found in monocyte-derived macrophages. Indeed, in CIPF dogs, monocyte-derived macrophages were enriched in genes associated with pro-fibrotic process including *FN1*, *SPP1*, *CXCL8* and *PLAU*, angiogenesis including *SPP1*, *VCAN* and *S100A4* and EMT including *VIM*, *FN1*, *SPP1* and *THY1*. Results of that study are in favour for a role of monocytes and monocyte-derived macrophages in the onset and/or the perpetuation of CIPF in WHWTs. Although further studies are required, the present data offer promise for the better understanding of CIPF pathogenesis as well as for identification of the potential role of overexpressed profibrotic genes as biomarkers and/or therapeutic targets of the disease.

Experimental section

Part 2

Study 4:

Characterization of the bronchoalveolar lavage fluid by single cell gene expression analysis in healthy dogs: a promising technique.

Frontiers in Immunology 11 :1707

Aline Fastrès, Dimitri Pirottin, Laurence Fievez, Thomas Marichal, Christophe J Desmet, Fabrice Bureau, Cécile Clercx

Abstract

Single-cell mRNA-sequencing (scRNA-seq) is a technique which enables unbiased, high throughput and high-resolution transcriptomic analysis of the heterogeneity of cells within a population. This recent technique has been described in humans, mice and other species in various conditions to cluster cells in populations and identify new subpopulations, as well as to study the gene expression of cells in various tissues, conditions and origins. In dogs, a species for which markers of cell populations are often limiting, scRNA-seq presents with elevated yet untested potential for the study of tissue composition. As a proof of principle, we used scRNA-seq to identify cellular populations of the bronchoalveolar lavage fluid (BALF) in healthy dogs (n = 4). A total of 5710 cells were obtained and analysed by scRNA-seq. Fourteen distinct clusters of cells were identified, further identified as macrophages/monocytes (4 clusters), T cells (2 clusters) and B cells (1 cluster), neutrophils (1 cluster), mast cells (1 cluster), mature or immature dendritic cells (1 cluster each), ciliated or non-ciliated epithelial cells (1 cluster each) and cycling cells (1 cluster). We used for the first time in dogs the scRNA-seq to investigate cellular subpopulations of the BALF of dog**.** This study hence expands our knowledge on dog lung immune cell populations, paves the way for the investigation at single-cell level of lower respiratory diseases in dogs, and establishes that scRNA-seq is a powerful tool for the study of dog tissue composition.

Introduction

The cells can be considered as the fundamental unit in biology. They are working in concert to respond to stimuli in order to maintain health. However, until recently, they were only characterized and distinguished using microscopy-based methods, flow cytometry, or bulk RNA sequencing, all techniques that are quite limiting for demonstration of cell heterogeneity (Herderschee *et al.*, 2015; Proserpio and Mahata, 2015; Haque *et al.*, 2017; Kiselev *et al.*, 2019). With the development of next-generation sequencing technologies, it is now possible to profile the transcriptome of each individual cell composing a sample. The single-cell mRNA sequencing (scRNA-seq) enables high throughput and high-resolution transcriptomic analysis of the cellular heterogeneity with an unbiased assessment of the cells as it gives the opportunity to identify cells without relying on previously known cell markers. It has become a powerful tool to identify cell subpopulations sharing similar transcriptome within a population, as well as to provide information related to cell fate, development, lineage, physiology, homeostasis and underlying molecular mechanisms (Haque *et al.*, 2017; Stubbington *et al.*, 2017; Papalexi and Satija, 2018). The use of this recent technique has been described in humans (Muraro *et al.*, 2016; Mould *et al.*, 2019; Suryawanshi *et al.*, 2019), mice (He *et al.*, 2018) and other species (Davie *et al.*, 2018; Farnsworth *et al.*, 2020) in various conditions and samples. In dogs, the use of this technique has not yet been reported so far.

Bronchoscopy and combined analysis of the bronchoalveolar lavage fluid (BALF) are largely used in the diagnosis of canine lower airway diseases either acute or chronic (Finke, 2013; Nelson and Couto, 2014). In dogs, bronchoalveolar lavage is a well-tolerated procedure and few adverse effects are reported (Finke, 2013; Nelson and Couto, 2014). Common analyses performed on BALF include determination of total (TCC) and differential cell counts (DCC) (including macrophages, neutrophils, lymphocytes, eosinophils and mast cells count), cytological examination of cytospin preparations, bacterial cultures and detection of specific respiratory pathogens using quantitative polymerase chain reactions (Finke, 2013; Nelson and Couto, 2014). Only few studies have characterized the lymphocyte populations in the canine BALF by flow cytometry (Dirscherl *et al.*, 1995; Vail, Mahler and Soergel, 1995; Clercx *et al.*, 2002; Out *et al.*, 2002; Spużak *et al.*, 2008) while the other cell types have not been studied. In depth examination of BALF cellular composition and subpopulations as well as the comparison of these cell subpopulations in healthy and diseased conditions could lead to the identification of new cell subsets involved in disease and could help to better understand the pathophysiology of lung diseases, the cell adaptations in disease context as well as to find new or more specific therapeutic targets (Stubbington *et al.*, 2017; Vegh and Haniffa, 2018).

In this study, we aimed to use the scRNA-seq technique in healthy client-owned dogs to analyse BALF cell subpopulations. Results will contribute to provide a base resource regarding cell

subpopulations composing the BALF of healthy dogs which could be of great interest for further investigations of the BALF cell subpopulations in disease.

Materials and methods

1. Dog population

For the scRNA-seq analysis, BALFs were obtained from healthy dogs prospectively recruited at the veterinary clinic of the University of Liège (CVU, Liège, Belgium) between December 2017 and June 2018. All dogs were privately owned, and samples were obtained with owners' consent. The study was validated by the ethical committee of the University of Liège (approval no. 1435).

The healthy status of the dogs was confirmed by history, normal physical examination, blood work (plasma biochemistry and haematology), bronchoscopy and analysis of the BALF (including a macroscopic evaluation, a TCC and a DCC). Dogs from various breed and age were chosen to better represent the diversity of the canine population.

2. Samples collection

BALFs were obtained under anaesthesia with butorphanol at 0.2 mg/kg (Butomidor®, Richter Pharma AG, Wels, Austria) as premedication and propofol (Diprivan®, Asen Pharma Trading Limited, Dublin, Ireland) infusion on demand.

Dogs were not intubated for the procedure. A bronchoscope (FUJINON© Paediatric Video-Bronchoscope EB-530S), cleaned and disinfected using the washer-disinfector Serie 4 (Soluscope®, Aubagne, France), was inserted into the bronchi until the extremity was wedged. Three to four mL/kg of a sterile NaCl 0.9% solution divided into 3 aliquots were instilled through the endoscope channel into the lung (2 aliquots were obtained in the right diaphragmatic lobe and one in the left diaphragmatic lobe) and directly reabsorbed by gentle suction into the same sterile recipient. About 1 mL of BALF was kept for total and differential cell count calculation performed using respectively a hemacytometer and a cytospin preparation (centrifugation at 221 g, for 4 minutes at 20°C, Thermo Shandon Cytospin©4), by counting a total of 200 cells at high power field. The rest of the BALF was then transferred within 15 to 20 minutes following collection on ice to the GIGA laboratory of Cellular and Molecular Immunology.

3. Single-cell RNA sequencing

a. BALF samples preparation

BALFs were filtered to remove mucus and total cell count was assessed using haemocytometer and Türk coloration (Supplementary Table 1). BALFs were then centrifuged at 400 g for 7 minutes and the pellet resuspended in phosphate-buffered saline solution (Gibco™ 1x DPBS, Cat.14190-169) to obtain a cell concentration around 1,000 cells/µL. A second filtration through a cell

strainer (BD Falcon™, Biosciences, USA, Cat.352350) was performed to remove any remaining cell debris and large clumps and cells were again counted with Trypan blue staining to assess cell viability considered as acceptable above 70% (Supplementary Table 1). The volume of the cell suspension was then adjusted to obtain a final cell concentration between 500 and 1000 cells/µL suspended in phosphate-buffered saline solution containing 0.04% (w/v) bovine serum albumin (Supplementary Table 1).

For each sample, approximatively 3500 cells (Supplementary Table 1) were loaded into the Chromium™ Controller (10x Genomics, Pleasanton, CA, USA) approximatively 30 minutes after the first filtration and were then partitioned into nanolitre scale vesicles containing 10x barcoded beads from Chromium™ Single Cell 3' Gel Bead Kit v2 (10x Genomics, Pleasanton, CA, USA) according to manufacturer's instructions. The following steps take place in the vesicles containing cell: [1] cell lysis, [2] capture of polyadenylated mRNAs oligonucleotides containing cell specific 16 bp barcode and 10 bp Unique Molecular Identifier (UMI) and [3] reverse transcription of mRNAs into cell specific barcoded cDNAs on a Veriti© 96-Well Thermal Cycler (ThermoFisher Scientific, Merelbeke, Belgium).

b. Single-cell library preparation and sequencing

Emulsion breakage, cDNA amplification and libraries construction were performed using Chromium™ Single Cell 3' Reagent kit v2 (10x Genomics, Pleasanton, CA, USA) according to manufacturer's instructions as already described (Schyns *et al.*, 2019). Briefly, cDNAs obtained were amplified in a Veriti© 96-Well Thermal Cycler. Amplified cDNA products were cleaned up, quality controlled and quantified. Illumina's P5, P7 and Read2 primers, as well as Sample Index were then added to generate sequencing libraries. The barcoded sequencing libraries were also quality controlled and quantified by quantitative PCR (KAPA Biosystems Library Quantification Kit for Illumina platforms). Sequencing libraries were loaded on an Illumina NextSeq500. The sequencing depth was set at 50,000 reads per cell, taking into account that approximately 2000 cells should be captured (55-60% efficiency). Cell Ranger software (v1.2.0) (10x Genomics, Pleasanton, CA, USA) was used to demultiplex Illumina BCL files to FASTQ files (cellranger mkfastq), to perform alignment to dog genome (CanFam3.1, GenBank assembly accession: GCA_000002285.2), filtering, UMIs counting and to produce gene-barcode matrices (cellranger count).

c. Data analysis and visualization

Analyses were performed using R package Seurat (version 3.1.2) (Stuart *et al.*, 2019). Briefly, we have first selected cells with a minimum of 100 and a maximum of 2,500 unique mapped genes to exclude low-quality cells or empty droplets and cell doublets or multiplets respectively. Only genes

present in at least 3 different cells were kept. Expression values were normalized to 10,000 transcripts per cell and the 'FindVariableFeatures' function was used to identify the top 2000 variable genes in each BALF sample. 'FindIntegrationAnchors' and 'IntegrateData' functions were used to combine the data of all BALF specimens, while minimizing batch effects. Next, a linear transformation using the 'ScaleData' function was applied so that highly-expressed genes do not dominate. A principal component analysis (PCA) was performed on the scaled data using the command 'RunPCA'. The statistically principal components taken into account for the next analysis were identified using the 'PCElbowPlot' and the 'DimHeatmap' functions and were set to 1:30. A K-nearest neighbour graph, based on the Euclidean distance in PCA space and the Jaccard similarity index, was obtained using the 'FindNeighbors' function. Cells were then clustered with the 'FindClusters' command based on the Louvain algorithm. Several cluster resolutions were tested, and the resolution of 0.3 was chosen, since higher resolutions created additional subdivisions of non-well-defined clusters or clusters containing singlets, which were considered not biologically relevant. The data were visualized by a non-linear dimensional reduction, the t-distributed stochastic neighbour embedding (t-SNE) plots, using the 'RunTSNE' function, with the number of dimensions to use set to 30 (PC 1:30).

Cell types within each cluster were characterized based on the identification of differentially expressed genes (DEGs) specific for each cluster compared to all others. The 'FindMarkers' function was used to identify DEGs across clusters. Clusters with the same identified cell type were also further characterized by comparing DEGs between each other. The differential expression was measured using non-parametric Wilcoxon rank sum tests adjusted for multiple testing with Bonferroni correction. Only DEGs with an adjusted P-value < 0.05 were retained. The genes not well annotated were further blasted on the Ensembl genome browser (v99.31) (Cunningham *et al.*, 2019) for dog species to increase the annotation rate. Specific cell markers average expression and percentage of cells expressing the indicated genes within clusters were visualized with the 'DotPlot' function. Alternatively, the 'FeaturePlot' function was used to show specific gene expression within single cells.

The different common biological processes between clusters with the same identified cell type were also assessed using the gene set enrichment analysis (GSEA) using the online GSEA-P software (Subramanian *et al.*, 2005). GSEA was carried out by computing overlaps between significantly enriched genes calculated between clusters with the same identified cell type and gene ontology (GO) biological process gene sets using hypergeometric tests with Benjamini Hochberg correction for multiple testing (P-value adjusted). Only the 10 first gene sets that best overlapped with our gene set were retained.

4. Statistical analysis

Single-cell mRNA sequencing data from the 4 samples were pooled for all analysis. A P-value lower than 0.05 was considered as significant. Details about statistical analysis for the scRNA-seq data and the gene set enrichment analysis can be found in the “Data analysis and visualization” section above.

Results

1. Dogs population characteristics

Four healthy client-owned dogs were recruited for the bronchoalveolar lavage procedure. The cohort was exclusively composed by adult females including one 4-year-old French bulldog, one 6-year-old Australian shepherd, one 9-year-old West Highland white terrier and one 11-year-old Yorkshire terrier.

2. BALF cells analysis

Information about TCC and DCC for each BALF can be found in the Table 1.

Table 1: *Total and differential cell count in each bronchoalveolar lavage fluid.*

		BALF 1	**BALF 2**	**BALF 3**	**BALF 4**
TCC, cells/µL		440	880	570	180
DCC, %	Macrophages	70	80	91	71
	Neutrophils	10	12	3	12
	Lymphocytes	18	5	3	10
	Eosinophils	1	3	1	2
	Mast cells	0	0	0	0
	Epithelial cells	1	0	2	5

BALF 1, female Yorkshire terrier of 11-year-old; BALF 2, female French bulldog of 4-year-old; BALF 3, female West Highland white terrier of 9-year-old; BALF 4, female Australian shepherd of 6-year-old; TCC, total cell count; DCC, differential cell count.

3. Single-cell RNA sequencing

The transcriptomic profile from a total of 5710 cells was obtained from each of the four BALF specimens using 10x Genomics based scRNA-seq analysis. Cells had a mean read depth of ~54,000 reads per cell. Summary of sequencing and mapping quality control metrics for each BALF sample is presented in Table 2. The distribution of transcripts and genes counts can be found in the Supplementary Figure 2A and B.

Cells from all dogs were compiled after identification of anchors using Seurat. The clustering in Seurat allowed the detection of 14 well-defined clusters (Figure 1A). The contribution of each individual sample in the compiled t-SNE figure is displayed in Figure 1B and C. Cells coming from each of the four BALF specimens were present in all identified clusters except for the cluster 11 which did not contain cells from BALF 1 (Figure 1C). The average expression of all transcripts detected by clusters is provided in the Supplementary Table 2.

Table 2: *Metrics about mapping and characteristics of the detected cells of each BALF sample.*

					BALF 1	**BALF 2**	**BALF 3**	**BALF 4**
Number of cells passing quality control					1,309	1,072	1,298	2,031
Reads mapped confidently to genome, %					68.1	68.6	59.8	72.4
Reads mapped confidently to transcriptome, %					26.5	30.4	23.9	30.7
Median genes/cell					485 (229-1163)	780 (350-1313)	834 (376-1046)	407 (215.25-953)
Median UMIs/cell					1020 (321-3351)	1942 (720-4003)	1888.5 (678-2671)	837 (430-2669)
Total genes detected	11,343	11,133	10.839	11,543				

Data were generated after passing quality control including the exclusion of cells with < 100 and > 2500 genes. Reads mapped confidently to genome are the number of reads that mapped only to the genome. Reads mapped confidently to transcriptome are the fraction of the reads mapped to a unique gene in the transcriptome and are considered for UMI counting. Median genes per cell correspond to the median number of genes with at least one UMI count. Total genes detected is the detected number of genes with at least one UMI count in any cell. BALF 1, female Yorkshire terrier of 11-year-old; BALF 2, female French bulldog of 4-year-old; BALF 3, female West Highland white terrier of 9-year-old; BALF 4, female Australian shepherd of 6-year-old; UMI, unique molecular identifier.

The cell identity of each cluster was determined based on the DEGs in each cluster compared to all others. All DEGs are reported in the Supplementary Table 3. In each cluster, a selection of the most overexpressed transcripts able to differentiate cell types according to the literature is displayed in Table 3. Cells of clusters 0, 3, 5 and 8 expressing *MARCO* and/or *MSR1* and/or *HLA-DRB1* and/or *CD163* and/or *CD86* and/or *MRC1* and/or *CD68* and/or *CD63* were identified as macrophages/monocytes (Mantovani *et al.*, 2013; Gundra *et al.*, 2014; Gibbings *et al.*, 2015; Gibbings *et al.*, 2017; Stifano and Christmann, 2016; Patel, Harris and Fitzgerald, 2017; Trombetta *et al.*, 2018; Byrne *et al.*, 2020). Cells of cluster 1 and 2 expressing *CD3* markers were identified as T lymphocytes (Patel, Harris and Fitzgerald, 2017; Alcover, Alarcon and Bartolo, 2018). Cells of clusters 4 and 12 expressing *TFF1*, *TFF3* and *KRT19* or just *KRT19* respectively, were identified as epithelial cells (Yi and Ku, 2013; Emidio *et al.*, 2019). Cells of clusters 7 and 13 expressing *CD83* and either *CD1E* or CCR7 respectively, were identified as dendritic cells (DC). Finally, cells of cluster 6 expressing *CD62L* and *ITGAM* were identified as neutrophils (Condliffe *et al.*, 1996), cells of cluster 9 expressing *PCLAF*, *TOP2A* and *Ki-67* as cycling cells (Mould *et al.*, 2019), cells of cluster 10 expressing *BCR*, *FCRLA* and *CD19* as B lymphocytes (Volkova *et al.*, 2007; X. Li *et al.*, 2017b; Haran *et al.*, 2020) and finally, cells of cluster 11 expressing *MS4A2*, *FCER1G*, *KIT* and *CD63* as mast cells (Kabashima *et al.*, 2018) (Table 3 and Figure 2). The proportions of the different identified cell types in the global dataset corresponded to 50.4% of macrophages/monocytes, 28.9% of lymphocytes B and T, 9.5% of epithelial cells, 4.1% of neutrophils, 3.9% of DC 2.2% of cycling cells and 1.0% of mast cells. Of

note, we were not able to identify eosinophils, cells known to be present in BALF (Nelson and Couto, 2014).

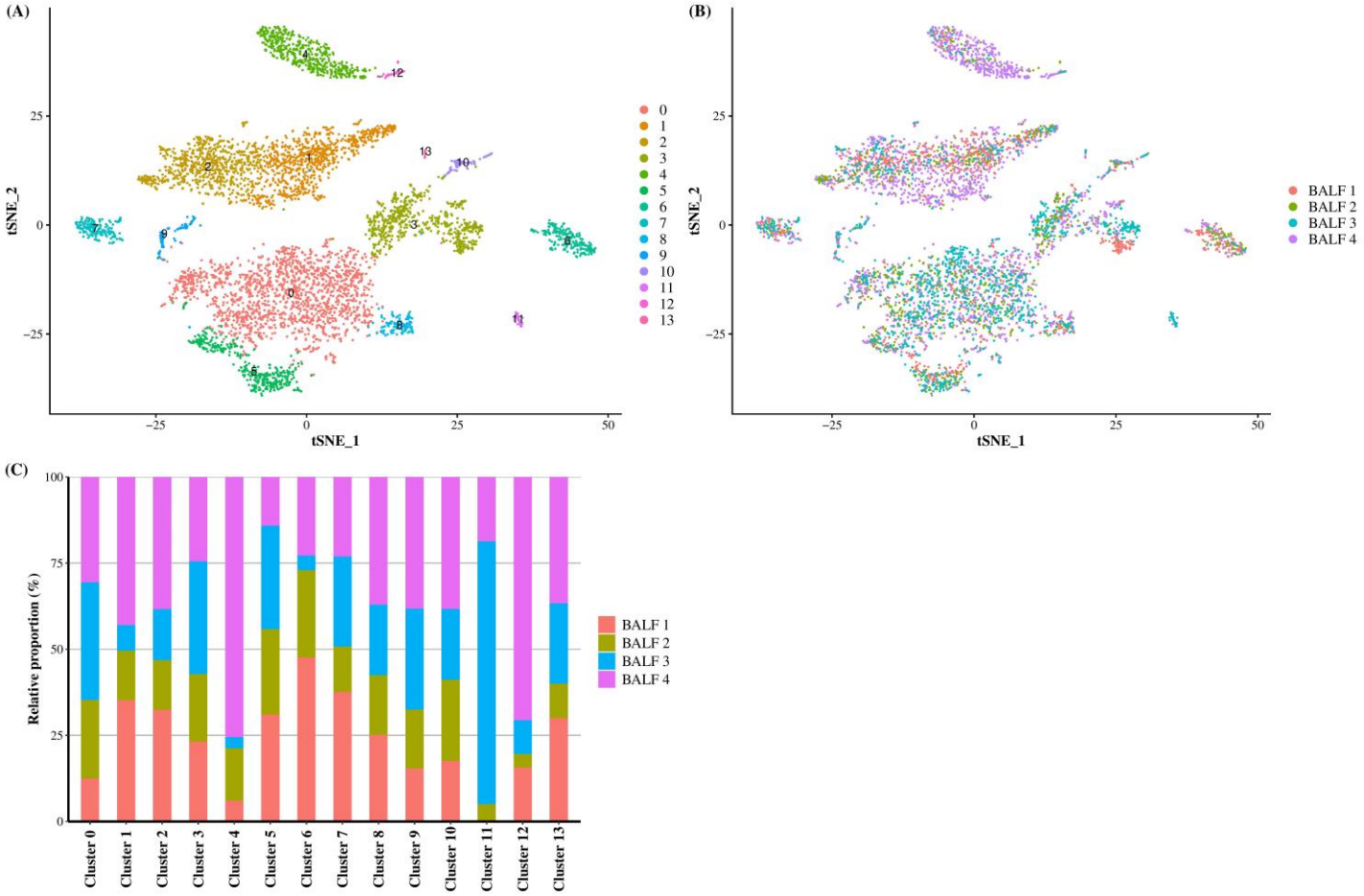

Figure 1: *Compiled t-SNE plot of the cell clusters.* ***(A)*** *t-SNE plot of all cells (n = 5710) representing the cell clusters analysed by scRNA-seq. Each colour corresponds to one cluster assigned via the graph-based clustering method with a resolution of 0.3.* ***(B)*** *Batch alignment across bronchoalveolar lavage fluid (BALF) specimens, each colour representing the cells coming from one sample.* ***(C)*** *Bar plot showing the relative proportion of the cell from each BALF sample into each cluster. BALF 1, female Yorkshire terrier of 11-year-old; BALF 2, female French bulldog of 4-year-old; BALF 3, female West Highland white terrier of 9-year-old; BALF 4, female Australian shepherd of 6-year-old.*

Table 3: *Selection of significant DEGs able to differentiate cell type in each cluster based on literature.*

		Cluster 0		**Cluster 1**		**Cluster 2**		**Cluster 3**		**Cluster 4**		**Cluster 5**		**Cluster 6**		**Cluster 7**		**Cluster 8**		**Cluster 9**		**Cluster 10**		**Cluster 11**		**Cluster 12**		**Cluster 13**	
		Avg logFC	pct	Avg logFC	pct	Avg logFC	pct	Avg logFC	pct	Avg logFC	pct	Avg logFC	pct	Avg logFC	pct	Avg logFC	pct	Avg logFC	pct	Avg logFC	pct	Avg logFC	pct	Avg logFC	pct	Avg logFC	pct	Avg logFC	pct
Macro-phages/ Monocytes markers	*MARCO*	**1.03**	83	-1	48	-0.99	60	**0.28**	25	-0.97	0	**0.35**	94	-0.97	51	-0.95	38					-0.91	20	-0.96	0	-0.94	24	-0.96	27
	MSR1	**0.99**	88	-1.23	46	-1.2	59	**0.63**	35	-1.2	16					-1.24	17									-1.22	20	-1.22	27
	HLA-DRB1	**0.85**	100	-1.18	84	-1.5	87			-3.27	26			-2.47	76	**1.33**	100	**0.63**	100					-3.25	19	-2.23	22	-2.1	73
	CD163	**0.7**	87	-1.31	24	-1.28	20	**1.17**	45	-1.25	14			-1.13	39							-1.22	16						
	CD86	**0.66**	86	-1.27	52	-1.16	59	**0.86**	57	-1.31	0			-1.03	52	**0.76**	91	**0.4**	79	-0.80	50			-1.25	76	-1.22	16		
	MRC1	**0.6**	91	-1.68	44	-1.69	54			-1.71	12	-0.52	92	-1.68	65			**0.43**	83			-1.51	43			-1.67	26	-1.6	20
	CD68	**0.97**	86	-1.19	36	-1.16	54			-1.18	0	**0.84**	96									-1.13	27	-0.79	3	-1.01	18		
	CD63	**0.85**	99	-0.98	64	-1.17	68	-0.26	49	-1	30	**0.39**	100	-0.5	43			**0.32**	97			-1.12	72	**1.76**	97	-0.51	33		
DC markers	*CD1E*															**0.87**	79	**0.26**	55										
	CD83	**0.26**	71	-1.06	7	-1.08	16			-0.78	17					**0.57**	83					-0.57	27			-1.04	8	**2.63**	100
	CCR7																											**3.24**	93
T cells markers	*CD3E*	-1.75	58	**1.37**	77	**1.54**	87			-1.56	4			-1.57	55	-1.43	25			**0.26**	73								
	CD3D	-1.6	56	**1.41**	72	**1.39**	83			-1.32	2	-1.39	55			-1.27	39									-1.39	22		
Epithelial cells markers	*TFF3*			-3.92	61	-4.15	67	-3.29	79	**6.18**	99	-4.17	93	-3.5	54							-3.24	77					-4.46	67
	TFF1			-3.31	58	-3.42	64	-2.31	78	**5.4**	95	-3.3	93	-2.66	77									-3.82	81	-3.39	28		
	KRT19	-1.84	60					-1.15	67	**3.32**	81			-1.66	52	-1.63	37					-1.64	60	-1.65	10	**2.09**	69		
Neutrophils markers	*SELL (CD62L)*	-0.25	72	-0.8	57	-0.91	48	-0.63	22	-1.18	7	-0.56	89	**2.84**	77	-0.6	82									-1.19	14		
	ITGAM													**1.47**	71														
Cycling cells markers	*ENSCAFG00000030087 (PCALF)*																			**2.75**	96								
	TOP2A																			**1.43**	82								
	ENSCAFG00000013255 (Ki67)																			**0.75**	45								
B cells markers	*ENSCAFG00000030258 (BCR)*					-1.51	64	-1.19	47	-2.02	15	-1.99	75			-1.91	81					**5.37**	87	-2.29	39				
	FCRLA																					**1.57**	72						
	CD19																					**0.77**	59						
Mast cells markers	*MS4A2*	-0.6	33	-0.51	39	-0.45	56	-0.39	75	-0.49	2			**0.78**	44							-0.33	11	**3.71**	78				
	KIT									-0.30	1					**0.42**	81							**3.13**	100				
	FCER1G	**0.58**	98	-1.89	21	-2.17	49			-2.19	4			**1.46**	83			**0.5**	94			-2.08	58	**2.21**	92	-2.09	26		

The avg logFC was calculated by comparing each cluster to all other clusters. Only significant data were reported in the table (P < 0.05). DEGs, differentially expressed genes; Avg logFC, average log2 fold; pct, percentage of cells in the cluster expressing the gene; DC, dendritic cells.

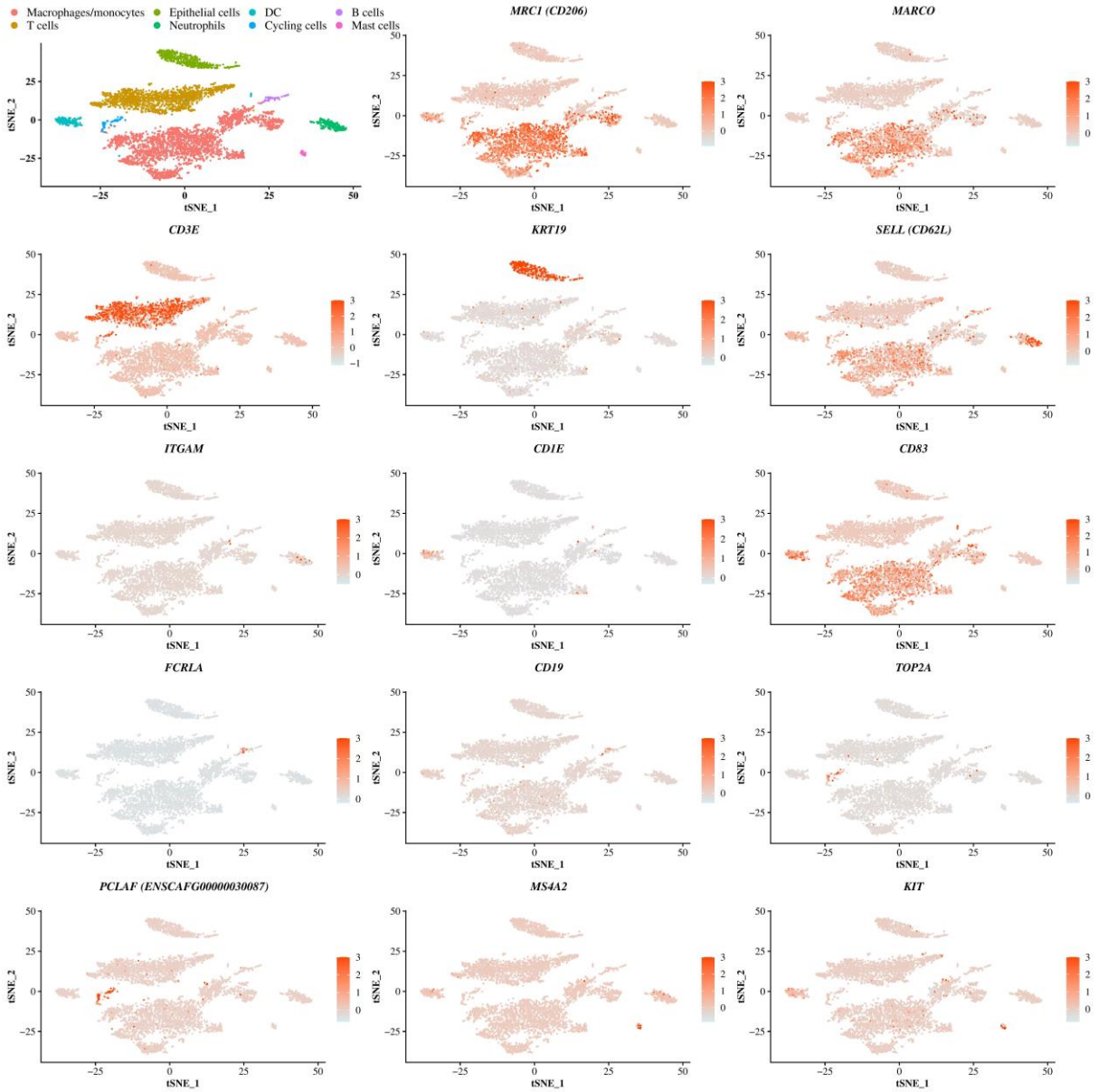

Figure 2: *Identification of cell identity corresponding to the clusters. t-SNE plot showing the cells identity based on the expression of differentially expressed genes representative of each cells type including genes coding for the macrophage receptor with collagenous structure (MARCO), the macrophage mannose receptor (MRC1, encoding CD206), the T-cell surface glycoprotein CD3 epsilon chain (CD3E), the cytokeratin 19 (KRT19), the selectin (SELL, encoding CD62L), the integrin alpha M (ITGAM), the T-cell surface glycoprotein CD1e (CD1E), the CD83 molecule, the Fc receptor like A (FCRLA), the CD19 molecule, the DNA topoisomerase II alpha (TOP2A), the proliferating cell nuclear antigen clamp associated factor (ENSCAFG00000030087, encoding PCLAF), the membrane spanning 4-domains A2 (MS4A2) and the mast/stem cell growth factor receptor (KIT). DC, dendritic cell.*

DEGs and biological processes were further compared between clusters sharing the same cell identity, namely macrophages/monocytes, T lymphocytes, epithelial cells and DC, to better characterize each cluster.

The graph-based clustering of merged single-cells identified four transcriptionally distinct clusters of macrophages/monocytes. In this study, *MARCO*, a class A scavenger receptor involved in host defence and demonstrated to be highly expressed in embryonic-derived or alveolar macrophages (AMs) and not expressed in monocyte-derived macrophages was used to identify AMs (Gibbings *et al.*, 2015; Byrne *et al.*, 2020). *MARCO* was overexpressed in the clusters 0, 3 and 5 compared to all remaining clusters (Figure 2 and Supplementary Table 3).

The first cluster of AMs (cluster 0) represented the majority of the macrophages/monocytes cells and showed a unique transcriptional signature including upregulation of transcripts coding for cell surface markers such as MHC-II molecules (e.g., *DLA-DQA1*, *DLA-DRA*, *DLA-DMA*), *CD63*, the Fc fragment of IgG receptor IIIa (*FCGR3A*, encoding *CD16*), the selectin L (*SELL*, encoding *CD62L*), the *CD36* molecule, the *CD68* molecule and the lysosomal associated membrane protein 2 (*LAMP2*) (Supplementary Table 4). Other most upregulated transcripts (average log2 fold change (avg_logFC) > 0.5, P < 0.05) included the apolipoprotein E (*APOE*) known as an anti-inflammatory, anti-proliferative and immune-modulatory protein (Kockx, Traini and Kritharides, 2018) and transcripts involved in the immune response such as for example the bactericidal permeability increasing protein (*BPI*) and the complement C1q A chain (*C1QA*) (Figure 3 and Supplementary Table 4). The principal biological functions exerted by cells in cluster 0 are reported in Table 4.

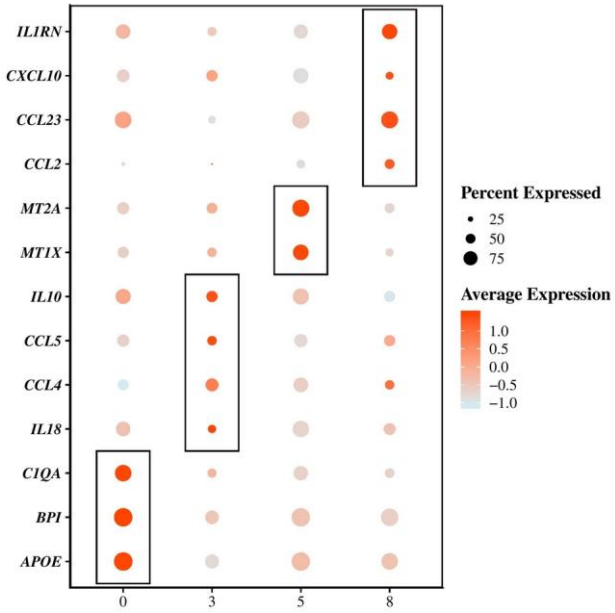

Figure 3: *Single-cell mRNA-sequencing based identification of 4 distinct subpopulations of macrophages/monocytes in the bronchoalveolar lavage fluid of dogs. Dot plots showing the average expression of the indicated genes as well as the percentage of cells expressing the genes within each cluster of macrophages/monocytes. An example of transcripts significantly (P-value adjusted < 0.05) differentially upregulated (average log2 fold change > 0.5) between the clusters 0, 3, 5 and 8 are depicted.*

Table 4: *Top 10 gene set overlap between significantly upregulated genes in cluster 0, 3, 5 and 8 compared to each other and the gene ontology (GO) biological process gene set.*

	Gene Set Name	Genes in Gene Set (K)	Positive DEGs included	Genes in Overlap (k)	k/K	FDR q-value
Cluster 0 vs 3, 5 and 8	Myeloid leukocyte activation	650	88	28	0.0431	1.23E-24
	Leukocyte mediated immunity	867	88	30	0.0346	3.06E-24
	Cell activation involved in immune response	705	88	28	0.0397	3.36E-24
	Myeloid leukocyte mediated immunity	550	88	26	0.0473	3.36E-24
	Exocytosis	899	88	29	0.0323	8.10E-23
	Immune effector process	1253	88	32	0.0255	1.42E-22
	Cell activation	1424	88	32	0.0225	6.03E-21
	Secretion	1638	88	31	0.0189	4.86E-18
	Defence response	1709	88	26	0.0152	2.40E-12
	Innate immune response	984	88	21	0.0213	2.50E-12
Cluster 3 vs 0, 5 and 8	Response to cytokine	1192	251	45	0.0378	4.29E-18
	Regulation of immune system process	1631	251	47	0.0288	1.22E-14
	Positive regulation of protein metabolic process	1633	251	46	0.0282	3.81E-14
	Cell activation	1424	251	43	0.0302	3.81E-14
	Cell motility	1719	251	46	0.0268	1.95E-13
	Response to oxygen containing compound	1616	251	44	0.0272	4.45E-13
	Locomotion	1943	251	48	0.0247	6.01E-13
	Defence response	1709	251	44	0.0257	2.46E-12
	Regulation of cell activation	608	251	27	0.0444	3.06E-12
	Interspecies interaction between organisms	927	251	32	0.0345	7.69E-12
Cluster 5 vs 0, 3 and 8	Myeloid leukocyte activation	650	62	16	0.0246	1.70E-11
	Myeloid leukocyte mediated immunity	550	62	15	0.0273	1.70E-11
	Exocytosis	899	62	17	0.0189	5.14E-11
	Cell activation involved in immune response	705	62	15	0.0213	2.91E-10
	Leukocyte mediated immunity	867	62	16	0.0185	2.91E-10
	Secretion	1638	62	20	0.0122	2.91E-10
	Cell activation	1424	62	18	0.0126	2.95E-09
	Immune effector process	1253	62	17	0.0136	3.90E-09
	Cellular homeostasis	971	62	14	0.0144	1.69E-07
	Homeostatic process	1913	62	18	0.0094	2.57E-07
Cluster 8 vs 0, 3 and 5	Defence response	1709	59	20	0.0117	1.22E-09
	Cell motility	1719	59	19	0.0111	7.91E-09
	Cytokine mediated signalling pathway	787	59	14	0.0178	1.49E-08
	Locomotion	1943	59	19	0.0098	3.31E-08
	Inflammatory response	722	59	13	0.018	4.87E-08
	Leukocyte migration	488	59	11	0.0225	1.29E-07
	Response to cytokine	1192	59	15	0.0126	1.29E-07
	Response to bacterium	681	59	12	0.0176	2.45E-07
	Response to biotic stimulus	1023	59	13	0.0127	1.88E-06
	Regulation of immune system process	1631	59	15	0.0092	6.45E-06

Gene set enrichment analysis carried on by computing overlaps between significantly upregulated genes (P < 0.05, avg_logFC > 0.25) and the gene ontology biological process gene set. "Genes in Gene Set" refers to the number of genes in the gene set, "Positive DEGs included" corresponds to the number of positive differentially expressed genes in the cluster of interest compared to the others and "Genes in Overlap" to the number of genes upregulated in the cluster and involved in the biological process. Avg_logFC, average log2 fold change.

Compared with macrophages composing clusters 0, 5 and 8, the AMs composing cluster 3 overexpressed (avg_logFC > 0.5, P < 0.05) transcripts encoding cell surface markers such as the macrophage mannose receptor (*MRC1*, encoding *CD206*), the integrin subunit alpha 5 (*ITGA5*), the scavenger receptor *CD163*, the *CD80* molecule and the *CD83* molecule (Supplementary Table 4). The cells in cluster 3 also largely overexpressed transcripts (avg_logFC > 0.5, P < 0.05) encoding cytokines, including the interleukin 18 (*IL18*), the C-C motif chemokine ligand 4 and 5 (*CCL4* and *CCL5*) and the interleukin 10 (*IL10*) (Figure 3 and Supplementary Table 4). Such combination of pro-inflammatory and immunoregulatory cytokines is consistent with the enriched functional properties of the cells in cluster 3 which include regulation of the immune response and cell activation (Table 4).

AMs in cluster 5, in comparison with cells from clusters 0, 3 and 8 also overexpressed transcripts encoding cell surface markers (avg_logFC > 0.5, P < 0.05), including the *CD9* molecule, the CD5 molecule like (*CD5L*), *CD68*, the carcinoembryonic antigen related cell adhesion molecule 5 (*CEACAM5*) and the *CD300C* molecule (Supplementary Table 4). The principal functions of AMs composing cluster 5 were quite similar to those associated with AMs in cluster 0. However, those cells seemed to be more involved in cellular homeostasis (Table 4), mostly metal ion homeostasis. Indeed, the most enriched transcripts in the cluster 5 were the metallothionein 1X (*MT1X*) and the metallothionein 2A (*MT2A*) which encode anti-oxidant proteins that are important in the homeostasis of metal in the cell, and in the detoxification of heavy metals (Figure 3 and Supplementary Table 4) (Zalewska, Trefon and Milnerowicz, 2014; Ling *et al.*, 2016).

The cells in cluster 8 compared with other clusters did not overexpress the transcript encoding *MARCO* and were not considered as AMs. Overexpressed transcripts coding for surface markers in cluster 8 compared with clusters 0, 3 and 5 included *MHC-II* (*DLA-DQA1*) and *MHC-I* (*DLA-88*) molecules, the tumour necrosis factor superfamily member 13b (*TNFSF13B*), the colony stimulating factor 2 receptor subunit beta (*CSF2RB*), the integrin subunit alpha X (*ITGAX*) and the *CD1e* molecule (Supplementary Table 4). The cells in cluster 8 were characterized by the overexpression (avg_logFC > 0.5, P < 0.05) of transcripts encoding cytokines including the interleukin 1 receptor antagonist (*IL1RN*), the C-C motif chemokine ligand 23 (*CCL23*), the C-C motif chemokine ligand 2 (*CCL2*) and the C-X-C motif chemokine ligand 10 (*CXCL10*) (Figure 3 and Supplementary Table 4). The high level of cytokine transcripts in cluster 8 is consistent with the enrichment for processes related to the inflammatory response, the defence response and the response to cytokines (Table 4).

By looking at the DEGs and the GSEA between cluster 1 and cluster 2 corresponding each to T cells (Supplementary Table 5, and Table 5), we were able to characterize cells in cluster 1 as cytotoxic or $CD8^+$ T cells. Indeed, the transcripts encoding granzyme B, K and A (*GZMB*, *GZMK* and *GZMA* respectively) were overexpressed with an avg_logFC > 1 in cluster 1 compared to cluster 2 (Supplementary Table 5). Those genes are expressed by cytotoxic T lymphocytes and natural

killer cells (Lieberman, 2003; Hidalgo *et al.*, 2008). Other transcripts with an avg_logFC > 1 in cluster 1 compared to cluster 2 included the killer cell lectin like receptor D1 and K1 (*KLRD1* and *KLRK1* respectively) also expressed primarily in natural killer cells and $CD8^+$ T cells (Godlove, Chiu and Weng, 2007; Hidalgo *et al.*, 2008). Finally, the *CD8b* molecule was also overexpressed in cluster 1 (Supplementary Table 5).

When comparing cluster 2 to cluster 1, enriched biological processes were more in favour of $CD4^+$ T cells, as reported in table 5. Although classical surface marker of this cell type was not expressed by the cells in our dataset (e.g., *CD4*), the cells in cluster 2 overexpressed transcripts encoding for the interleukin 7 receptor (*IL7R)* and the *CD40* ligand (*CD40L*) commonly found in $CD4^+$ T cells (Lesley *et al.*, 2006; Rodriguez-Perea *et al.*, 2016). Principal overexpressed transcripts in cluster 2 included *ICOS* (inducible T cell costimulatory) an important costimulatory factor expressed in activated T cells (Hutloff *et al.*, 1999; Tafuri *et al.*, 2001; Lischke *et al.*, 2012), *PLAC8* (placenta associated 8), *GATA3* (GATA binding protein 3) and *ANXA1* (annexin A1) (Supplementary Table 5). Those transcripts are associated with the activation of $CD4^+$ T cells, T cell differentiation in $CD4^+$ T cells and immune response modulation (Rogulski *et al.*, 2005; Zhu *et al.*, 2006; Gavins and Hickey, 2012; Huang *et al.*, 2016), which is coherent with the functions of $CD4^+$ T cells as reported in Table 5.

Table 5: *Top 10 gene set overlap between significantly upregulated genes in cluster 1 and 2 compared to each other and the gene ontology (GO) biological process gene set.*

	Gene Set Name	Genes in Gene Set (K)	Positive DEGs included	Genes in Overlap (k)	k/K	FDR q-value
Cluster 1 vs 2	Regulation of immune system process	1631	24	13	0.008	1.85E-08
	Innate immune response	984	24	11	0.0112	2.20E-08
	Regulation of immune response	1094	24	11	0.0101	4.58E-08
	Natural killer cell mediated immunity	65	24	5	0.0769	9.46E-07
	Defence response	1709	24	11	0.0064	3.10E-06
	Regulation of natural killer cell chemotaxis	9	24	3	0.3333	2.26E-05
	Natural killer cell chemotaxis	11	24	3	0.2727	3.81E-05
	Lymphocyte mediated immunity	344	24	6	0.0174	5.41E-05
	Lymphocyte chemotaxis	62	24	4	0.0645	5.41E-05
	Cell activation	1424	24	9	0.0063	8.11E-05
Cluster 2 vs 1	Regulation of lymphocyte activation	478	37	12	0.0251	1.38E-10
	Regulation of cell activation	608	37	12	0.0197	8.27E-10
	Regulation of T cell activation	313	37	10	0.0319	8.27E-10
	T cell activation	459	37	11	0.024	8.27E-10
	Regulation of cell death	1723	37	16	0.0093	2.23E-09
	Lymphocyte activation	721	37	12	0.0166	2.88E-09
	Apoptotic process	1980	37	16	0.0081	1.30E-08
	Biological adhesion	1417	37	14	0.0099	2.16E-08
	Cell activation	1424	37	14	0.0098	2.16E-08
	Leukocyte cell-cell adhesion	336	37	9	0.0268	2.16E-08

Gene set enrichment analysis carried on by computing overlaps between significantly upregulated genes (P < 0.05, avg_logFC > 0.25) and the gene ontology biological process gene set. "Genes in Gene Set" refers to the number of genes in the gene set, "Positive DEGs included" corresponds to the

number of positive differentially expressed genes in the cluster of interest compared to the other and "Genes in Overlap" to the number of genes upregulated in the cluster and involved in the biological process. Avg_logFC, average log2 fold change.

Diverse epithelial populations were captured and corresponded to clusters 4 and 12. Cluster 12 was identified as composed by ciliated epithelial cells as it included functions such as cilium movement, microtubule-based process and movement, cytoskeleton and cell projection organization (Table 6). Indeed, the most enriched transcript in cluster 12 compared to cluster 4 included notably the transcripts encoding *SNTN* (sentan, cilia apical structure protein), *DPCD* (deleted in primary ciliary dyskinesia homolog (mouse)), *ROPN1L* (rhophilin associated tail protein 1 like), *SPA17* (sperm autoantigenic protein 17) and *WDR78* (WD repeat domain 78) for example (Supplementary Table 6).

Table 6: *Top 10 gene set overlap between significantly upregulated genes in cluster 4 and 12 compared to each other and the gene ontology (GO) biological process gene set.*

	Gene Set Name	**Genes in Gene Set (K)**	**Positive DEGs included**	**Genes in Overlap (k)**	**k/K**	**FDR q-value**
Cluster 12 vs 4	Microtubule based process	734	93	14	0.0191	7.90E-06
	Epithelial cilium movement	23	93	5	0.2174	7.90E-06
	Cilium movement	65	93	6	0.0923	2.00E-05
	Cytoskeleton organization	1298	93	17	0.0131	2.00E-05
	Microtubule based movement	277	93	9	0.0325	3.13E-05
	Regulation response to stress	1497	93	17	0.0114	8.91E-05
	Cell projection organization	1512	93	16	0.0106	5.00E-04
	Reproduction	1459	93	15	0.0103	1.49E-03
	Actin filament bundle organization	155	93	6	0.0387	1.59E-03
	Central nervous system development	980	93	12	0.0122	2.54E-03

Gene set enrichment analysis carried on by computing overlaps between significantly upregulated genes ($P < 0.05$, avg_logFC > 0.25) and the gene ontology biological process gene set. No overlap was found between the gene set and upregulated genes of the cluster 4 compared to the cluster 12. "Genes in Gene Set" refers to the number of genes in the gene set, "Positive DEGs included" corresponds to the number of positive differentially expressed genes in the cluster of interest compared to the other and "Genes in Overlap" to the number of genes upregulated in the cluster and involved in the biological process. Avg_logFC, average log2 fold change.

Cells in cluster 7 and 13 were identified as DC. Compared with cells in cluster 13, cells in cluster 7 overexpressed (avg_logFC > 1) transcripts coding for MHC-II and MHC-I molecules (i.e., *HLA-DRB1*, *HLA-DQA1*, *DLA-DMA*, *DLA-DQA1*, *DLA-DRA*, *DLA-DOA*, *DLA-88* and *DLA-79*) (Supplementary Table 7) and their major functions concerned the activation of immune cells and the defence response.

Overexpressed surface marker transcripts identified in cells of cluster 13 compared to cluster 7 (avg_logFC > 1) included the C-C motif chemokine receptor 7 and the C-X-C motif chemokine

receptor 4 (*CCR7* and *CXCR4*, respectively), the *CD83* molecule and the programmed cell death 1 ligand 2 (*PDCD1LG2*) (Supplementary Table 7). The major functions of cells in cluster 13 concerned mostly the regulation of the activation of immune cells (Table 7). Because of their overexpression of *CD83* and *CCR7*, we considered that DC of cluster 13 correspond to mature DC (Xin *et al.*, 2009; Wolkow, Gebska and Korbut, 2018).

Table 7. *Top 10 gene set overlap between significantly upregulated genes in clusters 7 and 13 compared to each other and the gene ontology (GO) biological process gene set.*

	Gene Set Name	**Genes in Gene Set (K)**	**Positive DEGs included**	**Genes in Overlap (k)**	**k/K**	**FDR q-value**
Cluster 7 vs 13	Cell activation	1424	218	59	0.0414	3.15E-31
	Myeloid leukocyte activation	650	218	43	0.0662	4.95E-30
	Myeloid leukocyte mediated immunity	550	218	38	0.0691	5.41E-27
	Cell activation involved in immune response	705	218	41	0.0582	1.26E-26
	Immune effector process	1253	218	51	0.0407	1.26E-26
	Exocytosis	899	218	44	0.0489	8.25E-26
	Leukocyte mediated immunity	867	218	43	0.0496	1.90E-25
	Secretion	1638	218	54	0.033	3.62E-24
	Defence response	1709	218	51	0.0298	1.02E-20
	Regulation of immune system process	1631	218	46	0.0282	1.96E-17
Cluster 13 vs 7	Cell activation	1424	85	23	0.0162	2.66E-10
	Regulation of lymphocyte activation	478	85	14	0.0293	6.34E-09
	Lymphocyte activation	721	85	16	0.0222	6.34E-09
	Regulation of immune system process	1631	85	22	0.0135	6.34E-09
	Regulation of cell activation	608	85	15	0.0247	6.34E-09
	Regulation of T cell activation	313	85	12	0.0383	6.34E-09
	Response to biotic stimulus	1023	85	18	0.0176	8.72E-09
	T cell activation	459	85	13	0.0283	2.55E-08
	Cytokine production	759	85	15	0.0198	9.27E-08
	Response to cytokine	1192	85	17	0.0143	6.25E-07

Gene set enrichment analysis carried on by computing overlaps between significantly upregulated genes ($P < 0.05$, avg_logFC > 0.25) and the gene ontology biological process gene set. "Genes in Gene Set" refers to the number of genes in the gene set, "Positive DEGs included" corresponds to the number of positive differentially expressed genes in the cluster of interest compared to the other and "Genes in Overlap" to the number of genes upregulated in the cluster and involved in the biological process. Avg_logFC, average log2 fold change.

Discussion

In this paper, we report for the first-time a comprehensive single-cell expression profiling of the canine BALF cells in healthy condition. We were able to cluster cells in 14 distinct subsets identified as macrophages/monocytes, $CD8^+$ T cells, $CD4^+$ T cells, epithelial cells, ciliated epithelial cells, mature DC and DC, neutrophils, B cells, mast cells and cycling cells.

Until recently, cells of the dog BALF were only characterized by microscopic evaluation or, in rare cases, by flow cytometry. The cell populations identified by these techniques included macrophages, $CD4^+$ and $CD8^+$ lymphocytes, neutrophils, eosinophils, mast cells and epithelial cells (Dirscherl *et al.*, 1995; Vail, Mahler and Soergel, 1995; Rajamäki *et al.*, 2001; Clercx *et al.*, 2002; Out *et al.*, 2002; Spużak *et al.*, 2008; Finke, 2013; Nelson and Couto, 2014). With the use of the scRNA-seq, we highlighted the presence of 14 subpopulations of cells using an unbiased technique. We were able to characterized the cells composing those subpopulations in depth and to deduce their main functions based on their transcriptome. In addition to offer a way to overcome the lack of qualitative reagents designed for flow cytometry in dogs, the scRNA-seq allows a better characterization of cell heterogeneity without prior knowledge by highlighting, in better agreement with pulmonary physiology, all cell types and cell functions. Indeed, the scRNA-seq provides comprehensive profiles of cells without limitations due to pre-selected cells by probing a few selected markers (Islam *et al.*, 2011; Stubbington *et al.*, 2017; Papalexi and Satija, 2018; See *et al.*, 2018; Vegh and Haniffa, 2018).

Four subpopulations of macrophages/monocytes were found. Among them, 3 subpopulations corresponded to AMs based on their expression of *MARCO* (Gibbings *et al.*, 2015; Byrne *et al.*, 2020). AMs are the most abundant cells found in the airways in homeostatic conditions. They are self-maintaining with minimal contributions from circulating monocytes in healthy conditions (Laar *et al.*, 2016; Ardain, Marakalala and Alasdair, 2019; Byrne *et al.*, 2020). The first subpopulation of AMs, representing the major cell subpopulation, exerted functions involved in immune defence and response. The second was enriched in a combination of pro and anti-inflammatory cytokines transcripts and exerted functions involved in the regulation of the immune response. Finally, the third population had similar functions as the first with more implications in the homeostasis and the detoxification of metal ions. The last subpopulation was not considered as AMs and could correspond to monocytes-derived macrophages or monocytes. Indeed, the cluster was the smallest and expressed macrophages markers but not *MARCO*.

We found a large population of non-ciliated cells and a small population of ciliated cells corresponding to tracheobronchial epithelial cells.

T lymphocytes were subdivided into 2 subpopulations identified as $CD8^+$ and $CD4^+$ with a majority of $CD8^+$ T cells which was already reported in healthy dogs particularly in aged animals (Dirscherl *et al.*, 1995; Spużak *et al.*, 2008). Indeed, cells in cluster 1 expressed the *CD8b* molecule. However, cells in cluster 2 did not express neither *CD8* nor *CD4* while they overexpressed markers associated with classical $CD4^+$ T cells such as *GATA3*, *IL7R* and the *CD40* ligand (Lesley *et al.*, 2006; Zhu *et al.*, 2006; Huang *et al.*, 2016; Rodriguez-Perea *et al.*, 2016). The absence of *CD4* mRNA expression could be due to weakness or absence of transcription of this protein (See *et al.*, 2018). Indeed, in dogs, a population of $CD8^-CD4^-$ T cell has been described representing approximatively 15% of the $TCR\alpha\beta^+$ T cells in the lung, also expressing *GATA3* (Rabiger *et al.*, 2019). Cells from cluster 2 cells possibly belong to this population.

B cells were identified using *BCR*, *FCRLA* and *CD19* markers (Volkova *et al.*, 2007; X. Li *et al.*, 2017b; Haran *et al.*, 2020). *CD19* has only recently been described as B cell marker in dogs (Haran *et al.*, 2020) which highlights the benefice of the scRNA-seq for the identification of new surface markers to better isolate different cell types (Stubbington *et al.*, 2017; Papalexi and Satija, 2018). Common B cell surface markers used and described in dogs include *CD21* and *CD79A* (Faldyna *et al.*, 2007). In this study, *CD21* mRNA was not detected which could be due to absent or weak transcription of this protein (See *et al.*, 2018). *CD79A* was expressed in B cells but its expression was low and it was not significantly differentially expressed in the cluster 10 compared to others.

The identified granulocytic populations included neutrophils and mast cells. Basophils and mast cells shared common markers including *MS4A2*, *KIT* and *FCER1G* used in our study (Kabashima *et al.*, 2018). However, overexpressed DEGs in cluster 11 cells also included chymase (encoding *CMA1*) and tryptase enzymes (encoding *PPSAB1* and *TSP2*) which are almost entirely mast cell-specific (Caughey, 2016; Kabashima *et al.*, 2018; Varricchi *et al.*, 2018). The cells in cluster 11 also expressed *CD63* which is considered as one of the most useful markers of mast cell and basophil activation (Kabashima *et al.*, 2018; Varricchi *et al.*, 2018). We did not identify mast cells in BALF 1 which is probably due to the small proportion of that cell type into BALF samples (Nelson and Couto, 2014). Indeed, it represents only 1.0% of the total cells recovered in this analysis and it is possible that rare cell populations may not be properly captured with the 10X Genomics Chromium system (See *et al.*, 2018). We were not able to identify a cluster of eosinophils, which are normally present in dog BALF specimens (Nelson and Couto, 2014). Although the number of eosinophils found in the BALF of healthy dogs is rather low (Nelson and Couto, 2014) and may not be properly captured, their total absence from our dataset is most likely related to their high content of RNase (Sattasathuchana and

Steiner, 2014) inducing the rapid degradation of mRNA, thus preventing their detection by scRNA-seq.

Finally, two subpopulations of DC were also found one being identified as mature DC because of its higher expression of *CD83* and *CCR7* (Xin *et al.*, 2009; Wolkow, Gebska and Korbut, 2018).

The use of the scRNA-seq in dogs has some limitations. The principal impediment to apply scRNA-seq to canine samples is the necessity to map sequenced RNAs on a sufficiently well annotated database to be able to identify genes. The percentage of reads mapped confidently to the transcriptome in this study was considered as low (~28%) as it is expected to be > 30% (10X Genomics, 2020). This can be due to a poor annotation of the reference transcriptome (overlapping genes for example), but could also be related to a poor library, sequencing or reads quality [1]. However, despite this suboptimal mapping, we were able to identify cell clusters and deduce clusters principal functions based on the cell transcriptome obtained. Another limitation is the lack of information for the identification of specific cell markers in dogs. For example, in the 4 clusters identified as macrophages/monocytes, AMs were recognized only by their expression of *MARCO*. In the literature in human and mouse, the expression of *SIGLECF*, *MERTK*, *CD14*, *CCR2* and *Ly-6c* are commonly used to distinguish AMs from monocytes and monocyte-derived macrophages (Misharin *et al.*, 2013; Gibbings *et al.*, 2015, 2017; McQuattie-Pimentel, Budinger and Ballinger, 2018; Mould *et al.*, 2019; Schyns *et al.*, 2019). However, those markers were not detected in our dataset. The use of the 10X Genomics Chromium system although being unbiased, time saving and allowing high throughput and high-resolution transcriptomic analysis, also implies that rare cell populations may not be properly captured and that sensitivity is reduced decreasing the detection of weakly expressed genes (See *et al.*, 2018). It is possible that common markers used to identify different cell types are only weakly expressed making cell populations difficult to identify. Finally, a limited number of dogs was used in the study. Indeed, as the use of the scRNA-seq is quite expensive, only 4 BALF samples were analysed with a relatively low median number of cells and reads per sample (~1,300 cells and ~54,000 reads, respectively). The 4 selected dogs included young to old adult dogs from 4 breeds differing in size and body conformation, in order to be, as much as possible, representative of the whole healthy canine population, even if no males were sampled. However, we don't expect the sex to alter BALF cells transcriptome. While it has been shown that the age could alter the cell proportions in the BALF from healthy dogs (Mercier *et al.*, 2011), we are not aware of studies assessing its effect on BALF cells transcriptome either. To our knowledge, no study has specifically investigated the effect of the sex and the breed on canine BALF cells proportions and transcriptome. Besides, in the present study, cells coming from each of the four BALF specimens were present in nearly all identified clusters indicating that similar cell populations were present in all dogs.

Conclusion

ScRNA-seq is a new technique which enables unbiased, high throughput and high-resolution transcriptomic analysis and which can be used to identify cell populations in the BALF of healthy dogs. In this study, we provide a comprehensive single-cell transcriptome tool. It represents a highly informative dataset for the identification and subsequent interpretation of cell populations and molecular signatures alterations in lung diseases in dogs.

Acknowledgments

The authors would like to thank Albert Belinda and Romijn Sylvain for their helpful and kind assistance to obtain bronchoalveolar lavage fluid samples.

References

10X Genomics. (2020). Troubleshooting Cell Ranger. Available at: https://support.10xgenomics.com/single-cell-gene-expression/software/pipelines/latest/troubleshooting#alerts (Accessed: 16 March 2020).

Alcover A., Alarcon B. and Di Bartolo V. (2018). Cell biology of T cell receptor expression and regulation. Annual review of Immunology, 36, pp. 103–125. doi: 10.1146/annurev-immunol-042617-053429.

Ardain A., Marakalala M. J. and Alasdair L. (2019). Tissue-resident innate immunity in the lung. Immunology, 159, pp. 245–256. doi: 10.1111/imm.13143.

Byrne A.J., Powell J.E., Sullivan B.J.O., Ogger P.P., Hoffland A., Cook J., et al. (2020). Dynamics of human monocytes and airway macrophages during healthy aging and after transplant. Journal of Experimental Medicine, 217(3), e20191236. doi: 10.1084/jem.20191236.

Caughey G.H. (2016). Mast cell proteases as pharmacological targets. European Journal of Pharmacology, 778, pp. 44–55. doi: 10.1016/j.ejphar.2015.04.045.

Clercx C., Peeters D., German A.J., Khelil Y., McEntee K., Vanderplasschen A., et al. (2002). An immunologic investigation of canine eosinophilic bronchopneumopathy. Journal of Veterinary Internal Medicine, 16(3), pp. 229–237. doi: 10.1111/j.1939-1676.2002.tb02362.x.

Condliffe A.M., Chilvers E.R., Haslett C., Dransfield I. (1996). Priming differentially regulates neutrophil adhesion molecule expression/function. Immunology, 89, pp. 105–111. doi: 10.1046/j.1365-2567.1996.d01-711.x.

Cunningham F., Achuthan P., Akanni W., Allen J., Amode M.R., Armean I.M., et al. (2019). Ensembl 2019. Nucleic Acids Research, 47, pp. 745–751. doi: 10.1093/nar/gky1113.

Davie K., Janssens J., Koldere D., De Waegeneer M., Pech U., Kreft L., et al. (2018). A single-cell transcriptome atlas of the aging drosophila brain. Cell Press, 174(4), pp. 982-998.e20. doi: 10.1016/J.CELL.2018.05.057.

Dirscherl P., Beiskerb W., Kremmer E., Mihalkov A., Voss C., Ziesenis A. (1995). Immunophenotyping of canine bronchoalveolar and peripheral blood lymphocytes. Veterinary Immunology and Immunopathology, 48, pp. 1–10. doi: 10.1016/0165-2427(94)05414-N.

Emidio N.B., Hoffmann W., Brierley S.M., Muttenthaler M. (2019). Trefoil factor family : unresolved questions and clinical perspectives. Trends in Biochemical Science, 44(5), pp. 387–390. doi: 10.1016/j.tibs.2019.01.004.

Faldyna M., Samankova P., Leva L., Cerny J., Oujezdska J., Rehakova Z., et al. (2007). Cross-reactive anti-human monoclonal antibodies as a tool for B-cell identification in dogs and pigs. Veterinary Immunology and Immunopathology, 119, pp. 56–62. doi: 10.1016/j.vetimm.2007.06.022.

Farnsworth D.R., Saunders L.M. and Miller A.C. (2020). A single-cell transcriptome atlas for zebrafish development. Developmental Biology, 452(2), pp. 100–108. doi: 10.1016/J.YDBIO.2019.11.008.

Finke M.D. (2013). Transtracheal wash and bronchoalveolar lavage. Topics in Companion Animal Medicine, 28(3), pp. 97–102. doi: 10.1053/j.tcam.2013.06.003.

Gavins F.N.E. and Hickey, M.J. (2012). Annexin A1 and the regulation of innate and adaptive immunity. Frontiers in Immunology, 3, 354. doi: 10.3389/fimmu.2012.00354.

Gibbings S.L., Goyal R., Desch A.N., Leach S.M., Prabagar M., Atif S.M., et al. (2015). Transcriptome analysis highlights the conserved difference between embryonic and postnatal-derived alveolar macrophages. Blood, 126(11), pp. 1357–1366. doi: 10.1182/blood-2015-01-624809.

Gibbings S.L., Thomas S.M., Atif S.M., Mccubbrey A.L., Desch A.N., Danhorn T., et al. (2017). Three unique interstitial macrophages in the murine lung at steady state. American Journal of Respiratory Cell and Molecular Biology, 57(1), pp. 66–76. doi: 10.1165/rcmb.2016-0361OC.

Godlove J., Chiu W.K. and Weng N. (2007). Gene expression and generation of CD28- CD8 T cells mediated by interleukin 15. Experimental Gerontology, 42(5), pp. 412–415. doi: 10.1038/jid.2014.371.

Gundra U.M., Girgis N.M., Ruckerl D., Jenkins S., Ward L.N., Kurtz Z.D., et al. (2014). Alternatively activated macrophages derived from monocytes and tissue macrophages are phenotypically and functionally distinct. Blood, 123(20), pp. 110–122. doi: 10.1182/blood-2013-08-520619.

Haque A., Engel J., Teichmann S.A., Lönnberg T. (2017). A practical guide to single-cell RNA-sequencing for biomedical research and clinical applications. Genome Medicine, 9(1), pp. 1–12. doi: 10.1186/s13073-017-0467-4.

Haran K.P., Lockhart A., Xiong A., Radaelli E., Savickas P.J., Posey A., et al. (2020). Generation and validation of an antibody to canine CD19 for diagnostic and future therapeutic purposes. Veterinary Pathology, 57(2), pp. 241–252. doi: 10.1177/0300985819900352.

He L., Vanlandewijck M., Mäe M.A., Andrae J., Ando K., Del Gaudio F., et al. (2018). Single-cell RNA sequencing of mouse brain and lung vascular and vessel-associated cell types. Sciences Data, 5, 180160. doi: 10.1038/sdata.2018.160.

Herderschee J., Fenwick C., Pantaleo G., Roger T., Calandra T. (2015). Emerging single-cell technologies in immunology. Journal of Leukocyte Biology, 98, pp. 23–32. doi: 10.1189/jlb.6RU0115-020R.

Hidalgo L.G., Einecke G., Allanach K., Halloran P.F. (2008). The transcriptome of human cytotoxic T cells : similarities and disparities among allostimulated CD4 + CTL , CD8 + CTL and NK cells. American Journal of Transplantation, 8, pp. 627–636. doi: 10.1111/j.1600-6143.2007.02128.x.

Huang P., Zhou Y., Liu Z., Zhang P. (2016). Interaction between ANXA1 and GATA-3 in immunosuppression of CD4 + T Cells. Mediators of Inflammation, 2016, 1701059. doi: 10.1155/2016/1701059.

Hutloff A., Dittrich A.M., Beier K.C., Eljaschewitsch B., Kraft R., Anagnostopoulos I., et al. (1999). ICOS is an inducible T-cell co-stimulator structurally and functionally related to CD28. Nature, 397, pp. 263–266. doi: 10.1038/16717.

Islam S., Kjallquist U., Moliner A., Zajac P., Fan J.B., Lonnerberg P., et al. (2011). Characterization of the single-cell transcriptional landscape by highly multiplex RNA-seq Saiful. Genome Research, 21, pp. 1160–1167. doi: 10.1101/gr.110882.110.1160.

Kabashima K., Nakashima C., Nonomura Y., Otsuka A., Cardamone C., Parente R., et al. (2018). Biomarkers for evaluation of mast cell and basophil activation. Immunological Reviews, 282, pp. 114–120. doi: 10.1111/imr.12639.

Kiselev V.Y., Andrews T.S. and Hemberg M. (2019). Challenges in unsupervised clustering of single-cell RNA-seq data. Nature Reviews Genetics, 20(5), pp. 273–282. doi: 10.1038/s41576-018-0088-9.

Kockx M., Traini M. and Kritharides L. (2018). Cell-specific production, secretion, and function of apolipoprotein E. Journal of Molecular Medicine, 96, pp. 361–371. doi: 10.1007/s00109-018-1632-y.

Lesley R., Kelly L.M., Xu Y., Cyster J.G. (2006). Naive CD4 T cells constitutively express CD40L and augment autoreactive B cell survival. Immunology, 103(28), pp. 10717–10722. doi: 10.1073/pnas.0601539103.

Li X., Ding Y., Zi M., Sun L., Zhang W., Chen S., et al. (2017). CD19, from bench to bedside. Immunology Letters, 183, pp. 86–95. doi: 10.1016/j.imlet.2017.01.010.

Lieberman, J. (2003). The ABCs of granule-mediated cytotoxicity: new weapons in the arsenal. Nature Review in Immunology, 3, pp. 361–370. doi: https://doi.org/10.1038/nri1083.

Ling X.B., Wei H.W., Wang J., Kong Y.Q., Wu Y.Y., Guo J.L., et al. (2016). Mammalian metallothionein-2A and oxidative stress. International Journal of Molecular Sciences, 17, 1483. doi: 10.3390/ijms17091483.

Lischke T., Hegemann A., Gurka S., Vu D., Burmeister Y., Lam K., et al. (2012). Comprehensive analysis of CD4 + T cells in the decision between tolerance and immunity in vivo reveals a pivotal role for ICOS. The Journal of Immunology, 189, pp. 234–244. doi: 10.4049/jimmunol.1102034.

Mantovani A., Biswas S.K., Galdiero M.R., Sica A., Locati M. (2013). Macrophage plasticity and polarization in tissue repair and remodelling. Journal of Pathology, 229, pp. 176–185. doi: 10.1002/path.4133.

McQuattie-Pimentel A.C., Budinger G.R.S. and Ballinger M.N. (2018). Monocyte-derived alveolar macrophages : the dark side of lung repair? American Journal of Respiratory Cell and Molecular Biology, 58(1), pp. 5–6. doi: 10.1165/rcmb.2017-0328ED.

Mercier E., Bolognin M., Hoffmann A.C., Tual C., Day M.J., Clercx C. (2011). Influence of age on bronchoscopic findings in healthy beagle dogs. Veterinary Journal, 187(2), pp. 225–228. doi: 10.1016/j.tvjl.2009.12.007.

Misharin A.V, Morales-Nebreda L., Mutlu G.M., Budinger G.R.S., Perlman H. (2013). Flow cytometric analysis of macrophages and dendritic cell subsets in the mouse lung. American journal of respiratory cell and molecular biology, 49(4), pp. 503–510. doi: 10.1165/rcmb.2013-0086MA.

Mould K.J., Jackson N.D., Henson P.M., Seibold M., Janssen W.J. (2019). Single cell RNA sequencing identifies unique inflammatory airspace macrophage subsets. JCI insight, 4(5), pp. 1–17. doi: 10.1172/jci.insight.126556.

Muraro M.J., Dharmadhikari G., Grün D., Groen N., Dielen T., Jansen E.,et al. (2016). A single-cell transcriptome atlas of the human pancreas. Cell Press, 3(4), pp. 385-394.e3. doi: 10.1016/J.CELS.2016.09.002.

Nelson W.R. and Couto C.G. (2014). Diagnostic tests for the lower respiratory tract. In: Nelson W.R., Couto C.G. (eds). Small animal internal medicine 5th edition. Elsevier. St Louis, Missouri, pp. 263–296.

Out T.A., Wang S.Z., Rudolph K., Bice D.E. (2002). Local T-cell activation after segmental allergen challenge in the lungs of allergic dogs. Immunology, 105(4), pp. 499–508. doi: 10.1046/j.1365-2567.2002.01383.x.

Papalexi, E. and Satija, R. (2018). Single-cell RNA sequencing to explore immune cell heterogeneity. Nature Reviews Immunology, 18(1), pp. 35–45. doi: 10.1038/nri.2017.76.

Patel A., Harris K.A. and Fitzgerald F. (2017). What is broad-range 16S rDNA PCR? Archives of Disease in Childhood: Education and Practice Edition, 102(5), pp. 261–264. doi: 10.1136/archdischild-2016-312049.

Proserpio V. and Mahata B. (2015). Single-cell technologies to study the immune system. Immunology, 147, pp. 133–140. doi: 10.1111/imm12553.

Rabiger F.V., Rothe K., Von Buttlar H., Bismarck D., Büttner M., Moore P.F., et al. (2019). Distinct features of canine nn-conventional CD4−CD8α− double-negative TCRαβ+ vs. TCRγδ+ T cells. Frontiers in Immunology, 10, 2748. doi: 10.3389/fimmu.2019.02748.

Rajamäki M.M., Järvinen A., Saari S.A.M., Maisi P.S. (2001). Effect of repetitive bronchoalveolar lavage on cytologic findings in healthy dogs. American Journal of Veterinary Research, 62(1), pp. 14–17. doi: 10.2460/ajvr.2001.62.13.

Rodriguez-Perea A.L., Arcia E.D., Rueda C.M., Velilla P.A. (2016). Phenotypical characterization of regulatory T cells in humans and rodents. Clinical and Experimental Immunology, 185, pp. 281–291. doi: 10.1111/cei.12804.

Rogulski K., Li Y., Rothermund K., Pu L., Watkins S., Yi F., et al. (2005). Onzin , a c-Myc-repressed target, promotes survival and transformation by modulating the Akt – Mdm2 – p53 pathway. Oncogene, 24, pp. 7524–7541. doi: 10.1038/sj.onc.1208897.

Sattasathuchana P. and Steiner M. (2014). Canine eosinophilic gastrointestinal disorders. Animal Health Research Reviews, 15(1), pp. 76–86. doi: 10.1017/S1466252314000012.

Schyns J., Bai Q., Ruscitti C., Radermecker C., De Schepper S., Chakarov S., et al. (2019). Non-classical tissue monocytes and two functionally distinct populations of interstitial macrophages populate the mouse lung. Nature Communications, 10, 3964. doi: 10.1038/s41467-019-11843-0.

See, P., Lum J., Chen J., Ginhoux F. (2018). A single-cell sequencing guide for immunologists. Frontiers in Immunology, 9, 2425. doi: 10.3389/fimmu.2018.02425.

Spużak J., Chełmonska-soyta A., Krzysztof K., Jankowski M., Nicpon J., Błach J., et al. (2008). Application of flow cytometry in blood examination and bronchoalveolar lavage in healthy dogs. Medicine, 3(38), pp. 321–324.

Stifano G. and Christmann R.B. (2016). Macrophage involvement in systemic sclerosis : do we need more evidence? Current Rheumatology Reports, 18, 1–6. doi: 10.1007/s11926-015-0554-8.

Stuart T., Butler A., Hoffman P., Hafemeister C., Papalexi E., Mauck W.M.III, et al. (2019). Comprehensive integration of single-cell data resource comprehensive integration of single-cell data', Cell, 177(7), pp. 1888–1902. doi: 10.1016/j.cell.2019.05.031.

Stubbington M.J.T., Rozenblatt-Rosen O., Regev A., Teichmann S.A. (2017). Single cell transcriptomics to explore the immune system in health and disease. Science, 358(6359), pp. 58–63. doi: 10.1126/science.aan6828.

Subramanian A., Tamayo P., Mootha V.K., Mukherjee S., Ebert B.L., Gillettea M.A., et al. (2005). Gene set enrichment analysis: A knowledge-based approach for interpreting genome-wide expression profiles. Proceedings of the National Academy of Sciences, 102(43), pp. 15545–15550. doi: 10.1073/pnas.0506580102.

Suryawanshi H., Clancy R., Morozov P., Halushka M.K., Buyon J.P., Tuschl T. (2019). Cell atlas of the foetal human heart and implications for autoimmune-mediated congenital heart block. Cardiovascular Research, 116, 1446–1457. doi: 10.1093/cvr/cvz257.

Tafuri A., Shahinian A., Bladt F., Yoshinaga S.K., Jordana M., Wakeham A., et al. (2001). ICOS is essential for effective T-helper-cell responses. Nature, 409, pp. 105–109. doi: 10.1038/35051113.

Trombetta A.C., Goyal R., Desch A.N., Leach S.M., Prabagar M., Atif S.M., et al. (2018). A circulating cell population showing both M1 and M2 monocyte/macrophage surface markers characterizes systemic sclerosis patients with lung involvement. Respiratory Research, 19(186), pp. 1–12. doi: 10.1186/s12931-018-0891-z.

Vail D.M., Mahler P.A. and Soergel S.A. (1995). Differential cell analysis and phenotypic subtyping of lymphocytes in bronchoalveolar lavage fluid from clinically normal dogs. American Journal of Veterinary Research, 56(3), pp. 282–285.

Van De Laar L., Saelens W., De Prijck S., Martens L., Scott C.L., Van Isterdael G., et al. (2016). Yolk sac macrophages , fetal liver, and adult monocytes can colonize an empty niche and develop into functional tissue-resident macrophages. Immunity, 44(4), pp. 755–768. doi: 10.1016/j.immuni.2016.02.017.

Varricchi G., Raap U., Rivellese F., Gibbs B.F. (2018). Human mast cells and basophils — How are they similar how are they different ? Immunological Reviews, 282, pp. 8–34. doi: 10.1111/imr.12627.

Vegh P. and Haniffa M. (2018). The impact of single-cell RNA sequencing on understanding the functional organization of the immune system. Briefings in Functional Genomics, 17(4), pp. 265–272. doi: 10.1093/bfgp/ely003.

Volkova O.Y., Reshetnikova E.S., Mechetina L.V., Chikaev N.A., Najakshin A.M., Faizulin R.Z., et al. (2007). Generation and characterization of monoclonal antibodies specific for human FCRLA. Hybridoma, 26(2), pp. 78–85. doi: 10.1089/hyb.2006.043.

Wolkow P.P., Gebska A. and Korbut R. (2018). In vitro maturation of monocyte-derived dendritic cells results in two populations of cells with different surface marker expression, independently of applied concentration of interleukin-4. International Immunopharmacology, 57, pp. 165–171. doi: 10.1016/j.intimp.2018.02.015.

Xin H., Peng Y., Yuan Z., Guo H. (2009). In vitro maturation and migration of immature dendritic cells after chemokine receptor 7 transfection. Canadian Journal of Microbiology, 55(7), pp. 859–866. doi: 10.1139/W09-041.

Yi H. and Ku N.O. (2013). Intermediate filaments of the lung. Histochemisrty and Cell Biology, 140, pp. 65–69. doi: 10.1007/s00418-013-1105-x.

Zalewska M., Trefon J. and Milnerowicz H. (2014). The role of metallothionein interactions with other proteins. Proteomics, 14, pp. 1343–1356. doi: 10.1002/pmic.201300496.

Zhu J., Zhu J., Yamane H., Cote-Sierra J., Guo L., Paul W.E. (2006). GATA-3 promotes Th2 responses through three different mechanisms : induction of Th2 cytokine production, selective growth of Th2 cells and inhibition of Th1 cell-specific factors. Cell Research, 16, pp. 3–10. doi: 10.1038/sj.cr.7310002.

Supplemental material

The Supplementary Material for this article can be found online at: https://www.frontiersin.org/articles/10.3389/fimmu.2020.01707/full#supplementary-material.

The datasets presented in this study can be found in online repositories. The names of the repository/repositories and accession number(s) can be found below: https://www.ebi.ac.uk/arrayexpress/, E-MTAB-9265.

Experimental section

Part 2

Study 5 :

Identification of pro-fibrotic macrophage populations by single-cell transcriptomic analysis in West Highland white terriers affected with canine idiopathic pulmonary fibrosis.

Frontiers in Immunology 11

Aline Fastrès, Dimitri Pirottin, Laurence Fievez, Alexandru-Cosmin Tutunaru, Géraldine Bolen, Anne-Christine Merveille, Thomas Marichal, Christophe J. Desmet, Fabrice Bureau, Cécile Clercx

Abstract

Canine idiopathic pulmonary fibrosis (CIPF) affects old dogs from the West Highland white terrier (WHWT) breed and mimics idiopathic pulmonary fibrosis (IPF) in human. The disease results from deposition of fibrotic tissue in the lung parenchyma causing respiratory failure. Recent studies in IPF using single-cell RNA sequencing (scRNA-seq) revealed the presence of profibrotic macrophage populations in the lung, which could be targeted for therapeutic purpose. In dogs, scRNA-seq was recently validated for the detection of cell populations in bronchoalveolar lavage fluid (BALF) from healthy dogs. Here we used the scRNA-seq to characterize disease-related heterogeneity within cell populations of macrophages/monocytes (Ma/Mo) in the BALF from five WHWTs affected with CIPF in comparison with three healthy WHWTs. Gene set enrichment analysis was also used to assess pro-fibrotic capacities of Ma/Mo populations. Five clusters of Ma/Mo were identified. Gene set enrichment analyses revealed the presence of pro-fibrotic monocytes in higher proportion in CIPF WHWTs than in healthy WHWTs. In addition, monocyte-derived macrophages enriched in pro-fibrotic genes in CIPF compared with healthy WHWTs were also identified. These results suggest the implication of Ma/Mo clusters in CIPF processes, although, further research is needed to understand their role in disease pathogenesis. Overexpressed molecules associated with pulmonary fibrosis processes were also identified that could be used as biomarkers and/or therapeutic targets in the future.

Introduction

Canine idiopathic pulmonary fibrosis (CIPF) is defined as a progressive and abnormal accumulation of collagen in the lung parenchyma that threatens alveolar gas exchange and reduces lung compliance causing cough, exercise intolerance, and, finally, respiratory failure and death (Clercx, Fastrès and Roels, 2018; Laurila and Rajamäki, 2020). The disease affects predominantly middle-aged to old dogs from the West Highland white terrier (WHWT) breed (Clercx, Fastrès and Roels, 2018; Laurila and Rajamäki, 2020). Although the cause of CIPF is not identified, a genetic aetiology is suspected as it affects mainly one breed. Confirmation of the diagnostic remains challenging due to absence of available diagnostic biomarkers and necessity to exclude other diseases and comorbidities. It currently relies on either thoracic high-resolution computed tomography (HRCT) or histopathology of the lung tissue or both. Despite a lot of researches on CIPF, the pathophysiology remains unclear and no curative treatment are available (Clercx, Fastrès and Roels, 2018; Laurila and Rajamäki, 2020).

CIPF shares several clinical findings with human idiopathic pulmonary fibrosis (IPF). However, thoracic HRCT and histopathology show features associated with both human IPF and non-specific interstitial pneumonia demonstrating that CIPF and IPF are not strictly identical (Clercx, Fastrès and Roels, 2018; Laurila and Rajamäki, 2020). In spite of those differences, studying CIPF in WHWTs is worth to better understand IPF. Indeed, dogs, like human, are subjected to various environmental stresses which can have an impact on lung cells especially alveolar macrophages (AMs) (Puttur *et al.*, 2019). Moreover, CIPF is a disease that develops spontaneously in WHWTs (Clercx, Fastrès and Roels, 2018; Laurila and Rajamäki, 2020). Those characteristics make the dog a much more interesting model compared to the mouse experimental models. In human IPF and IPF mouse models, recent studies used single-cell mRNA sequencing (scRNA-seq) to detect altered cell populations compared with healthy conditions through an unbiased approach (Xu *et al.*, 2016; Gokey *et al.*, 2018; Xie *et al.*, 2018; Aran *et al.*, 2019; Morse *et al.*, 2019; Peyser *et al.*, 2019; Reyfman *et al.*, 2019; Zhang *et al.*, 2019; Joshi *et al.*, 2020; Tsukui *et al.*, 2020). Indeed, the technique allows high-throughput and high-resolution analysis of thousands of cells at the same time without requiring prior knowledge of cell markers to determine cell heterogeneity (See *et al.*, 2018; Poczobutt and Eickelberg, 2019; Stuart and Satija, 2019). With this method, a profibrotic role of specific macrophage and monocyte populations has been described in IPF patients and IPF mouse models (Aran *et al.*, 2019; Ji and Fan, 2019; Morse *et al.*, 2019; Peyser *et al.*, 2019; Reyfman *et al.*, 2019; Joshi *et al.*, 2020). An increased number of macrophages and proliferating myeloid cells was found in bleomycin-induced lung fibrosis mouse models, in the beginning of lung fibrosis development, before fibroblastic infiltration (Peyser *et al.*, 2019). Specific monocyte and macrophage clusters were identified in fibrosis conditions (Aran *et al.*, 2019; Morse *et al.*, 2019; Reyfman *et al.*, 2019; Joshi *et al.*, 2020).

AMs from IPF patients were enriched in functions involved in fibrotic processes including "extra-cellular matrix organization" and "regulation of cell migration" for example (Reyfman *et al.*, 2019). Pro-fibrotic macrophage but also monocyte clusters that expressed genes able to drive fibroblasts' proliferation were localized in areas of fibrosis (Aran *et al.*, 2019; Joshi *et al.*, 2020). All these findings indicate that targeting specific macrophage and monocyte clusters could be potentially useful for the prevention and the therapy of lung fibrosis (Ji and Fan, 2019).

Recently, cells of the bronchoalveolar lavage fluid (BALF) of healthy dogs have been characterized by scRNA-seq, providing a comprehensive single-cell expression profiling of the canine BALF cells in healthy conditions (Fastrès et al., 2020b). Fourteen distinct cell populations were identified including AMs (3 clusters), macrophages/monocytes (Ma/Mo) (1 cluster), $CD8^+$ T cells, $CD8^-CD4^-$ T cells, B cells, neutrophils, mature and immature dendritic cells (DCs), ciliated and non-ciliated epithelial cells, mast cells and cells in division (Fastrès et al., 2020b).

The objective of this study was to characterize, using scRNA-seq, disease-related heterogeneity within Ma/Mo populations in the BALF from WHWTs affected with CIPF compared with healthy WHWTs.

Materials and methods

1. Dog population

The scRNA-seq analysis was performed on BALF obtained from WHWTs affected with CIPF and healthy WHWTs. Dogs were prospectively recruited between March and October 2018 at the veterinary clinic of the University of Liège (Liège, Belgium) according to a protocol approved by the ethical committee of the University of Liège (approval no. 1435). All dogs were privately owned, and samples were obtained with owners' written consent.

The healthy or CIPF status of the dogs was confirmed according to a previously described approach (Heikkila-Laurila and Rajamaki, 2014) based on history, physical examination, complete blood work, 6-minutes walked distance (6MWD), thoracic HRCT, bronchoscopy and analysis of the BALF (including macroscopic evaluation and total (TCC) and differential (DCC) cell count). WHWTs under treatment including antimicrobials drugs and corticoids were excluded from the study.

2. BALF collection

BALF was obtained using the same protocol as previously described (Fastrès et al., 2020b). Briefly, under general anaesthesia, a bronchoscope (FUJINON© Paediatric Video-Bronchoscope EB-530S) was inserted into the lower airways of the dogs. Three to four mL/kg of sterile saline solution was instilled in the airways through the bronchoscope channel and directly reaspirated. A part of the crude BALF was used for TCC and DCC obtained using respectively a hemacytometer and a cytospin preparation. The rest of the collected fluid was then directly transferred on ice to the GIGA laboratory of cellular and molecular immunology (Liège, Belgium).

3. Single-cell RNA sequencing

ScRNA-seq was performed as already described (Schyns *et al.*, 2019; Fastrès et al., 2020b). Briefly, BALFs were processed to obtain a final cell suspension containing between 500 and 1,000 cells/µL suspended in phosphate-buffered saline solution (Gibco™ 1x DPBS, Cat.14190-169) containing 0.04% (w/v) bovine serum albumin. Cell viability assessed by Trypan blue staining was considered as acceptable above 80%. Details about BALF volume, final cell concentration and cell viability for each sample can be found in Supplementary Table 1.

For each sample, approximatively 3500 cells (Supplementary Table 1) were loaded into the Chromium™ Controller (10x Genomics, Pleasanton, CA, USA) and were then partitioned into nanolitre scale vesicles containing 10x barcoded beads from Chromium™ Single Cell 3' Gel Bead kit v2 (10x Genomics, Pleasanton, CA, USA) according to manufacturer's instructions. Reverse

transcription of mRNAs took place into vesicles on a Veriti© 96-Well Thermal Cycler (ThermoFisher Scientific, Merelbeke, Belgium) after cell lysis and capture of polyadenylated mRNAs.

Emulsion breakage, cDNA amplification and libraries construction were performed using Chromium™ Single Cell 3′ Reagent kit v2 (10x Genomics, Pleasanton, CA, USA) according to manufacturer's instructions as already described (Schyns *et al.*, 2019; Fastrès et al., 2020b). Libraries were assessed for quality (2100 Bioanalyser Instrument; Agilent, Santa Clara, CA, USA) and then sequenced on a NextSeq500 instrument (Illumina, San Diego, CA, USA).

Initial data pre-processing was performed using the Cell Ranger software (v1.2.0) (10x Genomics, Pleasanton, CA, USA). Reads were mapped to dog genome (CanFam3.1, GenBank assembly accession: GCA_000002285.2). The genes not well annotated were further blasted on the Ensembl genome browser (v99.31) (Cunningham *et al.*, 2019) for dog species.

Further data analyses were performed using R package Seurat (version 3.1.2) (Stuart *et al.*, 2019) after the selection of the cells with a minimum of 100 and a maximum of 2,500 unique genes mapped, the selection of the genes found in at least 3 different cells and the normalization of the expression values to 10,000 transcripts per cell. ScRNA-seq data coming from each dog were then merged for the next analyses which were done by following Stuart et al. (2019) instructions (Stuart *et al.*, 2019). Pre-ranked gene set enrichment analyses (GSEAs) were performed using GSEA-P software (v4.0.3) (Subramanian *et al.*, 2005). The enrichment score was determined using weighted Kolmogorov–Smirnov-like statistic with false discovery rate (FDR) correction for multiple testing (Subramanian *et al.*, 2005). A FDR cut-off of 25% was considered as appropriate (Subramanian *et al.*, 2005). GSEAs were computed between either the Gene Ontology (GO) Biological Process gene sets (v7.1) (Subramanian *et al.*, 2005), or the Hallmark gene sets (v7.1) (Subramanian *et al.*, 2005) or the Comparative Toxicogenomics Database Pulmonary fibrosis gene set (Davis *et al.*, 2019). Differentially expressed genes (DEGs) in different conditions were obtained using the "FindMarkers" command in Seurat (Stuart *et al.*, 2019). Differential gene expressions were measured using non-parametric Wilcoxon rank sum tests adjusted for multiple testing with Bonferroni correction. Only DEGs with an average log2 fold change (avg_logFC) > 0.25 and an adjusted P-value < 0.05 were retained.

4. Statistical analyses

A P-value lower than 0.05 was considered as significant. Details about statistical analyses for scRNA-seq data and GSEAs can be found in the section above. Statistics used for the comparison of the WHWTs groups are reported in Tables 1, 3 and 4.

Results

1. Study population

BALF samples were obtained from 3 healthy WHWTs and 5 WHWTs affected with CIPF. Characteristics of the dogs included in the study are reported in Table 1. No significant differences in age, gender and weight were reported between the groups (Table 1).

Table 1: *Characteristics of the West Highland white terriers either healthy or affected with canine idiopathic pulmonary fibrosis included in the study.*

		Healthy WHWTs (n = 3)	WHWTs affected with CIPF (n = 5)	*P*-value
Age, *y*		8.2 (5.4-8.7)	10.8 (10.2-12.7)	0.14[a]
Gender, *M/F*		2/1	1/4	0.46[b]
Weight, *kg*		8.4 (8.4-8.9)	9.5 (9.1-9.9)	0.14[a]
6MWD, *m*		506.1 (478.8-513.0)	356.4 (356.1-366.3)	0.04[a]
BALF analysis	TCC, *cells/µL*	760 (665-770)	2,620 (2,500-3,285)	0.04[a]
	Macrophages, *%*	78 (76.5-84.5)	71 (64-82)	0.39[a]
	Neutrophils, *%*	3 (2.5-3.5)	10 (9-21)	0.04[a]
	Lymphocytes, *%*	11 (7-16)	7 (7-16)	0.93[a]
	Eosinophils, *%*	1 (1-4)	2 (1-2)	0.93[a]
	Mast cells, *%*	0	0	/
	Epithelial cells, *%*	1 (0.5-1.5)	1 (0-1)	0.46[a]

Continuous data are not normally distributed according to the Shapiro-Wilk test and are then expressed in median and interquartile range. Groups were compared using either Mann-Whitney tests ([a]) or Chi-squared tests ([b]). WHWTs, West Highland white terriers; CIPF, canine idiopathic pulmonary fibrosis; M, male; F, female; 6MWD, 6-minutes walked distance; BALF, bronchoalveolar lavage fluid; TCC, total cell count.

CIPF diagnosis was confirmed in all CIPF WHWTs by thoracic HRCT which revealed extensive ground-glass opacity in all dogs. Other HRCT findings included a combination of mosaic pattern, bronchial wall thickening, parenchymal and subpleural bands, bronchomalacia and bronchiectasis. Among WHWTs affected with CIPF, 3/5 (60%) had an history of both exercise intolerance and cough and 2/5 (40%) only exhibited exercise intolerance. Crackles were heard on lung auscultation in all dogs. Three dogs (60%) had a restrictive dyspnoea. Among them, 2 also exhibited cyanosis. The 6MWD covered by each dog was in favour of exercise intolerance in all CIPF dogs. Moreover, the distance was significantly reduced in CIPF compared with healthy WHWTs (Table 1). At echocardiography, signs of secondary pulmonary arterial hypertension were present in all CIPF dogs. Changes in BALF cells analysis were consistent with non-specific chronic lung inflammation (Table 1).

Among control WHWTs included in the study, all were clinically healthy and did not have any signs or findings indicating pulmonary disease. Echocardiography excluded the presence of cardiac disease in all of them. Thoracic HRCT did not reveal significant abnormalities. BALF cells analysis was unremarkable (Table 1).

2. ScRNA-seq identifies multiple cell populations in the dog BALF

Droplet-based scRNA-seq analysis of BALF cells was performed with a median read depth of ~43,000 reads per cell. In total, 19,255 cells (6,703 from healthy and 12,552 from diseased dogs) coding for 11,722 unique genes were included in the final analysis. The median detected genes per cell was 788 (interquartile range 399-1191 genes/cells, Table 2). Individual metrics about mapping and cells are displayed in Table 2, the individual distribution for transcripts and genes counts is illustrated in Supplementary Figure 1A and B, respectively.

Table 2. *Metrics about mapping and characteristics of the detected cells in each bronchoalveolar lavage fluid specimen.*

Sample ID	Diagnosis	Number of cells passing quality control	Reads mapped confidently to genome, %	Reads mapped confidently to transcriptome, %	Median genes/ cell (range)	Median UMIs/ cell (range)	Total genes detected
WHWT 1	Healthy	3,060	67	24.4	741 (445-1,184)	1,711 (899-3,351)	12,354
WHWT 2	Healthy	2,345	67.2	24.7	1,091 (585-1,446)	2,809 (1,173-4,398)	12,988
WHWT 3	Healthy	1,298	59.8	23.9	834 (376-1,046)	1,889 (678-2,671)	10,839
CIPF 1	CIPF	2,551	69.2	24.6	1,147 (827-1,346)	2,934 (1,857-3,740)	12,988
CIPF 2	CIPF	2,686	67.3	23.4	618 (219-1,226)	1,362 (354-3,390)	12,478
CIPF 3	CIPF	2,564	74.8	30.4	503 (355-969)	960 (601-2,247)	11,819
CIPF 4	CIPF	2,556	71.5	28.1	867 (411-1,090)	1,939 (708-2,754)	11,722
CIPF 5	CIPF	2,195	73.1	27.5	453 (383-722)	833 (656-1,622)	11,921

Data were generated after passing quality control including the exclusion of cells with < 100 and > 2500 genes. Only genes present in more than 3 cells were kept. Reads mapped confidently to genome are the number of reads that mapped only to the genome. Reads mapped confidently to transcriptome are the fraction of the reads mapped to a unique gene in the transcriptome and are considered for UMI counting. Median genes per cell correspond to the median number of genes with at least one UMI count. Total genes detected is the detected number of genes with at least one UMI count in any cell. ID, identity; UMI, unique molecular identifier; WHWT, West Highland white terrier; CIPF, canine idiopathic pulmonary fibrosis.

Cells from all samples were combined and aligned to account for sample variations among dogs using Seurat package in R (version 3.1.2) (Stuart *et al.*, 2019). They were then clustered and

visualized using t-distributed stochastic neighbour embedding (t-SNE) plot with a resolution set at 0.3 and a number of dimensions to use set to 30 which resulted in the identification of 14 clusters (Figure 1A). After clustering, DEGs between each identified cluster were used to assign cell types to each cluster using previously established markers (Fastrès et al., 2020b). Cells populations found accordingly included Ma/Mo (5 clusters), $CD8^+$ and $CD8^-CD4^-$ T cells, mature and immature DCs, neutrophils, B cells, epithelial cells, mast cells and cycling cells (Figure 1B). DEGs detected in each cluster are provided in Supplementary Table 2. Principal markers used to identify cell populations can be found in Figure 1D. Each cell population included cells coming from healthy and diseased dogs (Figure 1C and Table 3). No significant differences were reported in relative proportions of the different cell types between healthy WHWTs and WHWTs affected with CIPF, except for mature DCs (Table 3).

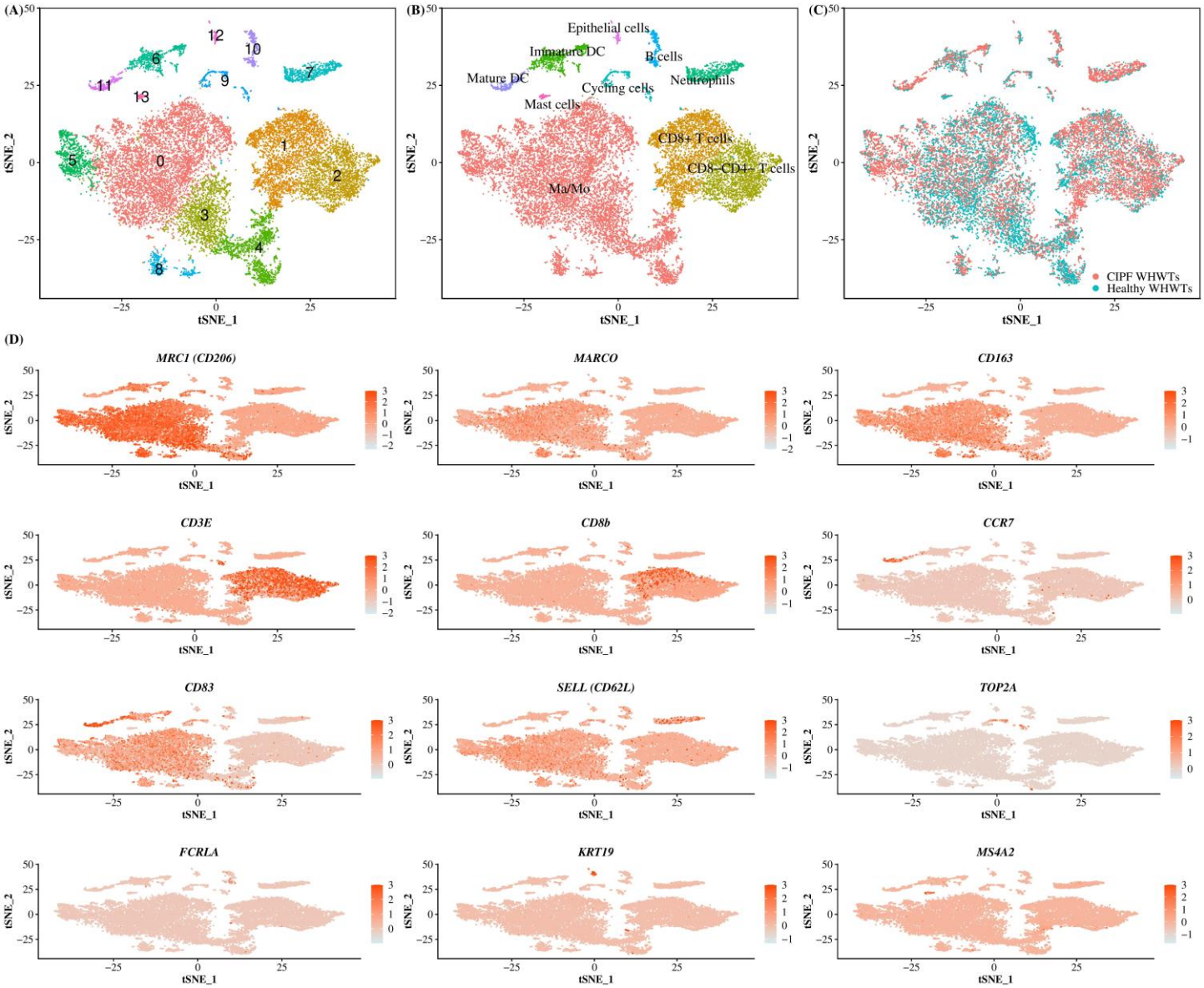

Figure 1. *Single-cell RNA sequencing analysis identifies multiple cell populations in the canine bronchoalveolar lavage fluids (BALFs). The scRNA-seq analysis was performed on a single-cell*

suspension generated from 8 BALFs obtained from 3 healthy West Highland white terriers (WHWTs) and 5 WHWTs affected with canine idiopathic pulmonary fibrosis (CIPF). Cells were visualized using t-distributed stochastic neighbour embedding (t-SNE) plots. (A) Cell clusters identified. (B) Cell populations identified. (C) Cells are coloured according to the status of dogs either healthy or affected with CIPF. (D) Expression of differentially expressed genes representative of each cell population. Ma/Mo, macrophages/monocytes; DC, dendritic cell; MRC1, macrophage mannose receptor; MARCO, macrophage receptor with collagenous structure; CD163, scavenger receptor cysteine-rich type 1 protein M130; CD3E, T-cell surface glycoprotein CD3 epsilon chain; CD8b, T-cell surface glycoprotein CD8 beta chain ; CCR7, C-C chemokine receptor type 7 ; CD83, CD83 molecule; SELL, selectin; TOP2A, DNA topoisomerase II alpha; FCRLA, Fc receptor like A; KRT19, cytokeratin 19; MS4A2, membrane spanning 4-domains A2.

Table 3. *Relative cells repartition between healthy and CIPF WHWTs in each cell population.*

	Healthy WHWTs	CIPF WHWTs	*P*-value
Ma/Mo	69.5 ± 4.7	52.7 ± 26.3	0.332
$CD8^+$ T cells	10.9 ± 10.0	17.6 ± 15.4	0.533
$CD8^-CD4^-$ T cells	7.1 ± 1.1	14.7 ± 9.0	0.210
Immature DC	4.6 ± 3.1	3.7 ± 1.6	0.586
Neutrophils	1.6 ± 2.1	4.5 ± 6.7	0.498
Cycling cells	2.2 ± 0.5	1.8 ± 0.7	0.456
B cells	1.5 ± 0.6	2.1 ± 1.4	0.557
Mature DC	0.4 ± 0.1	2.1 ± 1.0	0.041
Epithelial cells	1.0 ± 0.6	0.6 ± 0.2	0.160
Mast cells	1.2 ± 1.8	0.3 ± 0.3	0.270

Relative cell proportion were compared between healthy West Highland white terriers (WHWTs) and WHWTs affected with canine idiopathic pulmonary fibrosis (CIPF) using t-tests after verification of the distribution normality using Shapiro-Wilk tests. Data are expressed in mean percentage ± standard deviation.

3. ScRNA-seq analysis reveals fibrosis-associated transcriptomic changes in Ma/Mo clusters

3.1. Comparison between Ma/Mo clusters

After Ma/Mo isolation from other cell populations, we repeated clustering on those cells to better characterize changes associated with CIPF. It resulted in the identification of 5 transcriptionally distinct Ma/Mo clusters (M0, M1, M2, M3 and M4) (Figure 2A). Average expression of all the genes expressed by each Ma/Mo cluster can be found in Supplementary Table 3. Relative contributions of each Ma/Mo cluster into each group of dogs either healthy or diseased are displayed in Figure 2B and C. Cells repartition between healthy and diseased WHWTs was similar into each cluster except in the cluster M2 which contained more cells in WHWTs affected with CIPF (Figure 2B, C and Table 4). We then estimated differential genes expression between each cluster of Ma/Mo and performed

GSEAs to better characterize Ma/Mo clusters independently of the disease status of the dogs. All DEGs identified in each cluster compared to others are displayed in Supplementary Table 4. Results of the enrichment analyses performed by mapping DEGs identified in each cluster compared to others, to Hallmark gene sets or GO Biological Process gene sets are provided in Supplementary Table 5.

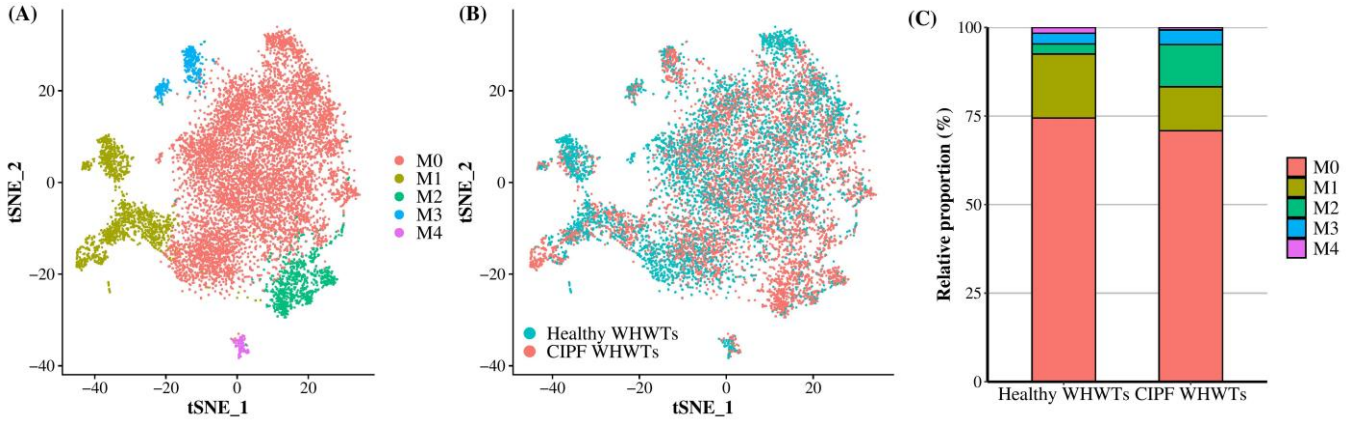

Figure 2. *Macrophages/monocytes (Ma/Mo) clusters identified. Cells identified as Ma/Mo after the annotation of scRNA-Seq data obtained from 3 healthy West Highland white terriers (WHWTs) and 5 WHWTs affected with canine idiopathic pulmonary fibrosis (CIPF) were selected and then clustered allowing the identification of 5 distinct clusters.* ***(A)*** *Clusters identified. Cells were visualized using a t-distributed stochastic neighbour embedding (t-SNE) plot.* ***(B)*** *t-SNE plot of Ma/Mo coloured according to the disease status of the WHWTs either healthy or affected with CIPF.* ***(C)*** *Bar plot of the relative proportion in each disease status of each Ma/Mo cluster.*

Table 4. *Relative cells repartition between healthy and CIPF WHWTs in each Ma/Mo cluster.*

	Healthy WHWTs	CIPF WHWTs	*P*-value
M0	73.6 ± 4.1	67.2 ±10.0	0.342
M1	18.8 ± 4.1	14.2 ± 6.6	0.329
M2	2.9 ± 0.2	13.5 ± 4.7	0.009
M3	3.2 ±1.1	4.4 ± 1.8	0.356
M4	1.4 ± 1.0	0.7 ± 0.4	0.185

Relative cell proportion in each macrophages/monocytes (Ma/Mo) cluster were compared between healthy West Highland white terriers (WHWTs) and WHWTs affected with canine idiopathic pulmonary fibrosis (CIPF) using t-tests after verification of the distribution normality using Shapiro-Wilk tests. Data are expressed in mean percentage ± standard deviation.

Resident AMs were identified based on *MARCO* expression (Figure 3), a class A scavenger receptor (Gibbings *et al.*, 2015; Gibbings *et al.*, 2017; Reyfman *et al.*, 2019; Fastrès et al., 2020b; Joshi *et al.*, 2020) and corresponded to cells in clusters M0 and M3 (Figure 2A, Supplementary Tables 3 and 4). They represented the majority of the cells composing Ma/Mo population (Figure 2A, C and Table 4). Cells in these clusters were enriched in biological processes relevant to AMs including "Hallmark reactive oxygen species pathways" for M0 cells and "GO adaptative immune response",

"GO antigen processing and presentation of peptide or polysaccharide antigen via MHC class II", "GO activation and regulation of immune response" and "GO pattern recognition receptor signalling pathway" for M3 cells (Supplementary Table 5). Cells in cluster M1 were considered as monocyte-derived macrophages as they expressed markers from both macrophages, including *MARCO*, *PPARG* (encoding peroxisome proliferator activated receptor gamma), *CD68*, *MRC1* (encoding macrophage mannose receptor, *CD206*), *MSR1* (encoding macrophage scavenger receptor 1, *CD204*) and *CD16* (Gautier *et al.*, 2012; Bharat *et al.*, 2016; Stifano and Christmann, 2016; Yu *et al.*, 2016; Reyfman *et al.*, 2019; Byrne *et al.*, 2020), and monocytes, including *CD11c* (encoding integrin subunit alpha X, *ITGAX*), *CD16*, *CD49d* (encoding integrin subunit alpha 4, *ITGA4*), *CD49e* (encoding integrin subunit alpha 5, *ITGA5*) and *CX3CR1* (encoding fractalkine receptor) (Figure 3, Supplementary Tables 3 and 4) (Ammon *et al.*, 2000; Gundra *et al.*, 2014; Bharat *et al.*, 2016; Byrne *et al.*, 2020). A cluster of monocytes which corresponded to cluster M2 was also identified. Indeed, M2 cells expressed only monocytes markers (Figure 3) including *CSF2RB* (encoding colony stimulating factor 2 receptor subunit beta, *CD131*), *CD11c*, *CD11b* (encoding integrin subunit alpha M, *ITGAM*), *CD49d*, *CD49e* and *CX3CR1* (Figure 3, Supplementary Tables 3 and 4) (Ammon *et al.*, 2000; Gundra *et al.*, 2014; Croxford *et al.*, 2015; Bharat *et al.*, 2016; Byrne *et al.*, 2020). Cells in cluster M1 were enriched in functions associated with the immune response activation including "Hallmark inflammatory response", "GO interferon gamma production" and "GO leukocyte cell-cell adhesion", while cells in cluster M2 were more involved in "GO leukocyte migration" and "GO cell motility" (Supplementary Table 5), functions essential when monocytes are recruited from blood into tissues. M4 cells also expressed macrophages and monocytes markers including notably *MHC-II* markers, *CD63*, *CD68*, *CD16* and *CD49d* (Ammon *et al.*, 2000; Gundra *et al.*, 2014; Patel and Metcalf, 2019; Byrne *et al.*, 2020; Joshi *et al.*, 2020), but they also overexpressed *CD3* genes compared with other clusters (Figure 3 and Supplementary Tables 3 and 4) which are known to be T-lymphocyte markers (Alcover, Alarcon and Bartolo, 2018). Enriched processes associated with M4 cluster were mainly focused on inflammatory response (Supplementary Table 5).

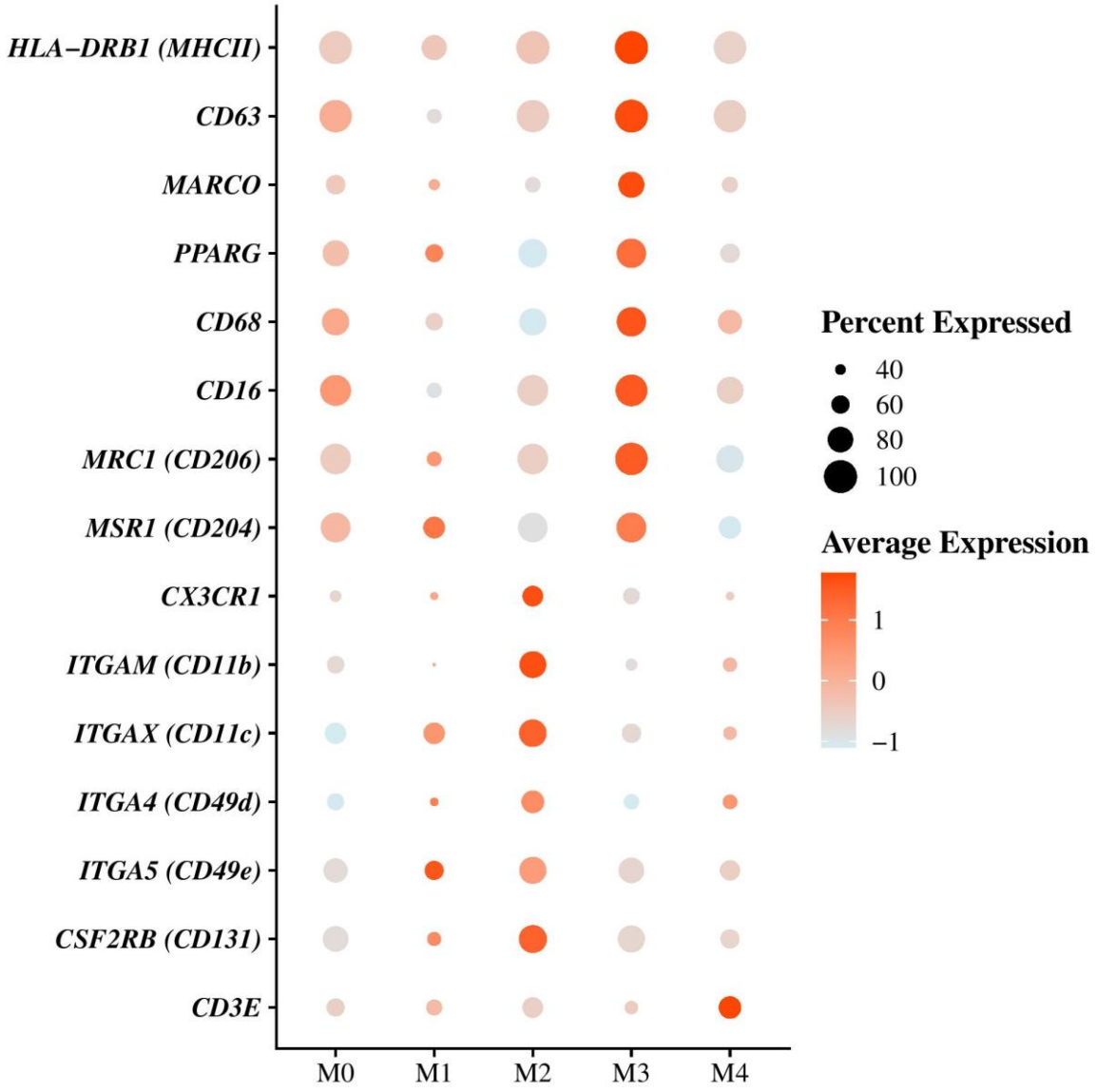

Figure 3. *Differential genes expression analysis between macrophages/monocytes (Ma/Mo) clusters. Dot plot showing the expression of the principal gene markers used to characterize each Ma/Mo cluster. Dot size represents the percentage of cells expressing the genes, while the dot colour represents the average expression of the indicated genes.*

For each cluster independently of the animal status (healthy or affected with CIPF), we also performed a GSEA to determine whether overexpressed genes in each cluster, in comparison with other clusters, could be associated with signatures of pulmonary fibrosis using the Comparative Toxicogenomics Database Pulmonary fibrosis gene set (Davis *et al.*, 2019). Only cells in cluster M1 and M2 showed significant enrichment for pulmonary fibrosis with a normalized enrichment score (NES) of 1.87 and 1.85, respectively (FDR *q*-value = 0.007 and 0.002) (Figure 4A and B). Differentially overexpressed genes identified in relation with pulmonary fibrosis included *SFTPC* (encoding surfactant protein C), *CCL5* (encoding C-C motif chemokine ligand 5), *FN1* (encoding

fibronectin 1), *CXCL8* (encoding C-X-C motif chemokine ligand 8), *ATP11A* (encoding ATPase phospholipid transporting 11A) and *SPP1* (encoding osteopontin) in cluster M1 and *CCL2* (encoding C-C motif chemokine ligand 2), *SPP1*, *FN1*, *CCL3* (encoding C-C motif chemokine ligand 3), *TIMP1* (encoding metallopeptidase inhibitor 1), *IL1RN* (encoding interleukin 1 receptor antagonist), *CXCL8* and *CCL4* (encoding C-C motif chemokine ligand 4) in cluster M2 (Figure 4C). M0 cells were negatively enriched for pulmonary fibrosis with a NES of -2.04 (FDR *q*-value = 0.002). The other clusters were not significantly associated with pulmonary fibrosis processes (FDR *q*-value = 0.145 and 0.289 for cells of cluster M3 and M4, respectively).

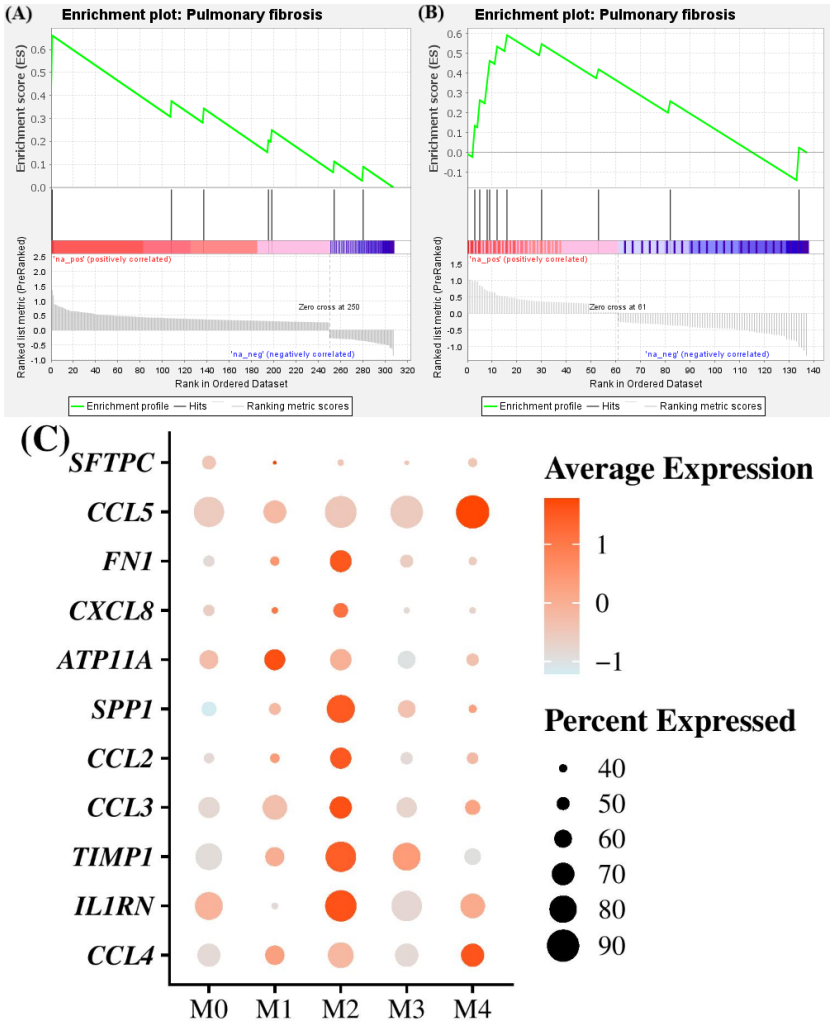

Figure 4. *Enrichment in pulmonary fibrosis processes in M1 and M2 macrophages/monocytes clusters compared to others.* ***(A-B)*** *Gene set enrichment analyses between Comparative Toxicogenomics Database Pulmonary Fibrosis gene set and differentially expressed genes in M1 and M2 clusters, respectively, compared to others.* ***(C)*** *Dot plot showing the expression of genes involved in pulmonary fibrosis processes found to be upregulated in cluster M1 and M2 compared to others. Dot size represents the percentage of cells expressing the genes, while the dot colour represents the average expression of the indicated genes.*

3.2. Comparison between animal status

Differential gene expression between cells from healthy WHWTs and WHWTs affected with CIPF in each Ma/Mo cluster was also assessed (Supplementary Table 6) and was essentially found for cells in cluster M1. DEGs in cluster M1 between CIPF and healthy WHWTs were mapped to the Comparative Toxicogenomics Database Pulmonary fibrosis gene set to assess pulmonary fibrosis signatures. NES in pulmonary fibrosis processes was at 2.01 (FDR *q*-value = 0.008) (Figure 5A). Genes involved in pulmonary fibrosis processes found to be upregulated in CIPF compared with healthy WHWTs in cluster M1 included *FN1*, *SPP1*, *CXCL8* and *PLAU* (encoding plasminogen activator urokinase) (Figure 5D-G). The differential expression between healthy and CIPF WHWTs of those molecules in all Ma/Mo clusters is illustrated in Supplementary Figure 2. Moreover, in cluster M1, enrichment analysis with Hallmark gene sets indicated that cells from CIPF WHWTs were enriched for processes known to be associated with fibrosis including "epithelial mesenchymal transition (EMT)" (Figure 5B) and "angiogenesis" (Figure 5C) (NES of 1.86 and 1.88; FDR *q*-value = 0.039 and 0.068, respectively). Genes associated with these 2 gene sets and overexpressed in CIPF dogs included *VIM* (encoding vimentin), *FN1*, *SPP1*, *THY1* (encoding Thy-1 cell surface antigen, *CD90*) for "EMT" gene set and *SPP1*, *VCAN* (encoding large fibroblast proteoglycan) and *S100A4* (encoding S100 calcium binding protein A4) for "angiogenesis" gene set (Supplementary Table 6).

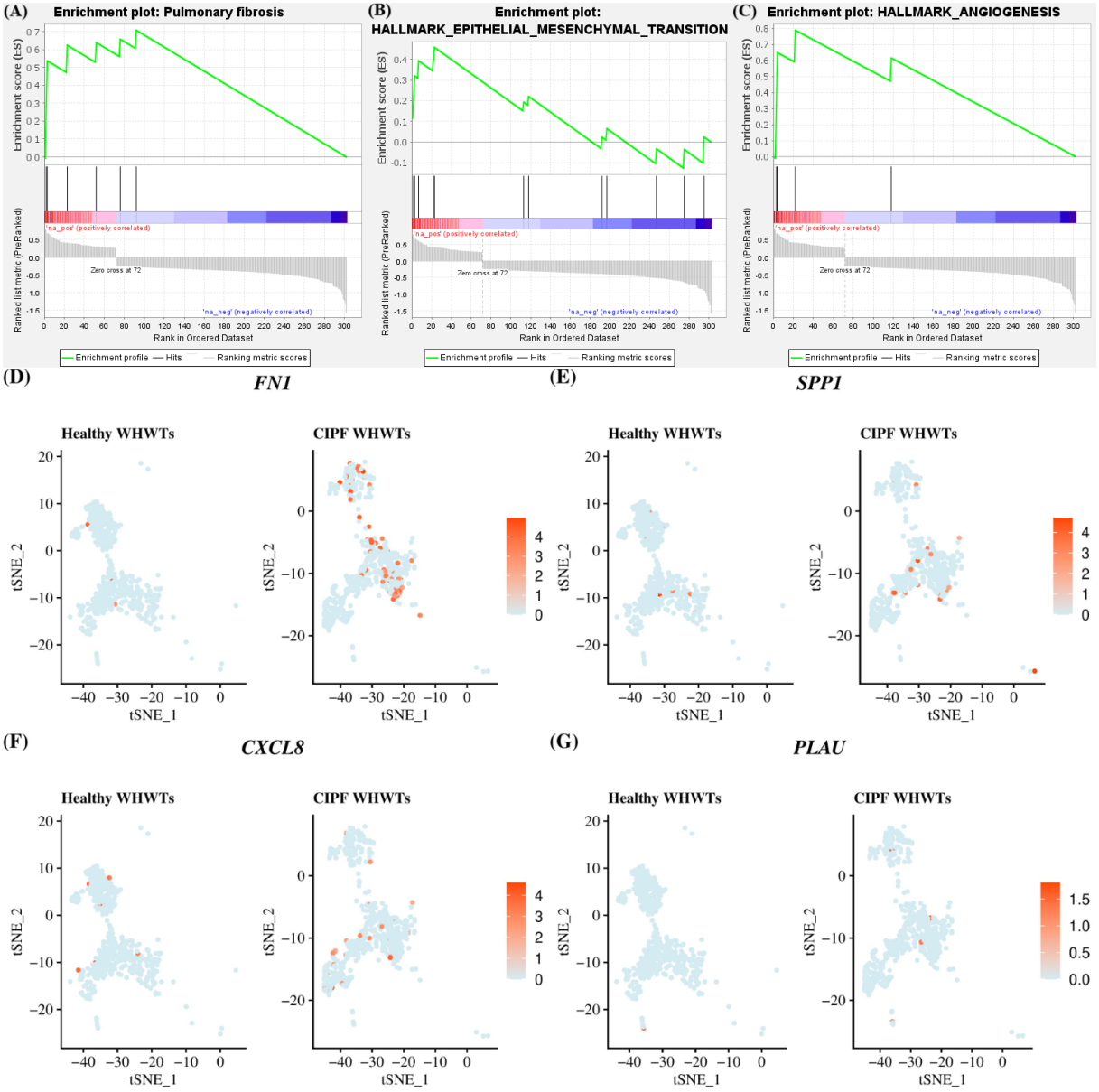

Figure 5. *M1 macrophages/monocytes cluster enrichment in pulmonary fibrosis processes in CIPF compared with healthy dogs. (A-C) Gene set enrichment analyses in M1 cluster between differentially expressed genes in West Highland white terriers (WHWTs) affected with canine idiopathic pulmonary fibrosis (CIPF) compared to healthy WHWTs and the Comparative Toxicogenomics Database Pulmonary fibrosis gene set and epithelial mesenchymal transition and angiogenesis Hallmark gene sets. (D-G) T-distributed stochastic neighbour embedding (t-SNE) plot of cluster M1 cells showing overexpressed genes in CIPF compared with healthy WHWTs, associated with pulmonary fibrosis according to the Comparative Toxicogenomics Database Pulmonary fibrosis gene set. Colour represents the average expression of the indicated genes.*

Discussion

In this study, we analysed Ma/Mo clusters in the BALF from healthy WHWTs compared with WHWTs affected with CIPF. Five Ma/Mo clusters were identified. Among them, we described a cluster of monocytes present in larger proportion in CIPF WHWTs than in healthy WHWTs. Expression of cells in this cluster was enriched for pulmonary fibrosis processes and 8 genes associated with fibrosis were overexpressed in this cluster including *CCL2, SPP1, FN1, CCL3, TIMP1, IL1RN, CXCL8* and *CCL4.* We also identified a cluster of monocyte-derived macrophages enriched for inflammatory and pulmonary fibrosis processes in which the gene expression differed between CIPF and healthy WHWTs with an enrichment for pulmonary fibrosis but also EMT and angiogenesis processes. We identified 4 overexpressed genes associated with pulmonary fibrosis processes in CIPF compared with healthy dogs in this cluster including *FN1, SPP1, CXCL8* and *PLAU.*

In this study, similar cell populations and clusters were identified compared with previously published data on scRNA-seq analysis in BALFs from healthy dogs and included Ma/Mo, T cells either $CD8^+$ or $CD8^-CD4^-$, DCs either mature or immature, neutrophils, B cells, epithelial cells, mast cells and cycling cells (Fastrès et al., 2020b). We were not able to differentiate between ciliated and non-ciliated epithelial cells which can be due to either the low proportion or the absence of ciliated epithelial cells in our samples (Nelson and Couto, 2020) as rare cell populations may be missed using scRNA-seq (See *et al.*, 2018). As already reported (Fastrès et al., 2020b), eosinophils were not identified using scRNA-seq, probably secondary to their RNase content conducting to the degradation of mRNAs in those cells (Sattasathuchana and Steiner, 2014).

In healthy conditions, lung macrophages are known to be extremely heterogeneous and play a crucial role in the regulation of the homeostasis of the lung. In addition to their immune defence function, they also exerted an indispensable role in organ development, maintenance of homeostasis and repair (Ji and Fan, 2019; Puttur *et al.*, 2019). In the lung, the majority of the macrophages are AMs which are resident and self-renewing macrophages (Puttur *et al.*, 2019). They have been identified in this study by their expression of *MARCO* and corresponded to cells of cluster M0 and M3 (Gibbings *et al.*, 2015; Puttur *et al.*, 2019; Fastrès et al., 2020b). In inflammatory conditions, the lung is rapidly infiltrated by recruited monocytes which gradually differentiate into monocyte-derived macrophages and then AMs (Puttur *et al.*, 2019). Here, we observed a higher proportion of monocytes (cells from cluster M2) in CIPF dogs that are probably recruited secondary to lung fibrosis in higher proportion than in healthy dogs. This increased number of macrophages and myeloid cells was also reported as an early event in bleomycin-induced lung fibrosis mouse model (Peyser *et al.*, 2019). As M2 cluster cells were enriched in pulmonary fibrosis processes, we suggest that their increased

proportion in CIPF condition could participate to the onset and/or to the perpetuation of the fibrosis process in WHWTs.

The Ma/Mo involved in pro-fibrotic processes in this study can be considered as immature macrophages as they were identified as either monocyte-derived macrophages (cluster M1) or monocytes (cluster M2). Recently, transcriptomic profiling of macrophages collected over the time course of bleomycin induced fibrosis showed that during monocyte maturation, genes linked to fibrosis are most highly expressed during their differentiation and progressively downregulated with the maturation of the cells into AMs (Misharin *et al.*, 2017). This is in line with results obtained in this study and suggests that recently recruited macrophages (clusters M1 and M2) have greater fibrotic capacity than mature AMs (clusters M0 and M3). Targeting those particularly pro-fibrotic recruited immature macrophage clusters could be a potential novel strategy for the prevention and the therapy of CIPF.

DEGs between healthy and CIPF WHWTs were essentially found in the M1 cluster. Moreover, M1 cells in CIPF dogs were enriched for EMT, angiogenesis and pulmonary fibrosis processes. EMT is considered as one of the phenomena by which collagen-producing fibroblasts and myofibroblasts accumulate, creating a pro-fibrotic environment (Salton, Volpe and Confalonieri, 2019). Indeed, epithelial cells differentiate to acquire features of mesenchymal cells including invasion, migration and production of extracellular matrix (Salton, Volpe and Confalonieri, 2019). Altered EMT process is the most widely accepted pathogenetic mechanism in IPF patient (Salton, Volpe and Confalonieri, 2019) and could also participate in the development of CIPF as suggested by this study. Angiogenesis is another well-known mechanism involved in IPF, which is targeted by Nintedanib, an anti-angiogenesis molecule used in human for its properties against the vascular endothelial growth factor (VEGF) pathway (Rivera-ortega *et al.*, 2018). Involvement of angiogenesis in CIPF has only been assessed through the measurement of VEGF concentration in serum without results (Roels *et al.*, 2015a). To the authors' best knowledge, none of the molecules identified in the present study and linked to angiogenesis has been studied in CIPF.

Among genes found to be associated with pulmonary fibrosis processes, only *CCL2* and *CXCL8* have already been associated with CIPF (Clercx, Fastrès and Roels, 2018). Indeed, it has been shown that mRNA expression of *CXCL8* and *CCL2* was increased in CIPF lungs compared with controls (Clercx, Fastrès and Roels, 2018). Moreover, *CCL2* and *CXCL8* chemokine concentrations were increased in CIPF WHWTs compared with healthy WHWTs in both serum and BALF and only in BALF respectively (Clercx, Fastrès and Roels, 2018). The osteopontin (*SPP1* gene) is a glycoprotein secreted by numerous cell types including macrophages which has been proved to be closely related to IPF (Berman *et al.*, 2004; Pardo *et al.*, 2005; Dong and Ma, 2017; Morse *et al.*, 2019; Wang *et al.*, 2019). Indeed, high level of expression and increased BALF protein concentration

have been reported in IPF mouse models but also in IPF patients (Pardo *et al.*, 2005). Such findings suggest that osteopontin could be used as a potential biomarker and a therapeutic target for treating fibrotic lung diseases (Dong and Ma, 2017). The fibronectin 1 (*FN1* gene) is a mediator of cell matrix adhesions. It promotes myofibroblast differentiation and is found in abundance in the lungs of IPF patients (Upagupta *et al.*, 2018). *CCL3* and *CCL4*, also known as macrophage inflammatory protein 1-alpha and beta, are chemoattractant cytokines (Capelli *et al.*, 2005; Bhavsar, Miller and Al-Sabbagh, 2015; Lee *et al.*, 2018) suspected to play a role in sustaining inflammation and the chronic course of IPF by recruiting inflammatory cells such as neutrophils (Capelli *et al.*, 2002; Capelli *et al.*, 2005; Lee *et al.*, 2018). Their expression in CIPF dogs could be related to the higher rate of neutrophils found in the BALF of CIPF compared to healthy dogs. The tissue inhibitor of metalloproteinase 1 (*TIMP-1* gene) probably contributes, through its control of matrix metalloproteinase catalytic activity, to provide a non-degrading fibrillar collagen microenvironment in IPF patient as well as in IPF mouse model (Selman *et al.*, 2000; Pardo *et al.*, 2016). It has also a potential value as biomarker in patients with IPF (Todd *et al.*, 2020). The interleukin-1 receptor antagonist (encoding *IL-1RA*) is a cytokine produced by alternatively activated AMs. The protein level was increased in IPF patients compared with healthy volunteers (Stahl *et al.*, 2013; Schupp *et al.*, 2015) and in patients with acute exacerbation of IPF compared with stable IPF patients suggesting that this protein could be of interest as diagnostic and prognostic marker (Schupp *et al.*, 2015). The role of the plasminogen activator urokinase (*PLAU* gene) in pulmonary fibrosis is not clear. The protein level has been showed to be low in BALF of IPF patient (Günther *et al.*, 2000; Schuliga *et al.*, 2018) and the molecule was showed to be protective against fibrosis development in IPF mouse model (Navaratnam *et al.*, 2014). Recently, the protective role of the plasminogen activator was controverted as its presence was associated with increased plasmin formation which in turn activates structural and inflammatory cells driven fibrosis (Schuliga *et al.*, 2018). *PLAU* overexpression in this study indicates that fibrinolytic processes are present in CIPF dogs. Whether it is protective or not remains unclear. Further studies are needed to better assess the potential role of all these molecules in CIPF pathogenesis and their utility as biomarkers of disease progression and as potential therapeutic target.

The present study had some limitations. First, the analysis of scRNA-seq data remains limited by the poor annotation of canine genomic dataset highlighting the need for further studies to optimize the use of this technique in healthy and diseased dogs. Indeed, the percentage of reads mapped confidently to the transcriptome had to be from at least 30% (10X Genomics, 2020), which is not the case in this study. Secondly, our study involved a relatively low number of dogs either healthy or affected with CIPF. Indeed, even if the transcriptomic profiling costs are falling, the use of the scRNA-seq remains currently quite expensive. However, even with this small number of subjects and with the lack of annotation of the canine genome, we were able to identify the different cell populations, their genes expression and their DEGs in CIPF condition. We were also able to detect the

genes already identified as involved in CIPF such as *CXCL8* and *CCL2*. Finally, it should be noted that in some Ma/Mo clusters, DEGs included markers normally expressed by other cell types, mainly in M4 cluster which expressed Ma/Mo and T cells markers. This likely results from contamination from ambient RNA released during BALF processing. This contamination is a known limitation that can occur in scRNA-seq experiments (Zheng *et al.*, 2017; Hwang, Lee and Bang, 2018). Another explanation would be that these cells are in fact doublets. Doublets are a known confounding factor in scRNA-seq analysis (Ilicic *et al.*, 2016) that can be reduced by decreasing cell number introduced in the Chromium™ Controller (Bloom, 2018) and by filtering out cells with a really high gene count (Ilicic *et al.*, 2016) as it was done in this study.

Conclusion

Using scRNA-seq in BALF specimens from healthy WHWTs and WHWTs affected with CIPF, we were able to reveal the presence of pro-fibrotic monocytes, more abundant in CIPF than in healthy WHWTs, reflecting the inflammation that occurs in fibrotic lung. The presence of those monocytes enriched with pro-fibrotic genes probably participates to the onset and/or the perpetuation of CIPF in WHWTs. Moreover, monocyte-derived macrophages enriched in pro-fibrotic genes in CIPF compared with healthy WHWTs were also identified. This cluster was also enriched with EMT and angiogenesis processes, which are known to play an important role in IPF.

The results of that study offer promise for the better understanding of the role of macrophages in CIPF pathogenesis and the identification of new biomarkers and therapeutic targets to better diagnose, follow and treat the disease.

Acknowledgments

The authors thanks Albert Belinda, Romijn Sylvain, and Kim-Thu Phan for their assistance in dog's contention and samples obtention.

References

10X Genomics. (2020). Troubleshooting Cell Ranger. Available at: https://support.10xgenomics.com/single-cell-gene-expression/software/pipelines/latest/troubleshooting#alerts (Accessed: 16 March 2020).

Alcover A., Alarcon B. and Di Bartolo V. (2018). Cell biology of T-cell receptor expression and regulation. Annual Review of Immunology, 36, pp. 103–125. doi: 10.1146/annurev-immunol042617-053429.

Ammon C., Meyer S.P., Schwarzfischer L., Krause S.W., Andreesen R., Kreutz M. (2000). Comparative analysis of integrin expression on monocyte-derived macrophages and monocyte-derived dendritic cells. Immunology, 100, pp. 364–369. doi: 10.1046/j.1365-2567.2000.00056.x.

Aran D., Looney A.P., Liu L., Wu E., Fong V., Hsu A., et al. (2019). Reference-based analysis of lung single-cell sequencing reveals a transitional profibrotic macrophage. Nature Immunology, 20, pp. 63–72. doi: 10.1038/s41590-018-0276-y.

Berman J.S., Serlin D., Li X., Whitley G., Hayes J., Rishikof D.C., et al. (2004). Altered bleomycin-induced lung fibrosis in osteopontin-deficient mice. American Journal of Physiology-Lung Cellular and Molecular Physiology, 286, pp. 1311–1138. doi: 10.1152/ajplung.00394.2003.

Bharat A., Bhorade S., Morales-Nebreda L., McQuattie-Pimentel A., Soberanes S., Ridge K., et al. (2016). Flow cytometry reveals similarities between lung macrophages in humans and mice. American Journal of Respiratory Cell and Molecular Biology, 54, pp. 147–149. doi: 10.1017/CBO9781107415324.004.

Bhavsar I., Miller C.S. and Al-Sabbagh M. (2015). Macrophage inflammatory protein-1 alpha (MIP-1 alpha)/CCL3: as a biomarker. In: Preedy V.R., Patel V.B. (eds). General methods in biomarker research and their applications. Dordrecht, The Netherlands, pp. 223–249. doi: 10.1007/978-94-007-7696-8_27.

Bloom J.D. (2018). Estimating the frequency of multiplets in single-cell RNA sequencing from cell-mixing experiments. PeerJ, 6, 5578. doi: 10.7717/peerj.5578.

Byrne A.J., Powell J.E., Sullivan B.J.O., Ogger P.P., Hoffland A., Cook J,. et al. (2020). Dynamics of human monocytes and airway macrophages during healthy aging and after transplant. Journal of Experimental Medicine, 217, e20191236. doi: 10.1084/jem.20191236.

Capelli A., Di Stefano A., Gnemmi I., Donner C.F. (2005). CCR5 expression and CC chemokine levels in idiopathic pulmonary fibrosis. European Respiratory Journal, 25, pp. 701–707. doi: 10.1183/09031936.05.00082604.

Capelli A., Di Stefano A., Lusuardi M., Gnemmi I., Donner C.F. (2002). Increased macrophage inflammatory protein-1a and macrophage inflammatory protein-1b levels in bronchoalveolar lavage fluid of patients affected by different stages of pulmonary sarcoidosis. American Journal of Respiratory and Critical Care Medicine, 165, pp. 236–241. doi: 10.1164/rccm2106084.

Clercx C., Fastrès A. and Roels E. (2018). Idiopathic pulmonary fibrosis in the West Highland white terrier: an update. Veterinary Journal, 242, 53–58. doi: 10.1016/j.tvjl.2018.10.007.

Croxford A.L., Lanzinger M., Hartmann F.J., Schreiner B., Mair F., Pelczar P., et al. (2015). The cytokine GM-CSF drives the inflammatory signature of CCR2+ monocytes and licenses autoimmunity. Immunity, 43, pp. 502–514. doi: 10.1016/j.immuni.2015.08.010.

Cunningham F., Achuthan P., Akanni W., Allen J., Amode M.R., Armean I.M., et al. (2019). Ensembl 2019. Nucleic Acids Research, 47, pp. 745–751. doi: 10.1093/nar/gky1113.

Davis A.P., Grondin C.J., Johnson R.J., Sciaky D., McMorran R., Wiegers J., et al. (2019). The comparative toxicogenomics database: update 2019. Nucleic Acids Research, 47, pp. 948–954. doi: 10.1093/nar/gky868.

Dong J. and Ma Q. (2017) Osteopontin enhances multi-walled carbon nanotube-triggered lung fibrosis by promoting TGF- β1 activation and myofibroblast differentiation. Particle and Fibre Toxicology, 14, 18. doi: 10.1186/s12989-017-0198-0.

Fastrès A., Pirottin D., Fievez L., Marichal T., Desmet C.J., Bureau F., et al. (2020b). Characterization of the bronchoalveolar lavage fluid by single cell gene expression analysis in healthy dogs: a promising technique. Frontiers in Immunology, 11, 1707. doi: 10.3389/fimmu.2020.01707.

Gautier E.L., Shay T., Miller J., Greter M., Jakubzick C., Ivanov S., et al. (2012). Gene-expression profiles and transcriptional regulatory pathways that underlie the identity and diversity of mouse tissue macrophages. Nature Immunology, 13, pp. 1118–1128. doi: 10.1038/ni.2419.

Gibbings S.L., Goyal R., Desch A.N., Leach S.M., Prabagar M., Atif S.M., et al. (2015). Transcriptome analysis highlights the conserved difference between embryonic and

postnatal-derived alveolar macrophages. Blood, 126, pp. 1357–1366. doi: 10.1182/blood-2015-01-624809.

Gibbings S.L., Thomas S.M., Atif S.M., Mccubbrey A.L., Desch A.N., Danhorn T., et al. (2017). Three Unique interstitial macrophages in the murine lung at steady state. American Journal of Respiratory Cell and Molecular Biology, 57, pp. 66–76. doi: 10.1165/rcmb.2016-0361OC.

Gokey J.J., Snowball J., Sridharan A., Speth J.P., Black K.E., Hariri L.P., et al. (2018). MEG3 is increased in idiopathic pulmonary fibrosis and regulates epithelial cell differentiation. JCI Insight, 3, e122490. doi: 10.1172/jci.insight.122490.

Gundra U.M., Girgis N.M., Ruckerl D., Jenkins S., Ward L.N., Kurtz Z.D., et al. (2014). Alternatively activated macrophages derived from monocytes and tissue macrophages are phenotypically and functionally distinct. Blood, 123, pp.110–122. doi: 10.1182/blood-2013-08-520619.

Günther A., Mosavi P., Ruppert C., Heinemann S., Temmesfeld B., Velcovsky H.G., et al. (2000). Enhanced tissue factor pathway activity and fibrin turnover in the alveolar compartment of patients with interstitial lung disease. Thrombosis and Haemostasis, 83, pp. 853–60. doi: 10.1055/s-0037-1613933.

Heikkila-Laurila H.P. and Rajamaki M.M. (2014). Idiopathic pulmonary fibrosis in West Highland white terriers. Veterinary Clinics of North America: Small Animal Practice, 44, pp. 129–142. doi: 10.1016/j.cvsm.2013.08.003.

Hwang B., Lee J.H. and Bang D. (2018). Single-cell RNA sequencing technologies and bioinformatics pipelines. Experimental & Molecular Medicine, 50, 96. doi: 10.1038/s12276-018-0071-8.

Ilicic T., Kim J.K., Kolodziejczyk A.A., Bagger F.O., McCarthy D.J., Marioni J.C., et al. (2016). Classification of low-quality cells from single-cell RNA-seq data. Genome Biology, 17, 29. doi: 10.1186/s13059-016-0888-1.

Ji J. and Fan J. (2019). Discovering myeloid cell heterogeneity in the lung by means of next generation sequencing. Military Medical Research, 6, 33. doi: 10.1186/s40779-019-0222-9.

Joshi N., Watanabe S., Verma R., Jablonski R.P., Chen C., Cheresh P., et al. (2020). A spatially restricted fibrotic niche in pulmonary fibrosis is sustained by M-CSF/M-CSFR signalling in monocyte-derived alveolar macrophages. European Respiratory Journal, 55, 1900646. doi: 10.1183/13993003.00646-2019.

Laurila H.P. and Rajamäki M.M. (2020). Update on canine idiopathic pulmonary fibrosis in West Highland white terriers. Veterinary Clinics of North America: Small Animal Practice, 50, 431–46. doi: 10.1016/j.cvsm.2019.11.004.

Lee J., Arisi I., Puxeddu E., Mramba L.K., Amicosante M., Swaisgood C.M., et al. (2018). Bronchoalveolar lavage (BAL) cells in idiopathic pulmonary fibrosis express a complex pro-inflammatory, pro-repair, angiogenic activation pattern, likely associated with macrophage iron accumulation. PloS One, 13, e0194803. doi: 10.1371/journal.pone.0194803.

Misharin A.V., Morales-Nebreda L., Reyfman P.A., Cuda C.M., Walter J.M., McQuattie-Pimentel A.C., et al. (2017). Monocyte-derived alveolar macrophages drive lung fibrosis and persist in the lung over the life span. Journal of Experimental Medicine, 214, pp. 2387–2404. doi: 10.1084/jem.20162152.

Morse C., Tabib T., Sembrat J., Buschur K.L., Bittar H.T., Valenzi E., et al. (2019). Proliferating SPP1/MERTK-expressing macrophages in idiopathic pulmonary fibrosis. European Respiratory Journal, 54, 1802441. doi: 10.1183/13993003.02441-2018.

Navaratnam V., Fogarty A.W., McKeever T., Thompson N., Jenkins G., Johnson S.R., et al. (2014). Presence of a prothrombotic state in people with idiopathic pulmonary fibrosis: A population-based case-control study. Thorax, 69, 207–215. doi: 10.1136/thoraxjnl-2013-203740.

Nelson W.R. and Couto C.G. (2020). Diagnostic tests for the lower respiratory tract. In: Nelson W.R., Couto C.G. (eds). Small animal internal medicine, 6th edition. Elsevier. St Louis, Missouri, pp. 287–320.

Pardo A., Cabrera S., Maldonado M., Selman M. (2016). Role of matrix metalloproteinases in the pathogenesis of idiopathic pulmonary fibrosis. Respiratory Research, 17, 23. doi: 10.1186/s12931-016-0343-6.

Pardo A., Gibson K., Cisneros J., Richards T.J., Yang Y., Becerril C., et al. (2005). Up-regulation and profibrotic role of osteopontin in human idiopathic pulmonary fibrosis. PloS Medicine, 2, e251. doi: 10.1371/journal.pmed.0020251.

Patel V.I. and Metcalf J.P. (2019). Airway macrophage and dendritic cell subsets in the resting human lung. Critical Reviews in Immunology, 38, pp. 303–331. doi: 10.1615/CritRevImmunol.2018026459.

Peyser R., MacDonnell S., Gao Y., Cheng L., Kim Y., Kaplan T., et al. (2019). Defining the activated fibroblast population in lung fibrosis using single-cell sequencing. American Journal of Respiratory Cell and Molecular Biology, 61, pp. 74–85. doi: 10.1165/rcmb.2018-0313OC.

Poczobutt J.M. and Eickelberg O. (2019). Defining the cell types that drive idiopathic pulmonary fibrosis using single-cell. American Journal of Respiratory and Critical Care Medicine, 199, pp. 1454–1456. doi: 10.1164/rccm.201901-0197ED.

Puttur F., Gregory L.G., Lloyd C.M., Fleming S.A. (2019). Airway macrophages as the guardians of tissue repair in the lung. Immunology & Cell Biology, 97, pp. 246–257. doi: 10.1111/imcb.12235.

Reyfman P.A., Walter J.M., Joshi N., Anekalla K.R., Mcquattie-pimentel A.C., Chiu S., et al. (2019). Single-cell transcriptomic analysis of human lung provides insights into the pathobiology of pulmonary fibrosis. American Journal of Respiratory and Critical Care Medicine, 199, pp. 1517–1536. doi: 10.1164/rccm.201712-2410OC.

Rivera-Ortega P., Hayton C., Blaikley J., Leonard C., Chaudhuri N. (2018). Nintedanib in the management of idiopathic pulmonary fibrosis: clinical trial evidence and real-world experience. Therapeutic Advances in Respiratory Disease, 12, 1753466618800618. doi: 10.1177/1753466618800618.

Roels E., Krafft E., Antoine N., Farnir F., Laurila H.P., Holopainen S., et al. (2015). Evaluation of chemokines CXCL8 and CCL2, serotonin, and vascular endothelial growth factor serum concentrations in healthy dogs from seven breeds with variable predisposition for canine idiopathic pulmonary fibrosis. Research in Veterinary Science, 101, pp. 57–62. doi: 10.1016/J.RVSC.2015.05.020.

Salton F., Volpe M.C. and Confalonieri M. (2019). Epithelial-mesenchymal transition in the pathogenesis of idiopathic pulmonary fibrosis. Medicina, 55, 83. doi: 10.3390/medicina55040083.

Sattasathuchana P. and Steiner M. (2014). Canine eosinophilic gastrointestinal disorders. Animal Health Research Reviews, 15, pp. 76–86. doi: 10.1017/S1466252314000012.

Schuliga M., Grainge C., Westall G., Knight D. (2018). The fibrogenic actions of the coagulant and plasminogen activation systems in pulmonary fibrosis. The International Journal of Biochemistry & Cell Biology, 97, pp. 108–117. doi: 10.1016/j.biocel.2018.02.016.

Schupp J.C., Binder H., Jäger B., Cillis G., Zissel G., Müller-quernheim J., et al. (2015). Macrophage activation in acute exacerbation of idiopathic pulmonary fibrosis. PloS One, 10, e0116775. doi: 10.1371/journal.pone.0116775.

Schyns J., Bai Q., Ruscitti C., Radermecker C., De Schepper S., Chakarov S., et al. (2019). Non-classical tissue monocytes and two functionally distinct populations of interstitial macrophages populate the mouse lung. Nature Communications, 10, 3964. doi: 10.1038/s41467-019-11843-0.

See P., Lum J., Chen J., Ginhoux F. (2018). A Single-cell sequencing guide for immunologists. Frontiers in Immunology, 9, 2425. doi: 10.3389/fimmu.2018.02425.

Selman M., Ruiz V., Cabrera S., Segura L., Ramirez R., Barrios R., et al. (2000). TIMP-1, -2, -3, and -4 in idiopathic pulmonary fibrosis. A prevailing nondegradative lung microenvironment? American Journal of Physiology-Lung Cellular and Molecular Physiology, 279, pp. 562–574. doi: 10.1152/ajplung.2000.279.3.L562.

Stahl M., Schupp J., Jaǧer B., Schmid M., Zissel G., MuẄller-Quernheim J., et al. (2013). Lung collagens perpetuate pulmonary fibrosis via CD204 and M2 macrophage activation. PloS One, 8, e81382. doi: 10.1371/journal.pone.0081382.

Stifano G. and Christmann R.B. (2016). Macrophage involvement in systemic sclerosis: do we need more evidence? Current Rheumatology Reports, 18, 2. doi: 10.1007/s11926-015-0554-8.

Stuart T., Butler A., Hoffman P., Hafemeister C., Papalexi E., Mauck III W.M., et al. (2019). Comprehensive integration of single-cell data. Cell, 177, pp. 1888–1902. doi: 10.1016/j.cell.2019.05.

Stuart T. and Satija R. (2019). Integrative single-cell analysis. Nature Reviews Genetics, 20, pp. 257–272. doi: 10.1038/s41576-019-0093-7.

Subramanian A., Tamayo P., Mootha V.K., Mukherjee S., Ebert B.L., Gillettea M.A., et al. (2005). Gene set enrichment analysis: A knowledge-based approach for interpreting genome-wide expression profiles. Proceedings of the National Academy of Sciences, 102, pp. 15545–15550. doi: 10.1073/pnas.0506580102.

Todd J.L., Vinisko R., Liu Y., Neely M.L., Overton R., Flaherty K.R., et al. (2020). Circulating matrix metalloproteinases and tissue metalloproteinase inhibitors in patients with idiopathic

pulmonary fibrosis in the multicenter IPF-PRO Registry cohort. BMC Pulmonary Medicine, 20, 64. doi: 10.1186/s12890-020-1103-4.

Tsukui T., Sun K.H., Wetter J.B., Wilson-Kanamori J.R., Hazelwood L.A., Henderson N.C., et al. (2020). Collagen-producing lung cell atlas identifies multiple subsets with distinct localization and relevance to fibrosis. Nature Communications, 11, 1920. doi: 10.1038/s41467-020-15647-5.

Upagupta C., Shimbori C., Alsilmi R., Kolb M. (2018). Matrix abnormalities in pulmonary fibrosis. European Respiratory Review, 27, 180033. doi: 10.1183/16000617.0033-2018.

Wang H., Wang M., Xiao K., Zhang X., Wang P., Qi H., et al. (2019). Bioinformatics analysis on differentially expressed genes of alveolar macrophage in IPF. Experimental Lung Research, 45, pp. 288–296. doi: 10.1080/01902148.2019.1680765.

Xie T., Wang Y., Deng N., Huang G., Taghavifar F., Geng Y., et al. (2018). Single-cell deconvolution of fibroblast heterogeneity in mouse pulmonary fibrosis. Cell Reports, 22, pp. 3625–3640. doi: 10.1016/j.celrep.2018.03.010.

Xu Y., Mizuno T., Sridharan A., Du Y., Guo M., Tang J., et al. (2016). Single-cell RNA sequencing identifies diverse roles of epithelial cells in idiopathic pulmonary fibrosis. JCI Insight, 1, e90558. doi: 10.1172/jci.insight.90558.

Yu Y.R.A., Hotten D.F., Malakhau Y., Volker E., Ghio A.J., Noble P.W., et al. (2016). Flow cytometric analysis of myeloid cells in human blood, bronchoalveolar lavage, and lung tissues. American Journal of Respiratory Cell and Molecular Biology, 54, pp. 13–24. doi: 10.1165/rcmb.2015-0146OC.

Zhang Y., Jiang M., Nouraie M., Roth M.G., Tabib T., Winters S., et al. (2019). GDF15 is an epithelial-derived biomarker of idiopathic pulmonary fibrosis. American Journal of Physiology-Lung Cellular and Molecular Physiology, 317, pp. 510–521. doi: 10.1152/ajplung.00062.2019.

Zheng G.X.Y., Terry J.M., Belgrader P., Ryvkin P., Bent Z.W., Wilson R., et al. (2017). Massively parallel digital transcriptional profiling of single cells. Nature Communications, 8, 14049. doi: 10.1038/ncomms14049.

Supplemental material

The Supplementary Material for this article can be found online at: https://www.frontiersin.org/articles/10.3389/fimmu.2020.611749/full#supplementary-material.

The datasets presented in this study can be found in online repositories. The names of the repository/repositories and accession number(s) can be found below: https://www.ebi.ac.uk/arrayexpress/, E-MTAB-9623.

Discussion - Perspectives

Discussion - Perspectives

In this work we firstly aimed to characterize the LM in dogs and to describe alterations of the LM especially in WHWTs affected with CIPF.

The LM was poorly studied in dogs at the beginning of this work as stated in the introduction. Therefore, our first objective was to describe the LM in healthy dogs and to identify the parameters able to alter it before assessing LM modifications associated with CIPF. In healthy conditions, we were able to confirm that the LM is quite stable in adult dogs (Study 2), as already reported by Ericsson and colleagues (2016). It is not surprising since the stability of the LM in adults has also been confirmed in men, mice and rats (Barfod *et al.*, 2015; Dickson *et al.*, 2015; Finn *et al.*, 2018). By regrouping reports common to all studies published on the LM in healthy dogs, including ours (Study 1 and study 2), comprising a total of 88 dogs (37 experimental beagles and 51 client-owned dogs from different breeds), we postulated that the core LM in dogs (bacteria common for all healthy dogs) was composed by four major phyla including Proteobacteria, Actinobacteria, Firmicutes and Bacteroidetes and included at least *Cutibacterium*, *Streptococcus*, *Acinetobacter* and *Pseudomonas* genera (Ericsson *et al.*, 2016; Roels *et al.*, 2017c; Fastrès *et al.*, 2017b).

Predictable modifications of the LM were encountered after oral antimicrobial drug administration in healthy dogs (Study 1), an effect previously reported in mice and rats (Barfod *et al.*, 2015; Dickson *et al.*, 2018; Finn *et al.*, 2019). The majority of the changes induced by antimicrobial drug administration returned to normal within approximatively 2 weeks after the drug discontinuation indicating that a wash-out period of 2 weeks should be sufficient to avoid antimicrobial drug effect on the LM in dogs. However, in our study, we used AC, an antimicrobial drug commonly used as first-line antibiotic in dogs with lower respiratory disease, and it should be remembered that the use of another antimicrobial drug in diseased dogs could have a different effect and duration on microbial communities. We also showed that differences in dogs' living conditions were associated with alterations of the LM (Study 2). Indeed, LM clustered separately between experimental and domestic living conditions. An environmental impact on the LM is not surprising as the LM is suspected to largely result from bacterial immigration (microaspiration, bacterial inhalation, and direct mucosal dispersion) (Dickson *et al.*, 2016). Differences in the type of food by affecting the gut microbial composition can then alter lung bacteria due to microaspirations. Moreover, the housing conditions and the geographical area impact the bacterial composition of inhaled air (Gleeson, Eggli and Maxwell, 1997; Dickson *et al.*, 2016; Dickson, Erb-Downward, *et al.*, 2017; Huang *et al.*, 2020). Indeed, bacterial communities of indoor area were shown to be affected by outdoor factors such as vegetation, urbanization and airborne particulate matter (Weikl *et al.*, 2016). Differences reported in LM between dogs from the same breed but living in different countries also tend to confirm that geographic position of the dogs, and more globally their environment, have an impact on the LM

(Ericsson *et al.*, 2016; Fastrès, *et al.*, 2017b; Fastrès *et al.*, 2019; Fastrès *et al.*, 2020a). Of note, differences in the LM of experimental beagles reported between the study from Ericsson and colleagues (2016) and our results (Study 1 and study 2) could also come from differences in procedures both to obtain the samples and to analyse the LM (Beck, 2014; Marsh *et al.*, 2018; Boers, Jansen and Hays, 2019). Increased standardization of studies on LM in dogs but also in other species would be beneficial to allow results from such studies to be compared with more confidence. Finally, we showed a mild but significant impact of the breed on the LM (Study 2).

We then investigated changes of the LM in an acute pulmonary disease and validated the use of the 16S rDNA amplicon sequencing technique to identify bacteria in canine lung infection (Study 3). In dogs with confirmed *B. bronchiseptica* pulmonary infection, a dysbiosis of the LM was observed. Indeed, we described a shift in the β-diversity with an increase in bacterial load associated with a decrease in α-diversity and richness. LM was dominated by one or two bacteria which mainly corresponded to *B. bronchiseptica* and *M. cynos*, a common co-infective bacterium found in CIRC-D (Priestnall *et al.*, 2014; Maboni *et al.*, 2019). Similar changes in the LM were also reported in acute respiratory diseases in other dogs and men (Dickson, Erb-Downward and Huffnagle, 2014; Dickson *et al.*, 2016; Vientós-plotts *et al.*, 2019). In our study, other bacteria present in a relative abundance of more than 5% and considered as potentially co-infective were also identified. Some were already described in CIRC-D like other *Mycoplasma* species (Viitanen, Lappalainen and Rajamäki, 2015; Decaro *et al.*, 2016) and *Pseudomonas* sp. (Ford, 2012), and others were reported as pathogen in pneumonia in dogs and/or in men like *Stenotrophomonas* sp., *Ureaplasma* sp., *Escherichia-Shigella* sp. and *Elizabethkingia meningoseptica* (Chalker, 2005; Jean *et al.*, 2014; Rheinwald *et al.*, 2015; Johnson *et al.*, 2016; Lappin *et al.*, 2017; Vientós-plotts *et al.*, 2019). Although it is not clear whether those bacteria were just colonizing or co-infective, they could have had an impact on disease progression and response to treatment. Indeed, in CIRD-C, more severe and chronic clinical signs have been associated with the presence of co-infections (Maboni *et al.*, 2019), and our diseased population included referral cases with median clinical signs duration of 1 month. Finally, a good agreement was found between results obtained with 16S rDNA amplicon sequencing and traditional techniques used to diagnose pulmonary infections in dogs such as culture and qPCR. Such agreement was also reported by Vientós-plotts and colleagues (2019). Taken together, results of this study revealed the benefit of the use of 16S rDNA amplicon sequencing to find new potential pathogens as well as rare and slow-growing bacteria. More generally, this technique shows a more global vision of all bacterial changes which could help clinicians, in complement with conventional bacterial detection techniques, to guide antimicrobial drugs and to predict disease outcomes and response to treatment as established in human acute respiratory disorders (Woo *et al.*, 2008; Dickson *et al.*, 2017b; Johansson *et al.*, 2019; Vientós-plotts *et al.*, 2019; Dickson *et al.*, 2020). Indeed, in human with pneumonia and parapneumonic effusions, for example, the percentage of bacterial detection was significantly higher

using 16S rDNA amplicon sequencing compared to conventional culture (Johansson *et al.*, 2019). In the majority of the cases, the same organism was identified by both techniques as it was the case in our study and in the study from Vientós-plotts and colleagues (2019). In addition, in ARDS and critically ill patients, some LM parameters like the detection of bacteria commonly associated with the gut (e.g., species of the Lachnospiraceae, Bacteroidaceae and Enterobacteriaceae families) and the increase in lung bacterial load have been associated with systemic inflammation and poorer outcomes (Dickson *et al.*, 2017; Dickson *et al.*, 2020).

In CIPF dogs, we found that LM alterations are more likely associated with the breed than with the disease (Study 2). Except for the identification of *Brochothrix* and *Pseudarcicella* as discriminant genera, no statistical differences were highlighted between diseased and healthy WHWTs. *Brochothrix*, *Curvibacter*, *Pseudarcicella* and a genus belonging to Flavobacteriaceae family were significantly increased in healthy WHWTs compared with other breeds and higher in CIPF compared with healthy WHWTs but not significantly. As those bacteria are preferentially found as contaminant in food and water (Ding and Yokota, 2010; Kasalický *et al.*, 2013; Hahn *et al.*, 2014; McBride, 2014; Stanborough *et al.*, 2017) and could then be ingested by the dogs and be part of the proximal gut microbiota, we postulated that their presence in CIPF dogs could be related to the higher rate of GER reported in this breed (Määttä *et al.*, 2018). The specific LM found in WHWTs could be associated with their predisposition to CIPF.

In human IPF, a correlation between blood cell transcriptomic profile and the LM was found by using network analysis (Huang *et al.*, 2017; Molyneaux *et al.*, 2017b). For example, overexpression of transcripts involved in bacterial and immune response were associated with higher bacterial load, the presence of specific bacteria such as *Neisseria* and the diagnosis of IPF (Molyneaux *et al.*, 2017b). In addition, the increase abundance of *Streptococcus* was associated with a reduce in expression of immune-response genes and both of these changes correlate with disease progression (Huang *et al.*, 2017). In transplanted lungs, specific changes in the LM were associated with distinct innate cell gene expression profiles. In particular, the presence of specific bacteria was shown to alter macrophage gene expression into pro-inflammatory (e.g., *Staphylococcus* and *Pseudomonas*), or remodelling profiles (e.g., *Prevotella* and *Streptococcus*) (Bernasconi *et al.*, 2016). In this work, we don't explore the association between LM dysbiosis and BALF immune cell expression profile that we assessed in the second part of this work. Indeed, in absence of a clear association between a disturbed LM and the disease, such analysis was considered as not relevant. We think that the LM alterations in CIPF dogs should be assessed in larger independent cohorts of dogs to confirm changes associated with the disease before any further investigations related to the association between specific LM disturbances and specific macrophage polarization. Follow-up studies starting before the onset of the disease, as well as during CIPF course would be required to better assess the role of LM in CIPF predisposition

and progression, as well as its utility as potential diagnostic and/or prognostic biomarker. Such studies however require to screen regularly a large number of apparently healthy ageing WHWTs during a prolonged period of time until they get the disease or die from another cause. Although we started to enrol dogs in the screening and follow-up program, much more cases are needed. Another concern is related to the fact that confirmation of CIPF is challenging, especially in early cases as stated in the introduction. Finally, comparing the LM with the oral microbiota and the proximal gut microbiota in WHWTs could be useful to validate our hypothesis related to increased microaspirations at the origin of the enrichment of water and food bacteria in the LM of WHWTs as a potential trigger of CIPF development and maintenance.

For the second part of this work, we wished to characterize BALF cell populations using an unbiased technique which has never been used in dogs before and to assess the presence of specific pro-fibrotic macrophage clusters in WHWTs affected with CIPF compared with healthy ones.

We first validated the use of the scRNA-seq in the BALF of healthy dogs (Study 4). The use of the scRNA-seq allowed the identification and the description of 14 cell clusters corresponding to 8 different cell populations including Ma/Mo, T cells, neutrophils, DCs, epithelial cells, B cells, mast cells and proliferating cells. Among those populations, only macrophages, T cells, neutrophils, mast cells and epithelial cells were previously described in canine BALF samples by cytology and/or flow cytometry (Dirscherl *et al.*, 1995; Vail, Mahler and Soergel, 1995; Clercx *et al.*, 2002; Out *et al.*, 2002; Spużak *et al.*, 2008; Finke, 2013; Nelson and Couto, 2014). Unfortunately, we were not able to find eosinophils, a cell type commonly found in BALF (Nelson and Couto, 2014). This is probably due to their high content of RNAse able to destroy RNAs preventing their detection by transcriptomic analysis (Sattasathuchana and Steiner, 2014). Cell populations identified by scRNA-seq in healthy canine BALF were similar to cell populations found in healthy human BALF. Indeed, in human, macrophages, neutrophils, T cells, natural killer cells, DCs, B cells, mast cells and epithelial cells have been described in scRNA-seq studies (Morse *et al.*, 2019; Liao *et al.*, 2020). In addition to the identification of new cell populations in canine BALF, the scRNA-seq also allowed to better characterize cells by clustering them based on their transcriptome, measuring DEGs between clusters and deducing their main functions. Indeed, BALF cell clusters were found for Ma/Mo, T cell, DC and epithelial cell populations in dogs. Three clusters of AMs were described, exerting functions in immune defence and response, immune response regulation, and cell homeostasis and detoxification of metal ions, respectively. A fourth macrophagic cluster was found and corresponded to monocytes or monocyte-derived macrophages. Epithelial cells were subdivided into ciliated or non-ciliated cells, T cells into $CD8^+$ and $CD4^-CD8^-$, and DCs into mature and immature DCs. Except for T cells, cell clusters have not yet been investigated in term of transcriptome and principal functions in BALF from

healthy dogs (Dirscherl *et al.*, 1995; Vail, Mahler and Soergel, 1995; Clercx *et al.*, 2002; Out *et al.*, 2002; Spużak *et al.*, 2008; Finke, 2013; Nelson and Couto, 2014). Thanks to this work, we showed that scRNA-seq can be used in canine BALF and could also probably be used in other types of canine samples. We also highlighted the benefit to use scRNA-seq to better analyse cell heterogeneity and functions in an unbiased way. Finally, this canine BALF cell atlas provides an interactive and accessible resource to allow cell specific changes in gene expression exploration, in healthy and diseased lung, which is susceptible to accelerate discovery and translation to other species.

We then investigated macrophage clusters in CIPF compared with healthy WHWTs (Study 5). Indeed, aside from their antimicrobial role, macrophages have been largely involved in the pathogenesis of fibrotic lung diseases and are considered as potent source of profibrotic molecules including TGF-β1, PDGF, FGF, IGF1, VEGF, MMPs, tissue inhibitor of metalloproteinases, chemokines, *etc.* (Kolahian *et al.*, 2016; Desai *et al.*, 2018; Heukels *et al.*, 2019). In IPF mouse models, depletion of Ma/Mo was shown to reduce pulmonary fibrosis, while their adoptive transfer during fibrogenesis was shown to exacerbate fibrosis (Gibbons *et al.*, 2011). Moreover, depending on the cellular and environmental context, macrophages can exert pro-fibrotic and pro-inflammatory effects (Desai *et al.*, 2018; Zhang *et al.*, 2018). Both of these effects can promote fibrosis by preventing ECM degradation, and maintaining tissue inflammation causing alveolar epithelium injuries, respectively (Heukels *et al.*, 2019). In CIPF WHWTs, specific pro-fibrotic macrophage clusters were found in BALF samples overexpressing genes associated with pulmonary fibrosis, angiogenesis and EMT processes. These findings suggest a role for macrophages in CIPF pathogenesis.

In man, specific pro-fibrotic macrophage clusters were also identified by scRNA-seq in IPF patients. In all scRNA-seq studies on IPF, pro-fibrotic macrophage clusters were characterized by overexpression of *SPP1* which was suggested to be the hallmark for pro-fibrotic macrophages in IPF patients (Morse *et al.*, 2019; Reyfman *et al.*, 2019; Adams *et al.*, 2020). Macrophages overexpressing *SPP1* were suggested to have a role in activation of myofibroblasts and ECM development (Morse *et al.*, 2019; Adams *et al.*, 2020). Reports of studies in lung tissue of fibrosis mouse models, in which *SPP1* expression and protein level were increased, support the role for SPP1 in the ECM production and hence the fibrosis development in the lung (Takahashi *et al.*, 2001; Berman *et al.*, 2004; Dong and Ma, 2017). Indeed, in lung fibrosis mouse models, deletion of *SPP1* was shown to reduce upregulated expression of *FN1* and collagen type 1, two major proteins involved in the formation and the remodelling of fibrotic ECM, as well as *MMP2* (Berman *et al.*, 2004; Dong and Ma, 2017). TGF-β1 induction and activation, fibroblasts accumulation and activation, and myofibroblast accumulation were also reduced compared to a lung fibrosis mouse model non depleted for *SPP1* (Dong and Ma, 2017). Similarly to reports on IPF and lung fibrosis mouse models, *SPP1* was also overexpressed in

our 2 pro-fibrotic macrophage clusters when compared to all others and overexpressed in diseased compared with healthy dogs in monocyte-derived macrophages. The overexpression of this transcript in our identified pro-fibrotic macrophage clusters tends to validate their involvement in the fibrosis process occurring in CIPF.

The overexpression of other pro-fibrotic molecules found in CIPF pro-fibrotic macrophage clusters such as *CCL2, CXCL8, FN1, TIMP1* and *IL1RN* was also reported in pro-fibrotic macrophage clusters in IPF (Morse *et al.*, 2019; Reyfman *et al.*, 2019). At the protein level, an increase in BALF and serum CCL2 concentration and in BALF CXCL8 concentration was found in CIPF compared with healthy WHWTs, which is in line with our results (Roels *et al.*, 2015b). However, none of the other overexpressed molecules have yet been investigated at the protein level in the disease.

Finally, in our study, pro-fibrotic monocytes and monocyte-derived macrophages don't seem to arise as a new population in CIPF WHWTs. Indeed, the 2 clusters are present in both healthy and CIPF WHWTs. However, differences were found between healthy and diseased WHWTs in both clusters. Monocytes were present in greater proportion in diseased compared to healthy WHWTs and monocyte-derived macrophages showed transcriptomic modifications between healthy and diseased dogs. The presence of same Ma/Mo clusters in IPF as in normal lungs was also reported by Morse and colleagues (2019) who also described transcriptomic modifications between healthy and diseased lungs including an increase in *SPP1* expression in IPF lungs.

Although a role for neutrophils, T cells, DCs and mast cells was described in IPF (Heukels *et al.*, 2019), we failed to identify DEGs between CIPF and healthy WHWTs in those cell types. However, an increase number of neutrophils at cytology was reported in CIPF compared with healthy WHWTs which is in agreement with previous studies in CIPF WHWTs on BALF cell count analysis (Heikkila-Laurila and Rajamaki, 2014). The increase in neutrophils could be related to the overexpression of *CCL3* and *CCL4* in pro-fibrotic monocytes, also reported in IPF, which are known to be chemoattractant cytokines for neutrophils (Capelli *et al.*, 2002, 2005; Lee *et al.*, 2018; Heukels *et al.*, 2019).

The identification and detailed description of aberrant Ma/Mo populations in the CIPF BALF may lead to identification of novel cell type–specific therapies and biomarkers which rises a lot of perspectives for CIPF research. The best candidates as biomarkers and/or therapeutic targets in overexpressed pro-fibrotic molecules included FN1, SPP1 and CXCL8 which were overexpressed in pro-fibrotic monocytes and in monocyte-derived macrophages compared to other Ma/Mo clusters and which were also overexpressed in CIPF compared with healthy WHWTs in monocyte-derived macrophages. As already said, CXCL8 protein concentration was already investigated for its potential utility as biomarker and was increased in BALF samples between CIPF and healthy WHWTs (Roels *et*

al., 2015b). FN1 is considered as one of the most dominant components of ECM with collagens I and III (Upagupta *et al.*, 2018). It is found in abundance in IPF lungs and is essential for myofibroblasts differentiation (Upagupta *et al.*, 2018). In addition, human macrophagic *FN1* expression and production was increased in IPF patients and this macrophagic-produced FN1 was shown to recruit fibroblasts inducing lung architectural distortion (Rennard *et al.*, 1981; Morse *et al.*, 2019; Reyfman *et al.*, 2019). Targeting such molecule or macrophages-producing FN1 could be useful to reduce fibroblasts accumulation and differentiation. As already said, SPP1 seems to be the hallmark of pro-fibrotic macrophages identified in pulmonary fibrosis by scRNA-seq and has a role in fibrosis development (Morse *et al.*, 2019; Reyfman *et al.*, 2019; Adams *et al.*, 2020). Next to its potential utility as biomarker in CIPF, SPP1 is also suggested to be targeted as treatment in human IPF (Dong and Ma, 2017) and could represent a good option in CIPF dogs according to our results. In lung fibrosis mouse models, a link was also found between SPP1 and FN1. Indeed, as already said, mice depleted for *SPP1* showed a decrease in *FN1* expression associated with a reduction of lung fibrosis extent (Takahashi *et al.*, 2001; Dong and Ma, 2017), which support the potential benefit for the targeting of SPP1 to slow or stop CIPF progression and to act at the same time on FN1 amount.

The scRNA-seq as a tool for unbiased cellular approach, although strongly efficient, is yet in development and currently, the development of new software based on gene expression profile such as Niche Net (Browaeys, Saelens and Saeys, 2020) allows to investigate cell-cell interactions and to have a functional understanding of cell–cell communication. The use of this new software would be helpful to investigate the links between pro-fibrotic Ma/Mo populations and other cells and to provide a better understanding of the role of pro-fibrotic Ma/Mo populations in CIPF pathogenesis.

Finally, in our scRNA-seq analysis, we only focused on BALF Ma/Mo which represent a part but not all Ma/Mo present in the lungs and that might be involved in CIPF pathogenesis. Indeed, in addition to the monocytes recruited into the lung which can be found in the interstitium, specific clusters of macrophages, called interstitial macrophages (IMs), ideally positioned in the interstitium and especially exerting anti-inflammatory functions have also been described (Liegeois *et al.*, 2018; Schyns *et al.*, 2019). Modifications of IMs have been found in mice with induced hypoxemia. Indeed, the number of IMs was shown to transiently increase and their transcriptome was showed to change towards expression of anti-inflammatory genes, in response to the low blood oxygen level (Pugliese *et al.*, 2017). Accordingly, this increase in immunoregulatory activity might play a role in CIPF dogs with known hyoxemia. In mice with bleomycin-induced and radiation-induced lung fibrosis, IMs were also shown to aquire pro-fibrotic signature, potentially at the origin of lung fibrosis (Shi *et al.*, 2021). However, recently, a protective role of IMs was also described in early development of bleomycin-induced IPF, in which the depletion of IMs induced higher collagen deposition and inflammatory cells recruitement (Chakarov *et al.*, 2019). Althought the role of IMs as protective or causative agent in

lung fibrosis needs to be confirmed, such studies showed that investigating Ma/Mo clusters in the interstitial compartment appears interesting to better understand all the mechanisms driven by Ma/Mo in the disease pathogenesis. Moreover, pro-fibrotic epithelial and fibroblastic clusters also localised into the lung tissue have been described in IPF scRNA-seq studies (Nemeth, Schundner and Frick, 2020). Establishing the whole lung cell atlas in dogs will be the next step to identify modifications induced by CIPF in an unbiased way and in a more global vision in the entire lung tissue including those IM, epithelial and fibroblastic cells.

Limitations

This work has several limitations. The principal limitation is the difficulty to recruit large numbers of well-phenotyped WHWTs affected with CIPF. Indeed, CIPF remains a rare disease easily confounded by owners and veterinarians with ageing and other cardiopulmonary diseases, respectively (Clercx, Fastrès and Roels, 2018; Laurila and Rajamäki, 2020). Moreover, diagnosis requires performance of several complementary examinations including thoracic HRCT and even if disease confirmation can only be obtained through lung tissue histopathological examination, lung biopsies are only performed after the animal death as the balance between risk and benefit is too high (Clercx, Fastrès and Roels, 2018; Laurila and Rajamäki, 2020). Therefore, despite large communication about the WHWT project launched at the veterinary clinic of Liège University, we were only able to recruit 17 WHWTs suspected to have CIPF based on thoracic HRCT and followed every 6 months during the course of this work. Among them 10 died during the study period but lung tissue was collected in only 6 of these dogs in which CIPF was confirmed by histology. Six healthy control WHWTs were also recruited but only 2 of them have had a follow-up every year. The limited number of dogs has a great impact on results, especially with the use of sequencing technologies that provide huge amount of data. Indeed, the amount of data has an impact on statistical power of analyses and prevents the detection of statistically significant small effects (Desquilbet *et al*., 2015).

Another limitation inherent in dog studies is the lack of specifically-design research tools and materials for dogs. Poor annotation of canine genome databases limits genome databases-based results. For example, in scRNA-seq studies, a threshold of 30% of reads mapped confidently to the transcriptome is required which was not reached in our studies (10X Genomics, 2020). Although it did not prevent us from having consistent results, it probably masked information and prevented us from optimizing the use of this technique. In dogs also, there is a lack of well-described cell markers. Usually, cell population markers are derived from human or rodent studies and are not always adapted to canine cell populations as noted in our first study on scRNA-seq. Moreover, classical validations of scRNA-seq studies usually based on flow cytometry or immunohistochemistry methods are limited by the lack of antibodies able to bind reliably to canine cells.

Other limitations linked to the use of the 16S rDNA amplicon sequencing and the scRNA-seq techniques have been addressed in details in the introduction and have to be kept in mind when interpreting data obtained by such methods. More specifically, the study of the LM, because of its low bacterial load, requires strict controls to avoid samples contamination at each analysis steps (Salter *et al.*, 2014; Marsh *et al.*, 2018). Accordingly, in all of our studies, PCSs were obtained from each dog and processed alongside the samples. In all of them, the post-PCR quality control did not identify PCR products > 1 ng/µL, necessary to have reliable sequencing analysis results (Taminiau and Daube, unpublished data). Moreover, when bacterial loads were compared between PCSs and samples, a significant 2 log fold change difference was found in all of our studies. Positive and negative controls were also used for the sequencing step to validate each run. The absence of a standardized technique to explore LM also prevents good comparison between studies that remain sparse in dogs. The use of the scRNA-seq also has limitations. First, it requires fresh samples to avoid RNA contamination from dead or broken cells (Zheng *et al.*, 2017; Salomon *et al.*, 2019). Doublets can also result in misinterpretation of the results (Chen, Ning and Shi, 2019). Accordingly, we analysed BALF samples within one hour after collection to limit the presence of broken or dead cells in our samples and a percentage of viability above 80% was considered as acceptable. As detection and withdrawal of possible broken or dead cells and doublets is crucial, cells containing less than 100 genes (dead or broken cells) or more than 2500 genes (doublets) were excluded from our analyses. We also screened our samples for mitochondrial genes to search for dead or broken cells without identification of such genes. Finally, poorly expressed RNA might not be captured by the scRNA-seq technique (See *et al.*, 2018; Chen, Ning and Shi, 2019), although we reach a plateau of detected genes in the majority of our sample on the saturation curve by having a sequencing depth stated at 50,000 reads. Rare cells populations might also not be captured (See *et al.*, 2018; Chen, Ning and Shi, 2019), and eosinophils doesn't seem to be recruited by the scRNA-seq technique.

Conclusion

To conclude, this work increases knowledge on CIPF pathogenesis by focusing on the potential involvement of the LM and BALF macrophages in the disease.

We established that the LM in healthy dogs is composed by 4 major phyla, the Proteobacteria, the Actinobacteria, the Firmicutes and the Bacteroidetes and includes at least *Cutibacterium*, *Streptococcus*, *Acinetobacter* and *Pseudomonas* genera. We also showed that the LM is relatively stable in healthy adult dogs and is mainly influenced by the living conditions of the dogs, although the breed also has an impact. We showed that the 16S rDNA amplicon sequencing is a reliable technique to identify bacteria in lung infectious diseases, and that the dysbiosis associated with acute lung conditions is characterized by an increase in bacterial burden and a decrease in richness and α-diversity, with the domination of one or two bacteria. We also showed that a treatment with

antimicrobials drugs induces LM alterations and that a wash-out period of at least 2 weeks should be followed before sampling to minimize antimicrobial drug-induced dysbiosis. Unfortunately, we were not able to identify significant specific LM alterations associated with CIPF but we reported a specific LM in dogs of the WHWT breed which could be associated with the predisposition to the disease.

After validation of the use of the scRNA-seq in BALF from healthy dogs, a technique never used in dogs before, we were able to identify in healthy and CIPF WHWTs 2 Ma/Mo clusters, further characterized as monocytes and monocyte-derived macrophages, enriched in pro-fibrotic genes compared with other Ma/Mo clusters. Although those two clusters were present in healthy WHWTs, monocytes were in lesser cell proportion compared to CIPF dogs and differences in gene expression including notably an enrichment in pro-fibrotic genes was found in monocyte-derived macrophages in CIPF compared with healthy WHWTs. Those results are in favour of a role of macrophages in CIPF development and perpetuation. However, more studies are required to validate those results and identify potential therapeutic targets in link with macrophages clusters or their expression products.

Even if CIPF remains complex and still poorly understood, this work offers promising perspectives for future projects with always the objectives to improve disease detection, follow-up, understanding, and treatment.

Bibliography

10X Genomics. (2020). Troubleshooting Cell Ranger. Available at: https://support.10xgenomics.com/single-cell-gene-expression/software/pipelines/latest/troubleshooting#alerts (Accessed: 16 March 2020).

Abranches J., Zeng L., Kajfasz J.K., Palmer S., Chakraborty B., Wen Z., et al. (2018). Biology of oral *Streptococci*. Microbiology Spectrum, 6(5), pp. 426–434. doi: 10.1128/9781683670131.ch26.

Adams T.S., Schupp J.C., Poli S., Ayaub E.A., Neumark N., Ahangari F., et al. (2020). Single-cell RNA-seq reveals ectopic and aberrant lung-resident cell populations in idiopathic pulmonary fibrosis. Science Advances, 6, eaba1983. doi: 10.1126/sciadv.aba1983.

Agler C.S., Friedenberg S., Olivry T., Meurs K.M., Olby N.J. (2019). Genome-wide association analysis in West Highland white terriers with atopic dermatitis. Veterinary Immunology and Immunopathology, 209, pp. 1–6. doi: 10.1016/j.vetimm.2019.01.004.

Al Alam D., Danopoulos S., Grubbs B., Ali N.A.B.M., MacAogain M., Chotirmall S.H., et al. (2020). Human fetal lungs harbor a microbiome signature. American Journal of Respiratory and Critical Care Medicine, 201, pp. 1002–1006. doi: 10.1164/RCCM.201911-2127LE.

Alcover A., Alarcon B. and Di Bartolo V. (2018). Cell biology of T-cell receptor expression and regulation. Annual Review of Immunology, 36, pp. 103–125. doi: 10.1146/annurev-immunol042617-053429.

Alfaro T.M. and Cordeiro C.R. (2020). Comorbidity in idiopathic pulmonary fibrosis - what can biomarkers tell us? Therapeutic Advances in Respiratory Disease Review, 14, pp. 1–10. doi: 10.1177/https.

American Thoracic Society (ATS) and the European Respiratory Society (ERS) (2000). Idiopathic pulmonary fibrosis: diagnosis and treatment. International consensus statement. American Journal of Respiratory and Critical Care Medicine, 161, pp. 646–664. doi: 10.1164/ajrccm.161.2.ats3-00.

Amis T.C. and Kurpershoek C. (1986). Pattern of breathing in brachycephalic dogs. American Journal of Veterinary Research, 47(10), pp. 2200–2204.

Ammon C., Meyer S.P., Schwarzfischer L., Krause S.W., Andreesen R., Kreutz M. (2000). Comparative analysis of integrin expression on monocyte-derived macrophages and monocyte-derived dendritic cells. Immunology, 100, pp. 364–369. doi: 10.1046/j.1365-2567.2000.00056.x.

Anand S. and Mande S.S. (2018). Diet, microbiota and gut-lung connection. Frontiers in Microbiology, 9, p. 2147. doi: 10.3389/fmicb.2018.02147.

Anderton, T.L., Maskell, D.J. and Preston A. (2004). Ciliostasis is a key early event during colonization of canine tracheal tissue by *Bordetella bronchiseptica*. Microbiology, 150, pp. 2843–2855. doi: 10.1099/mic.0.27283-0.

Antunes L.C.S., Imperi F., Carattoli A., Visca P. (2011). Deciphering the multifactorial nature of acinetobacter baumannii pathogenicity. PLoS One, 6(8), e22674. doi: 10.1371/journal.pone.0022674.

Aran D., Looney A.P., Liu L., Wu E., Fong V., Hsu A., et al. (2019). Reference-based analysis of lung single-cell sequencing reveals a transitional profibrotic macrophage. Nature Immunology, 20, pp. 63–72. doi: 10.1038/s41590-018-0276-y.

Ardain A., Marakalala M. J. and Alasdair L. (2019). Tissue-resident innate immunity in the lung. Immunology, 159, pp. 245–256. doi: 10.1111/imm.13143.

Balakrishnan A. and Tong C.W. (2020). Clinical application of pulmonary function testing in small animals. Veterinary Clinics of North America: Small Animal Practice. Elsevier Inc, 50, pp. 273–294. doi: 10.1016/j.cvsm.2019.10.004.

Barfod K.K., Vrankx K., Mirsepasi-Lauridsen H.C., Hansen J.S., Hougaard K.S., Larsen S.T., et al. (2015). The murine lung microbiome changes during lung inflammation and intranasal vancomycin treatment. The Open Microbiology Journal, 9, pp. 167–179. doi: 10.2174/1874285801509010167.

Barnes T., Brown K.K., Corcoran B., Glassberg M.K., Kervitsky D.J., Limper A.H., et al. (2019). Research in pulmonary fibrosis across species: unleashing discovery through comparative biology. American Journal of the Medical Sciences, 357, pp. 399–404. doi: 10.1016/j.amjms.2019.02.005.

Bassis C.M., Erb-Downward J.R., Dickson R.P., Freeman C.M., Schmidt T.M., Young V.B., et al. (2015). Analysis of the upper respiratory tract microbiotas as the source of the lung and gastric microbiotas in healthy individuals. mBio, 6(2), e00037-15. doi: 10.1128/mBio.00037-15.

Beck J.M. (2014). ABCs of the lung microbiome. Annals of the American Thoracic Society, 11(1), pp. 5–8. doi: 10.1513/AnnalsATS.201306-188MG.

Beck J.M., Young V.B. and Huffnagle G.B. (2012). The Microbiome of the lung. Translational Research, 160(4), pp. 258–266. doi: 10.1016/j.trsl.2012.02.005.

Bédard Méthot D., Leblanc É. and Lacasse Y. (2019). Meta-analysis of gastroesophageal reflux disease and idiopathic pulmonary fibrosis. Chest, 155(1), pp. 33–43. doi: 10.1016/J.CHEST.2018.07.038.

Bemis D. and Appel M. (1977). Aerosol Nolvasan treatment of *Bordetella bronchiseptica* in dogs. Veterinary Clinic of North America: Small Animal Practice, 72(1), pp. 53–55.

Berman J.S., Serlin D., Li X., Whitley G., Hayes J., Rishikof D.C., et al. (2004). Altered bleomycin-induced lung fibrosis in osteopontin-deficient mice. American Journal of Physiology-Lung Cellular and Molecular Physiology, 286, pp. 1311–1138. doi: 10.1152/ajplung.00394.2003.

Bernasconi E., Pattaroni C., Koutsokera A., Pison C., Kessler R., Benden C., et al. (2016). Airway microbiota determines innate cell inflammatory or tissue remodeling profiles in lung transplantation. American Journal of Respiratory and Critical Care Medicine, 194(10), pp. 1252–1263. doi: 10.1164/rccm.201512-2424OC.

Bernaerts F., Talavera J., Leemans J., Hamaide A., Claeys S., Kirschvink N., et al. (2010). Description of original endoscopic findings and respiratory functional assessment using barometric whole-body plethysmography in dogs suffering from brachycephalic airway obstruction syndrome. The Veterinary Journal, 183(1), pp. 95–102. doi: 10.1016/j.tvjl.2008.09.009.

Bharat A., Bhorade S., Morales-Nebreda L., McQuattie-Pimentel A., Soberanes S., Ridge K., et al. (2016). Flow cytometry reveals similarities between lung macrophages in humans and mice. American Journal of Respiratory Cell and Molecular Biology, 54, pp. 147–149. doi: 10.1017/CBO9781107415324.004.

Bhavsar I., Miller C.S. and Al-Sabbagh M. (2015). Macrophage inflammatory protein-1 alpha (MIP-1 alpha)/CCL3: as a biomarker. In: Preedy V.R., Patel V.B. (eds). General methods in biomarker research and their applications. Dordrecht, The Netherlands, pp. 223–249. doi: 10.1007/978-94-007-7696-8_27.

Biesbroek G., Tsivtsivadze E., Sanders E.A., Montijn R., Veenhoven R.H., Keijser B.J., et al. (2014). Early respiratory microbiota composition determines bacterial succession patterns and respiratory health in children. American Journal of Respiratory and Critical Care Medicine, 190, pp. 1283–1292. doi: 10.1164/rccm.201407-1240OC.

Bindels L.B., Neyrinck A.M., Salazar N., Taminiau B., Druart C., Muccioli G.G., et al. (2015). Non digestible oligosaccharides modulate the gut microbiota to control the development of leukemia and associated cachexia in mice. PLoS One, 10(6), e0131009. doi: 10.1371/journal.pone.0131009.

Blanchard A.C. and Waters V.J. (2019). Microbiology of cystic fibrosis airway disease. Seminars in Respiratory and Critical Care Medicine, 40, pp. 727–736. doi: 10.1055/s-0039-1698464.

Bloom J.D. (2018). Estimating the frequency of multiplets in single-cell RNA sequencing from cell-mixing experiments. PeerJ, 6, 5578. doi: 10.7717/peerj.5578.

Boers S.A., Jansen R. and Hays J.P. (2019). Understanding and overcoming the pitfalls and biases of next-generation sequencing (NGS) methods for use in the routine clinical microbiological diagnostic laboratory. European Journal of Clinical Microbiology and Infectious Diseases, 38, pp. 1059–1070. doi: 10.1007/s10096-019-03520-3.

Bonella F., Hegedues B., Langer S., Honshoven F., Gottstein E., Theegarten D., et al. (2019). Serum KL-6 as a biomarker for interstitial lung diseases in a clinical setting: application of a fully automated immunoassay. European Respiratory Journal, 54, 4697. doi: 10.1183/13993003.congress-2019.PA4697.

Browaeys R., Saelens W. and Saeys Y. (2020). NicheNet: modelling intercellular communication by linking ligands to target genes. Nature Methods, 17, pp. 159–162. doi: 10.1038/s41592-019-0667-5.

Brown R.L., Sequeira R.P. and Clarke T.B. (2017). The microbiota protects against respiratory infection via GM-CSF signalling. Nature Communications, 8, 1512. doi: 10.1038/s41467-017-01803-x.

Brusse-Keizer M., Vander Valk P., van der Zanden R.W., Nijdam L., van der Palen J., Hendrix R., et al. (2015). Amoxicillin concentrations in relation to beta-lactamase activity in sputum during exacerbations of chronic obstructive pulmonary disease. International Journal of COPD, 10, pp. 455–461. doi: 10.2147/COPD.S70355.

Buboltz A.M., Nicholson T.L., Weyrich L.S., Harvill E.T. (2009). Role of the Type III Secretion System in a hypervirulent lineage of *Bordetella bronchiseptica.* Infection and Immunity, 77(9), pp. 3969–3977. doi: 10.1128/IAI.01362-08.

Byrne A.J., Powell J.E., Sullivan B.J.O., Ogger P.P., Hoffland A., Cook J., et al. (2020). Dynamics of human monocytes and airway macrophages during healthy aging and after transplant. Journal of Experimental Medicine, 217, e20191236. doi: 10.1084/jem.20191236.

Canonne A.M., Billen F., Tual C., Ramery E., Roels E., Perters I., Clercx C. (2016). Quantitative PCR and cytology of bronchoalveolar lavage fluid in dogs with Bordetella bronchiseptica infection. Journal of veterinary internal medicine, 30(4), pp. 1204–1209. doi: 10.1111/jvim.14366.

Canonne A.M., Roels E., Billen F., Benchekroun G., Clercx C. (2018). Comparison of two aerosolized gentamicin protocols for *Bordetella bronchiseptica* lower airway infection in dogs. Journal of Veterinary Internal Medicine, 32, pp. 2306–2307. doi: 10.1111/jvim.15092.

Capelli A., Di Stefano A., Gnemmi I., Donner C.F. (2005). CCR5 expression and CC chemokine levels in idiopathic pulmonary fibrosis. European Respiratory Journal, 25, pp. 701–707. doi: 10.1183/09031936.05.00082604.

Capelli A., Di Stefano A., Lusuardi M., Gnemmi I., Donner C.F. (2002). Increased macrophage inflammatory protein-1a and macrophage inflammatory protein-1b levels in bronchoalveolar lavage fluid of patients affected by different stages of pulmonary sarcoidosis. American Journal of Respiratory and Critical Care Medicine, 165, pp. 236–241. doi: 10.1164/rccm2106084.

Cattelan N., Dubey P., Arnal L., Yantorno O.M., Deora R. (2016). Bordetella biofilms: a lifestyle leading to persistent infections. Pathogens and Disease, 74, ftv108. doi: 10.1093/femspd/ftv108.

Caughey G.H. (2016). Mast cell proteases as pharmacological targets. European Journal of Pharmacology, 778, pp. 44–55. doi: 10.1016/j.ejphar.2015.04.045.

Chakarov S., Lim H.Y., Tan L., Lim S.Y., See P., Lum J., et al. (2019). Two distinct interstitial macrophage populations coexist across tissues in specific subtissular niches. Science, 363, 1190. doi: 10.1126/science.aau0964.

Chalker V. (2005). Canine mycoplasmas. Research in Veterinary Science, 79(1), pp. 1–8. doi: 10.1016/j.rvsc.2004.10.002.

Chanda D., Otoupalova E., Smith S.R., Volckaert T., De Langhe S.P., Thannickal V.J. (2019). Developmental pathways in the pathogenesis of lung fibrosis', Molecular Aspects of Medicine, 65, pp. 56–69. doi: 10.1016/j.mam.2018.08.004.

Charlson E.S., Bittinger K., Haas A.R., Fitzgerald A.S., Frank I., Yadav A., et al. (2011). Topographical continuity of bacterial populations in the healthy human respiratory tract. American Journal of Respiratory and Critical Care Medicine, 184, pp. 957–963. doi: 10.1164/rccm.201104-0655OC.

Chen G., Ning B. and Shi T. (2019). Single-cell RNA-seq technologies and related computational data analysis. Frontiers in Genetics, 10, 317. doi: 10.3389/fgene.2019.00317.

Chung K.F. (2017). Clinical reviews in allergy and immunology airway microbial dysbiosis in asthmatic patients: A target for prevention and treatment? Journal of Allergy and Clinical Immunology, 139(4), pp. 1071–1081. doi: 10.1016/j.jaci.2017.02.004.

Ciofu O. and Tolker-Nielsen T. (2019). Tolerance and resistance of *Pseudomonas aeruginosa* biofilms to antimicrobial agents-How *P. aeruginosa* can escape antibiotics. Frontiers in Microbiology, 10,913. doi: 10.3389/fmicb.2019.00913.

Clarridge J.E. (2004). Impact of 16S rRNA gene sequence analysis for identification of bacteria on clinical microbiology and infectious diseases. Clinical Microbiology Reviews, 17, pp. 840–862. doi: 10.1128/CMR.17.4.840-862.2004.

Clercx C., Peeters D., German A.J., Khelil Y., McEntee K., Vanderplasschen A., et al. (2002). An immunologic investigation of canine eosinophilic bronchopneumopathy. Journal of Veterinary Internal Medicine, 16(3), pp. 229–237. doi: 10.1111/j.1939-1676.2002.tb02362.x.

Clercx C., Fastrès A. and Roels E. (2018). Idiopathic pulmonary fibrosis in the West Highland white terrier: an update. Veterinary Journal, 242, 53–58. doi: 10.1016/j.tvjl.2018.10.007.

Clercx C. and Peeters D. (2007). Canine eosinophilic bronchopneumopathy. Veterinary Clinics of North America - Small Animal Practice, 37, pp. 917–35. doi: 10.1016/j.cvsm.2007.05.007.

Coburn B., Wang P.W., Caballero J.D., Clark S.T., Brahma V., Donaldson S., et al. (2015). Lung microbiota across age and disease stage in cystic fibrosis. Scientific Reports, 5, 10241. doi: 10.1038/srep10241.

Codony F., Dinh-Thanh M. and Agustí G. (2020). Key factors for removing bias in viability PCR-based methods: a review. Current Microbiology, 77, pp. 682–687. doi: 10.1007/s00284-019-01829-y.

Cole J.R., Chai B., Marsh T.L., Farris R.J., Wang Q., Kulam S.A., et al. (2003). The Ribosomal Database Project (RDP-II): Previewing a new autoaligner that allows regular updates and the new prokaryotic taxonomy. Nucleic Acids Research, 31, pp. 442–443. doi: 10.1093/nar/gkg039.

Condliffe A.M., Chilvers E.R., Haslett C., Dransfield I. (1996). Priming differentially regulates neutrophil adhesion molecule expression/function. Immunology, 89, pp. 105–111. doi: 10.1046/j.1365-2567.1996.d01-711.x.

Corcoran B.M., Cobb M., Martin M.W.S., Dukes-McEwan J., French A., Luis-Fuentes V. (1999). Chronic pulmonary disease in West Highland white terriers. Veterinary record, 144, pp. 611–616.

Corcoran B.M., Dukes-McEwan J., Rhind S., French A. (1999). Idiopathic pulmonary fibrosis in a Staffordshire bull terrier with hypothyroidism. Journal of Small Animal Practice, 40(4), pp. 185–188. doi: 10.1111/j.1748-5827.1999.tb03788.x.

Corcoran B.M., King L.G., Schwarz T., Hammond G., Sullivan M. (2011). Further characterisation of the clinical features of chronic pulmonary disease in West Highland white terriers. Veterinary Record, 168(13), pp. 355–355. doi: 10.1136/vr.c6519.

Costa A.N., da Costa F.M., Campos S.V., Salles R.K., Athanazio R.A., Costa A.N., et al. (2018). The pulmonary microbiome: challenges of a new paradigm. Jornal Brasileiro de Pneumologia, 44(5), pp. 424–432. doi: 10.1590/s1806-37562017000000209.

Croxford A.L., Lanzinger M., Hartmann F.J., Schreiner B., Mair F., Pelczar P., et al. (2015). The cytokine GM-CSF drives the inflammatory signature of CCR2+ monocytes and licenses autoimmunity. Immunity, 43, pp. 502–514. doi: 10.1016/j.immuni.2015.08.010.

Cruaud P., Vigneron A., Fradette M.S., Dorea C.C., Culley A.I., Rodriguez M.J., et al. (2020). Annual bacterial community cycle in a seasonally ice-covered river reflects environmental and climatic conditions. Limnology and Oceanography, 65, pp. S21–S37. doi: 10.1002/lno.11130.

Crystal R.G. Fulmer J.D., Roberts W.C., Moss M.L., Line B.R., Reynolds H.Y. (1976). Idiopathic pulmonary fibrosis clinical, histologic, radiographic, physiologic, scintigraphic, cytologic, and biochemical aspects. Annals of internal medicine, 85(6), pp. 769–788. doi: 10.7326/0003-4819-85-6-769.

Cunningham F., Achuthan P., Akanni W., Allen J., Amode M.R., Armean I.M., et al. (2019). Ensembl 2019. Nucleic Acids Research, 47, pp. 745–751. doi: 10.1093/nar/gky1113.

Davie K., Janssens J., Koldere D., De Waegeneer M., Pech U., Kreft L., et al. (2018). A single-cell transcriptome atlas of the aging drosophila brain. Cell Press, 174(4), pp. 982-998.e20. doi: 10.1016/J.CELL.2018.05.057.

Davis A.P., Grondin C.J., Johnson R.J., Sciaky D., McMorran R., Wiegers J., et al. (2019). The comparative toxicogenomics database: update 2019. Nucleic Acids Research, 47, pp. 948–954. doi: 10.1093/nar/gky868

Decaro N., Mari V, Larocca V., Losurdo M., Lanave G., Stella M., et al. (2016). Molecular surveillance of traditional and emerging pathogens associated with canine infectious respiratory disease. Veterinary Microbiology, 192, pp. 21–25. doi: 10.1016/j.vetmic.2016.06.009.

Derynck R. and Budi E.H. (2019). Specificity, versatility and control of TGF-β family signalling. Science Signaling, 12, eaav5183. doi: 10.1126/scisignal.aav5183.

Desai O., Winkler J., Minasyan M., Herzog E.L. (2018). The role of immune and inflammatory cells in idiopathic pulmonary fibrosis. Frontiers in Medicine, 5, 43. doi: 10.3389/fmed.2018.00043.

DeSantis T.Z., Hugenholtz P., Larsen N., Rojas M., Brodie E.L., Keller K., et al. (2006). Greengenes, a chimera-checked 16S rRNA gene database and workbench compatible with ARB. Applied and Environmental Microbiology, 72, pp. 5069–5072. doi: 10.1128/AEM.03006-05.

Desquilbet L. (2015). Puissance statistique d'une étude version 3. Available at: https://eve.vet-alfort.fr/course/view.php?id=353 (Accessed: 3 May 2018).

Dickson R.P., Erb-Downward J.R., Falkowski N.R., Hunter E.M., Ashley S.L., Huffnagle G.B. (2018). The lung microbiota of healthy mice are highly variable, cluster by environment, and reflect variation in baseline lung innate immunity. American Journal of Respiratory and Critical Care Medicine, 198(4), pp. 497–508. doi: 10.1164/rccm.201711-2180OC.

Dickson R.P., Erb-Downward J.R., Freeman C.M., McCloskey L., Beck J.M., Huffnagle G.B., et al. (2015). Spatial variation in the healthy human lung microbiome and the adapted island model of lung biogeography. Annals of the American Thoracic Society, 12(6), pp. 821–830. doi: 10.1513/AnnalsATS.201501-029OC.

Dickson R.P., Erb-Downward J.R., Freeman C.M., McCloskey L., Falkowski N.R., Huffnagle G.B., et al. (2017a). Bacterial topography of the healthy human lower respiratory tract. mBio, 8(1), e02287-16. doi: 10.1128/mBio.02287-16.

Dickson R.P., Erb-Downward J.R. and Huffnagle G.B. (2014). Towards an ecology of the lung: New conceptual models of pulmonary microbiology and pneumonia pathogenesis. The Lancet Respiratory Medicine, 2(3), pp. 238–246. doi: 10.1016/S2213-2600(14)70028-1.

Dickson R.P., Erb-Downward J.R., Martinez F.J., Huffnagle G.B. (2016). The Microbiome and the Respiratory Tract. Annual Review of Physiology, 78(1), pp. 481–504. doi: 10.1146/annurev-physiol-021115-105238.

Dickson R.P., Erb-Downward J.R., Prescott H.C., Martinez F.J., Curtis J.L., Lama V.N., et al. (2014). Analysis of culture-dependent versus culture-independent techniques for identification of bacteria in clinically obtained bronchoalveolar lavage fluid. Journal of Clinical Microbiology, 52(10), pp. 3605–3613. doi: 10.1128/JCM.01028-14.

Dickson R.P. and Huffnagle G.B. (2015). The lung microbiome: new principles for respiratory bacteriology in health and disease. PLoS Pathogens, 11(7), e1004923. doi: 10.1371/journal.ppat.1004923.

Dickson R.P., Schultz M.J., van der Poll T., Schouten L.R., Falkowski N.R., Luth J.E., et al. (2020). Lung microbiota predict clinical outcomes in critically ill patients. American Journal of Respiratory and Critical Care Medicine, 201(5), pp. 555–563. doi: 10.1164/rccm.201907-1487OC.

Dickson R.P., Singer B.H., Newstead M.W., Falkowski N.R., Erb-Downward J.R., Standiford T.J., et al. (2017b). Enrichment of the lung microbiome with gut bacteria in sepsis and the acute respiratory distress syndrome. Nature Microbiology, 1, 16113. doi: 10.1038/nmicrobiol.2016.113.

Ding L. and Yokota A. (2010). *Curvibacter fontana* sp. nov., a microaerobic bacteria isolated from well water. The Journal of General and Applied Microbiology, 56(3), pp. 267–271. doi: 10.2323/jgam.56.267.

Dirscherl P., Beiskerb W., Kremmer E., Mihalkov A., Voss C., Ziesenis A. (1995). Immunophenotyping of canine bronchoalveolar and peripheral blood lymphocytes. Veterinary Immunology and Immunopathology, 48, pp. 1–10. doi: 10.1016/0165-2427(94)05414-N.

Doggett N.A., Mukundan H., Lefkowitz E.J., Slezak T.R., Chain P.S., Morse S., et al. (2016). Culture-independent diagnostics for health security. Health Security, 14, pp. 122–142. doi: 10.1089/hs.2015.0074.

Dominguez-Bello M.G., Costello E.K., Contreras M., Magri M., Hidalgo G., Fierer N., et al. (2010). Delivery mode shapes the acquisition and structure of the initial microbiota across multiple body habitats in newborns. Proceedings of the National Academy of Sciences of the United States of America, 107, pp. 11971–11975. doi: 10.1073/pnas.1002601107.

Dong J. and Ma Q. (2017). Osteopontin enhances multi-walled carbon nanotube-triggered lung fibrosis by promoting TGF-β1 activation and myofibroblast differentiation. Particle and Fibre Toxicology, 14, 18. doi: 10.1186/s12989-017-0198-0.

Dréno B., Pécastaings S., Corvec S., Veraldi S., Khammari A., Roques C. (2018). *Cutibacterium acnes* (*Propionibacterium acnes*) and *acne vulgaris*: a brief look at the latest updates. Journal of European Academy of Dermatology and Venereology, 32(2), pp. 5–14. doi: 10.1111/jdv.15043.

Dumas A., Bernard L., Poquet Y., Lugo-Villarino G., Neyrolles O. (2018). The role of the lung microbiota and the gut – lung axis in respiratory infectious diseases. Cellular Microbiology, 20, e12966. doi: 10.1111/cmi.12966.

Eckersall P.D. and Bell R. (2010). Acute phase proteins: Biomarkers of infection and inflammation in veterinary medicine. The Veterinary Journal, 185, pp. 23–27. doi: 10.1016/j.tvjl.2010.04.009.

Edgar R.C., Haas B.J., Clemente J.C., Quince C., Knight R. (2011). UCHIME improves sensitivity and speed of chimera detection. Bioinformatics, 27(16), pp. 2194–2200. doi: 10.1093/bioinformatics/btr381.

Emidio N.B., Hoffmann W., Brierley S.M., Muttenthaler M. (2019). Trefoil factor family: unresolved questions and clinical perspectives. Trends in Biochemical Science, 44(5), pp. 387–390. doi: 10.1016/j.tibs.2019.01.004.

Erb-Downward J.R., Thompson D.L., Han M.K., Freeman C.M., McCloskey L., Schmidt L.A., et al. (2011). Analysis of the lung microbiome in the “healthy” smoker and in COPD. PLoS One, 6(2), e16384. doi: 10.1371/journal.pone.0016384.

Ericsson A.C., Personett A.R., Grobman M.E., Rindt H., Reinero C.R. (2016). Composition and predicted metabolic capacity of upper and lower airway microbiota of healthy dogs in relation to the faecal microbiota. PLoS One, 11(5), e0154646. doi: 10.1371/journal.pone.0154646.

Faldyna M., Samankova P., Leva L., Cerny J., Oujezdska J., Rehakova Z., et al. (2007). Cross-reactive anti-human monoclonal antibodies as a tool for B-cell identification in dogs and pigs. Veterinary Immunology and Immunopathology, 119, pp. 56–62. doi: 10.1016/j.vetimm.2007.06.022.

Farnsworth D.R., Saunders L.M. and Miller A.C. (2020). A single-cell transcriptome atlas for zebrafish development. Developmental Biology, 452(2), pp. 100–108. doi: 10.1016/J.YDBIO.2019.11.008.

Farris B. (2020). Chapter 15: Acute hypoxemic respiratory failure: idiopathic pulmonary fibrosis. In: Esquinas A.M. and Vargas N. (eds). Ventilatory support and oxygen therapy in elder, palliative and end-of-life care patients. Springer Nature, Cham, Switzerland, pp. 115–122. doi: 10.1007/978-3-030-26664-6.

Fastrès A., Felice F., Roels E., Moermans C., Corhay J.L., Bureau F., et al. (2017a). The lung microbiome in idiopathic pulmonary fibrosis: a promising approach for targeted therapies. International Journal of Molecular Sciences, 18(12), 2735. doi: 10.3390/ijms18122735.

Fastrès A., Pirottin D., Fievez L., Marichal T., Desmet C.J., Bureau F., et al. (2020b). Characterization of the bronchoalveolar lavage fluid by single cell gene expression analysis in healthy dogs: a promising technique. Frontiers in Immunology, 11, 1707. doi: 10.3389/fimmu.2020.01707.

Fastrès A., Roels E., Bolen G., Tutunaru A.C., Antoine N., Farnir F., et al. (2018). Investigation of serum Krebs Von den Lungen 6 concentration as a predisposing factor and in the diagnosis of canine idiopathic pulmonary fibrosis in the West Highland white terrier. Proceedings of the 28th ECVIM-CA Congress, Rotterdam, The Netherlands. Journal of Veterinary Internal Medicine, 33(2), pp. 1084-1085. doi: 10.1111/jvim.15372.

Fastrès A., Roels E., Tanimiau B., Rajamäki M.M., Daube G., Clercx C. (2017b). Possible effect of environment on lung microbiota in the healthy West Highland white terrier. Proceedings of the 4th FARAH-Day. Liège, Belgium, p. 67.

Fastrès A., Roels E., Vangrinsven E., Taminiau B., Jabri H., Taminiau B., et al. (2020a). Influence of the type of breed, living conditions and canine idiopathic pulmonary fibrosis. BMC Microbiology, 20, 84. doi: 10.1186/s12866-020-01784-w.

Fastrès A., Taminiau B., Vangrinsven E., Tutunaru A.C., Moyse E., Farnir F, et al. (2019). Effect of an antimicrobial drug on lung microbiota in healthy dogs. Heliyon. Elsevier, 5(11), e02802. doi: 10.1016/J.HELIYON.2019.E02802.

Favrot C., Rostaher A., Fischer N., Olivry T., Zwickl L., Audergon S. (2020). Atopic dermatitis in West Highland white terriers – part I : natural history of atopic dermatitis in the first three years of life. Veterinary Dermatology, 31, 106-e16. doi: 10.1111/vde.12801.

Federhen S. (2012). The NCBI Taxonomy database. Nucleic Acids Research, 40, pp. 136–143. doi: 10.1093/nar/gkr1178.

File T.M. (2007). The development of pharmacokinetically enhanced amoxicillin/clavulanate for the management of respiratory tract infections in adults. International Journal of Antimicrobial Agents, 30, pp. 131–134. doi: 10.1016/j.ijantimicag.2007.07.038.

Filho F.S.L., Alotaibi N.M., Ngan D., Tam S., Yang J., Hollander Z., et al. (2019). Sputum microbiome is associated with 1-year mortality after chronic obstructive pulmonary disease hospitalizations. American Journal of Respiratory and Critical Care Medicine, 199, pp. 1205–1213. doi: 10.1164/rccm.201806-1135OC.

Fillion-Bertrand G., Dickson R.P., Boivin R., Lavoie J.P., Huffnagle G.B., Leclere M. (2018). Lung microbiome is influenced by the environment and asthmatic status in an equine model of asthma. American Journal of Respiratory Cell and Molecular Biology, 60(2), pp. 189–197. doi: 10.1165/rcmb.2017-0228OC.

Finke M.D. (2013). Transtracheal wash and bronchoalveolar lavage. Topics in Companion Animal Medicine, 28(3), pp. 97–102. doi: 10.1053/j.tcam.2013.06.003.

Finn S.M.B., Scheuermann U., Holzknecht Z.E., Parker W., Granek J.A., Lin S.S., et al. (2018). Effect of gastric fluid aspiration on the lung microbiota of laboratory rats. Experimental Lung Research, 44, pp. 201–210. doi: 10.1080/01902148.2018.1482976.

Finn S.M.B., Scheuermann U., Holzknecht Z.E., Gao Q., Ibrahim M.M., Parker W., et al. (2019). The effect of levofloxacin on the lung microbiota of laboratory rats. Experimental Lung Research, 45, pp. 200–208. doi: 10.1080/01902148.2019.1639225.

Ford, R. (2012). Canine infectious tracheobronchitis. In Greene CE. Infectuous diseases of the dog and cat. 4th ed. Elsevier. Saint Louis, Missouri, pp. 55–65.

Fraher M.H., O'Toole P.W. and Quigley E.M.M. (2012). Techniques used to characterize the gut microbiota: A guide for the clinician. Nature Reviews Gastroenterology and Hepatology, 9, pp. 312–322. doi: 10.1038/nrgastro.2012.44.

Gautier E.L., Shay T., Miller J., Greter M., Jakubzick C., Ivanov S., et al. (2012). Gene-expression profiles and transcriptional regulatory pathways that underlie the identity and diversity of mouse tissue macrophages. Nature Immunology, 13, pp. 1118–1128. doi: 10.1038/ni.2419.

Gavins F.N.E. and Hickey, M.J. (2012). Annexin A1 and the regulation of innate and adaptive immunity. Frontiers in Immunology, 3, 354. doi: 10.3389/fimmu.2012.00354.

Gibbings S.L., Goyal R., Desch A.N., Leach S.M., Prabagar M., Atif S.M., et al. (2015). Transcriptome analysis highlights the conserved difference between embryonic and postnatal-derived alveolar macrophages. Blood, 126, pp. 1357–1366. doi: 10.1182/blood-2015-01-624809.

Gibbings S.L., Thomas S.M., Atif S.M., Mccubbrey A.L., Desch A.N., Danhorn T., et al. (2017). Three Unique interstitial macrophages in the murine lung at steady state. American Journal of Respiratory Cell and Molecular Biology, 57, pp. 66–76. doi: 10.1165/rcmb.2016-0361OC.

Gibbons M.A., MacKinnon A.C., Ramachandran P., Dhaliwal K., Duffin R., Phythian-Adams A. T., et al. (2011). Ly6Chi monocytes direct alternatively activated profibrotic macrophage regulation of lung fibrosis. American Journal of Respiratory and Critical Care Medicine, 184, pp. 569–581. doi: 10.1164/rccm.201010-1719OC.

Glass D.S., Grossfeld D., Renna H.A., Agarwala P., Spiegler P., Kasselman L.J., et al. (2020). Idiopathic pulmonary fibrosis: Molecular mechanisms and potential treatment approaches. Respiratory Investigation, 58, pp. 320–335. doi: 10.1016/j.resinv.2020.04.002.

Glassberg M.K. (2019). Overview of idiopathic pulmonary fibrosis, evidence-based guidelines, and recent developments in the treatment landscape. American Journal of Managed Care, 25, pp. S195–S203.

Gleeson K., Eggli D. and Maxwell S. (1997). Quantitative aspiration during sleep in normal subjects. Chest, 111, pp. 1266–1272. doi: 10.1378/chest.111.5.1266.

Glendinning L., Wright S., Pollock J., Tennant P., Collie D., McLachlana G. (2016). Variability of the sheep lung microbiota. Applied and Environmental Microbiology, 82(11), pp. 3225–3238. doi: 10.1128/AEM.00540-16.

Godlove J., Chiu W.K. and Weng N. (2007). Gene expression and generation of CD28- CD8 T cells mediated by interleukin 15. Experimental Gerontology, 42(5), pp. 412–415. doi: 10.1038/jid.2014.371.

Gokey J.J., Snowball J., Sridharan A., Speth J.P., Black K.E., Hariri L.P., et al. (2018). MEG3 is increased in idiopathic pulmonary fibrosis and regulates epithelial cell differentiation. JCI Insight, 3, e122490. doi: 10.1172/jci.insight.122490.

Grimminger F., Günther A. and Vancheri C. (2015). The role of tyrosine kinases in the pathogenesis of idiopathic pulmonary fibrosis. European Respiratory Journal, 45, pp. 1426–1433. doi: 10.1183/09031936.00149614.

Guiot J., Moermans C., Henket M., Corhay J.L., Louis R. (2017). Blood biomarkers in idiopathic pulmonary fibrosis. Lung, 195(3), pp. 273–280. doi: 10.1007/s00408-017-9993-5.

Gundra U.M., Girgis N.M., Ruckerl D., Jenkins S., Ward L.N., Kurtz Z.D., et al. (2014). Alternatively activated macrophages derived from monocytes and tissue macrophages are phenotypically and functionally distinct. Blood, 123, pp.110–122. doi: 10.1182/blood-2013-08-520619.

Günther A., Mosavi P., Ruppert C., Heinemann S., Temmesfeld B., Velcovsky H.G., et al. (2000). Enhanced tissue factor pathway activity and fibrin turnover in the alveolar compartment of patients with interstitial lung disease. Thrombosis and Haemostasis, 83, pp. 853–60. doi: 10.1055/s-0037-1613933.

Ha H., Debnath B. and Neamati N. (2017). Role of the CXCL8-CXCR1/2 axis in cancer and inflammatory diseases. Theranostics, 7, pp. 1543–1588. doi: 10.7150/thno.15625.

Hahn M.W., Schmidt J., Taipale S.J., Doolittle W.F., Koll U. (2014). *Rhodoluna lacicola* gen. nov., sp. nov., a planktonic freshwater bacterium with stream-lined genome. International Journal of Systematic and Evolutionary Microbiology, 64, pp. 3254–3263. doi: 10.1099/ijs.0.065292-0.

Hamai K., Iwamoto H., Ishikawa N., Horimasu Y., Masuda T., Miyamoto S., et al. (2016). Comparative Study of circulating MMP-7, CCL18, KL-6, SP-A, and SP-D as disease markers of idiopathic pulmonary fibrosis. Disease Markers, 2016, 4759040. doi: 10.1155/2016/4759040.

Han M.L., Zhou Y., Murray S., Tayob N., Noth I., Lama V.N., et al. (2014). Lung microbiome and disease progression in idiopathic pulmonary fibrosis: an analysis of the COMET study. The Lancet, 2, pp. 548–556. doi: 10.1016/S2213-2600(14)70069-4.

Haque A., Engel J., Teichmann S.A., Lönnberg T. (2017). A practical guide to single-cell RNA-sequencing for biomedical research and clinical applications. Genome Medicine, 9(1), pp. 1–12. doi: 10.1186/s13073-017-0467-4.

Haran K.P., Lockhart A., Xiong A., Radaelli E., Savickas P.J., Posey A., et al. (2020). Generation and validation of an antibody to canine CD19 for diagnostic and future therapeutic purposes. Veterinary Pathology, 57(2), pp. 241–252. doi: 10.1177/0300985819900352.

Harrison N.K. (2009). Pulmonary infection in Wegener's granulomatosis and idiopathic pulmonary fibrosis. Thorax, 64, pp. 647–649. doi: 10.1136/thx.2009.116418.

He L., Vanlandewijck M., Mäe M.A., Andrae J., Ando K., Del Gaudio F., et al. (2018). Single-cell RNA sequencing of mouse brain and lung vascular and vessel-associated cell types. Sciences Data, 5, 180160. doi: 10.1038/sdata.2018.160.

Hedlund E. and Deng Q. (2018). Single-cell RNA sequencing: Technical advancements and biological application. Molecular Aspects of Medicine, 59, pp. 36–46. doi: 10.1016/j.mam.2017.07.003.

Heikkilä H.P., Krafft E., Jespers P., McEntee K., Rajamäki M.M., Clercx C. (2013). Procollagen type III amino terminal propeptide concentrations in dogs with idiopathic pulmonary fibrosis compared with chronic bronchitis and eosinophilic bronchopneumopathy. The Veterinary Journal, 196, pp. 52–56. doi: 10.1016/J.TVJL.2012.07.023.

Heikkilä H.P., Lappalainen A.K., Day M.J., Clercx C., Rajamäki M.M. (2011). Clinical, bronchoscopic, histopathologic, diagnostic imaging, and arterial oxygenation findings in West Highland white terriers with idiopathic pulmonary fibrosis. Journal of Veterinary Internal Medicine, 25, pp. 433–439. doi: 10.1111/j.1939-1676.2011.0694.x.

Heikkila-Laurila H.P. and Rajamaki M.M. (2014). Idiopathic pulmonary fibrosis in West Highland white terriers. Veterinary Clinics of North America: Small Animal Practice, 44, pp. 129–142. doi: 10.1016/j.cvsm.2013.08.003.

Helps C.R., Lait P., Damhuis A., Björnehammar U., Bolta D., Brovida C., et al. (2005). Factors associated with upper respiratory tract disease caused by feline herpesvirus, feline calicivirus, *Chlamydophila felis* and *Bordetella bronchiseptica* in cats: Exerience from 218 European catteries. Veterinary Record, 156(21), pp. 669–673. doi: 10.1136/vr.156.21.669.

Herderschee J., Fenwick C., Pantaleo G., Roger T., Calandra T. (2015). Emerging single-cell technologies in immunology. Journal of Leukocyte Biology, 98, pp. 23–32. doi: 10.1189/jlb.6RU0115-020R.

Heukels P., Moor C.C., von der Thüsen J.H., Wijsenbeek M.S., Kool M. (2019). Inflammation and immunity in IPF pathogenesis and treatment. Respiratory Medicine, 147, pp. 79–91. doi: 10.1016/j.rmed.2018.12.015.

Heul V.A., Planer J. and Kau A.L. (2019). The human microbiota and asthma. Clinical Reviews in Allergy and Immunology, 57(3), pp. 350–363.

Hewitt R.J. and Molyneaux P.L. (2017). The respiratory microbiome in idiopathic pulmonary fibrosis. Annals of Translational Medicine, 5(12), 250. doi: 10.21037/atm.2017.01.56.

Hidalgo L.G., Einecke G., Allanach K., Halloran P.F. (2008). The transcriptome of human cytotoxic T cells: similarities and disparities among allostimulated CD4 + CTL, CD8 + CTL and NK cells. American Journal of Transplantation, 8, pp. 627–636. doi: 10.1111/j.1600-6143.2007.02128.x.

Hilty M., Burke C., Pedro H., Cardenas P., Bush A., Bossley C., et al. (2010). Disordered microbial communities in asthmatic airways. PLoS One, 5(1), e8578. doi: 10.1371/journal.pone.0008578.

Hochhegger B., Marchiori E., Zanon M., Rubin A.S., Fragomeni R., Altmayer S., et al. (2019). Imaging in idiopathic pulmonary fibrosis: Diagnosis and mimics. Clinics, 74, e225. doi: 10.6061/clinics/2019/e225.

Hogan D.A., Willger S.D., Dolben E.L., Hampton T.H., Stanton B.A., Morrison H.G., et al. (2016). Analysis of lung microbiota in bronchoalveolar lavage, protected brush and sputum samples from subjects with mild-to-moderate cystic fibrosis lung disease. PLoS One, 11, e0149998. doi: 10.1371/journal.pone.0149998.

Holopainen S., Rautala E., Lilja-Maula L., Lohi H., Rajamäki M.M., Lappalainen A.K. (2019). Thoracic high resolution CT using the modified VetMousetrap TM device is a feasible method for diagnosing canine idiopathic pulmonary fibrosis in awake West Highland white terriers. Veterinary Radiology & Ultrasound, 60, pp. 525–532. doi: 10.1111/vru.12779.

Homova (2018). Available at: https://www.mothur.org/wiki/Homova (Accessed: 21 October 2019).

Honeybourne D. (1994). Antibiotic penetration into lung tissues. Thorax, 49(2), pp. 104–106. doi: 10.1136/thx.49.2.104.

Hooda S., Minamoto Y., Suchodolski J.S., Swanson K.S. (2012). Current state of knowledge: the canine gastrointestinal microbiome. Animal health research reviews, 13(1), pp. 78–88. doi: 10.1017/S1466252312000059.

Hu Y., Wang L.S., Jin Y.P., Du S.S., Du Y.K., He X., et al. (2017). Serum Krebs von den Lungen-6 level as a diagnostic biomarker for interstitial lung disease in Chinese patients. Clinical Respiratory Journal, 11(3), pp. 337–345. doi: 10.1111/crj.12341.

Huang P., Zhou Y., Liu Z., Zhang P. (2016). Interaction between ANXA1 and GATA-3 in immunosuppression of CD4 + T Cells. Mediators of Inflammation, 2016, 1701059. doi: 10.1155/2016/1701059.

Huang T., Zhang M., Tong X., Chen J., Yan G., Fang S., et al. (2019). Microbial communities in swine lungs and their association with lung lesions. Microbial Biotechnology, 12, pp. 289–304. doi: 10.1111/1751-7915.13353.

Huang Y., Ma S.F., Espindola M.S., Vij R., Oldham J.M., Huffnagle G.B., et al. (2017). Microbes are associated with host innate immune response in idiopathic pulmonary fibrosis. American Journal of Respiratory and Critical Care Medicine, 196(2), pp. 208–219. doi: 10.1164/rccm.201607-1525OC.

Huang Y.J. and LiPuma J.J. (2017). The microbiome in cystic fibrosis. Clinical Chest Medicine, 37, pp. 59–67. doi: 10.1016/j.ccm.2015.10.003.

Huang Z., Pan Z., Yang R., Bi Y., Xiong X. (2020). The canine gastrointestinal microbiota: early studies and research frontiers. Gut Microbes, 11, pp. 635–654. doi: 10.1080/19490976.2019.1704142.

Hutloff A., Dittrich A.M., Beier K.C., Eljaschewitsch B., Kraft R., Anagnostopoulos I., et al. (1999). ICOS is an inducible T-cell co-stimulator structurally and functionally related to CD28. Nature, 397, pp. 263–266. doi: 10.1038/16717.

Hwang B., Lee J.H. and Bang D. (2018). Single-cell RNA sequencing technologies and bioinformatics pipelines. Experimental & Molecular Medicine, 50, 96. doi: 10.1038/s12276-018-0071-8.

Ilicic T., Kim J.K., Kolodziejczyk A.A., Bagger F.O., McCarthy D.J., Marioni J.C., et al. (2016). Classification of low-quality cells from single-cell RNA-seq data. Genome Biology, 17, 29. doi: 10.1186/s13059-016-0888-1.

Invernizzi R. and Molyneaux P.L. (2019). The contribution of infection and the respiratory microbiome in acute exacerbations of idiopathic pulmonary fibrosis. European Respiratory Review, 28, 190045. doi: 10.1183/16000617.0045-2019.

Ishikawa N., Hattori N., Yokoyama A., Kohno N. (2012). Utility of KL-6/MUC1 in the clinical management of interstitial lung diseases. Respiratory Investigation. Elsevier, 50(1), pp. 3–13. doi: 10.1016/j.resinv.2012.02.001.

Islam S., Kjallquist U., Moliner A., Zajac P., Fan J.B., Lonnerberg P., et al. (2011). Characterization of the single-cell transcriptional landscape by highly multiplex RNA-seq Saiful. Genome Research, 21, pp. 1160–1167. doi: 10.1101/gr.110882.110.1160.

Jany J.L. and Barbier G. (2008). Culture-independent methods for identifying microbial communities in cheese. Food Microbiology, 25, pp. 839–848. doi: 10.1016/j.fm.2008.06.003.

Jean S.S., Lee W.S., Chen F.L., Ou T.Y., Hsueh P.R. (2014). *Elizabethkingia meningoseptica*: an important emerging pathogen causing healthcare-associated infections. Journal of Hospital Infection, 86, pp. 244–249. doi: 10.1016/j.jhin.2014.01.009.

Ji J. and Fan J. (2019). Discovering myeloid cell heterogeneity in the lung by means of next generation sequencing. Military Medical Research, 6, 33. doi: 10.1186/s40779-019-0222-9.

Johansson N., Vondracek M., Backman-Johansson C., Sköld M.C., Andersson-Ydsten K., Hedlund J. (2019). The bacteriology in adult patients with pneumonia and parapneumonic effusions: increased yield with DNA sequencing method. European Journal of Clinical Microbiology & Infectious Diseases, 38, pp. 297–304. doi: 10.1007/s10096-018-3426-0.

Johnson L. R., Johnson E.G., Vernau W., Kass P.H., Byrne B.A. (2016). Bronchoscopy, imaging, and concurrent diseases in dogs with bronchiectasis: (2003 – 2014). Journal of Veterinary Internal Medecine, 30, pp. 247–254. doi: 10.1111/jvim.13809.

Johnson L.R. and Stern J.A. (2020). Clinical features and outcome in 25 dogs with respiratory-associated pulmonary hypertension treated with sildenafil. Journal of Veterinary Internal Medicine, 35, pp. 65–73. doi: 10.1111/jvim.15679.

Johnson V.S., Corcoran B.M., Wotton P.R., Schwarz T., Sullivan M. (2005). Thoracic high-resolution computed tomographic findings in dogs with canine idiopathic pulmonary fibrosis. Journal of small animal practice, 46(8), pp. 381–388. doi: 10.1111/j.1748-5827.2005.tb00334.x.

Joshi N., Watanabe S., Verma R., Jablonski R.P., Chen C., Cheresh P., et al. (2020). A spatially restricted fibrotic niche in pulmonary fibrosis is sustained by M-CSF/M-CSFR signalling in monocyte-derived alveolar macrophages. European Respiratory Journal, 55, 1900646. doi: 10.1183/13993003.00646-2019.

Joshi N. Walter, J.M. and Misharin A.V. (2018). Alveolar macrophage. Cellular Immunology, 330, pp. 86–90. doi: 10.1016/j.cellimm.2018.01.005.

Jubinville E., Veillette M., Milot J., Maltais F., Comeau A.M., Levesque R.C., et al. (2018). Exacerbation induces a microbiota shift in sputa of COPD patients. PLoS One, 13(3), e0194355. doi: 10.1371/journal.pone.0194355.

Kabashima K., Nakashima C., Nonomura Y., Otsuka A., Cardamone C., Parente R., et al. (2018). Biomarkers for evaluation of mast cell and basophil activation. Immunological Reviews, 282, pp. 114–120. doi: 10.1111/imr.12639.

Kämpfer P., Busse H.J., Longaric I., Rosselló-Móra R., Galatis H., Lodders N. (2012). Pseudarcicella hirudinis gen. nov., sp. nov., isolated from the skin of the medical leech hirudo medicinalis. International Journal of Systematic and Evolutionary Microbiology, 62(9), pp. 2247–2251. doi: 10.1099/ijs.0.037390-0.

Kanagawa T. (2003). Bias and artifacts in multitemplate polymerase chain reactions (PCR). Journal of Bioscience and Bioengineering, 96, pp. 317–323. doi: 10.1016/s1389-1723(03)90130-7.

Karvone A.M., Kirjavainen P.V., Taubel M., Jayaprakash B., Adams R.I., Sordillo J.E., et al. (2019). Indoor bacterial microbiota and development of asthma by 10.5 years of age. Journal of Allergy and Clinical Immunology, 144(5), pp. 1402–1410. doi: 10.1016/j.jaci.2019.07.035.

Kasalický V., Jezbera J., Hahn M.W., Šimek K. (2013). The diversity of the *Limnohabitans* genus, an important group of freshwater bacterioplankton, by characterization of 35 isolated strains. PLoS One, 8(3), e58209. doi: 10.1371/journal.pone.0058209.

Kaur S.P., Rao R. and Nanda S. (2011). Amoxicillin: A broad spectrum antibiotic. International Journal of Pharmacy and Pharmaceutical Sciences, 3(3), pp. 30–37.

Kim M., Morrison M. and Yu Z. (2010). Evaluation of different partial 16S rRNA gene sequence regions for phylogenetic analysis of microbiomes. Journal of Microbiological Methods, 84, pp. 81–87. doi: 10.1016/j.mimet.2010.10.020.

Kiselev V.Y., Andrews T.S. and Hemberg M. (2019). Challenges in unsupervised clustering of single-cell RNA-seq data. Nature Reviews Genetics, 20(5), pp. 273–282. doi: 10.1038/s41576-018-0088-9.

Kishaba T. (2019a). Acute exacerbation of idiopathic pulmonary fibrosis. Medicina, 55, 70. doi: 10.3390/medicina55030070.

Kishaba T. (2019b). Evaluation and management of idiopathic pulmonary fibrosis. Respiratory Investigatio., 57, pp. 300–311. doi: 10.1016/j.resinv.2019.02.003.

Klappenbach J.A., Saxman P.R., Cole J.R., Schmidt T.M. (2001). rrndb: the ribosomal RNA operon copy number database. Nucleic Acids Research, 29, pp. 181–184.

Kockx M., Traini M. and Kritharides L. (2018). Cell-specific production, secretion, and function of apolipoprotein E. Journal of Molecular Medicine, 96, pp. 361–371. doi: 10.1007/s00109-018-1632-y.

Kolahian S., Fernandez I.E., Eickelberg O., Hartl D. (2016). Immune mechanisms in pulmonary fibrosis. American Journal of Respiratory Cell and Molecular Biology, 55, pp. 309–322. doi: 10.1165/rcmb.2016-0121TR.

Kostric M., Milger K., Krauss-Etschmann S., Engel M., Vestergaard G., Schloter M., et al. (2018). Development of a Stable Lung Microbiome in Healthy Neonatal Mice. Microbial Ecology. Microbial Ecology, 75(2), pp. 529–542. doi: 10.1007/s00248-017-1068-x.

Kozich J.J., Westcott S.L., Baxter N.T., Highlander S.K., Schloss P.D. (2013). Development of a dual-index sequencing strategy and curation pipeline for analysing amplicon sequence data on the MiSeq. Applied and Environmental Microbiology, 79(17), pp. 5112–5120. doi: 10.1128/AEM.01043-13.

Krafft E., Heikkilä H.P., Jespers P., Peeters D., Day M.J., Rajamäki M.M., Mc Entee K., et al. (2011). Serum and bronchoalveolar lavage fluid endothelin-1 concentrations as diagnostic biomarkers of canine idiopathic pulmonary fibrosis. Journal of Veterinary Internal Medicine, 25, pp. 990–996. doi: 10.1111/j.1939-1676.2011.0766.x.

Krafft E., Laurila H.P., Peters I.R., Bureau F., Peeters D., Day M.J., et al. (2013). Analysis of gene expression in canine idiopathic pulmonary fibrosis. The Veterinary Journal, 198, pp. 479–486. doi: 10.1016/j.tvjl.2013.08.018.

Krafft E., Lybaert P., Roels E., Laurila H.P., Rajamäki M.M., Farnir F., et al. (2014). Transforming growth factor beta 1 activation, storage, and signalling pathways in idiopathic pulmonary fibrosis in dogs. Journal of Veterinary Internal Medicine, 28(6), pp. 1666–1675. doi: 10.1111/jvim.12432.

Langille M.G., Zaneveld J., Caporaso J.G., McDonald D., Knights D., Reyes J.A. et al. (2013). Analysis Predictive functional profiling of microbial communities using 16S rRNA marker gene sequences. Nature Biotechnology, 31(9), pp. 814–823. doi: 10.1038/nbt.2676.

Lappin M.R., Blondeau J., Boothe D., Breitschwerdt E.B., Guardabassi L., Lloyd D.H., et al. (2017). Antimicrobial use guidelines for treatment of respiratory tract disease in dogs and cats: antimicrobial guidelines working group of the international society for companion animal infectious diseases. Journal of Veterinary Internal Medicine, 31, pp. 279–294. doi: 10.1111/jvim.14627.

Laurila H.P. and Rajamäki M.M. (2020). Update on canine idiopathic pulmonary fibrosis in West Highland white terriers. Veterinary Clinics of North America: Small Animal Practice, 50, 431–46. doi: 10.1016/j.cvsm.2019.11.004.

Lee J., Arisi I., Puxeddu E., Mramba L.K., Amicosante M., Swaisgood C.M., et al. (2018). Bronchoalveolar lavage (BAL) cells in idiopathic pulmonary fibrosis express a complex pro-inflammatory, pro-repair, angiogenic activation pattern, likely associated with macrophage iron accumulation. PloS One, 13, e0194803. doi: 10.1371/journal.pone.0194803.

Lesley R., Kelly L.M., Xu Y., Cyster J.G. (2006). Naive CD4 T cells constitutively express CD40L and augment autoreactive B cell survival. Immunology, 103(28), pp. 10717–10722. doi: 10.1073/pnas.0601539103.

Li N., He F., Liao B., Zhou Y., Li B., Ran P. (2017a). Exposure to ambient particulate matter alters the microbial composition and induces immune changes in rat lung. Respiratory Research. Respiratory Research, 18, 143. doi: 10.1186/s12931-017-0626-6.

Li X., Ding Y., Zi M., Sun L., Zhang W., Chen S., et al. (2017b). CD19, from bench to bedside. Immunology Letters, 183, pp. 86–95. doi: 10.1016/j.imlet.2017.01.010.

Li Z., Wang X., Di D., Pan R., Gao Y., Xiao C., et al. (2021). Comparative analysis of the pulmonary microbiome in healthy and diseased pigs. Molecular Genetics and Genomics, 296, pp. 21–31. doi: 10.1007/s00438-020-01722-5.

Liao M., Liu Y., Yuan J., Wen Y., Xu G., Zhao J., et al. (2020). Single-cell landscape of bronchoalveolar immune cells in patients with COVID-19', Nature Medicine, 26, pp. 842–844. doi: 10.1038/s41591-020-0901-9.

Lieberman, J. (2003). The ABCs of granule-mediated cytotoxicity: new weapons in the arsenal. Nature Review in Immunology, 3, pp. 361–370. doi: https://doi.org/10.1038/nri1083.

Liegeois M., Legrand C., Desmet C.J., Marichal T., Bureau F. (2018). The interstitial macrophage: A long-neglected piece in the puzzle of lung immunity. Cellular Immunology, 330, pp. 91–96. doi: 10.1016/j.cellimm.2018.02.001.

Lilja-Maula L.I.O., Laurila H.P., Syrjä P., Lappalainen A.K., Krafft E., Clercx C., et al. (2014). Long-term outcome and use of 6-minute walk test in West Highland white terriers with idiopathic pulmonary fibrosis. Journal of Veterinary Internal Medicine, 28, pp. 379–385. doi: 10.1111/jvim.12281.

Lilja-Maula L.I.O., Palviainen M.J., Heikkilä H.P., Raekallio M.R., Minna M. Rajamäki M.M. (2013). Proteomic analysis of bronchoalveolar lavage fluid samples obtained from West Highland white terriers with idiopathic pulmonary fibrosis, dogs with chronic bronchitis, and healthy dogs. American Journal of Veterinary Research, 74, pp. 148–154. doi: 10.2460/ajvr.74.1.148.

Lilja-Maula L.I.O., Syrjä P., Laurila H.P., Sutinen E., Palviainen M., Ritvos O., et al. (2015). Upregulation of alveolar levels of activin B, but not activin A, in lungs of west highland white terriers with idiopathic pulmonary fibrosis and diffuse alveolar damage. Journal of Comparative Pathology, 152, pp. 192–200. doi: 10.1016/j.jcpa.2014.11.006.

Lilja-Maula L.I.O., Syrjä P., Laurila H.P., Sutinen E., Rönty M.., Koli K., et al. (2014). Comparative study of transforming growth factor-β signalling and regulatory molecules in human and canine idiopathic pulmonary fibrosis. Journal of Comparative Pathology, 150(4), pp. 399–407. doi: 10.1016/j.jcpa.2013.12.001.

Ling X.B., Wei H.W., Wang J., Kong Y.Q., Wu Y.Y., Guo J.L., et al. (2016). Mammalian metallothionein-2A and oxidative stress. International Journal of Molecular Sciences, 17, 1483. doi: 10.3390/ijms17091483.

Lischke T., Hegemann A., Gurka S., Vu D., Burmeister Y., Lam K., et al. (2012). Comprehensive analysis of CD4 + T cells in the decision between tolerance and immunity in vivo reveals a pivotal role for ICOS. The Journal of Immunology, 189, pp. 234–244. doi: 10.4049/jimmunol.1102034.

Lloyd C.M. and Marsland B.J. (2017). Lung homeostasis: influence of age, microbes, and the immune system. Immunity, 46(4), pp. 549–561. doi: 10.1016/j.immuni.2017.04.005.

Lobetti R.G., Milner R. and Lane E. (2001). Chronic idiopathic pulmonary fibrosis in five dogs. Journal of the American Animal Hospital Association, 37(2), pp. 119–127. doi: 10.5326/15473317-37-2-119.

Löfdahl A., Tornling G., Wigén J., Larsson-Callerfelt A.K., Wenglén C., Westergren-Thorsson G. (2021). Pathological insight into 5-HT2b receptor activation in fibrosing interstitial lung disease. International Journal of Molecular Sciences, 22, p. 225. doi: 10.3390/ijms22010225.

Lorenzo J.M., Munekata P.E., Dominguez R., Pateiro M., Saraiva J.A., Franco D. (2018). Main groups of microorganisms of relevance for food safety and stability: General aspects and overall description. In Innovative technologies for food preservation: Inactivation of spoilage and pathogenic microorganisms. Elsevier. St Louis, Missouri: Elsevier Inc., pp. 53–107. doi: 10.1016/B978-0-12-811031-7.00003-0.

Low R.B., Giancola M.S., King T.E. Jr, Chapitis J., Vacek P., Davis G.S. (1992). Serum and bronchoalveolar lavage of N-terminal type III procollagen peptides in idiopathic pulmonary fibrosis. American Review of Respiratory Disease, 146, pp. 701–706. doi: 10.1164/ajrccm/146.3.701.

Lynch D.A., Sverzellati N., Travis W.D., Brown K.K., Colby T.V., Galvin J.R., et al. (2018). Diagnostic criteria for idiopathic pulmonary fibrosis: a Fleischner Society White Paper. The Lancet, 6, pp. 138–153. doi: 10.1016/S2213-2600(17)30433-2.

Määttä M., Laurila H.P., Holopainen S., Lilja-Maula L.I., Melamies M., Viitanen S.J., et al. (2017). Reflux aspiration can be detected in lungs of dogs with respiratory disease. Proceedings of the 27th ECVIM-CA Congress, St Julian's, Malta. Journal of Veterinary Internal Medicine, 32(6), pp. 2074–2081. doi: 10.1111/jvim.14858.

Määttä M., Laurila H.P., Holopainen S., Aaltonen K., Lilja-Maula L., Viitanen S., et al. (2020). Matrix metalloproteinase-2, -7, and -9 activities in dogs with idiopathic pulmonary fibrosis compared

to healthy dogs and dogs with other respiratory diseases. Journal of Veterinary Internal Medicine, 35(1), pp. 462-471. doi: 10.1111/jvim.15970.

Määttä M., Laurila H.P., Holopainen S., Lilja-Maula L., Melamies M., Viitanen S.J., et al. (2018). Reflux aspiration in lungs of dogs with respiratory disease and in healthy West Highland white terriers. Journal of Veterinary Internal Medicine, 32(6), pp. 2074–2081. doi: 10.1111/jvim.15321.

Maboni G., Seguel M., Lorton A., Berghaus R., Sanchez S. (2019). Canine infectious respiratory disease: New insights into the aetiology and epidemiology of associated pathogens. PLoS One, 14(4), e0215817. doi: 10.1371/journal.pone.0215817.

Macosko E.Z., Basu A., Satija R., Nemesh J., Shekhar K., Goldman M., Tirosh I., et al. (2015). Highly parallel genome-wide expression profiling of individual cells using nanolitre droplets. Cell, 161(5), pp. 1202–1214. doi: 10.1016/j.cell.2015.05.002.

Maddocks S. and Jenkins R. (2017). Chapter 4 - Quantitative PCR: things to consider. In: Understanding PCR. Academic Press, Cambridge, United Kingdom, pp. 45–52. doi: 10.1016/B978-0-12-802683-0.00004-6.

Mahalanobish S., Saha S., Dutta S., Sil P.C., et al. (2020). Matrix metalloproteinase: An upcoming therapeutic approach for idiopathic pulmonary fibrosis. Pharmacological Research, 152, 104591. doi: 10.1016/j.phrs.2019.104591.

Maher T.M. and Strek M.E. (2019). Antifibrotic therapy for idiopathic pulmonary fibrosis: time to treat. Respiratory Research, 20, 205. doi: 10.1186/s12931-019-1161-4.

Man W.H., De Steenhuijsen Piters W.A.A. and Bogaert D. (2017). The microbiota of the respiratory tract: Gatekeeper to respiratory healt. Nature Reviews Microbiology, 15, pp. 259–270. doi: 10.1038/nrmicro.2017.14.

Mantovani A., Biswas S.K., Galdiero M.R., Sica A., Locati M. (2013). Macrophage plasticity and polarization in tissue repair and remodelling. Journal of Pathology, 229, pp. 176–185. doi: 10.1002/path.4133.

Marsh R.L., Nelson M.T., Pope C.E., Leach A.J., Hoffman L.R., Chang A.B., et al. (2018). How low can we go? The implications of low bacterial load in respiratory microbiota studies. Pneumonia, 10(1), 7. doi: 10.1186/s41479-018-0051-8.

Mathieu E., Escribano-Vazquez U., Descamps D., Cherbuy C., Langella P., Riffault S., et al. (2018). Paradigms of lung microbiota functions in health and disease, particularly, in asthma. Frontiers in Physiology, 9, 1168. doi: 10.3389/fphys.2018.01168.

Mayhew D., Devos N., Lambert C., Brown J.R., Clarke S.C., Kim V.L., Magid-Slav M., et al. (2018). Longitudinal profiling of the lung microbiome in the AERIS study demonstrates repeatability of bacterial and eosinophilic COPD exacerbations. Thorax, 73, pp. 422–430. doi: 10.1136/thoraxjnl-2017-210408.

McBride M.J. (2014). The family Flavobacteriaceae. In: Rosenberg E., DeLong E.F., Lory S., Stackebrandt E., Thompson F. (eds). The prokaryotes. Springer-Verlag. Berlin, Germany, pp. 643–676.

Mckeown S., Richter A.G., O'Kane C., McAuley D.F., Thickett D.R. (2009). MMP expression and abnormal lung permeability are important determinants of outcome in IPF. European Journal of Pharmacology, 33, pp. 77–84. doi: 10.1183/09031936.00060708.

McQuattie-Pimentel A.C., Budinger G.R.S. and Ballinger M.N. (2018). Monocyte-derived alveolar macrophages: the dark side of lung repair? American Journal of Respiratory Cell and Molecular Biology, 58(1), pp. 5–6. doi: 10.1165/rcmb.2017-0328ED.

Mercer P.F., Chambers R.C. (2013). Coagulation and coagulation signalling in fibrosis. Biochimica et Biophysica Acta - Molecular Basis of Disease, 1832, pp. 1018–1027. doi: 10.1016/J.BBADIS.2012.12.013.

Mercier E., Bolognin M., Hoffmann A.C., Tual C., Day M.J., Clercx C. (2011). Influence of age on bronchoscopic findings in healthy beagle dogs. Veterinary Journal, 187(2), pp. 225–228. doi: 10.1016/j.tvjl.2009.12.007.

Misharin A.V., Morales-Nebreda L., Mutlu G.M., Budinger G.R., Perlman H. (2013). Flow cytometric analysis of macrophages and dendritic cell subsets in the mouse lung.', American journal of respiratory cell and molecular biology. American Thoracic Society, 49(4), pp. 503–10. doi: 10.1165/rcmb.2013-0086MA.

Misharin A.V., Morales-Nebreda L., Reyfman P.A., Cuda C.M., Walter J.M., McQuattie-Pimentel A.C., et al. (2017). Monocyte-derived alveolar macrophages drive lung fibrosis and persist in the lung over the life span. Journal of Experimental Medicine, 214, pp. 2387–2404. doi: 10.1084/jem.20162152.

Mizrahi-Man O., Davenport E.R. and Gilad Y. (2013). Taxonomic classification of bacterial 16S rRNA genes using short sequencing reads: evaluation of effective study designs. PLoS One, 8, pp. 18–23. doi: 10.1371/journal.pone.0053608.

Moffatt M.F. and Cookson W.O. (2017). The lung microbiome in health and respiratory diseases. Clinical Pulmonary Medicine, 17, pp. 525–529. doi: 10.7861/clinmedicine.17-6-525.

Molyneaux P.L., Cox M.J., Wells A.U., Kim H.C., Ji W., Cookson W.O.C., et al. (2017a). Changes in the respiratory microbiome during acute exacerbations of idiopathic pulmonary fibrosis. Respiratory Research, 18(1), 29. doi: 10.1186/s12931-017-0511-3.

Molyneaux P.L., Cox M.J., Willis-Owen S.A., Mallia P., Russell K.E., Russell A.M., et al. (2014). The role of bacteria in the pathogenesis and progression of idiopathic pulmonary fibrosis. American Journal of Respiratory and Critical Care Medicine, 190, pp. 906–913. doi: 10.1164/rccm.201403-0541OC.

Molyneaux P.L. and Maher T.M. (2013). The role of infection in the pathogenesis of idiopathic pulmonary fibrosis. European Respiratory Review, 22, pp. 376–381. doi: 10.1183/09059180.00000713.

Molyneaux P.L., Willis-Owen S.A.G., Cox M.J., James P., Cowman S., Loebinger M., et al. (2017b). Host-microbial interactions in idiopathic pulmonary fibrosis. American Journal of Respiratory and Critical Care Medicine, 195(12), pp. 1640–1650. doi: 10.1164/rccm.201607-1408OC.

Moore B.B., Kolodsick J.E., Thannickal V.J., Cooke K., Moore T.A., Hogaboam C., et al. (2005). CCR2-mediated recruitment of fibrocytes to the alveolar space after fibrotic injury. The American Journal of Pathology. American Society for Investigative Pathology, 166, pp. 675–684. doi: 10.1016/S0002-9440(10)62289-4.

Morris A., Beck J.M., Schloss P.D., Campbell T.B., Crothers K., Curtis J.L., et al. (2013). Comparison of the respiratory microbiome in healthy nonsmokers and smokers. American Journal of Respiratory and Critical Care Medicine, 187(10), pp. 1067–1075. doi: 10.1164/rccm.201210-1913OC.

Morse C., Tabib T., Sembrat J., Buschur K.L., Bittar H.T., Valenzi E., et al. (2019). Proliferating SPP1/MERTK-expressing macrophages in idiopathic pulmonary fibrosis. European Respiratory Journal, 54, 1802441. doi: 10.1183/13993003.02441-2018.

Mould K.J., Jackson N.D., Henson P.M., Seibold M., Janssen W.J. (2019). Single cell RNA sequencing identifies unique inflammatory airspace macrophage subsets. JCI insight, 4(5), pp. 1–17. doi: 10.1172/jci.insight.126556.

Muraro M.J., Dharmadhikari G., Grün D., Groen N., Dielen T., Jansen E., et al. (2016). A single-cell transcriptome atlas of the human pancreas. Cell Press, 3(4), pp. 385-394.e3. doi: 10.1016/J.CELS.2016.09.002.

Navaratnam V., Fogarty A.W., McKeever T., Thompson N., Jenkins G., Johnson S.R., et al. (2014). Presence of a prothrombotic state in people with idiopathic pulmonary fibrosis: A population-based case-control study. Thorax, 69, 207–215. doi: 10.1136/thoraxjnl-2013-203740.

NCBI (2019a). Taxonomy browser. *B. bronchiseptica*. Available at: https://www.ncbi.nlm.nih.gov/Taxonomy/Browser/wwwtax.cgi?id=518. (Accessed 06 September 2019).

NCBI (2019b). Taxonomy browser. *M. cynos*. Available at: https://www.ncbi.nlm.nih.gov/Taxonomy/Browser/wwwtax.cgi. (Accessed 06 September 2019).

Nelson W.R. and Couto C.G. (2014). Diagnostic tests for the lower respiratory tract. In: Nelson W.R., Couto C.G. (eds). Small animal internal medicine 5th edition. Elsevier. St Louis, Missouri, pp. 263–296.

Nelson W.R. and Couto C.G. (2020). Diagnostic tests for the lower respiratory tract. In: Nelson W.R., Couto C.G. (eds). Small animal internal medicine, 6th edition. Elsevier. St Louis, Missouri, pp. 287–320.

Nemeth J., Schundner A. and Frick M. (2020). Insights into development and progression of idiopathic pulmonary fibrosis from single cell RNA studies. Frontiers in Medicine, 7, 611729. doi: 10.3389/fmed.2020.611728.

Ngo J., Taminiau B., Fall P.A., Daube G., Fontaine J. (2018). Ear canal microbiota – a comparison between healthy dogs and atopic dogs without clinical signs of otitis externa. Veterinary Dermatology, 29(5), pp. 425-e140. doi: 10.1111/vde.12674.

Norris A.J., Naydan D.K. and Wilson D.W. (2005). Interstitial lung disease in West Highland White Terrier. Veterinary Pathology, 42(1), pp. 35–41. doi: 10.1354/vp.42-1-35.

Norris C.R., Griffey S.M. and Walsh P. (2002). Use of keyhole lung biopsy for diagnosis of interstitial lung diseases in dogs and cats: 13 cases (1998-2001). Journal of the American Veterinary Medical Association, 221(10), pp. 1453–1459. doi: 10.2460/javma.2002.221.1453.

Novik G., Savich V. and Kiseleva E. (2015). Microbiology in agriculture and human health. In Mohammad Manjur Shah (ed) Microbiology in Agriculture and Human Health. IntechOpen. London, United Kingdom, pp. 73–105. doi: 10.5772/60502.

O'Dwyer D.N., Dickson R.P. and Moore B.B. (2016). The lung microbiome, immunity, and the pathogenesis of chronic lung disease. The Journal of Immunology, 196(12), pp. 4839–4847. doi: 10.4049/jimmunol.1600279.

O'Dwyer D.N., Shanna A.L., Gurczynski S.J., Meng X., Wilke C., Falkowski N.R., et al. (2019). Lung microbiota contribute to pulmonary inflammation and disease progression in pulmonary fibrosis. American Journal of Respiratory and Critical Care Medicine, 199, pp. 1127–1138. doi: 10.1164/rccm.201809-1650OC.

Olson A.L., Gifford A.H., Inase N., Fernández Pérez E.R., Suda T. (2018). The epidemiology of idiopathic pulmonary fibrosis and interstitial lung diseases at risk of a progressive-fibrosing phenotype. European Respiratory Review, 27, 180077. doi: 10.1183/16000617.0077-2018.

O' Neill D.G., Ballantyne Z.F., Hendricks A., Church D.B., Brodbelt D.C., Pegram C. West Highland white terriers under primary veterinary care in the UK in 2016 : demography , mortality and disorders. (2019). Canine Genetics and Epidemiology, 6, 7. doi: 10.1186/s40575-019-0075-2.

Osafo-Addo A.D. and Herzog E.L. (2017). CCL2 and T cells in pulmonary fibrosis: An old player gets a new role. Thorax, 72(11), pp. 967–968. doi: 10.1136/thoraxjnl-2017-210517.

Out T.A., Wang S.Z., Rudolph K., Bice D.E. (2002). Local T-cell activation after segmental allergen challenge in the lungs of allergic dogs. Immunology, 105(4), pp. 499–508. doi: 10.1046/j.1365-2567.2002.01383.x.

Papalexi, E. and Satija, R. (2018). Single-cell RNA sequencing to explore immune cell heterogeneity. Nature Reviews Immunology, 18(1), pp. 35–45. doi: 10.1038/nri.2017.76.

Pardo A., Cabrera S., Maldonado M., Selman M. (2016). Role of matrix metalloproteinases in the pathogenesis of idiopathic pulmonary fibrosis. Respiratory Research, 17, 23. doi: 10.1186/s12931-016-0343-6.

Pardo A., Gibson K., Cisneros J., Richards T.J., Yang Y., Becerril C., et al. (2005). Up-regulation and profibrotic role of osteopontin in human idiopathic pulmonary fibrosis. PloS Medicine, 2, e251. doi: 10.1371/journal.pmed.0020251.

Parks D.H. and Beiko R.G. (2010). Identifying biologically relevant differences between metagenomic communities. Bioinformatics, 26(6), pp. 715–721. doi: 10.1093/bioinformatics/btq041.

Patel A., Harris K.A. and Fitzgerald F. (2017). What is broad-range 16S rDNA PCR? Archives of Disease in Childhood: Education and Practice Edition, 102(5), pp. 261–264. doi: 10.1136/archdischild-2016-312049.

Patel V.I. and Metcalf J.P. (2019). Airway macrophage and dendritic cell subsets in the resting human lung. Critical Reviews in Immunology, 38, pp. 303–331. doi: 10.1615/CritRevImmunol.2018026459.

Pattaroni C., Watzenboeck M.L., Schneidegger S., Kieser S., Wong N.C., Bernasconi E., et al. (2018). Early-life formation of the microbial and immunological environment of the human airways. Cell Host and Microbe, 24, pp. 857–865. doi: 10.1016/j.chom.2018.10.019.

Pennington, J. (1981). Penetration of antibiotics into respiratory secretions. Reviews of Infectious Disease, 3(1), pp. 67–73. doi: 10.1093/clinids/3.1.67.

Peyser R., MacDonnell S., Gao Y., Cheng L., Kim Y., Kaplan T., et al. (2019). Defining the activated fibroblast population in lung fibrosis using single-cell sequencing. American Journal of Respiratory Cell and Molecular Biology, 61, pp. 74–85. doi: 10.1165/rcmb.2018-0313OC.

Piersigilli F., Van Grambezen B., Hocq C., Danhaive O. (2020). Nutrients and microbiota in lung diseases of prematurity: The placenta-gut-lung triangle. Nutrients, 12, 469. doi: 10.3390/nu12020469.

Pietschke C., Treitz C., Forêt S., Schultze A., Künzel S., Tholey A., et al. (2017). Host modification of a bacterial quorum-sensing signal induces a phenotypic switch in bacterial symbionts. Proceedings of the National Academy of Sciences of the United States of America, 114(40), E8488–E8497. doi: 10.1073/pnas.1706879114.

Pilione M.R. and Harvill E.T. (2006). The *Bordetella bronchiseptica* type III secretion system inhibits gamma interferon production that is required for efficient antibody-mediated bacterial clearance. Infection and Immunity, 74(2), pp. 1043–1049. doi: 10.1128/IAI.74.2.1043.

Piras I.S., Bleul C., Siniard A., Wolfe A.J., De Both M.D., Hernandez A.G., et al. (2020). Association of common genetic variants in the CPSF7 and SDHAF2 genes with canine idiopathic pulmonary fibrosis in the West Highland white terrier. Genes, 11(6), 609. doi: 10.3390/genes11060609.

Plantier L., Cazes A., Dinh-Xuan A.T., Bancal C., Marchand-Adam S., Crestani B. (2018). Physiology of the lung in idiopathic pulmonary fibrosis. European Respiratory Review, 27, 170062. doi: 10.1183/16000617.0062-2017.

Plumb D.C. (2015) Plumb's veterinary drug handbook, eighth edition. Wiley-Blackwell. Ames, Iowa, pp.80-84.

Poczobutt J.M. and Eickelberg O. (2019). Defining the cell types that drive idiopathic pulmonary fibrosis using single-cell. American Journal of Respiratory and Critical Care Medicine, 199, pp. 1454–1456. doi: 10.1164/rccm.201901-0197ED.

Priestnall S.L., Mitchell J.A., Walker C.A., Erles K. (2014). New and emerging pathogens in canine infectious respiratory disease. Veterinary Pathology, 51(2), pp. 492–504. doi: 10.1177/0300985813511130.

Proserpio V. and Mahata B. (2015). Single-cell technologies to study the immune system. Immunology, 147, pp. 133–140. doi: 10.1111/imm12553.

Pruesse E., Quast C., Knittel K., Fuchs B.M., Ludwig W., Peplies J., et al. (2007). SILVA: A comprehensive online resource for quality checked and aligned ribosomal RNA sequence data compatible with ARB. Nucleic Acids Research, 35, pp. 7188–7196. doi: 10.1093/nar/gkm864.

Pugliese S.C., Kumar S., Janssen W.J., Graham B.B., Frid M.G., Riddle S.R., et al. (2017). A time and compartment specific activation of lung macrophages in hypoxic pulmonary hypertension. Journal of Immunology, 198, pp. 4802–4812. doi: 10.4049/jimmunol.1601692.A.

Puttur F., Gregory L.G., Lloyd C.M., Fleming S.A. (2019). Airway macrophages as the guardians of tissue repair in the lung. Immunology & Cell Biology, 97, pp. 246–257. doi: 10.1111/imcb.12235.

Rabiger F.V., Rothe K., Von Buttlar H., Bismarck D., Büttner M., Moore P.F., et al. (2019). Distinct features of canine non-conventional CD4−CD8α− double-negative TCRαβ+ vs. TCRγδ+ T cells. Frontiers in Immunology, 10, 2748. doi: 10.3389/fimmu.2019.02748.

Raghu G., Collard H.R., Egan J.J., Martinez F.J., Behr J., Brown K.K., et al. (2011). An official ATS/ERS/JRS/ALAT statement: Idiopathic pulmonary fbrosis: evidence-based guidelines for diagnosis and management. American Journal of Respiratory and Critical Care Medicine, 183, pp. 789–823. doi: 10.1164/rccm.2009-040GL.

Raghu G., Amatto V.C., Behr J., Stowasser S. (2015a). Comorbidities in idiopathic pulmonary fibrosis patients: a systematic literature review. European Respiratory Journal, 46, pp. 1113–1130. doi: 10.1183/13993003.02316-2014.

Raghu G., Martinez F.J., Brown K.K., Costabel U., Cottin V., Wells A.U., et al. (2015b). CC-chemokine ligand 2 inhibition in idiopathic pulmonary fibrosis: A phase 2 trial of carlumab. European Respiratory Journal, 46, pp. 1740–1750. doi: 10.1183/13993003.01558-2014.

Raghu G., Remy-Jardin M., Myers J.L., Richeldi L., Ryerson C.J., Lederer D.J., et al. (2018). Diagnosis of idiopathic pulmonary fibrosis an official ATS/ERS/JRS/ALAT clinical practice guideline. American Journal of Respiratory and Critical Care Medicine, 198, pp. e44–e68. doi: 10.1164/rccm.201807-1255ST.

Rajamäki M.M., Järvinen A., Saari S.A.M., Maisi P.S. (2001). Effect of repetitive bronchoalveolar lavage on cytologic findings in healthy dogs. American Journal of Veterinary Research, 62(1), pp. 14–17. doi: 10.2460/ajvr.2001.62.13.

Reinero C. (2019a). Interstitial lung diseases in dogs and cats part I: the idiopathic interstitial pneumonias. The Veterinary Journal, 243, pp. 48–54. doi: 10.1016/J.TVJL.2018.11.010.

Reinero C. (2019b). Interstitial lung diseases in dogs and cats part II: Known cause and other discrete forms. The Veterinary Journal, 243, pp. 55–64. doi: 10.1016/J.TVJL.2018.11.011.

Reinero C., Visser L.C., Kellihan H.B., Masseau I., Rozanski E., Clercx C., et al. (2020). ACVIM consensus statement guidelines for the diagnosis, classification, treatment, and monitoring of pulmonary hypertension in dogs. Journal of Veterinary Internal Medicine, 34, pp. 549–573. doi: 10.1111/jvim.15725.

Reinero C.R. and Cohn L.A. (2007). Interstitial lung diseases. Veterinary Clinics of North America - Small Animal Practice, 37, pp. 937–947. doi: 10.1016/j.cvsm.2007.05.008.

Reizenstein E., Johansson B., Mardin L., Abens J., Möllby R., Hallander H.O. (1993). Diagnostic evaluation of polymerase chain reaction discriminative for *Bordetella pertussis*, *B.*

parapertussis, and *B. bronchiseptica*. Diagnostic Microbiology and Infectious Disease, 17(3), pp. 185–191. doi: 10.1016/0732-8893(93)90094-N.

Rennard S.I. Hunninghake G.W., Bitterman P.B., Crystal R.G. (1981). Production of fibronectin by the human alveolar macrophage: Mechanism for the recruitment of fibroblasts to sites of tissue injury in interstitial lung diseases. Proceedings of the National Academy of Sciences, 78, pp. 7147–7151. doi: 10.1073/pnas.78.11.7147.

Reyfman P.A., Walter J.M., Joshi N., Anekalla K.R., Mcquattie-pimentel A.C., Chiu S., et al. (2019). Single-cell transcriptomic analysis of human lung provides insights into the pathobiology of pulmonary fibrosis. American Journal of Respiratory and Critical Care Medicine, 199, pp. 1517–1536. doi: 10.1164/rccm.201712-2410OC.

Rheinwald M., Hartmann K., Hähner M., Wolf G., Straubinger R.K., Schulz B. (2015). Antibiotic susceptibility of bacterial isolates from 502 dogs with respiratory signs. Veterinary record, 176(15), 383. doi: 10.1136/vr.102694.

Richardson H., Dicker A.J., Barclay H., Chalmers J.D. (2019). The microbiome in bronchiectasis. European Respiratory Review, 28(153), 190048. doi: 10.1183/16000617.0048-2019.

Richeldi L., Collar H.R. and Jones M.G. (2017). Idiopathic pulmonary fibrosis. The Lancet, 389(10082), pp. 1941–1952. doi: 10.1016/S0140-6736(17)30866-8.

Ricotta C. (2017). Of beta diversity, variance, evenness, and dissimilarity. Ecology and Evolution, 7, pp. 4835–4843. doi: 10.1002/ece3.2980.

Rivera-Ortega P., Hayton C., Blaikley J., Leonard C., Chaudhuri N. (2018). Nintedanib in the management of idiopathic pulmonary fibrosis: clinical trial evidence and real-world experience. Therapeutic Advances in Respiratory Disease, 12, 1753466618800618. doi: 10.1177/1753466618800618.

Rodriguez-Perea A.L., Arcia E.D., Rueda C.M., Velilla P.A. (2016). Phenotypical characterization of regulatory T cells in humans and rodents. Clinical and Experimental Immunology, 185, pp. 281–291. doi: 10.1111/cei.12804.

Roels E., Barrera C., Million L., Rajamäki M.M., Talbot J., Clercx C., et al. (2017b). Investigation of a fungal aetiology in canine idiopathic pulmonary fibrosis. Proceedings of the 27th ECVIM-CA Congress, St Julian's, Malta. Journal of Internal Veterinary Medicine, 32, p. 558. doi: 10.1111/jvim.14858.

Roels E., Bauer N., Lecut C., Moritz A., Gothot A., Clercx C. (2019). Haemostatic, fibrinolytic and inflammatory profiles in West Highland white terriers with canine idiopathic pulmonary fibrosis and controls. BMC Veterinary Research. BMC Veterinary Research, 15, 379. doi: 10.1186/s12917-019-2134-z.

Roels E., Couvreur T., Farnir F., Clercx C., Verschakelen J., Bolen G. (2017a). Comparison between sedation and general anaesthesia for high-resolution computed tomographic characterization of canine idiopathic pulmonary fibrosis in West Highland white terriers. Veterinary Radiology & Ultrasound, 58, pp. 284–294. doi: 10.1111/vru.12481.

Roels E., Dourcy M., Holopainen S., Rajamäki M.M., Gillet L., Ehlers B., et al. (2016). No evidence of herpesvirus infection in West Highland white terriers with canine idiopathic pulmonary fibrosis. Veterinary Pathology, 53, pp. 1210–1212. doi: 10.1177/0300985816641991.

Roels E., Fastrès A., McGeown P., Gommeren K., Saegerman C., Clercx C. (2018). Questionnaire-based survey of owner-reported environment and care of West Highland white terrier with or without idiopathic pulmonary fibrosis. Proceedings of the 28th ECVIM-CA Congress, Rotterdam, The Netherlands. Journal of Internal Veterinary Medicine, 33(2), p. 1084. doi: 10.1111/jvim.15372.

Roels E., Fastrès A., Merveille A.C., Bolen G., Teske E., Clercx C., et al. (2021). The prevalence of pulmonary hypertension assessed using the pulmonary vein-to-right pulmonary artery ratio and its association with survival in West Highland white terriers with canine idiopathic pulmonary fibrosis', BMC Veterinary Research, 17, 171. doi: 10.1186/s12917-021-02879-w.

Roels E., Krafft E., Antoine N., Farnir F., Laurila H.P., Holopainen S., et al. (2015a). Evaluation of chemokines CXCL8 and CCL2, serotonin, and vascular endothelial growth factor serum concentrations in healthy dogs from seven breeds with variable predisposition for canine idiopathic pulmonary fibrosis. Research in Veterinary Science, 101, pp. 57–62. doi: 10.1016/J.RVSC.2015.05.020.

Roels E., Krafft E., Farnir F., Holopainen S., Laurila H.P., Rajamäki M.M., et al. (2015b). Assessment of CCL2 and CXCL8 chemokines in serum, bronchoalveolar lavage fluid and lung tissue samples from dogs affected with canine idiopathic pulmonary fibrosis. The Veterinary Journal, 206, pp. 75–82. doi: 10.1016/J.TVJL.2015.06.001.

Roels E., Taminiau B., Darnis E., Neveu F., Daube G., Clercx C. (2017c). Comparative analysis of the respiratory microbiota of healthy dogs and dogs with canine idiopathic pulmonary fibrosis. Journal of Veterinary Internal Medicine, 31(1), pp. 230–231. doi: 10.1111/jvim.14600.

Rogers G.B., Shaw D., Marsh R.L., Carroll M.P., Serisier D.J., Bruce K.D. (2015). Respiratory microbiota: addressing clinical questions, informing clinical practice. Thorax, 70, pp. 74–81. doi: 10.1136/thoraxjnl-2014-205826.

Rognes T., Flouri T., Nichols B., Quince C., Mahé F. (2016). VSEARCH: a versatile open source tool for metagenomics. PeerJ, 4, e2584. doi: 10.7717/peerj.2584.

Rogulski K., Li Y., Rothermund K., Pu L., Watkins S., Yi F., et al. (2005). Onzin, a c-Myc-repressed target, promotes survival and transformation by modulating the Akt – Mdm2 – p53 pathway. Oncogene, 24, pp. 7524–7541. doi: 10.1038/sj.onc.1208897.

Rostaher A., Dolf G., Fischer N.M., Silaghi C., Akdis C., Zwickl L., et al. (2020). Atopic dermatitis in a cohort of West Highland white terriers in Switzerland . Part II : estimates of early life factors and heritability. Veterinary Dermatology, 31, 276-e66. doi: 10.1111/vde.12843.

Sakmanoglu A., Sayin Z., Ucan U.S., Pinarkara Y., Uslu A., Erganis O. (2017). Comparison of five methods for isolation of DNA from *Mycoplasma cynos*. Journal of Microbiological Methods, 140, pp. 70–73. doi: 10.1016/J.MIMET.2017.07.003.

Salisbury M.L., Han M.K., Dickson R.P., Molyneaux P.L. (2017). Microbiome in interstitial lung disease: from pathogenesis to treatment target. Current Opinion in Pulmonary Medicine, 23(5), pp. 404–410. doi: 10.1097/MCP.0000000000000399.

Salomon R., Kaczorowski D., Valdes-Mora F., Nordon R.E., Neild A., Farbehi N., et al. (2019). Droplet-based single cell RNAseq tools: A practical guide. Lab on a Chip, 19(10), pp. 1706–1727. doi: 10.1039/c8lc01239c.

Salter S.J., Cox M.J., Turek E.M., Calus S.T., Cookson W.O., Moffatt M.F., et al. (2014). Reagent and laboratory contamination can critically impact sequence-based microbiome analyses. BMC Biology, 12, 87. doi: 10.1186/s12915-014-0087-z.

Salton F., Volpe M.C. and Confalonieri M. (2019). Epithelial-mesenchymal transition in the pathogenesis of idiopathic pulmonary fibrosis. Medicina, 55, 83. doi: 10.3390/medicina55040083.

Sattasathuchana P. and Steiner M. (2014). Canine eosinophilic gastrointestinal disorders. Animal Health Research Reviews, 15, pp. 76–86. doi: 10.1017/S1466252314000012.

Scher J.U., Joshua V., Artacho A., Abdollahi-Roodsaz S., Öckinger J., Kullberg S. et al. (2016). The lung microbiota in early rheumatoid arthritis and autoimmunity. Microbiome, 4, 60. doi: 10.1186/s40168-016-0206-x.

Schloss P. (2013). Amova. Available at: https://www.mothur.org/wiki/Amova (Accessed: 21 October 2019).

Schloss P. (2018). Homova. Available at: https://www.mothur.org/wiki/Homova (Accessed: 21 October 2019).

Schober K.E. and Baade H. (2006). Doppler echocardiographic prediction of pulmonary hypertension in West Highland white terriers with chronic pulmonary disease. Journal of Veterinary Internal Medecine, 20, pp. 912–920. doi: 10.1111/j.1939-1676.2006.tb01805.x.

Schuliga M., Grainge C., Westall G., Knight D. (2018). The fibrogenic actions of the coagulant and plasminogen activation systems in pulmonary fibrosis. The International Journal of Biochemistry & Cell Biology, 97, pp. 108–117. doi: 10.1016/j.biocel.2018.02.016.

Schulz B.S., Kurz S., Weber K., Balzer H.J., Hartmaan K. (2014). Detection of respiratory viruses and *Bordetella bronchiseptica* in dogs with acute respiratory tract infections. The Veterinary Journal, 201(3), pp. 365–369. doi: 10.1016/J.TVJL.2014.04.019.

Schupp J.C., Binder H., Jäger B., Cillis G., Zissel G., Müller-quernheim J., et al. (2015). Macrophage activation in acute exacerbation of idiopathic pulmonary fibrosis. PloS One, 10, e0116775. doi: 10.1371/journal.pone.0116775.

Schyns J., Bai Q., Ruscitti C., Radermecker C., De Schepper S., Chakarov S., et al. (2019). Non-classical tissue monocytes and two functionally distinct populations of interstitial macrophages populate the mouse lung. Nature Communications, 10, 3964. doi: 10.1038/s41467-019-11843-0.

See P., Lum J., Chen J., Ginhoux F. (2018). A Single-cell sequencing guide for immunologists. Frontiers in Immunology, 9, 2425. doi: 10.3389/fimmu.2018.02425.

Segal L.N., Alekseyenko A.V., Clemente J.C., Kulkarni R., Wu B., Chen H., et al. (2013). Enrichment of lung microbiome with supraglottic taxa is associated with increased pulmonary inflammation. Microbiome, 1, 19. doi: 10.1186/2049-2618-1-19.

Segal L.N., Rom W.N. and Weiden, M.D. (2014). Lung microbiome for clinicians: New discoveries about bugs in healthy and diseased lungs. Annals of the American Thoracic Society, 11(1), pp. 108–116. doi: 10.1513/AnnalsATS.201310-339FR.

Segata N., Izard J, Waldron L., Gevers D., Miropolsky L., Garrett W.S., et al. (2011). Metagenomic biomarker discovery and explanation. Genome Biology, 12(6). doi: 10.1186/gb-2011-12-6-r60.

Selman M., Ruiz V., Cabrera S., Segura L., Ramirez R., Barrios R., et al. (2000). TIMP-1, -2, -3, and -4 in idiopathic pulmonary fibrosis. A prevailing nondegradative lung microenvironment? American Journal of Physiology-Lung Cellular and Molecular Physiology, 279, pp. 562–574. doi: 10.1152/ajplung.2000.279.3.L562.

Selman M. and Pardo A. (2020). The leading role of epithelial cells in the pathogenesis of idiopathic pulmonary fibrosis. Cellular Signalling, 66, 109482. doi: 10.1016/j.cellsig.2019.109482.

Sgalla G., Iovene B., Calvello M., Ori M., Varone F., Richeldi L. (2018). Idiopathic pulmonary fibrosis: pathogenesis and management. Respiratory Research, 19, 32. doi: 10.1186/s12931-018-0730-2.

Shi T., Denney L., An H., Ho L.P., Zheng Y. (2021). Alveolar and lung interstitial macrophages: Definitions, functions, and roles in lung fibrosis. Journal of Leukocyte Biology, 110, pp. 107–114. doi: 10.1002/JLB.3RU0720-418R.

Shukla S.D., Budden K.F., Neal R., Hansbro P.M. (2017). Microbiome effects on immunity, health and disease in the lung. Clinical and Translational Immunology, 6(3), e133-12. doi: 10.1038/cti.2017.6.

Simpson J.M., Martineau B., Jones W.E., Ballam J.M., Mackie R.I. (2002). Characterization of faecal bacterial populations in canines: Effects of age, breed and dietary fiber. Microbial Ecology, 44(2), pp. 186–197. doi: 10.1007/s00248-002-0001-z.

Singh N., Vats A., Sharma A., Arora A., Kumar A. (2017). The development of lower respiratory tract microbiome in mice. Microbiome, 5, 61. doi: 10.1186/s40168-017-0277-3.

Singh P., Carraher C. and Schwarzbauer J.E. (2010). Assembly of fibronectin extracellular matrix. Annual Review of Cell and Developmental Biology, 26, pp. 397–419. doi: 10.1146/annurev-cellbio-100109-104020.

Siqueira F.M., Pérez-Wohlfeil E., Carvalho F.M., Trelles O., Schrank I.S., Vasconcelos A.T.R., et al. (2017). Microbiome overview in swine lungs. PLoS One, 12, e0181503. doi: 10.1371/journal.pone.0181503.

Skinner J.A., Pilione M.R., Shen H., Harvill E.T., Yuk M.H. (2005). Bordetella type III secretion modulates dendritic cell migration resulting in immunosuppression and bacterial persistence. The Journal of Immunology, 175, pp. 4647–4652. doi: 10.4049/jimmunol.175.7.4647.

Slatko B.E., Gardner A.F. and Ausubel F.M. (2018). Overview of next generation sequencing technologies (and bioinformatics) in cancer. Current Protocols in Molecular Biology, 122, e59. doi: 10.1002/cpmb.59.

Sokai A., Tanizawa K., Handa T., Kanatani K., Kubo T., Ikezoe K., et al. (2017). Importance of serial changes in biomarkers in idiopathic pulmonary fibrosis. ERJ Open Research, 3, pp. 00019–2016. doi: 10.1183/23120541.00019-2016.

Somogyi V., Chaudhuri N., Torrisi S.E., Kahn N., Müller V., Kreuter M. (2019). The therapy of idiopathic pulmonary fibrosis: what is next? European Respiratory Review, 28, 190021. doi: 10.1183/16000617.0021-2019.

Spagnolo P., Molyneaux P.L., Bernardinello N., Cocconcelli E., Biondini D., Fracasso F., et al. (2019). The role of the lung' s microbiome in the pathogenesis and progression of idiopathic pulmonary fibrosis. International Journal of Molecular Sciences, 20, 5618. doi: 10.3390/ijms20225618.

Spużak J., Chełmonska-soyta A., Krzysztof K., Jankowski M., Nicpon J., Błach J., et al. (2008). Application of flow cytometry in blood examination and bronchoalveolar lavage in healthy dogs. Medicine, 3(38), pp. 321–324.

Stahl M., Schupp J., Jaǧer B., Schmid M., Zissel G., MuÏler-Quernheim J., et al. (2013). Lung collagens perpetuate pulmonary fibrosis via CD204 and M2 macrophage activation. PloS One, 8, e81382. doi: 10.1371/journal.pone.0081382.

Stanborough T., Fegan N., Powell S.M., Tamplin M., Chandry P.S. (2017). Insight into the genome of *Brochothrix thermosphacta*, a problematic meat spoilage bacterium. Applied and Environmental Microbiology, 83(5), e02786-16. doi: 10.1128/AEM.02786-16.

Stefano A. Di, Ricciardolo F.L.M., Caramori G., Adcock I.M., Chung K.F., Barnes P.J., et al. (2017). Bronchial inflammation and bacterial load in stable COPD is associated with TLR4

overexpression. European Respiratory Journal, 49, 1602006. doi: 10.1183/13993003.02006-2016.

Steinfeld A., Prenger-Berninghoff E., Bauer N., Weiß R., Moritz A. (2012). Bacterial susceptibility testings of the lower airways of diseased dogs. Tierarztl Prax Ausg K Kleintiere Heimtiere, 40(5), pp. 309–317. doi: 10.1055/s-0038-1623659.

Stifano G. and Christmann R.B. (2016). Macrophage involvement in systemic sclerosis: do we need more evidence? Current Rheumatology Reports, 18, 2. doi: 10.1007/s11926-015-0554-8.

Stoddard S.F. Smith B.J., Hein R., Roller B.R., Schmidt T.M. (2015). rrnDB: Improved tools for interpreting rRNA gene abundance in bacteria and archaea and a new foundation for future development. Nucleic Acids Research, 43, pp. D593–D598. doi: 10.1093/nar/gku1201.

Streit W.R. and Schmitz R.A. (2004). Metagenomics - The key to the uncultured microbes. Current Opinion in Microbiology, 7, pp. 492–498. doi: 10.1016/j.mib.2004.08.002.

Stuart T., Butler A., Hoffman P., Hafemeister C., Papalexi E., Mauck III W.M., et al. (2019). Comprehensive integration of single-cell data. Cell, 177, pp. 1888–1902. doi: 10.1016/j.cell.2019.05.

Stuart T. and Satija R. (2019). Integrative single-cell analysis. Nature Reviews Genetics, 20, pp. 257–272. doi: 10.1038/s41576-019-0093-7.

Stubbington M.J.T., Rozenblatt-Rosen O., Regev A., Teichmann S.A. (2017). Single cell transcriptomics to explore the immune system in health and disease. Science, 358(6359), pp. 58–63. doi: 10.1126/science.aan6828.

Subramanian A., Tamayo P., Mootha V.K., Mukherjee S., Ebert B.L., Gillettea M.A., et al. (2005). Gene set enrichment analysis: A knowledge-based approach for interpreting genome-wide expression profiles. Proceedings of the National Academy of Sciences, 102, pp. 15545–15550. doi: 10.1073/pnas.0506580102.

Suryawanshi H., Clancy R., Morozov P., Halushka M.K., Buyon J.P., Tuschl T. (2019). Cell atlas of the foetal human heart and implications for autoimmune-mediated congenital heart block. Cardiovascular Research, 116, 1446–1457. doi: 10.1093/cvr/cvz257.

Swigris J.J. and Brown K.K. (2010). The role of endothelin-1 in the pathogenesis of idiopathic pulmonary fibrosis. BioDrugs, 24, pp. 49–54. doi: 10.2165/11319550-000000000-00000.

Syrjä P., Heikkilä H.P., Lilja-Maula L., Krafft E., Clercx C., Day M.J., et al. (2013). The histopathology of idiopathic pulmonary fibrosis in West Highland white terriers shares features of both non-specific interstitial pneumonia and usual interstitial pneumonia in man. Journal of Comparative Pathology, 149(2–3), pp. 303–313. doi: 10.1016/j.jcpa.2013.03.006.

Sze M.A., Dimitriu P.A., Hayashi S., Elliott W.M., McDonough J.E., Gosselink J.V., et al. (2012). The lung tissue microbiome in chronic obstructive pulmonary disease. American Journal of Respiratory and Critical Care Medicine, 185(10), pp. 1073–1080. doi: 10.1164/rccm.201111-2075OC.

Tafuri A., Shahinian A., Bladt F., Yoshinaga S.K., Jordana M., Wakeham A., et al. (2001). ICOS is essential for effective T-helper-cell responses. Nature, 409, pp. 105–109. doi: 10.1038/35051113.

Takahashi F., Takahashi K., Okazaki T., Maeda K., Ienaga H., Maeda M., et al. (2001). Role of osteopontin in the pathogenesis of bleomycin-induced pulmonary fibrosis. American Journal of Respiratory Cell and Molecular Biology, 24, pp. 264–271. doi: 10.1165/ajrcmb.24.3.4293.

Takahashi Y., Saito A., Chiba H., Kuronuma K., Ikeda K., Kobayashi T., et al. (2018). Impaired diversity of the lung microbiome predicts progression of idiopathic pulmonary fibrosis. Respiratory Research. Respiratory Research, 19, 34. doi: 10.1186/s12931-018-0736-9.

Tashiro J., Rubio G.A., Limper A.H., Williams K., Elliot S.J., Ninou I., et al. (2017). Exploring animal models that resemble idiopathic pulmonary fibrosis. Frontiers in Medicine, 4, p. 118. doi: 10.3389/fmed.2017.00118.

Teo S.M., Mok D., Pham K., Kusel M., Serralha M., Troy N., et al. (2015). The infant nasopharyngeal microbiome impacts severity of lower respiratory infection and risk of asthma development. Cell Host and Microbe, 17, pp. 704–715. doi: 10.1016/j.chom.2015.03.008.

The Human Microbiome Project Consortium (2012). Structure, function and diversity of the healthy human microbiome. Nature, 486, pp. 207–214. doi: 10.1038/nature11234.

Thiemann S., Smit N. and Strowig T. (2016). Antibiotics and the intestinal microbiome: individual responses, resilience of the ecosystem, and the susceptibility to infections. Current Topics in Microbiology and Immunology, 398, pp. 123–146. doi: 10.1007/82_2016_504.

Thierry F., Handel I., Hammond G., King L.G., Corcoran B.M., Schwarz T. (2017). Further characterization of computed tomographic and clinical features for staging and prognosis of

idiopathic pulmonary fibrosis in West Highland white terriers. Veterinary Radiology and Ultrasound, 58(4), pp. 381–388. doi: 10.1111/vru.12491.

Todd J.L., Vinisko R., Liu Y., Neely M.L., Overton R., Flaherty K.R., et al. (2020). Circulating matrix metalloproteinases and tissue metalloproteinase inhibitors in patients with idiopathic pulmonary fibrosis in the multicenter IPF-PRO Registry cohort. BMC Pulmonary Medicine, 20, 64. doi: 10.1186/s12890-020-1103-4.

Torrisi S.E., Vancheri A., Pavone M., Sambataro G., Palmucci S., Vancheri C. (2018). Comorbidities of IPF: How do they impact on prognosis. Pulmonary Pharmacology & Therapeutics, 53, pp. 6–11. doi: 10.1016/j.pupt.2018.09.003.

Trombetta A.C., Goyal R., Desch A.N., Leach S.M., Prabagar M., Atif S.M., et al. (2018). A circulating cell population showing both M1 and M2 monocyte/macrophage surface markers characterizes systemic sclerosis patients with lung involvement. Respiratory Research, 19(186), pp. 1–12. doi: 10.1186/s12931-018-0891-z.

Tsukui T., Sun K.H., Wetter J.B., Wilson-Kanamori J.R., Hazelwood L.A., Henderson N.C., et al. (2020). Collagen-producing lung cell atlas identifies multiple subsets with distinct localization and relevance to fibrosis. Nature Communications, 11, 1920. doi: 10.1038/s41467-020-15647-5.

Ungefroren H., Id F.G., Kaufmann R., Settmacher U., Lehnert H., Id B.H.R. (2018). Signaling crosstalk of TGF-β/ALK5 and PAR2/PAR1 : A complex regulatory network controlling fibrosis and cancer. International Journal of Molecular Sciences, 19, 1568. doi: 10.3390/ijms19061568.

Upagupta C., Shimbori C., Alsilmi R., Kolb M. (2018). Matrix abnormalities in pulmonary fibrosis. European Respiratory Review, 27, 180033. doi: 10.1183/16000617.0033-2018.

Vail D.M., Mahler P.A. and Soergel S.A. (1995). Differential cell analysis and phenotypic subtyping of lymphocytes in bronchoalveolar lavage fluid from clinically normal dogs. American Journal of Veterinary Research, 56(3), pp. 282–285.

Van De Laar L., Saelens W., De Prijck S., Martens L., Scott C.L., Van Isterdael G., et al. (2016). Yolk sac macrophages, fetal liver, and adult monocytes can colonize an empty niche and develop into functional tissue-resident macrophages. Immunity, 44(4), pp. 755–768. doi: 10.1016/j.immuni.2016.02.017.

Vargas-Albores F., Martínez-Córdova L.R., Martínez-Porchas M., Calderón K., Lago-Lestón A. (2019). Functional metagenomics: a tool to gain knowledge for agronomic and veterinary sciences', Biotechnology and Genetic Engineering Reviews, 35, pp. 69–91. doi: 10.1080/02648725.2018.1513230.

Varricchi G., Raap U., Rivellese F., Gibbs B.F. (2018). Human mast cells and basophils — How are they similar how are they different? Immunological Reviews, 282, pp. 8–34. doi: 10.1111/imr.12627.

Vegh P. and Haniffa M. (2018). The impact of single-cell RNA sequencing on understanding the functional organization of the immune system. Briefings in Functional Genomics, 17(4), pp. 265–272. doi: 10.1093/bfgp/ely003.

Větrovský T. and Baldrian P. (2013). The variability of the 16S rRNA gene in bacterial genomes and its consequences for bacterial community analyses. PLoS One, 8(2), e57923. doi: 10.1371/journal.pone.0057923.

Vientós-plotts A.I., Ericsson A.C., Rindt H., Reinero C.R. (2019). Respiratory dysbiosis in canine bacterial pneumonia: standard culture vs. microbiome sequencing. Frontiers in Veterinary Science, 6, 354. doi: 10.3389/fvets.2019.00354.

Vieson M.D., Piñeyro P. and LeRoith T. (2012). A review of the pathology and treatment of canine respiratory infections. Veterinary Medicine: Research and Reports, 3, pp. 25–39. doi: 10.2147/VMRR.S25021.

Viitanen S.J., Laurila H.P., Lilja-Maula L.I., Melamies M.A., Rantala M., Rajamäki M.M. (2014). Serum C-reactive protein as a diagnostic biomarker in dogs with bacterial respiratory diseases. Journal of Veterinary Internal Medicine, 28(1), pp. 84–91. doi: 10.1111/jvim.12262.

Viitanen S.J., Lappalainen A. and Rajamäki M.M. (2015). Co-infections with respiratory viruses in dogs with bacterial pneumonia. Journal of Veterinary Internal Medicine, 29(2), pp. 544–551. doi: 10.1111/jvim.12553.

Visser L.C. Im M.K., Johnson L.R., Stern J.A. (2016). Diagnostic value of right pulmonary artery distensibility index in dogs with pulmonary hypertension: comparison with Doppler echocardiographic estimates of pulmonary arterial pressure. Journal of Veterinary Internal Medicine, 30, pp. 543–552. doi: 10.1111/jvim.13911.

Volkova O.Y., Reshetnikova E.S., Mechetina L.V., Chikaev N.A., Najakshin A.M., Faizulin R.Z., et al. (2007). Generation and characterization of monoclonal antibodies specific for human FCRLA. Hybridoma, 26(2), pp. 78–85. doi: 10.1089/hyb.2006.043.

Wakamatsu K., Nagata N., Kumazoe H., Oda K., Ishimoto H., Yoshimi M., et al. (2017). Prognostic value of serial serum KL-6 measurements in patients with idiopathic pulmonary fibrosis. Respiratory Investigation, 55(1), pp. 16–23. doi: 10.1016/j.resinv.2016.09.003.

Wakwaya Y. and Brown K.K. (2019). Idiopathic pulmonary fibrosis: epidemiology, diagnosis and outcome. American Journal of the Medical Sciences, 357(5), pp. 359–369. doi: 10.1016/j.amjms.2019.02.013.

Wallis A. and Spinks K. (2015). The diagnosis and management of interstitial lung disease., British Medical Journal, 350, h2072. doi: 10.1136/bmj.h2072.

Wang H., Wang M., Xiao K., Zhang X., Wang P., Qi H., et al. (2019). Bioinformatics analysis on differentially expressed genes of alveolar macrophage in IPF. Experimental Lung Research, 45, pp. 288–296. doi: 10.1080/01902148.2019.1680765.

Wang J., Lesko M., Badri M.H., Kapoor B.C., Wu B.G., Li Y., et al. (2017). Lung microbiome and host immune tone in subjects with idiopathic pulmonary fibrosis treated with inhaled interferon-γ. ERJ Open Research, 3(3), pp. 00008–2017. doi: 10.1183/23120541.00008-2017.

Wang J., Li F. and Tian Z. (2017). Role of microbiota on lung homeostasis and diseases. Science China Life Sciences, 60, pp. 1407–1415. doi: 10.1007/s11427-017-9151-1.

Wang Z., Bafadhel M., Haldar K., Spivak A., Mayhew D., Miller B.E., et al. (2016). Lung microbiome dynamics in COPD exacerbations. European Respiratory Journal, 47(4), pp. 1082–1092. doi: 10.1183/13993003.01406-2015.

Webb J. and Armstrong J. (2002). Chronic idiopathic pulmonary fibrosis in a West Highland white terrier. The Canadian veterinary journal, 43, pp. 703–705.

Weikl F., Tischer C., Probst A.J., Heinrich J., Markevych I., Jochner S., et al. (2016). Fungal and bacterial communities in indoor dust follow different environmental determinants. PLoS One, 11, e0154131. doi: 10.1371/journal.pone.0154131.

Weng D., Chen X.Q., Qiu H., Zhang Y., Li Q.H., Zhao M.M., et al. (2019). The role of infection in acute exacerbation of idiopathic pulmonary fibrosis. Mediators of Inflammation, 2019, 5160694. doi: 10.1155/2019/5160694.

Whaley S.L., Wolff R.K. and Muggenburg B.A. (1987). Clearance of nasal mucus in nonanesthetized and anesthetized dogs. American Journal of Veterinary Research, 48(2), pp. 204–206.

Williams K.J. (2014). Gammaherpesviruses and pulmonary fibrosis: evidence from humans, horses, and rodents. Veterinary Parasitology, 51(2), pp. 372–384. doi: 10.1177/0300985814521838.

Williams K. and Roman J. (2016). Studying human respiratory disease in animals - Role of induced and naturally occurring models. Journal of Pathology, 238, pp. 220–232. doi: 10.1002/path.4658.

Wind S., Crestani B., Thibault R., Lederlin M., Vernhet L., Valenzuela C., et al. (2019). Clinical pharmacokinetics and pharmacodynamics of nintedanib. Clinical Pharmacokinetics, 58, pp. 1131–1147. doi: 10.1007/s40262-019-00766-0.

Woese C.R. (1987). Bacterial evolution. Microbiological Reviews, 51, pp. 221–271. doi: 10.1128/mmbr.51.2.221-271.1987.

Woese C.R. and Fox G.E. (1977). Phylogenetic structure of the prokaryotic domain: The primary kingdoms. Proceedings of the National Academy of Sciences of the United States of America, 74, pp. 5088–5090. doi: 10.1073/pnas.74.11.5088.

Wolkow P.P., Gebska A. and Korbut R. (2018). In vitro maturation of monocyte-derived dendritic cells results in two populations of cells with different surface marker expression, independently of applied concentration of interleukin-4. International Immunopharmacology, 57, pp. 165–171. doi: 10.1016/j.intimp.2018.02.015.

Woo P.C.Y., Lau S.K.P., Teng J.L.L., Tse H., Yuen K.Y. (2008). Then and now: use of 16S rDNA gene sequencing for bacterial identification and discovery of novel bacteria in clinical microbiology laboratories. Clinical Microbiology and Infection, 14(10), pp. 908–934. doi: 10.1111/j.1469-0691.2008.02070.x.

Wygrecka M., Didiasova M., Berscheid S., Piskulak K., Taborski B., Zakrzewicz D. (2013). Protease-activated receptors (PAR)-1 and -3 drive epithelial-mesenchymal transition of alveolar epithelial cells – potential role in lung fibrosis. Thrombosis and Haemostasis, 110, pp. 295–307. doi: 10.1160/TH12-11-0854.

Wypych L.C., Wickramasinghe T.P. and Marsland B.J. (2020). The influence of the microbiome on respiratory health. Nature immunology, 20, pp. 1279–1290.

Xie T., Wang Y., Deng N., Huang G., Taghavifar F., Geng Y., et al. (2018). Single-cell deconvolution of fibroblast heterogeneity in mouse pulmonary fibrosis. Cell Reports, 22, pp. 3625–3640. doi: 10.1016/j.celrep.2018.03.010.

Xin H., Peng Y., Yuan Z., Guo H. (2009). In vitro maturation and migration of immature dendritic cells after chemokine receptor 7 transfection. Canadian Journal of Microbiology, 55(7), pp. 859–866. doi: 10.1139/W09-041.

Xu Y., Mizuno T., Sridharan A., Du Y., Guo M., Tang J., et al. (2016). Single-cell RNA sequencing identifies diverse roles of epithelial cells in idiopathic pulmonary fibrosis. JCI Insight, 1, e90558. doi: 10.1172/jci.insight.90558.

Xue M., Guo Z., Cai C., Sun B., Wang H. (2019). Evaluation of the diagnostic efficacies of serological markers KL-6, SP-A, SP-D, CCL2, and CXCL13 in idiopathic interstitial pneumonia. Respiration, 98, pp. 534–545. doi: 10.1159/000503689.

Yang D., Xing Y., Song X., Qian Y. (2020). The impact of lung microbiota dysbiosis on inflammation. Immunology, 159(2), pp. 156–166. doi: 10.1111/imm.13139.

Yatsunenko T., Rey F.E., Manary M.J., Trehan I., Dominguez-Bello M.G., Contreras M., et al. (2012). Human gut microbiome viewed across age and geography Tanya. Nature, 486, pp. 222–227. doi: 10.1038/nature11053.

Yi H. and Ku N.O. (2013). Intermediate filaments of the lung. Histochemisrty and Cell Biology, 140, pp. 65–69. doi: 10.1007/s00418-013-1105-x.

Yu C., Liu Y., Sun L., Wang D., Wang Y., Zhao S. (2017). Chronic obstructive sleep apnea promotes aortic remodelling in canines through miR-145/Smad3 signalling pathway. Oncotarget, 8(23), pp. 37705–37716. doi: 10.18632/oncotarget.17144.

Yu Y.R.A., Hotten D.F., Malakhau Y., Volker E., Ghio A.J., Noble P.W., et al. (2016). Flow cytometric analysis of myeloid cells in human blood, bronchoalveolar lavage, and lung tissues. American Journal of Respiratory Cell and Molecular Biology, 54, pp. 13–24. doi: 10.1165/rcmb.2015-0146OC.

Zalewska M., Trefon J. and Milnerowicz H. (2014). The role of metallothionein interactions with other proteins. Proteomics, 14, pp. 1343–1356. doi: 10.1002/pmic.201300496.

Zaura E., Brandt B., Teixeira de Mattos M.J., Buijs M., Caspers M., Rashid M., et al. (2015). Same exposure but two radically different responses to antibiotics: resilience of the salivary microbiome versus long-term microbial shifts in feces. mBio, 6(6), e01693-15. doi: 10.1128/mBio.01693-15.

Zhang D., Li S., Wang N., Tan H.Y., Zhang Z., Feng Y. (2020). The cross-talk between gut microbiota and lungs in common lung diseases. Frontiers in Microbiology, 11, 301. doi: 10.3389/fmicb.2020.00301.

Zhang L., Wang Y., Wu G., Xiong W., Gu W. and Wang C.Y. (2018). Macrophages: friend or foe in idiopathic pulmonary fibrosis? BMC Respiratory Research, 19, 170. doi: 10.1186/s12931-018-0864-2.

Zhang Y., Jiang M., Nouraie M., Roth M.G., Tabib T., Winters S., et al. (2019). GDF15 is an epithelial-derived biomarker of idiopathic pulmonary fibrosis. American Journal of Physiology-Lung Cellular and Molecular Physiology, 317, pp. 510–521. doi: 10.1152/ajplung.00062.2019.

Zheng G.X.Y., Terry J.M., Belgrader P., Ryvkin P., Bent Z.W., Wilson R., et al. (2017). Massively parallel digital transcriptional profiling of single cells. Nature Communications, 8, 14049. doi: 10.1038/ncomms14049.

Zhu J., Zhu J., Yamane H., Cote-Sierra J., Guo L., Paul W.E. (2006). GATA-3 promotes Th2 responses through three different mechanisms: induction of Th2 cytokine production, selective growth of Th2 cells and inhibition of Th1 cell-specific factors. Cell Research, 16, pp. 3–10. doi: 10.1038/sj.cr.7310002.

Zimmerman K.L., Panciera D.L., Panciera R.J., Oliver J.W., Hoffmann W.E., Binder E.M., et al. (2010). Hyperphosphatasemia and concurrent adrenal gland dysfunction in apparently healthy Scottish Terriers. Journal of the American Veterinary Medical Association, 237, pp. 178–186. doi: 10.2460/javma.237.2.178.

Presses de la Faculté de Médecine vétérinaire de l'Université de Liège

4000 Liège (Belgique)

D/2021/0480/9
ISBN 978-2-87543-175-2